

# TOUGH2 USER'S GUIDE, VERSION 2

*Karsten Pruess  
Curt Oldenburg  
George Moridis*

Earth Sciences Division, Lawrence Berkeley National Laboratory  
University of California, Berkeley, California 94720

November 1999  
revised September 2012

This work was supported by the Director, Office of Science, Office of Basic Energy Sciences,  
Materials Sciences and Engineering Division of the U.S. Department of Energy  
under Contract no. DE-AC02-05CH11231.



## **TOUGH2 USER'S GUIDE, VERSION 2**

Copyright © 2012

by

Karsten Pruess  
Curt Oldenburg  
George Moridis

The U.S. Department of Energy has the right to use this document  
for any purpose whatsoever including the right to reproduce  
all or any part thereof.

## DISCLAIMER

This document was prepared as an account of work sponsored by the United States Government. While this document is believed to contain correct information, neither the United States Government nor any agency thereof, nor The Regents of the University of California, nor any of their employees, makes any warranty, express or implied, or assumes any legal responsibility for the accuracy, completeness, or usefulness of any information, apparatus, product, or process disclosed, or represents that its use would not infringe privately owned rights. Reference herein to any specific commercial product, process, or service by its trade name, trademark, manufacturer, or otherwise, does not necessarily constitute or imply its endorsement, recommendation, or favoring by the United States Government or any agency thereof, or The Regents of the University of California. The views and opinions of authors expressed herein do not necessarily state or reflect those of the United States Government or any agency thereof or The Regents of the University of California.

Lawrence Berkeley National Laboratory is an equal opportunity employer

## ABSTRACT

TOUGH2 is a numerical simulator for nonisothermal flows of multicomponent, multiphase fluids in one, two, and three-dimensional porous and fractured media. The chief applications for which TOUGH2 is designed are in geothermal reservoir engineering, nuclear waste disposal, environmental assessment and remediation, and unsaturated and saturated zone hydrology. TOUGH2 was first released to the public in 1991; the 1991 code was updated in 1994 when a set of preconditioned conjugate gradient solvers was added to allow a more efficient solution of large problems.

Version 2.0 features several new fluid property modules and offers enhanced process modeling capabilities, such as coupled reservoir-wellbore flow, precipitation and dissolution effects, and multiphase diffusion. Numerous improvements in previously released modules have been made and new user features have been added, such as enhanced linear equation solvers, and writing of graphics files. The T2VOC module for three-phase flows of water, air and a volatile organic chemical (VOC), and the T2DM module for hydrodynamic dispersion in 2-D flow systems have been integrated into the overall structure of the code and are included in the Version 2.0 package. Data inputs are upwardly compatible with the previous version. Coding changes were generally kept to a minimum, and were only made as needed to achieve the additional functionalities desired. Version 2.1 has a restructured core and includes several bug fixes.

TOUGH2 is written in standard FORTRAN77 and can be run on any platform, such as workstations, PCs, Macintosh, mainframe and supercomputers, for which appropriate FORTRAN compilers are available. This report is a self-contained guide to application of TOUGH2 to subsurface flow problems. It gives a technical description of the TOUGH2 code, including a discussion of the physical processes modeled, and the mathematical and numerical methods used. Illustrative sample problems are presented along with detailed instructions for preparing input data.



## TABLE OF CONTENTS

LIST OF FIGURES.....	ix
LIST OF TABLES.....	xii
1. INTRODUCTION .....	1
2. HARDWARE REQUIREMENTS AND CODE INSTALLATION .....	4
3. METHODOLOGY AND ARCHITECTURE OF TOUGH2.....	6
3.1 Scope and Methodology .....	6
3.2 Program Structure and Execution .....	7
4. TOUGH2 ARRAY STRUCTURE.....	11
4.1 Primary Thermodynamic Variables .....	11
4.2 Thermophysical Property Arrays .....	13
4.3 Linear Equation Setup .....	16
4.4 Dimensioning of Major Arrays .....	17
5. PREPARATION OF INPUT DATA .....	19
5.1 TOUGH2 Input Data .....	19
5.2 Geometry Data .....	25
6. EQUATION-OF-STATE MODULES.....	29
6.1 EOS1 (water, water with tracer).....	30
6.2 EOS2 (water, CO <sub>2</sub> ) .....	33
6.3 EOS3 (water, air).....	35
6.4 EOS4 (water, air, with vapor pressure lowering capability) .....	37
6.5 EOS5 (water, hydrogen).....	39
6.6 EOS7 (water, brine, air) .....	40
6.7 EOS7R (water, brine, radionuclide 1, radionuclide 2, air).....	44
6.8 EOS8 (water, air, oil) .....	49
6.9 EOS9 (saturated-unsaturated flow) .....	51
6.10 EWASG (water, NaCl, non-condensable gas) .....	55
7. USER FEATURES .....	61
7.1 Initial Conditions and Restarting.....	61
7.2 Boundary Conditions and “Inactive” Elements .....	62
7.3 Sinks and Sources.....	64
7.4 Heat Exchange with Confining Beds .....	69

7.5 Block-by-block Permeability Modification .....	71
7.6 Linear Equation Solvers .....	72
8. OUTPUT FROM TOUGH2.....	75
9. SAMPLE PROBLEMS .....	78
9.1 Problem No. 1 (*sam1*) - Code Demonstration and Comparison with TOUGH (EOS3).....	79
9.2 Problem No. 2 (*rhp*) - Heat Pipe in Cylindrical Geometry (EOS3, EOS4).....	87
9.3 Problem No. 3 (*rvf*) - Heat Sweep in a Vertical Fracture (EOS1) .....	93
9.4 Problem No. 4 (*rfp*) - Five-spot Geothermal Production/Injection (EOS1, EOS2) .....	99
9.5 Problem No. 5 (*r1q*) - Coupled Wellbore Flow (EOS1) .....	104
9.6 Problem No. 6 (*rf1*) - Multiphase and Nonisothermal Processes in a System with Variable Salinity (EOS7) .....	107
9.7 Problem No. 7 (*rdif7*) - Thermal and Tracer Diffusion (EOS7R).....	111
9.8 Problem No. 8 (*rdica*) - Contamination of an Aquifer from VOC Vapors in the Vadose Zone (EOS7R).....	114
9.9 Problem No. 9 (*rcol8*) - Flushing Oil from a 1-D Column by Water Injection (EOS8).....	119
9.10 Problem No. 10 (*reos9a*) - Demonstration of Equilibrium (EOS9) .....	122
9.11 Problem No. 11 (*rpm*) - Demonstration of Permeability Modification Options (EOS9).....	125
9.12 Problem No. 12 (*rhbc*) - Production from a Geothermal Reservoir with Hypersaline Brine and CO <sub>2</sub> (EWASG) .....	130
10. CONCLUDING REMARKS .....	134
ACKNOWLEDGEMENT .....	137
REFERENCES .....	138
APPENDIX A. MASS AND ENERGY BALANCES .....	144
APPENDIX B. SPACE AND TIME DISCRETIZATION .....	148
APPENDIX C. DESCRIPTION OF FLOW IN FRACTURED MEDIA .....	152
APPENDIX D. MULTIPHASE DIFFUSION .....	155
APPENDIX E. TOUGH2 INPUT FORMATS .....	160
APPENDIX F. INPUT FORMATS FOR MESHMAKER .....	177
APPENDIX G. RELATIVE PERMEABILITY FUNCTIONS .....	184
APPENDIX H. CAPILLARY PRESSURE FUNCTIONS.....	188
SUBJECT INDEX.....	191

## LIST OF FIGURES

Figure 1. Example of coding for internal version control.....	3
Figure 2. Modular “MULKOM” architecture of TOUGH2.....	8
Figure 3. Structure of thermophysical property arrays in TOUGH2 .....	13
Figure 4. Linear equation structure .....	15
Figure 5. TOUGH2 input formats .....	22
Figure 6. User options for supplying geometry data.....	26
Figure 7. Henry’s law coefficients for dissolution of CO <sub>2</sub> in water.....	33
Figure 8. Model for converging-diverging pore channels.....	57
Figure 9. Porosity-permeability relationship for tubes-in-series model, after Verma and Pruess (1988). .....	58
Figure 10. Contour plot of flowing bottomhole pressures, in bars (from Table 17).....	68
Figure 11. TOUGH2 input file (first part) for sample problem 1 - code demonstration. ....	79
Figure 12. File MESH for sample problem 1.....	81
Figure 13. File INCON for sample problem 1.....	82
Figure 14. File GENER for sample problem 1.....	83
Figure 15. File SAVE for sample problem 1. ....	84
Figure 16. Part of printed output for sample problem 1.....	85
Figure 17. Calling sequence of program units in problem 1.....	86
Figure 18. Input file for problem 2 - heat pipe in cylindrical geometry. ....	88
Figure 19. Profiles of temperature, pressure, liquid saturation and air mass fraction.....	89
Figure 20. Selected output for problem 2 run with EOS4.....	90
Figure 21. Selected output for problem 2, run with EOS4 and including gas diffusion.....	91
Figure 22. Selected output for problem 2 run with EOS3.....	92
Figure 23. Schematic diagram of injection-production system in vertical fracture. Injection occurs at <i>I</i> , production at <i>P</i> . .....	93
Figure 24. Input file for problem 3 - heat sweep in a vertical fracture. ....	95
Figure 25. TOUGH2 printout of mesh pattern in problem 3. ....	96

Figure 26. Temperature distribution in fracture plane after 5 years. Injection and production regions are marked I and P, respectively. ....	97
Figure 27. Produced fluid temperature versus time for vertical fracture problem. ....	97
Figure 28. Five-spot well pattern with grid for modeling a 1/8 symmetry domain .....	99
Figure 29. TOUGH2/EOS1 input file for problem 4 - five-spot production/injection. (Only part of ELEME and CONNE data blocks is shown.).....	101
Figure 30. Output from MINC processing for problem 4.....	102
Figure 31. Selected output from problem 4 flow simulation. ....	103
Figure 32. Temperature profiles for problem 4 along a line from injection to production well after 36.5 yrs.....	103
Figure 33. Input for coupled reservoir-wellbore flow problem for TOUGH2/EOS1.....	105
Figure 34. Part of printed output for coupled reservoir-wellbore problem.....	106
Figure 35. Simulated flow rate ( $q$ ), flowing enthalpy ( $h$ ), flowing bottomhole pressure ( $P_{wb}$ ) and reservoir pressure in well grid block ( $P_{res}$ ) for a problem adapted from Hadgu et al. (1995). Results obtained for constant bottomhole pressure of $P_{wb} = 57.37$ bars, labeled $q_c$ , $h_c$ , and $P_{res,c}$ , are also shown. ....	106
Figure 36. TOUGH2 input file for EOS7 test problem.....	108
Figure 37. Iteration sequence and portion of the output after time step # 2.....	109
Figure 38. TOUGH2 output after 1 day of simulation time.....	110
Figure 39. Diffusion problem for EOS7R.....	112
Figure 40. Selected output for problem 7.....	113
Figure 41. Model system for examining migration of VOC from the vadose zone into an aquifer. ....	114
Figure 42. Part of TOUGH2 input data for mesh generation and for initializing an EOS7 run to obtain gravity-capillary equilibrium. ....	115
Figure 43. Abbreviated TOUGH2/EOS7R input data file for VOC migration problem. ....	116
Figure 44. Part of printout for VOC contamination problem after $t = 1$ year. ....	117
Figure 45. Time dependence of simulated aqueous VOC concentrations below the water table for fully coupled multiphase diffusion, and for separate treatment of gas and aqueous phase diffusive fluxes.....	118
Figure 46. Three-phase flow problem for EOS8: flushing oil from a 1-D column.....	120

Figure 47. Portion of printed output for 3-phase flow problem.....	121
Figure 48. EOS9 input file for demonstration of gravity-capillary equilibrium. ....	123
Figure 49. Portion of the printed output for the gravity-capillary equilibrium problem.....	124
Figure 50. EOS9 input file for demonstrating “logarithmic” permeability modifiers. ....	126
Figure 51. MESHMaker input, alternative SEED data, and EOS3-type initial conditions for permeability modification problem. ....	127
Figure 52. Part of printed output for running the input file of Fig. 50 with TOUGH2/EOS9, demonstrating “logarithmic” permeability modification.....	128
Figure 53. Part of printed output for running modified input file of Fig. 50 with TOUGH2/EOS3 for “logarithmic” permeability modification.....	128
Figure 54. Part of printed output for running modified input file of Fig. 50 with TOUGH2/EOS9 for “linear” permeability modification. ....	129
Figure 55. Part of printed output for running modified input file of Fig. 50 with TOUGH2/EOS9, using permeability modifiers provided in ELEME data block....	129
Figure 56. TOUGH2/EWASG input data for constant-rate production from a 1-D cylindrical reservoir.....	131
Figure 57. Simulated thermodynamic conditions for 1-D radial flow problem with salinity and non-condensable gas, plotted as a function of the similarity variable $x =$ $R^2/t$ . Results at $2 \times 10^6$ seconds are shown as lines, while the data at $t = 5 \times 10^5$ seconds are given as symbols.....	132
Figure 58. Iteration sequence for first five time steps of the hypersaline reservoir problem.....	133
Figure 59. Weighting procedures for absolute ( $k$ ) and relative permeability ( $k_r$ ) at grid block interfaces. ....	135
Figure 60. Space discretization and geometry data in the integral finite difference method....	148
Figure 61. Idealized double porosity model of a fractured porous medium. ....	152
Figure 62. Subgridding in the method of "multiple interacting continua" (MINC).....	153
Figure 63. Flow connections in the “dual permeability” model. Global flow occurs between both fracture ( $F$ ) and matrix ( $M$ ) grid blocks. In addition there is $F\text{-}M$ interporosity flow. ....	154
Figure 64. MESHMaker input formats. ....	178

## LIST OF TABLES

Table 1. TOUGH2 fluid property modules, as released in 1991 .....	2
Table 2. New fluid property modules for TOUGH2 .....	2
Table 3. TOUGH2 program structure .....	9
Table 4. Summary of major common blocks .....	18
Table 5. TOUGH2 input data blocks <sup>§</sup> .....	20
Table 6. TOUGH2 disk files .....	24
Table 7. Summary of EOS1 .....	30
Table 8. Summary of EOS2 .....	34
Table 9. Summary of EOS3 .....	36
Table 10. Summary of EOS4 .....	38
Table 11. Thermophysical properties of hydrogen .....	39
Table 12. Summary of EOS7 .....	42
Table 13. Summary of EOS7R .....	45
Table 14. Summary of EOS8 .....	49
Table 15. Summary of EOS9 .....	52
Table 16. Summary of EWASG .....	56
Table 17. Flowing bottomhole pressures (in Pa) at 1000 m feed zone depth for a well of 20 cm ( $\approx$ 8 inch) inside diameter producing at 7 bar wellhead pressure (calculated from HOLA; Aunzo et al., 1991). ....	68
Table 18. Parameters for fracture flow problem .....	94
Table 19. Parameters for five-spot problem .....	100
Table 20. TCE and PCE data for VOC contamination problem. ....	115
Table 21. Parameters for production from a saline reservoir with CO <sub>2</sub> . ....	130



## 1. Introduction

TOUGH2 is a general-purpose numerical simulation program for multi-dimensional fluid and heat flows of multiphase, multicomponent fluid mixtures in porous and fractured media. Chief application areas are in geothermal reservoir engineering, nuclear waste isolation studies, environmental assessment and remediation, and flow and transport in variably saturated media and aquifers.

The simulation capabilities available through TOUGH2 are quite diverse, and an attempt at a complete description would produce a rather unwieldy report. The present report is a self-contained document which provides a summary of mathematical models and numerical methods used, includes illustrative sample problems, and gives complete specifications for preparing input data. It is not intended to be read through from front to back. New users should skim through some of the more general material in sections 1-3 and 5, then install the TOUGH2 program on their computer, and try out some of the sample input files provided with the code. For some of the more complex modules, detailed specialized reports are available which will facilitate applications. This includes T2VOC (Falta et al., 1995), a module for three-phase, three-component, nonisothermal flow of water, air, and a volatile organic compound (VOC), T2DM (Oldenburg and Pruess, 1993, 1995), a module for strongly coupled flow and transport in 2-D systems with variable salinity and hydrodynamic dispersion, ECO2N for nonisothermal flows of water, NaCl, and a CO<sub>2</sub>-rich phase (Pruess, 2005), and ECO2M for mixtures of water, NaCl, CO<sub>2</sub>, including super- and subcritical conditions, and phase change between liquid and gaseous CO<sub>2</sub> (Pruess, 2011).

The TOUGH2 program consists of a number of functional units with flexible and transparent interfaces. Much of what the program units do is spelled out in internal comments and in printed output. The new program modules make increasing use of “self-documenting” features. TOUGH2 is distributed along with a number of input data files for sample problems. Besides providing benchmarks for proper code installation, these can serve as a self-teaching tutorial in the use of TOUGH2, and they provide templates to help jump-start new applications.

The original TOUGH2 code released in 1991 (Pruess, 1991a) provided five different fluid property or “EOS” (equation-of-state) modules. Labeled “EOS1” - “EOS5,” these included the main modules for geothermal and nuclear waste applications (see Table 1). The new Version 2.0 release of TOUGH2 includes improved versions of these five EOS-modules, as well as a number of new fluid property modules (see Table 2). In addition it provides a more flexible and comprehensive description of flow systems and processes, along with new user features, such as enhanced linear equation solvers, and direct outputting of graphics files.

A number of ancillary programs have been written to facilitate certain operations that occur in many TOUGH2 applications. Examples include the assignment of initial and boundary conditions, modification of MESH files, and extracting of graphics files from output data. A selection of “utility programs” and occasional updates of program modules are available for downloading from the TOUGH2 homepage on the web, at <http://esd.lbl.gov/TOUGH2/>.

Table 1. TOUGH2 fluid property modules, as released in 1991

Module	Capabilities
EOS1*	water, water with tracer
EOS2	water, CO <sub>2</sub>
EOS3*	water, air
EOS4	water, air, with vapor pressure lowering
EOS5*	water, hydrogen

\* optional constant-temperature capability

Table 2. New fluid property modules for TOUGH2

Module	Capabilities
EOS7*	water, brine, air
EOS7R*	water, brine, air, parent-daughter radionuclides
EOS8*	water, “dead” oil, non-condensable gas
EOS9	variably-saturated isothermal flow according to Richards’ equation
EWASG*	water, salt (NaCl), non-condensable gas (includes precipitation and dissolution, with porosity and permeability change; optional treatment of vapor pressure lowering effects)

\* optional constant-temperature capability

It is hoped that the “open” architecture of TOUGH2 will facilitate applications, and will encourage users to further develop and enhance the code. TOUGH2 includes a tight and visible “version control” system for meeting stringent demands on reliability and referenceability of code applications. Each program unit, when first called during a TOUGH2 simulation run, writes a brief (typically one line) message specifying its name, version number, date, and purpose. An example from the EOS subroutine of the EOS3 module is shown in Fig. 1. Version number and/or date are updated when significant modifications are made. This allows reference to user’s notes for code changes, and maintains a referenceable record of code changes and applications. All version messages are optionally printed to OUTPUT at the end of a simulation run; for an example see Fig. 17 (section 9.1)

```

SAVE ICALL
DATA ICALL/0/
ICALL=ICALL+1
IF(ICALL.EQ.1) WRITE(11,899)
C 899 FORMAT (/6X,'EOS'      1.0      28 MARCH    1991',6X,
C 899 FORMAT (/6X,'EOS'      1.01     26 JUNE     1992',6X,
C 899 FORMAT (/6X,'EOS'      1.01     24 March   1998',6X,
 899 FORMAT (/6X,'EOS'      1.01    11 January  1999',6X,
      X'*EOS3* ... THERMOPHYSICAL PROPERTIES MODULE FOR
WATER/AIR')

```

Figure 1. Example of coding for internal version control.

## **2. Hardware Requirements and Code Installation**

Version 2.0 of TOUGH2 was developed on an IBM RS/6000 workstation under a Unix-based operating system. The coding complies with the ANSI X3.9-1978 (FORTRAN77) standard. Like other members of the TOUGH/MULKOM family of codes, TOUGH2 requires 64-bit arithmetic. It is available as a FORTRAN77 program that is intrinsically single precision, and may be used on 64-bit processors, or on 32-bit processors whose compiler has an internal double-precision "switch". For example, on an IBM RS/6000 workstation with a 32-bit CPU compilation should be made with the option "-qautodbl=db1pad" to obtain 64-bit arithmetic; on Sun workstations the same effect is achieved by specifying the "-r8" compilation option. A version that is intrinsically double-precision is being prepared for execution on PCs and Macintoshes.

The standard TOUGH2 FORTRAN77 source code consists of the files `t2fm.f`, `t2cg22.f`, `meshm.f`, `eosx.f`, and `t2f.f`, where `eosx.f` is any one of a number of different fluid property (equation-of-state) modules. As an example of compilation, linking, and program execution we reproduce here the commands that would be used on a workstation, running a UNIX-based operating system. The example involves creating an executable "`xt2_eos1`", and then using input file "`rvf`" to run sample problem 3 (INCLUDE-file `*T2*` must be present in the source code directory)

### **IBM RS/6000**

```
f77 -o xt2_eos1 -qautodbl=db1pad \
      t2fm.f eos1.f t2cg22.f meshm.f t2f.f t2solv.f
```

### **DEC ALPHA**

```
f90 -o xt2_eos1 -r8 -i8 \
      t2fm.f eos1.f t2cg22.f meshm.f t2f.f t2solv.f
```

### **LINUX/gfortran**

```
gfortran -o xt2_eos1 -g -fdefault-real-8 -falign-commons \
          t2fm.f eos1.f t2cg22.f meshm.f t2f.f t2solv.f
```

### **LINUX/ifort**

```
ifort -o xt2_eos1 -g -r8 -i8 -align dcommons -check none \
       t2fm.f eos1.f t2cg22.f meshm.f t2f.f t2solv.f
```

Alternatively, provide compiler name and appropriate compiler options in file `makefile`, set `EOS = eos1` and type "make".

For compilation and linking on a PC, invoke the equivalent compiler options, specifically regarding 64-bit arithmetic. Run-time checks for array bound errors need to be disabled, and alignment of COMMON blocks should be invoked.

Execution of an input file `rvf` (third sample problem, see section 9.3) would be made with the command

```
xt2_eos1 < rvf > rvf.out
```

where output is printed to file `rvf.out`. On a PC, this command is executed in a DOS Command Prompt window.

Some of the EOS-modules include specialized versions of the same program units that appear in standard TOUGH2, creating a situation of "duplicate names" during the linking process. On most computers the linker will simply use the first program unit with a given name, and will ignore subsequent program units with the same name. On some computers the presence of duplicate names during linking will create a fatal error. The simplest way of avoiding this is to change the names of the unwanted program units. For example, EOS9 includes a modified version of subroutine MULTI. If a name conflict appears during linking, the user should, prior to compilation, simply change the name of MULTI in TOUGH2 file `t2f.f` to MULTIX, say.

Memory requirements of TOUGH2 depend on the problem size, and can be estimated from

$$M = 0.08 * (NEL + 2 * NCON) * NEQ * NEQ \quad (1)$$

where  $M$  is RAM in kilobytes,  $NEL$  is the number of grid blocks (elements),  $NCON$  is the number of connections between them, and  $NEQ$  is the number of equations (mass and heat balances) per grid block. Thus, a flow problem with up to 800 grid blocks, 2,400 connections, and 3 equations per grid block can be solved with 4 Megabytes of RAM, while simulation of a problem with 8,000 grid blocks, 24,000 connections, and 2 equations per grid block would require approximately 18 MB of RAM. Eq. (1) is approximate in that it does not account for size-independent storage requirements that need to be met even for small problems. The major problem-size dependent arrays can be easily re-dimensioned for different-size problems through PARAMETER statements in the main program (see section 4.4).

### **3. Methodology and Architecture of TOUGH2**

#### **3.1 Scope and Methodology**

TOUGH2 solves mass and energy balance equations that describe fluid and heat flow in general multiphase, multicomponent systems (Appendix A). Fluid advection is described with a multiphase extension of Darcy's law; in addition there is diffusive mass transport in all phases. Heat flow occurs by conduction and convection, the latter including sensible as well as latent heat effects. The description of thermodynamic conditions is based on the assumption of local equilibrium of all phases. Fluid and formation parameters can be arbitrary nonlinear functions of the primary thermodynamic variables.

For numerical simulation the continuous space and time variables must be discretized (see Appendix B). In all members of the TOUGH/MULKOM family of codes, space discretization is made directly from the integral form of the basic conservation equations, without converting them into partial differential equations. This "integral finite difference" method (IFDM; Edwards, 1972; Narasimhan and Witherspoon, 1976) avoids any reference to a global system of coordinates, and thus offers the advantage of being applicable to regular or irregular discretizations in one, two, and three dimensions. The IFDM also makes it possible, by means of simple preprocessing of geometric data, to implement double- and multiple-porosity methods for fractured media (see Appendix C; Pruess and Narasimhan, 1982, 1985; Pruess, 1983). No particular price needs to be paid for this flexibility; indeed, for systems of regular grid blocks referred to a global coordinate system the IFDM is completely equivalent to conventional finite differences. Time is discretized fully implicitly as a first-order backward finite difference. This together with 100% upstream weighting of flux terms at interfaces is necessary to avoid impractical time step limitations in flow problems involving phase (dis-)appearances, and to achieve unconditional stability (Peaceman, 1977).

The discretization results in a set of strongly coupled nonlinear algebraic equations (Appendix B), with the time-dependent primary thermodynamic variables of all grid blocks as unknowns. These equations are cast in residual form, i.e.,  $\{\text{residual}\} = \{\text{left-hand side}\} - \{\text{right-hand side}\} = 0$ , and are solved simultaneously, using Newton-Raphson iteration. Time steps can be automatically adjusted (increased or reduced) during a simulation run, depending on the convergence rate of the iteration process. Automatic time step adjustment is essential for an efficient solution of multiphase flow problems, where intrinsic time scales for significant changes in the flow system may vary by many orders of magnitude during a simulation run. Different methods are available to solve the linear equations arising at each iteration step, including

preconditioned conjugate gradient solvers, as well as sparse direct matrix methods (see section 7.6). While direct methods are more predictable and less problem-dependent in their performance, it is only through the application of iterative conjugate gradient methods that solutions for large grid systems (10,000 blocks or more) and three-dimensional problems can be accomplished (Moridis and Pruess, 1998).

The accuracy of TOUGH2 has been tested by comparison with many different analytical and numerical solutions, with results from laboratory experiments, and with field observations (see e.g., Moridis and Pruess, 1992; Pruess et al., 1996). However, it should be emphasized that the integration of many different modules into a single program structure is a difficult and potentially “hazardous” task. Many different options can be selected in different program modules. It is not practically possible to exhaustively cross-check the mutual compatibility and proper performance of all options. Users are cautioned that there is no finite process by which all program bugs that may be present can be identified and corrected. Fixing a bug may cause unanticipated problems elsewhere. Continuing vigilance and application testing are needed.

### 3.2 Program Structure and Execution

The governing equations for multiphase fluid and heat flow (see Appendix A) have the same mathematical form, regardless of the nature and number of fluid phases and components present. Based on this recognition, TOUGH2 was set up with a modular architecture (see Fig. 2), in which the main flow and transport module can interface with different fluid property modules. This gives TOUGH2 the flexibility to handle a wide variety of multicomponent, multiphase flow systems. The nature and properties of specific fluid mixtures enter into the governing equations only through thermophysical parameters, such as fluid density, viscosity, enthalpy, etc., which are provided by an appropriate “EOS” (equation-of-state) module. Such an architecture was first implemented in a research code known as MULKOM in the early 80s, and later formed the basis of TOUGH, a more specialized multiphase code for water-air-heat (Pruess, 1987). We now use the term “MULKOM” to denote the general architecture or “blueprint” of the code, while the specific FORTRAN77 implementation is called “TOUGH2.”

The coding of TOUGH2 is structured around two large arrays which hold, respectively, the primary thermodynamic variables for all grid blocks, and all other (secondary) thermophysical parameters needed to assemble the governing flow and transport equations (see section 4.2). These arrays are one-dimensional and hold data for all grid blocks of the computational mesh in sequential fashion. The solution of a flow problem essentially consists of a complete set of thermodynamic variables as a function of time. In TOUGH2, all arrays holding spatially

distributed information take the form of labeled COMMON blocks, one per array. This provides flexibility and convenience for adjusting array dimensions to different-size problems.

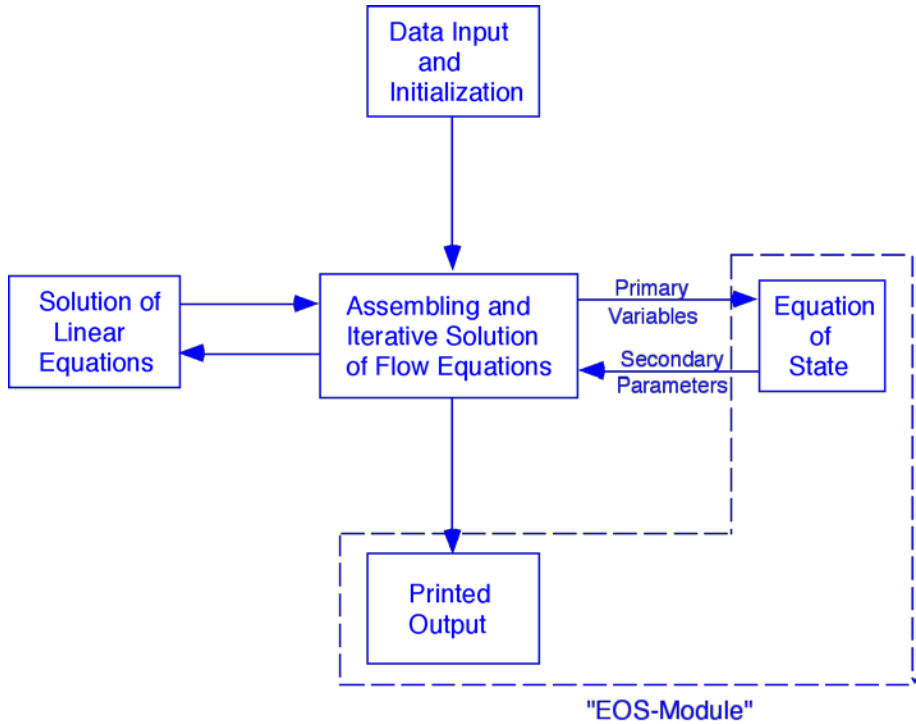


Figure 2. Modular “MULKOM” architecture of TOUGH2.

The subroutines contained in the TOUGH2 package can be grouped according to their functions as summarized in Table 3. The initialization of a simulation run is accomplished by the subroutines INPUT and RFILE in a flexible manner. Most of the necessary data are supplied from disk files, which can be either directly provided by the user, or can be generated internally from data provided in the INPUT file. The initialization stage also can generate a variety of computational grids, or meshes. The iteration sequence for time stepping is controlled by CYCIT. On the first time step, all thermophysical properties are initialized (subroutine EOS), and time step counter KCYC, iteration counter ITER, and convergence flag KON are defined. The iteration counter is incremented, and the accumulation and flow terms for all equations are assembled in subroutine MULTI. If sinks or sources are present MULTI calls subroutine QU, which in turn can call a series of satellite routines to perform functions such as calculating phase compositions of produced fluids, interpolating from tables, and obtaining flowing wellbore pressure corrections.

MULTI then computes all residuals, identifies the element index (NER) and equation index (KER) for the largest residual, and checks for convergence. If convergence is achieved (KON = 2), CONVER is called to update the primary variables. Otherwise control shifts to LINEQ, which functions as executive routine for the linear equation solution, and can call a variety of user-selectable linear equation solvers. Informative messages during the linear equation solution process are written onto a disk file called LINEQ. Printed output subject to different user controls can be generated with subroutines OUT and BALLA. Depending on the value of the convergence flag KON, the program will proceed to the next iteration (KON = 1), or to the next time step (KON = 2). If anything goes wrong - failure in computing thermophysical parameters, failure in solving the linear equations, failure to converge within a given maximum number of iterations - the time step will be repeated with a reduced time increment  $\Delta t$ .

Table 3. TOUGH2 program structure

subroutine(s)	function
TOUGH2 (main program)	executive routine; define problem-size dependent arrays, generate internal documentation
INPUT, RFILE (and satellite routines, including MESHMaker)	problem initialization
CYCIT	executive routine for time stepping
EOS (and satellites)	thermophysical properties and phase diagnostics
MULTI (and satellites)	assembly of mass and energy balance equations
QU (and satellites)	sink and source terms
LINEQ (and satellites)	solution of linear equations, provisional updating of thermodynamic variables
CONVER	conclusion of converged time steps, updating of thermodynamic variables and iteration counters
WRIFI, OUT, BALLA	output of results

Execution will continue until one of several termination criteria is reached, such as a user-specified total number of time steps, or a specified simulation time. In some cases a simulation may proceed with convergence achieved on the first iteration (ITER = 1). This can occur when time steps are chosen so small, or conditions are so close to steady state, that the convergence tolerances are satisfied without requiring any updating of thermodynamic variables. TOUGH2 has

coding to recognize such a condition. If convergence on ITER = 1 occurs for 10 consecutive time steps, this will be taken to indicate attainment of steady state, the current conditions will be written out, and execution will terminate.

Another termination criterion is monitored when automatic time step control is in effect. In this case execution will be stopped when convergence failure is encountered following two time steps for which convergence on ITER = 1 was achieved. The rationale for this is as follows. As conditions approach steady state, the rates of change in thermodynamic variables become small, and time steps will grow to very large values when automatic time step control is in effect. The off-diagonal elements in the Jacobian matrix are proportional to time step size, and may become so large that convergence of the linear equation system may no longer be achieved because of numerical roundoff. Thus we may have a situation where for a somewhat reduced time step convergence is achieved without requiring a linear equation solution (ITER = 1), while no convergence at all can be obtained when a linear equation solution is required. The aforementioned stopping criterion was designed to prevent such “no progress” calculations to go on and on for a potentially large number of user-specified time steps.

A general overview of TOUGH2 input data is presented in section 5; Appendices E and F provide a full reference to TOUGH2 input formats.

## 4. TOUGH2 Array Structure

### 4.1 Primary Thermodynamic Variables

TOUGH2 implements the assumption that locally all phases are in thermodynamic equilibrium. Let us now consider the number of primary thermodynamic variables that are needed to completely specify the thermodynamic state of a flow system consisting of  $NK$  components, which are distributed according to local thermodynamic equilibrium among  $NPH$  phases. From Gibbs' phase rule it follows that the number of thermodynamic degrees of freedom in such a system is

$$f = NK + 2 - NPH \quad (2)$$

In addition there are  $(NPH - 1)$  saturation degrees of freedom, because the  $NPH$  phase saturations (or phase volume fractions)  $S_\beta$  are constrained by the relationship

$$\sum_{\beta=1}^{NPH} S_\beta = 1 \quad (3)$$

The total number of primary thermodynamic variables (degrees of freedom) is therefore

$$\begin{aligned} NKI &= f + NPH - 1 \\ &= NK + 1 \end{aligned} \quad (4)$$

which is equal to the total number of balance equations per grid block, namely,  $NK$  mass balance and one energy balance equation. The thermodynamic state of a discretized flow system consisting of  $NEL$  volume elements, or grid blocks, is then completely specified by a set of  $NEL * NKI$  primary thermodynamic variables, to which correspond an equal number of mass and energy balance equations. For transient flow systems, these primary variables are time-dependent, and they represent the unknowns to be calculated in each time step.

An important consideration in the modeling of fluid and heat flow processes with phase change is the choice of the primary variables that define the thermodynamic state of the system. When a phase appears or disappears, the set of appropriate thermodynamic variables may change. In single-component flows involving water, for example, appropriate thermodynamic variables for describing single-phase conditions (subcooled liquid or superheated steam) are temperature  $T$  and pressure  $P$ . However, in two-phase conditions pressure and temperature are not independent, but

are related by the vapor-pressure relationship  $P = P_{sat}(T)$ . (When vapor pressure lowering effects are considered, the more complicated relationship Eq. A.7 applies.)

There are two alternative ways for dealing with this problem. One possibility is to use a set of “persistent” variables such as (pressure, enthalpy) or (density, internal energy), which remain independent even as phase conditions change, so that they can be used throughout the single- and two-phase regions. This approach has been successfully implemented in a number of multiphase codes (Pritchett, 1975; Faust and Mercer, 1975; Pruess et al., 1979; Pruess and Schroeder, 1980). A drawback of this approach is that parametric relationships for thermophysical properties are usually formulated in terms of the “natural” variables pressure and temperature, so that their computation as functions of “persistent” variables becomes either more difficult (requiring solution of implicit equations) or entails some sacrifice in accuracy. An alternative possibility is to use the variables (pressure, temperature) only for single-phase conditions, and to “switch” to variables (pressure, saturation) when a transition to two-phase conditions occurs. Experience has proven variable-switching to be a very robust method for treating multiphase systems, and this is the approach used in most TOUGH2 modules.

The choice of primary variables and the switching procedures for phase transitions are different in different equation-of-state modules (see section 6).

## 4.2 Thermophysical Property Arrays

In TOUGH2 all of the  $NEL*NK1$  primary variables are stored sequentially in a one-dimensional array  $X$ ; first the  $NK1$  variables for grid block # 1, then the  $NK1$  variables for grid block # 2, and so on (see Fig. 3). The starting location for primary variables for grid block  $N$  is  $NLOC+1$ , where  $NLOC = (N-1)*NK1$ .



Volume Element	Primary Variables		Volume Element	SECONDARY PARAMETERS	
				gas phase	aqueous phase
# 1	$x(1)$ • • • $x(NK1)$	→	# 1	phase saturation relative permeability viscosity density specific enthalpy capillary pressure diffusion factor 1 <sup>(§)</sup> diffusion factor 2 <sup>(&amp;)</sup>	$S$ $k_r$ $\mu$ $\rho$ $h$ $P_c$ $a$ $b$
# 2	$x(NK1+1)$ • • • $x(2*NK1)$			mass fractions component 1 • component NK	$X^1$ • $X^{NK}$
	• • • •				PAR(NB+1) • PAR(NB+NK) PAR(2*NBK)
# N	$x(NLOC+1)$ • • • $x(NLOC+NK1)$			temperature (miscellaneous)	$T$ PAR(NSEC-1) PAR(NSEC)
	• • • •			(second set of secondary parameters: $X(1)$ incremented)	PAR(NSEC+1) • PAR(2*NSEC)
# NEL	• • • $x(NEL*NK1)$		# 2		• • •
			# NEL		• • •

$$(\S) \quad a = \phi \tau_0 \tau_\beta \rho_\beta \quad (\&) \quad b = d_\beta^\kappa(T, P) / d_\beta^\kappa(T_0, P_0)$$

Figure 3. Structure of thermophysical property arrays in TOUGH2

The thermophysical properties (“secondary parameters”) needed to assemble the mass- and energy-balance equations for all volume elements are stored sequentially in a large array “PAR” (see Fig. 3). These parameters are calculated in the EOS module for the latest updated primary variables during the iteration process. The first group of  $NB$  ( $= 6$  or  $8$ ) secondary parameters includes 6 parameters needed for the accumulation and advective flow terms. If parameter  $NB$  is set equal to 8, these are followed by two parameters for the dependence of diffusion coefficients on primary variables (see Appendix D). Starting in location  $NB+1$ , there are  $NK$  component mass fractions, so that the total number of secondary parameters per fluid phase is  $NBK = NB + NK$ . By convention, the  $NBK$  gas phase parameters come first, followed by  $NBK$  parameters for the aqueous phase. Fig. 3 shows the PAR array structure for the case of two fluid phases, but the coding in TOUGH2 permits any number of phases, as specified by the parameter  $NPH$ . The  $NPH*NBK$  phase-specific parameters are followed by temperature  $T$  and an additional array member that is used for different purposes by different EOS modules. The total number of secondary parameters is  $NSEC = NPH*NBK + 2$ .

There are two additional arrays  $DX$  and  $DELX$  with structure identical to  $X$ . While  $X$  holds primary variables corresponding to the last successful (converged) time step,  $DX$  holds the increments calculated during the Newton-Raphson iteration process. Thus the latest updated primary variables are  $X + DX$ . Thermophysical properties are needed not only for calculating the residuals of the mass- and energy-balance equations (B.5), but also for calculating their derivatives in the Jacobian matrix  $\mathbf{J} = -\partial R_n / \partial x_i$  (see Eqs. B.6 and B.7;  $x_i$  denotes the collection of all primary independent thermodynamic variables). In order to avoid any restrictions in the manner that thermophysical parameters could be functionally dependent on primary variables, these derivatives are obtained by numerical differentiation. In order to calculate derivatives, the PAR-array must provide secondary parameters not only at the “state point” (latest  $X + DX$ ), but also for  $NEQ$  additional sets of primary variables in which one of the primary variables at a time is incremented by a small amount. Therefore, the total number of secondary parameters per grid block is  $(NEQ + 1)*NSEC$ . Secondary parameters for grid block # $N$  start after location #  $NLOC2 = (N - 1)*(NEQ + 1)*NSEC$  of the PAR array. The small increments used for numerical differentiation are typically of order  $10^{-8} * X$ , and are stored in an array  $DELX$ . The structure of the coupled linear equations solved at iteration step  $(p+1)$  is shown in Fig. 4. At the conclusion of a converged time step, the primary variables  $X$  are updated,  $X \not\propto X + DX$ .

volume element n	component balance $\kappa$	matrix row
# 1	1	1
	•	•
	•	•
NEQ		NEQ
---		
# 2	1	NEQ+1
	•	•
	•	•
NEQ		2*NEQ
---		
	•	•
	•	•
	•	•
	•	•
---		
# N	1	(N-1)*NEQ+1
	•	•
	•	•
	•	•
	•	•
---		
# NEL	•	•
	•	•
	•	•
NEQ		NEL*NEQ

$$\mathbf{J} \bullet \Delta \mathbf{x} = \mathbf{R}$$

$$-\frac{\partial R_n^\kappa}{\partial x_i} \Big|_p * x_{i,p+1} - x_{i,p} = R_n^\kappa \Big|_p$$

matrix column	1 ••• NEQ	NEQ+1 ••	•••
primary variable	1 ••• NEQ	1 •••	••• NEQ
volume element n	# 1	# 2 •••	# NEL

Figure 4. Linear equation structure

It was stated above that the number of mass- and energy-balance equations per grid block is the same as the number  $NKI$  of primary thermodynamic variables. In many applications, however, heat effects and temperature changes may be small, so that it would be sufficient to consider just the mass balance equations. The simplest way of forcing temperature changes to zero would be to assign the solid matrix an overwhelmingly large heat capacity, so that finite rates of heat exchange will cause negligible temperature change. This approach is perfectly acceptable and

useable with TOUGH2, but it has the disadvantage that the full number of balance equations must be solved, even though the energy balance reduces to the trivial statement  $\partial T/\partial t = 0$ . For certain EOS modules, TOUGH2 offers a more elegant way of running problems without temperature changes, at a considerable savings of computing time. By convention we always take the first  $NK$  equations per grid block to represent mass balances, while the energy balance equation comes last as #  $NK1$ . TOUGH2 uses a parameter  $NEQ$ , distinct from  $NK$ , to number the balance equations per grid block, and normally we would have  $NEQ = NK + 1$ . However, the user can choose to assign  $NEQ = NK$  in the input file; then no energy equations are set up or solved and the number of coupled equations is reduced by one per grid block, or a total of  $NEL$ . For the smaller set of  $NK$  equations we only solve for  $NK$  primary variables; thus the option  $NEQ = NK$  can only be used with those EOS modules that have temperature as primary variable #  $NK1$  (see Tables 1 and 2).

### 4.3 Linear Equation Setup

The data provided by the PAR-array are used in the flow module of TOUGH2 to assemble the linear equations (B.7) that are solved at each step of the Newton-Raphson iteration procedure. These equations are arranged and numbered sequentially, as shown in Fig. 4, with the first  $NK$  equations per grid block representing component mass balances, while the last equation (#  $NK1$ ) represents the energy balance. The row indices of the Jacobian matrix correspond to the component balance equations, while the column indices correspond to the sequence of primary variables in array  $X$ . If the option  $NEQ = NK$  is chosen, only  $NK$  mass balance equations will be set up per grid block. In this case only the first  $NK$  primary variables per grid block will contribute matrix columns, while variable #  $NK1$ , which must be temperature, remains passive and is not engaged or altered in the linear equation handling. However, all thermophysical parameters will be calculated at the temperature values specified in variable #  $NK1$ .

Note that the accumulation terms of the balance equations depend only on primary variables for one grid block, so that they will generate non-zero derivative terms only in an  $NEQ*NEQ$  submatrix that is located on the diagonal of the Jacobian  $J$ . The flow terms, being dependent on primary variables of two grid blocks, will generate two non-zero  $NEQ*NEQ$  submatrices of derivatives, which are located in the off-diagonal matrix locations corresponding to the two grid blocks.

In TOUGH2 all Jacobian matrix elements as well as the entries in the vector  $R$  of residuals are calculated in subroutine MULTI. The calculation first assigns all matrix elements arising from the accumulation terms, of which there are  $NEQ*NEQ$ . These are stored sequentially in a one-dimensional array CO; matrix elements for grid block  $N$  begin after location  $(N - 1)*NEQ*NEQ$  in

CO. The corresponding row and column indices are stored separately in arrays *IRN* and *ICN*, respectively. Calculation of the derivatives demands that each accumulation term is calculated  $NEQ + 1$  times; once for the state point ( $X + DX$ ), and  $NEQ$  times for each of the  $NEQ$  primary variables incremented ( $X + DX + DELX$ ). Additional contributions to diagonal terms in the Jacobian  $\mathbf{J}$  may arise from sink and source terms if present; these are assigned in subroutine *QU* called from *MULTI*. Subsequently all flux terms are evaluated. These depend in general on the  $2*NEQ$  primary variables of the two connected grid blocks, so that a total of  $2*NEQ + 1$  flux terms need to be evaluated for calculation of the state point as well as of all derivative terms. The total number of potentially non-zero elements in the Jacobian matrix is

$$NZ = NEL * NEQ^{**2} + 2 * NCON * NEQ^{**2} \quad (5)$$

After all matrix elements and members of the right-hand side vector of residuals have been assembled, the linear equations (B.7) are solved by one of several user-selectable algorithms, including sparse direct methods and a variety of preconditioned conjugate gradient algorithms (see section 7.6). The resulting increments in the primary variables are added to the array *DX*, and the process of linear equation setup and solution is repeated for the primary variables  $X + DX$ . This process continues until the residuals are reduced below a preset convergence tolerance (Eq. B.8). If convergence is not achieved within a specified maximum number of iterations (usually 8) the time step is repeated with reduced time increment.

#### 4.4 Dimensioning of Major Arrays

The major problem-size dependent arrays reside in labeled COMMON blocks, one array per block, which are dimensioned by means of a PARAMETER statement in the main (TOUGH2) program. An informational statement on permissible problem size (number of grid blocks, etc.) is provided in the printed output of a TOUGH2 run. When problem specifications exceed array dimensions the execution stops with a diagnostic printout. The user must then increase PARAMETER assignments accordingly. All arrays are given a dimension of 1 in the subroutines, and for re-dimensioning it is only necessary to revise the PARAMETER assignments in the main program; no other changes are needed. Some compilers will generate warnings or error messages when COMMON blocks are dimensioned differently in different program units. This can be avoided by compiling the main program separately from the subprograms. Subsequent linking of the object modules will properly communicate COMMON block addresses between main program and subprograms. A list of major arrays used in TOUGH2 and their dimensions is given in Table 4 below.

Table 4. Summary of major common blocks

Reference to	COMMON blocks	Length
Elements	E1 - E7, VINWES, AHTRAN XYZ1, XYZ2, XYZ3, VBC	NEL (= number of elements)
Primary variables	P1 - P7	NEL*NK1
Connections (interfaces)	C1 - C12  COMPO, PORVEL, FLOVP1, FLOVP2  DISP  DARVELM	NCON (= number of connections)  NCON*NPH  NCON*NPH*NK  NCON*NPH*(2*NEQ+1)
Sinks and sources	G1, G2, G3, G3A  G4 through G25, and G27 through G31  G26	MGTAB (= total number of tabular generation data)  NOGN (= number of sinks and sources)  NOGN*NPH
Secondary parameters	SECPAR	NEL*(NEQ+1)*NSEC
Linear equations <sup>†</sup>	L1, L2, L3  L4 L5, L8 L6 L7 CGARA6	NZ  NEL*NEQ 5*NEL*NEQ 8*NEL*NEQ 5*NEL*NEQ+NZ+32 38*NEL*NEQ+1000

<sup>†</sup> array dimensioning is made according to the needs of the conjugate gradient solvers; when the direct solver LUBAND is used, only a smaller-size problem can be accommodated

## 5. Preparation of Input Data

The data needed to characterize a flow system include hydrogeologic parameters and constitutive relations of the permeable medium (absolute and relative permeability, porosity, capillary pressure, etc.), thermophysical properties of the fluids (mostly provided internally), initial and boundary conditions of the flow system, and sinks and sources. In addition, TOUGH2 requires specification of space-discretized geometry, and various program options, computational parameters, and time-stepping information. Here we summarize the basic conventions adopted for TOUGH2 input data. A detailed explanation of TOUGH2 input data is given in Appendix E; input formats for internal grid generation through the MESHMaker module are explained in Appendix F. Some of the EOS modules have specialized input requirements (discussed in section 6).

The T2VOC and T2DM modules have special options and input requirements, which are explained in separate reports (T2VOC: Falta et al., 1995; T2DM: Oldenburg and Pruess, 1993, 1995).

### 5.1 TOUGH2 Input Data

Input can be provided to TOUGH2 in a flexible manner by means of one or several ASCII data files, with up to 80 characters per record. All TOUGH2 input is in fixed format and standard metric (SI) units, such as meters, seconds, kilograms, °C, and the corresponding derived units, such as Newtons, Joules, and Pascal = N/m<sup>2</sup> for pressure.

In the standard TOUGH2 input file data are organized in blocks which are defined by five-character keywords typed in columns 1-5; see Table 5 and Fig. 5. The first record must be a problem title of up to 80 characters. The last record usually is ENDCY; alternatively, ENDI may be used if no flow simulation is to be carried out (useful for mesh generation). Data records beyond ENDCY (or ENDI) will be ignored. Some data blocks, such as those specifying reservoir domains (ROCKS), volume elements (ELEME), connections (CONNE), and sinks/sources (GENER), have a variable number of records, while others have a fixed number of records. The end of variable-length data blocks is indicated by a blank record. The data blocks between the first and last one can be provided in arbitrary order, except that block ELEME, if present, must precede block CONNE. The blocks ELEME and CONNE must either be both provided through the INPUT file, or must both be absent, in which case alternative means for specifying geometry data will be employed (see section 5.2, below). The block GENER can be omitted if there are no sinks and sources in the problem. If block START is present, consisting of one data record with START typed in columns 1-5, the block INCON can be incomplete, with elements in arbitrary order, or can be absent altogether. Elements for which no initial conditions are specified in INCON will

then be assigned domain-specific initial conditions from block INDOM, if present, or will be assigned default initial conditions given in block PARAM, along with default porosities given in block ROCKS. If START is not present, INCON must contain information for all elements, in exactly the same order as they are listed in block ELEME.

Table 5. TOUGH2 input data blocks<sup>§</sup>

Keyword	Function
TITLE (first record)	one data record (single line) with a title for the simulation problem
MESHM	optional; parameters for internal grid generation through MESHMaker
ROCKS	hydrogeologic parameters for various reservoir domains
MULTI	optional; specifies number of fluid components and balance equations per grid block; applicable only for certain fluid property (EOS) modules
SELEC	used with certain EOS-modules to supply thermophysical property data
START	optional; one data record for more flexible initialization
PARAM	computational parameters; time stepping and convergence parameters; program options
DIFFU	diffusivities of mass components
FOFT	optional; specifies grid blocks for which time series data are desired
COFT	optional; specifies connections for which time series data are desired
GOFT	optional; specifies sinks/sources for which time series data are desired
RPCAP	optional; parameters for relative permeability and capillary pressure functions
TIMES	optional; specification of times for generating printout
*ELEME	list of grid blocks (volume elements)
*CONNE	list of flow connections between grid blocks
*GENER	optional; list of mass or heat sinks and sources
INDOM	optional; list of initial conditions for specific reservoir domains
*INCON	optional; list of initial conditions for specific grid blocks
NOVER (optional)	optional; if present, suppresses printout of version numbers and dates of the program units executed in a TOUGH2 run
ENDCY (last record)	one record to close the TOUGH2 input file and initiate the simulation
ENDFI	alternative to “ENDCY” for closing a TOUGH2 input file; will cause flow simulation to be skipped; useful if only mesh generation is desired

<sup>§</sup> Blocks labeled with a star \* can be provided as separate disk files, in which case they would be omitted from the INPUT file.

Between data blocks an arbitrary number of records with arbitrary data may be present that do not begin with any of the TOUGH2 keywords. This is useful for inserting comments about problem specifications directly into the input file. TOUGH2 will gather all these comments and will print the first 50 such records in the output file.

Much of the data handling in TOUGH2 is accomplished by means of disk files, which are written in a format of 80 characters per record, so that they can be edited and modified with any text editor. Table 6 summarizes the disk files other than (default) INPUT and OUTPUT used in TOUGH2; examples are given for sample problem 1 in section 9.1. The initialization of the arrays for geometry, generation, and initial condition data is always made from the disk files MESH (or MINC), GENER, and INCON. A user can either provide these files at execution time, or they can be written from TOUGH2 input data during the initialization phase of the program. If no data blocks GENER and INCON are provided in the input file, and if no disk files GENER and INCON are present, defaults will take effect (no generation; domain-specific initial conditions from block INDOM, or defaults from block PARAM). If a user intends to use these defaults, (s)he has to make sure that at execution time no disk files INCON or GENER are present from a previous run (or perhaps from a different problem). A safe way to use default GENER and INCON is to specify “dummy” data blocks in the input file, consisting of one record with GENER or INCON, followed by a blank record.

The format of data blocks ELEME, CONNE, GENER, and INCON is basically the same when these data are provided as disk files as when they are given as part of the input file. However, specification of these data through the input file rather than as disk files offers some added conveniences, which are useful when a new simulation problem is initiated. For example, a sequence of identical items (volume elements, connections, sinks or sources) can be specified through a single data record. Also, indices used internally for cross-referencing elements, connections, and sources will be generated internally by TOUGH2 rather than having them provided by the user. MESH, GENER, and INCON disk files written by TOUGH2 can be merged into an input file without changes, keeping the cross-referencing information.

TOUGH2 INPUT FORMATS							
<b>TITLE</b>							
<b>ROCKS</b>	1	*	2	*	3	*	4
MAT	NAD	DROK	POR	PER (1)	PER (2)	PER (3)	CWET
COM		EXPAN	CDRY	TORTX	GK	XKD3	SPHT
IRP		RP (1)	RP (2)	RP (3)	RP (4)	RP (5)	RP (6)
ICP		CP (1)	CP (2)	CP (3)	CP (4)	CP (5)	CP (6)
<b>MULTI</b>	(optional) 1	*	2	*	3	*	4
NK	NEQ	NPH	NB	NKIN			
<b>START</b>	(optional) 1	*	2	*	3	*	4
				MOP: 1 2 3 4 5 6 7 8 9 0 1 2 3 4			
<b>PARAM</b>	1	*	2	*	3	*	4
KDATA	NOTE	MCYC	MSEC	MCYPR	MOP (l), l=1,24		TEXP
	TSTART	TIMAX	DELTEN or NDLT	DELMX	ELST		BE
	DLT (1)	DLT (2)	DLT (3)				
						DLT (M)	(M≤8*NDLT)
	RE1	RE2	U	WUP	WNR	DFAC	
	DEP (1)		DEP (2)		DEP (3)		DEP (4)
MATSLV	<b>SOLVR</b>	(optional) 1	*	2	*	3	*
ZPROCS	ZPROCS	RITMAX	CLOSUR				
OPROCS							
<b>RPCAP</b>	(optional) 1	*	2	*	3	*	4
	IRP		RP (1)	RP (2)	RP (3)	RP (4)	RP (5)
	ICP		CP (1)	CP (2)	CP (3)	CP (4)	CP (5)
						CP (6)	CP (7)
<b>ELEM</b>	1	*	2	*	3	*	4
	EL	NE	NSEQ	NADD	MA1 MA2	VOLX	AHTX
						PMX	X
							Y
							Z
<b>CONN</b>	1	*	2	*	3	*	4
	EL1	NE1	EL2	NE2	NSEQ	NAD1	NAD2
						ISOT	
						D1	D2
						AREAX	BETAX
							SIGX
<b>GENER</b>	1	*	2	*	3	*	4
	EL	NE	SL	NS	NSEQ	NADD	NADS
						LTAB	
						TYPE	GX
							EX
							HX
	F1(1)		F1(2)				F1 (LTAB)
	F2(1)		F2(2)				F2 (LTAB)
	F3(1)		F3(2)				F3 (LTAB)
<b>INCON</b>	1	*	2	*	3	*	4
	EL	NE	NSEQ	NADD		PORX	
						X1	X2
						X3	X4

Figure 5. TOUGH2 input formats

TOUGH2 INPUT FORMATS (continued)															
<b>INDOM</b> (optional)	1	*	2	*	3	*	4	*	5	*	6	*	7	*	8
MAT															
	X1		X2		X3		X4								
<b>DIFFU</b> (optional)	1	*	2	*	3	*	4	*	5	*	6	*	7	*	8
FDDIAG(I,1), I=1, NPH															
FDDIAG(I,2), I=1, NPH															
<b>SELEC</b> (optional)	1	*	2	*	3	*	4	*	5	*	6	*	7	*	8
IE(1)    IE(2)    IE(3)    IE(4)    IE(5)    IE(6)    IE(7)    IE(8)    IE(9)    IE(10)    IE(11)    IE(12)    IE(13)    IE(14)    IE(15)    IE(16)															
FE(1)    FE(2)    FE(3)    FE(4)    FE(5)    FE(6)    FE(7)    FE(8)															
FE(9)    FE(10)    FE(11)    FE(12)    FE(13)    FE(14)    FE(15)    FE(16)															
FE(17)															
															FE(8*IE(1))
<b>TIMES</b> (optional)	1	*	2	*	3	*	4	*	5	*	6	*	7	*	8
ITI    ITE    DELAF    TINTER															
TIS (1)    TIS (2)    TIS (3)    TIS (ITI)															
<b>MESHM</b> (optional)	1	*	2	*	3	*	4	*	5	*	6	*	7	*	8
<b>FOFT</b> (optional)	1	*	2	*	3	*	4	*	5	*	6	*	7	*	8
EOFT															
<b>COFT</b> (optional)	1	*	2	*	3	*	4	*	5	*	6	*	7	*	8
ECOFT															
<b>GOFT</b> (optional)	1	*	2	*	3	*	4	*	5	*	6	*	7	*	8
EGOFT															
<b>NOVER</b> (optional)	1	*	2	*	3	*	4	*	5	*	6	*	7	*	8
<b>ENDFI</b> (optional)	1	*	2	*	3	*	4	*	5	*	6	*	7	*	8
<b>ENDCY</b>	1	*	2	*	3	*	4	*	5	*	6	*	7	*	8

Figure 5. TOUGH2 input formats (continued)

Table 6. TOUGH2 disk files

File	Use
MESH (unit 4)	written in subroutine INPUT from ELEME and CONNE data, or in module MESHMAKER from mesh specification data; read in RFILE to initialize all geometry data arrays used to define the discretized flow problem
GENER (unit 3)	written in subroutine INPUT from GENER data; read in RFILE to define nature, strength, and time-dependence of sinks and sources
INCON (unit 1)	written in subroutine INPUT from INCON data; read in RFILE to provide a complete specification of thermodynamic conditions
SAVE (unit 7)	written in subroutine WRIFI to record thermodynamic conditions at the end of a TOUGH2 simulation run; compatible with formats of file or data block INCON for initializing a continuation run
MINC (unit 10)	written in module MESHMAKER with MESH-compatible specifications, to provide all geometry data for a fractured-porous medium mesh (double porosity, dual permeability, etc.); read (optionally) in subroutine RFILE to initialize geometry data for a fractured-porous system
LINEQ (unit 15)	written during linear equation solution, to provide informative messages on linear equation solution
TABLE (unit 8)	written in CYCIT to record coefficients of semi-analytical heat exchange at the end of a TOUGH2 simulation run read (optionally) in subroutine QLOSS to initialize heat exchange coefficients in a continuation run
FOFT (unit 12)	written in FGTAB to provide time series data for elements for plotting
COFT (unit 14)	written in FGTAB to provide time series data for connections for plotting
GOFT (unit 13)	written in FGTAB to provide time series data for sinks/sources for plotting
VERS (unit 11)	written in all TOUGH2 program units with informational message on version number, date, and function; read in main program and printed to default OUTPUT at the conclusion of a TOUGH2 simulation run; printing of version information is suppressed when keyword NOVER is present in INPUT file

## 5.2 Geometry Data

### *General Concepts*

Handling of flow geometry data in TOUGH2 is upward compatible with TOUGH input formats and data handling. As in other "integral finite difference" codes (Edwards, 1972; Narasimhan and Witherspoon, 1976), flow geometry is defined by means of a list of volume elements ("grid blocks"), and a list of flow connections between them (Appendix B). This formulation can handle regular and irregular flow geometries in one, two, and three dimensions. Single- and multiple-porosity systems (porous and fractured media) can be specified, and higher-order methods, such as seven- and nine-point differencing, can be implemented by means of appropriate specification of geometric data (Pruess and Bodvarsson, 1983).

In TOUGH2, volume elements are identified by names that consist of a string of five characters, '12345'. These are arbitrary, except that the last two characters (#4 and 5) must be numbers; an example of a valid element name is "ELE10". Flow connections are specified as ordered pairs of elements, such as "(ELE10, ELE11)". A variety of options and facilities are available for entering and processing geometric data (see Fig. 6). As in TOUGH, element volumes and domain identification can be provided by means of a data block ELEME in the INPUT file, while a data block CONNE can be used to supply connection data, including interface area, nodal distances from the interface, and orientation of the nodal line relative to the vertical. These data are internally written to a disk file MESH, which in turn initializes the geometry data arrays used during the flow simulation. It is also possible to omit the ELEME and CONNE data blocks from the INPUT file, and provide geometry data directly on a disk file MESH.

### *Meshmaker*

TOUGH2 offers an additional way for defining flow system geometry by means of a special program module MESHMaker. This can perform a number of mesh generation and processing operations and is invoked with the keyword MESHMaker in the INPUT file. The MESHMaker module itself has a modular structure; present sub-modules include RZ2D for generating two-dimensional radially symmetric (R-Z) meshes, and XYZ for one-, two-, and three-dimensional rectilinear (Cartesian) grids. Multiple-porosity processing for simulation of flow in naturally fractured reservoirs can be invoked by means of a keyword MINC, which stands for "multiple interacting continua" (see Appendix C). The MINC-process operates on the data of the primary (porous medium) mesh as provided on disk file MESH, and generates a "secondary" mesh containing fracture and matrix elements with identical data formats on file MINC. (The file MESH used in this process can be either directly supplied by the user, or it can have been internally generated either from data in INPUT blocks ELEME and CONNE, or from RZ2D or XYZ mesh-

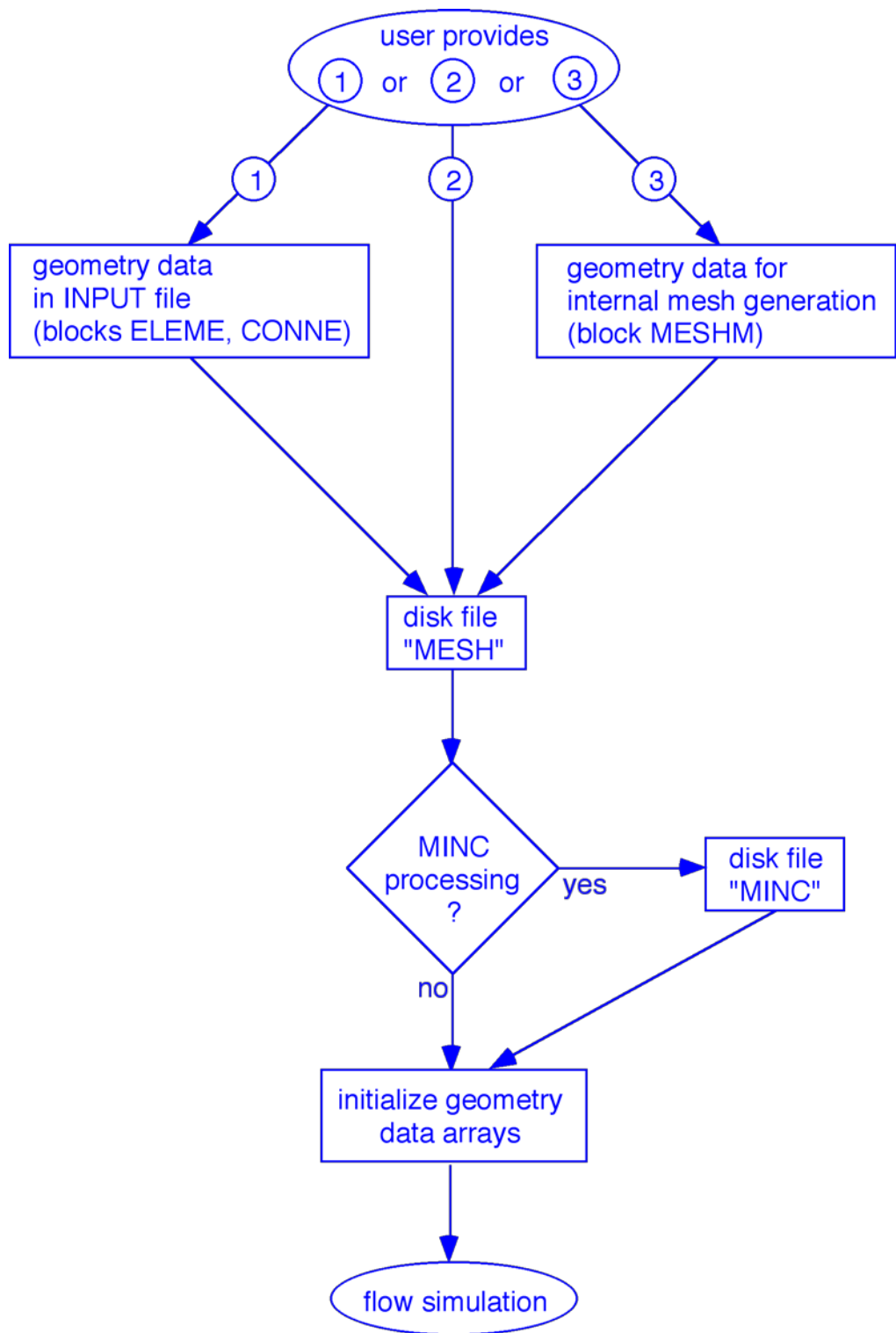


Figure 6. User options for supplying geometry data.

making.) The MINC process of sub-partitioning porous medium grid blocks into fracture and matrix continua will only operate on active grid blocks, while inactive grid blocks are left unchanged as single porous medium blocks. By convention, elements encountered in data block ELEME (or file MESH) are taken to be “active” until the first element entry with a zero or negative volume is encountered. The first element with volume less than or equal to zero, and all subsequent elements, are taken to be “inactive.” In order to exclude selected reservoir domains from the MINC process, the user needs to preprocess or edit the ELEME data block before MINC partitioning is made, and assemble all grid blocks that are to remain single porous media at the end, then place a “dummy” block of zero volume in front of them. The concept of inactive blocks is also used in a second, unrelated manner to maintain time-independent Dirichlet boundary conditions (see section 7.2).

As a convenience for users desiring graphical display of data, the internal mesh generation process will also write nodal point coordinates on file MESH. These data are written in 3E10.4 format into columns 51-80 of each grid block entry in data block ELEME. Generally speaking, no internal use whatsoever is made of nodal point coordinates in TOUGH2; the single exception is for optional initialization of a gravity-capillary equilibrium with EOS9 (see sections 6.9 and 9.10).

Specific naming conventions have been adopted in the internal mesh generation process. For RZ2D, the last two characters directly number the radial grid blocks, from 1 through 99. Character #3 is blank for the first 99 radial blocks, and then runs through the sequence 1, 2, ..., 9, A, B, ..., Z for a maximum total of 3599 radial blocks. The second character counts up to 35 grid layers as 1, 2, ..., 9, A, B, ..., Z. The first character is 'A' for the first 35 layers, and is incremented to B, C, ..., Z, 1, 2, ..., 9 for subsequent groups of 35 layers.

For rectilinear meshes generated by XYZ, characters 4 and 5 together number the grid blocks in the X-direction, while character #3 = 1, 2, ..., 9, A, B, ..., Z numbers Y direction grid blocks, and character #2, running through the same sequence as #3, numbers grid blocks in the Z-direction. Overflows in any of these (more than 99 X-blocks, more than 35 Y- or Z-blocks) advance character #1 through the sequence A, B, C, ..., Z. Both RZ2D and XYZ assign all grid blocks to domain #1 (first entry in block ROCKS); a user desiring changes in domain assignments must do so by hand, either through editing of the MESH file with a text editor, or by means of preprocessing with an appropriate utility program, or by appropriate source code changes in subroutines WRZ2D and GXYZ. TOUGH2 runs that involve RZ2D or XYZ mesh generation will produce a special printout, showing element names arranged in their actual geometric pattern. An example is given in section 9.3.

The naming conventions for the MINC process are somewhat different from those originally adopted in the GMINC program (Pruess, 1983), and are as follows. For a primary grid block with name '12345,' the corresponding fracture subelement in the secondary mesh is named ' 2345' (character #1 replaced with a blank for easy recognition). The successive matrix continua are labeled by running character #1 through 2, ..., 9, A, B, ..., Z. The domain assignment is incremented by 1 for the fracture grid blocks, and by 2 for the matrix grid blocks. Thus, domain assignments in data block ROCKS should be provided in the following order: the first entry is the single (effective) porous medium, then follows the effective fracture continuum, and then the rock matrix. An example is given in sample problem 4 (\*rfp\*), see p. 99.

Users should be aware that the MINC process may lead to ambiguous element names when the inactive element device is used to keep a portion of the primary mesh as unprocessed porous medium.

Mesh generation and/or MINC processing can be performed as part of a simulation run. Alternatively, by closing the input file with the keyword ENDFI (instead of ENDCY), it is possible to skip the flow simulation and only execute the MESHMaker module to generate a MESH or MINC file. These files can then be used, with additional user-modifications by hand if desired, in subsequent flow simulations. MESHMaker input formats are described in Appendix F, and examples of practical applications are given in the sample problems. Execution of MESHMaker produces printed output which is self-explanatory.

## 6. Equation-of-State Modules

The thermophysical properties of fluid mixtures needed for assembling the governing mass- and energy-balance equations are provided by “equation-of-state” (EOS) modules. The flow module of TOUGH2 is coded in general fashion to set up and solve mass balances for an arbitrary number of NK components that are distributed among NPH phases. As explained in more detail in the description of individual EOS modules, below, fluid phase conditions are recognized from the numerical values of the primary variables. Besides providing values for all secondary (thermophysical) parameters as functions of the primary thermodynamic variables, i.e., assigning all data in the PAR-array, the EOS module fulfills three additional important functions:

- (i) the phase conditions pertaining to a given set of primary variables are identified for all volume elements (grid blocks);
- (ii) the appearance or disappearance of phases is recognized as primary variables change during the Newton-Raphson iteration process;
- (iii) primary variables are switched and properly re-initialized in response to a change of phase.

The primary variables/secondary parameters concept as implemented in TOUGH2 essentially eliminates any direct connection between the choice of primary variables and the secondary parameters that are used to set up the flow equations. This provides maximum flexibility and convenience in the choice of primary variables, because only secondary parameters are used in the flow equations. There is one exception to this separation, namely, in all fluid property modules except EOS9 the pressure of a reference phase (usually gas) is by convention always the first primary variable, and it is used directly in the flow equations.

The various EOS modules included in the TOUGH2 package can represent different fluid mixtures. Below we describe these modules in some detail; a summary of EOS specifications and usage also appears in the printed output produced from a TOUGH2 run. For some EOS modules, additional information is available in separate reports to which we provide references. Note that only one EOS module at a time should be linked with the other TOUGH2 modules to form an executable code.

## 6.1 EOS1 (water, water with tracer)

This is the most basic EOS module, providing a description of pure water in its liquid, vapor, and two-phase states. All water properties (density, specific enthalpy, viscosity, saturated vapor pressure) are calculated from the steam table equations as given by the International Formulation Committee (1967). The formulation includes subregion 1 (subcooled water below  $T = 350$  °C), subregion 2 (superheated steam), and subregion 6 (saturation line up to  $T = 350$  °C). In these regions, density and internal energy are represented within experimental accuracy. Viscosity of liquid water and steam are represented to within 2.5 % by correlations given in the same reference. For details of the formulation, its accuracy and range of validity, refer to the original publication. In Version 2.0 of TOUGH2, the previously used subroutines for the steam table equations have been replaced with faster routines that were kindly provided by Michael O'Sullivan (University of Auckland, New Zealand). Vapor pressure lowering from capillary and adsorption effects are neglected; thus, in two-phase conditions vapor pressure is equal to saturated vapor pressure of bulk liquid.

A summary of EOS1 specifications and parameters is given in Table 7. The default parameter settings are ( $NK, NEQ, NPH, NB$ ) = (1, 2, 2, 6) for solving mass and energy balances

Table 7. Summary of EOS1

<u>Components</u>	# 1: water # 2: “water 2” (optional)
<u>Parameter choices</u>	( $NK, NEQ, NPH, NB$ ) = (1, 2, 2, 6) one water component, nonisothermal (default) (1, 1, 2, 6) only liquid, or only vapor; isothermal (2, 3, 2, 6) two-waters, nonisothermal*
	molecular diffusion can be modeled by setting $NK = 2, NB = 8$
<u>Primary Variables</u>	single-phase conditions $(P, T, [X])$ - (pressure, temperature, [mass fraction of water 2] <sup>†</sup> ) two-phase conditions $(P_g, S_g, [X])$ - (gas phase pressure, gas saturation, [mass fraction of water 2] <sup>†</sup> )

\* two waters cannot be run in isothermal mode, because in this case temperature is not the last primary variable

† optional, for  $NK = 2$  only

for a single water component. The option  $NEQ = 1$  is available for running single-phase flow problems that involve only liquid water, or only superheated steam, under constant temperature conditions. EOS1 also has a capability for representing two waters of identical physical properties, which contain different trace constituents. This option can be invoked by specifying ( $NK$ ,  $NEQ$ ,  $NPH$ ,  $NB$ ) = (2, 3, 2, 6) in data block MULTI (see below). With this option, two water mass balances will be set up, allowing separate tracking of the two components. For example, one could specify the water initially present in the flow system as “water 1,” while water being injected is specified as “water 2.” When the two-waters option is chosen molecular diffusion can also be modeled. As with other EOS-modules, this is accomplished by setting parameter  $NB$  equal to 8 (see Appendices D and E).

The primary variables are ( $P$ ,  $T$ ) for single-phase points, ( $P_g$ ,  $S_g$ ) for two-phase points. For the convenience of the user it is possible to initialize two-phase points as ( $T$ ,  $S_g$ ); when the numerical value of the first primary variable is less than 374.15, this will automatically be taken to indicate that this represents temperature rather than pressure, and will cause variables to be converted internally from ( $T$ ,  $S_g$ ) to ( $P_{sat}(T)$ ,  $S_g$ ) prior to execution. When the two-waters option is used, primary variables are ( $P$ ,  $T$ ,  $X$ ) for single-phase points, and ( $P_g$ ,  $S_g$ ,  $X$ ) for two-phase points, where  $X$  is the mass fraction of “water 2” present. All thermophysical properties (density, specific enthalpy, viscosity) are assumed independent of the component mixture; i.e., independent of mass fraction  $X$ . This approximation is applicable for problems in which the identity of different waters is distinguished by the presence of different trace constituents, which occur in concentrations low enough to not appreciably affect the thermophysical properties.

The phase diagnostic procedures are as follows. When initializing a problem, each grid block has two primary variables ( $X1$ ,  $X2$ ). The meaning of  $X2$  depends on its numerical value: for  $X2 > 1.5$ ,  $X2$  is taken to be temperature in °C, otherwise it is gas saturation. (Although physically saturation is restricted to the range  $0 \leq S \leq 1$ , it is necessary to allow saturations to exceed 1 during the Newton-Raphson iteration.) If  $X2$  is temperature this indicates that single-phase conditions are present; specifically, for  $P (= X1) > P_{sat}(T)$  we have single-phase liquid, otherwise we have single-phase steam. Subsequent to initialization, the phase condition is identified simply based on the value of  $S_g$  as stored in the PAR array.  $S_g = 0$ : single-phase liquid,  $S_g = 1$ : single-phase vapor,  $0 < S_g < 1$ : two-phase.

Phase change is recognized as follows. For single-phase points the temperature (second primary variable) is monitored, and the corresponding saturation pressure is compared with actual fluid pressure  $P$ . For a vapor (liquid) point to remain vapor (liquid), we require that  $P < P_{sat}$  ( $P >$

$P_{sat}$ ); if this requirement is violated, a transition to two-phase conditions takes place. The primary variables are then switched to  $(P_g, S_g)$ , and these are initialized as  $P_g = P_{sat}(T)$ ,  $S_g = 0.999999$  if the point was in the vapor region, and  $S_g = 0.000001$  if it was in the liquid region. For two-phase points  $S_g$  is monitored; we require that  $0 < S_g < 1$  for a point to remain two-phase. If  $S_g < 0$  this indicates disappearance of the gas phase; the primary variables are then switched to  $(P, T)$ , and the point is initialized as single-phase liquid, with  $T$  taken from the last Newton-Raphson iteration, and  $P = 1.000001 * P_{sat}(T)$ . For  $S_g > 1$  the liquid phase disappears; again the primary variables are switched to  $(P, T)$ , and the point is initialized as single-phase vapor, with  $T$  taken from the last Newton-Raphson iteration, and  $P = 0.999999 * P_{sat}(T)$ . Note that in these phase transitions we preserve temperature rather than pressure from the last iteration. This is preferable because in most flow problems temperature tends to be more slowly varying than pressure.

## 6.2 EOS2 (water, CO<sub>2</sub>)

This is an updated version of the fluid property module originally developed by O'Sullivan et al. (1985) for describing fluids in gas-rich geothermal reservoirs, which may contain CO<sub>2</sub> mass fractions ranging from a few percent to occasionally 80% or more (Atkinson et al., 1980). EOS2 accounts for non-ideal behavior of gaseous CO<sub>2</sub>, and dissolution of CO<sub>2</sub> in the aqueous phase with heat of solution effects. According to Henry's law, the partial pressure of a non-condensable gas (NCG) in the gas phase is proportional to the mol fraction  $x_{aq}^{NCG}$  of dissolved NCG in the aqueous phase,

$$P_{NCG} = K_h x_{aq}^{NCG} \quad (6)$$

The Henry's law coefficient  $K_h$  for dissolution of CO<sub>2</sub> in water is strongly dependent on temperature. The correlation used in the previous release of EOS2 had been developed by O'Sullivan et al. (1985) for the elevated temperature conditions encountered in geothermal reservoirs. It is accurate to within a few percent of experimental data in the temperature range of 40 °C ≤  $T$  ≤ 330 °C, but becomes rather inaccurate at lower temperatures and even goes to negative values for  $T < 30$  °C (see Fig. 7). Subroutine HENRY in EOS2 was replaced with a new routine that uses the correlation developed by Battistelli et al. (1997), which is accurate for 0 °C ≤  $T$  ≤ 350 °C. The Battistelli et al. formulation agrees well with another correlation that was developed by S. White (1996, private communication).

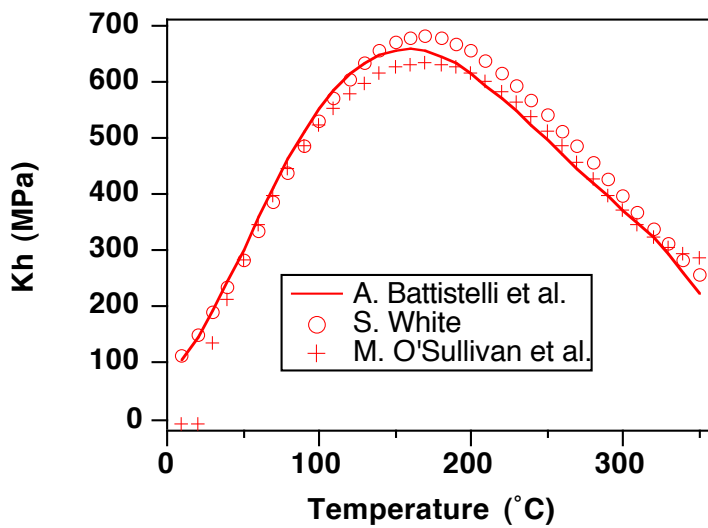


Figure 7. Henry's law coefficients for dissolution of CO<sub>2</sub> in water.

The viscosity of vapor - CO<sub>2</sub> mixtures is described with a formulation due to Pritchett et al. (1981); other thermophysical property correlations are based on the model of Sutton and McNabb (1977).

Specifications and parameters of EOS2 are summarized in Table 8. A more detailed description and application to geothermal reservoir problems are given in the paper by O'Sullivan et al. (1985).

Table 8. Summary of EOS2

<u>Components</u>	# 1: water # 2: CO <sub>2</sub>
<u>Parameter choices</u>	(NK, NEQ, NPH, NB) = (2, 3, 2, 6) molecular diffusion can be modeled by setting NB = 8
<u>Primary Variables</u>	single-phase conditions (P, T, PCO <sub>2</sub> ) - (pressure, temperature, CO <sub>2</sub> partial pressure) two-phase conditions (P <sub>g</sub> , S <sub>g</sub> , PCO <sub>2</sub> ) - (gas phase pressure, gas saturation, CO <sub>2</sub> partial pressure)

### 6.3 EOS3 (water, air)

This module is an adaptation of the EOS module of the TOUGH simulator, and implements the same thermophysical properties model (Pruess, 1987). All water properties are represented by the steam table equations as given by the International Formulation Committee (1987). Air is approximated as an ideal gas, and additivity is assumed for air and vapor partial pressures in the gas phase,  $P_g = P_a + P_v$ . The viscosity of air-vapor mixtures is computed from a formulation given by Hirschfelder et al. (1954). The solubility of air in liquid water is represented by Henry's law, Eq. 6. Henry's constant for air dissolution in water is a slowly varying function of temperature, varying from  $6.7 \times 10^9 P_a$  at  $20^\circ\text{C}$  to  $1.0 \times 10^{10} P_a$  at  $60^\circ\text{C}$  and  $1.1 \times 10^{10} P_a$  at  $100^\circ\text{C}$  (Loomis, 1928). Because air solubility is small, this kind of variation is not expected to cause significant effects, and a constant  $K_h = 10^{10} P_a$  was adopted.

EOS3 differs from the EOS module of TOUGH in one important respect, namely, the choice of primary thermodynamic variables. In TOUGH we have  $(P, T, X)$  for single-phase conditions,  $(P_g, S_g, T)$  for two-phase conditions. The choice made in EOS3 of TOUGH2 is  $(P, X, T)$  for single-phase,  $(P_g, S_g + 10, T)$ . The rationale for the seemingly bizarre choice of  $S_g + 10$  as a primary variable is as follows. As an option, we wish to be able to run isothermal two-phase flow problems with the specification  $NEQ = NK$ , so that the then superfluous heat balance equation needs not be engaged. This requires that temperature  $T$  be the third primary variable. The logical choice of primary variables would then appear to be  $(P, X, T)$  for single-phase and  $(P_g, S_g, T)$  for two-phase conditions. However, both  $X$  and  $S_g$  vary over the range  $(0, 1)$ , so that this would not allow a distinction of single-phase from two-phase conditions solely from the numerical range of primary variables. By taking the second primary variable for two-phase conditions to be  $X_2 = 10 + S_g$ , the range of that variable is shifted to the interval  $(10, 11)$ , and a distinction between single and two-phase conditions can be easily made. As a convenience to users, we retain the capability to optionally initialize flow problems with TOUGH-style primary variables by setting  $MOP(19) = 1$ . A summary of EOS specifications is given in Table 9.

Table 9. Summary of EOS3

<u>Components</u>	# 1: water # 2: air
<u>Parameter choices</u>	
$(NK, NEQ, NPH, NB) =$	(2, 3, 2, 6) water and air, nonisothermal (default) (2, 2, 2, 6) water and air, isothermal molecular diffusion can be modeled by setting NB = 8
<u>Primary Variables</u> *	
	single-phase conditions $(P, X, T)$ - (pressure, air mass fraction, temperature) two-phase conditions $(P_g, S_g + 10, T)$ - (gas phase pressure, gas saturation plus 10, temperature)

\* By setting  $MOP(19) = 1$ , initialization can be made with TOUGH-style variables  $(P, T, X)$  for single-phase,  $(P_g, S_g, T)$  for two-phase.

## 6.4 EOS4 (water, air, with vapor pressure lowering capability)

The specification of thermophysical properties in this EOS differs from EOS3 in that provision is made for vapor pressure lowering effects. The new version of EOS4 has added capabilities for initializing problems, and it can optionally be run in single-component (water only, no air) mode. Vapor pressure is expressed by Kelvin's equation (Eq. A.7); it is a function not only of temperature, but depends also on capillary pressure, which in turn is a function of saturation. The primary variables are  $(P, T, P_a)$  for single-phase conditions and  $(P_g, S_g, P_a)$  for two-phase conditions, where  $P_a$  is the partial pressure of air. Note that in two-phase conditions temperature is not among the primary variables. It is implicitly determined from the relationship  $P_g - P_a = P_v$ , with  $P_v = P_v(T, S_l)$  as given in Eq. A.7.

It would be possible to use other sets of primary variables; in particular, temperature could be used also in two-phase conditions. Our test calculations for a number of examples indicated, however, that the choice  $(P_g, S_g, P_a)$  usually leads to better convergence behavior than the choice  $(P_g, S_g, T)$ . The reason for the numerically inferior behavior of the latter set is in the air mass balance. With the variables  $(P_g, S_g, T)$ , the amount of air present in a grid block becomes controlled by the difference between total gas pressure  $P_g$  and effective vapor pressure  $P_v = P_{sat}(T)f_{VPL}(T, S_l)$  (Eq. A.7), which can be subject to very severe numerical cancellation. From the applications viewpoint, however, initialization of a flow problem with the set  $(P_g, S_g, T)$  may be much more physical and convenient. EOS4 allows the initialization of two-phase points as  $(P_g, S_g, T)$ ; this capability can be selected by specifying  $MOP(19) = 1$  in the INPUT file. When using  $MOP(19) = 1$ , the second primary variable upon initialization can also be relative humidity RH, expressed as a fraction ( $0 < RH \leq 1$ ); this choice is made by entering the second primary variable as a negative number, which will serve as a flag to indicate that it means (negative of) relative humidity, and will be internally converted to saturation in the initialization phase. The conversion consists of iteratively solving Kelvin's equation for given  $RH = f_{VPL}(T, S_l)$  for  $S_l$ . Users need to beware that relative humidity specifications must be within the range that is feasible for the capillary pressure functions used. If maximum capillary pressures are not strong enough to accommodate a chosen value of  $RH$ , a diagnostic will be printed and execution will terminate.

As a further convenience to users, the choice  $MOP(19) = 2$  allows EOS4 to be initialized with EOS3 variables of  $(P, X, T)$  for single-phase,  $(P_g, S_g + 10, T)$  for two-phase. This way continuation runs with EOS4 can be made from EOS3-generated conditions. Note that, when using  $MOP(19) \neq 0$  options, data block or file INCON must terminate on a blank record (' '). If '+++' is encountered in INCON, it is assumed that primary variables are provided in agreement with internal usage;  $MOP(19)$  is then reset to zero and an informative message is printed.

Vapor pressure lowering effects raise new issues because they make it possible for a liquid phase to exist under conditions where vapor partial pressure and gas phase total pressure are less than the saturation pressure. What is the appropriate pressure at which liquid phase density, enthalpy and viscosity are to be evaluated? We believe that a physically plausible choice is to take  $P_l = \max(P_g, P_{sat})$ , and this has been implemented in EOS4. The implementation faces a difficulty, however, because temperature is not among the primary variables in two-phase conditions, so that  $P_{sat}$  is only implicitly known; moreover, vapor pressure lowering effects are functionally dependent on liquid phase density, which is also a function of temperature. This leads to a potentially unstable situation with regard to the choice of liquid phase pressure under conditions where  $P_g \approx P_{sat}$ , which happens to be a common occurrence in boiling regions. In order to avoid this problem we evaluate liquid water density in the Kelvin equation for vapor pressure lowering (Eq.A.7) always at  $P_l = P_{sat}$ , which will be an excellent approximation due to the small compressibility of liquid water. In all accumulation and flow terms the density of liquid water is evaluated at  $P_l = \max(P_g, P_{sat})$ . Vapor pressure lowering can be optionally suppressed by setting  $MOP(20) = 1$ . A summary of EOS4 specifications is given in Table 10.

Table 10. Summary of EOS4

<u>Components</u>	# 1: water # 2: air
<u>Parameter choices</u>	
( $NK, NEQ, NPH, NB$ ) =	(2, 3, 2, 6) water and air, nonisothermal (default) (1, 2, 2, 6) water only (no air), nonisothermal
<ul style="list-style-type: none"> <li>• <math>MOP(20) = 1</math> optionally suppresses vapor pressure lowering effects</li> <li>• molecular diffusion can be modeled by setting <math>NB = 8</math></li> </ul>	
<u>Primary Variables</u> *†	
single-phase conditions $(P, T, P_a)$ - (pressure, temperature, air partial pressure)	
two-phase conditions $(P_g, S_g, P_a)$ - (gas phase pressure, gas saturation, air partial pressure)	

\* By setting  $MOP(19) = 1$ , initialization of two-phase conditions can be made with  $(P_g, S_g, T)$ , or with  $(P_g, -RH, T)$ , where RH is relative humidity ( $0 < RH \leq 1$ ).

† By setting  $MOP(19) = 2$ , initialization can be made with EOS3-style variables  $(P, X, T)$  for single-phase ( $X$  is air mass fraction),  $(P_g, S_g + 10, T)$  for two-phase.

## 6.5 EOS5 (water, hydrogen)

In a number of waste disposal projects, corrosive metals are to be emplaced in geologic formations beneath the water table. These will evolve a mixture of gases, with hydrogen being the chief constituent. The EOS5 fluid property module was developed to study the behavior of groundwater systems in which hydrogen releases is taking place. It is a close “cousin” of EOS3, the main difference being that the air component is replaced by hydrogen, with considerably different thermophysical properties (see Table 11). The assignment and handling of primary thermodynamic variables in EOS5 is identical to EOS3 (see Table 9). The main differences in the assignment of secondary parameters are as follows. Density of gaseous hydrogen is computed from the ideal gas law. Viscosity and water solubility of hydrogen are interpolated from the data given in Table 11. For temperatures in excess of 25 °C, the solubility at 25 °C is used. The parameter specifications of EOS5 are identical to those of EOS3 as given in Table 9, with air replaced by hydrogen.

Table 11. Thermophysical properties of hydrogen

density at $P = 1$ bar	experimental*	ideal gas law†
$T = 280$ K	0.086546 kg/m <sup>3</sup>	0.08660 kg/m <sup>3</sup>
$T = 300$ K	0.080776 kg/m <sup>3</sup>	0.08082 kg/m <sup>3</sup>
<hr/>		
viscosity*		
	$T = 0$ °C	$T = 100$ °C
$P = 1$ bar	$8.40 \times 10^{-6}$ Pa·s	$10.33 \times 10^{-6}$ Pa·s
$P = 100$ bar	$8.57 \times 10^{-6}$ Pa·s	$10.44 \times 10^{-6}$ Pa·s
<hr/>		
solubility in water at $P = 1$ bar§		
$T = 0$ °C	$1.92 \times 10^{-6}$ g H <sub>2</sub> /g H <sub>2</sub> O	
$T = 25$ °C	$1.54 \times 10^{-6}$ g H <sub>2</sub> /g H <sub>2</sub> O	

\* from Vargaftik (1975), p. 39.

† universal gas constant  $R = 8314.56$  J/mol/°C; molecular weight of hydrogen 2.0160 kg/mol.

§ after Dean (1985); solubility at different pressures is computed from Henry’s law.

## 6.6 EOS7 (water, brine, air)

An extension of the EOS3 module for water/air mixtures, EOS7 represents the aqueous phase as a mixture of (pure) water and brine. This approach is very useful for flow problems in which salinity does not reach saturated levels (Reeves et al., 1986; Herbert et al., 1988). The salinity of the aqueous phase is described by means of the brine mass fraction,  $X_b$ , and density and viscosity are interpolated from the values for the water and brine endmembers. Salinity-dependent air solubility is also taken into account, but no allowance is made for reduction of vapor pressure with salinity. The brine is modeled as NaCl solution, while the non-condensable gas is air, although the treatment could be adapted, with minor modifications, to other brines and gases. The representation of the temperature and pressure dependence of thermophysical properties is somewhat more general than that of Reeves et al. (1986), retaining the flexibility of the TOUGH2 formulation for nonisothermal processes.

EOS7 can describe phase conditions ranging from single-phase liquid to two-phase to single-phase gas. However, the approach of describing variably saline fluids not as mixtures of water and salt but as mixtures of water and brine has specific limitations which need to be considered in applications. For example, in problems with significant boiling it would be possible for salinity to reach saturated levels, corresponding to brine mass fraction  $X_b = 1$  (supposing that the brine component was chosen as fully saturated salt solution). Upon further boiling solid salt would precipitate, but solubility limits and solids precipitation are not taken into account in the approach used in EOS7. (These can be modeled with the EWASG module, see section 6.10.) As evaporation continues from a saline aqueous phase, eventually brine mass fraction would increase beyond  $X_b = 1$ , in which case other mass fractions would become negative, and non-physical results would be obtained. From a physical viewpoint brine mass fraction in the gas phase should always be equal to zero, but the only way the brine mass balance can be maintained during phase transitions from two-phase to single-phase vapor conditions is by allowing  $X_{b,\text{gas}}$  to vary freely. Users need to carefully examine problem setups and results to guard against unphysical results in applications that involve boiling.

We now briefly summarize the treatment of thermophysical properties in EOS7; a more detailed discussion is available in a laboratory report (Pruess, 1991b). The density of the aqueous phase is calculated from the assumption, shown to be very accurate by Herbert et al. (1988), that fluid volume is conserved when water and brine are mixed. Mixture density  $\rho_m$  can then be expressed in terms of water and brine densities as follows.

$$\frac{1}{\rho_m} = \frac{1-X_b}{\rho_w} + \frac{X_b}{\rho_b} \quad (7)$$

Eq. (7) applies to densities at fixed pressure and temperature conditions. In order to achieve a simple approximation for fluid density at variable temperatures and pressures, EOS7 takes compressibility and expansivity of brine to be equal to those of water. This will provide a reasonable approximation at least for a limited range of temperatures and pressures around the reference conditions ( $P_0$ ,  $T_0$ ). The default reference brine has a density of 1185.1 kg/m<sup>3</sup> at reference conditions of  $P_0 = 1$  bar,  $T_0 = 25$  °C, corresponding to an NaCl solution of 24.98 wt-%, or 5.06 molar (Potter and Brown, 1977; cited after Finley and Reeves, 1982). The user may specify different reference conditions and brine densities. Effects of salinity on the enthalpy of the aqueous phase are ignored.

Following Herbert et al. (1988), salinity effects on aqueous phase viscosity are modeled with a polynomial correction to the viscosity of pure water. Mixture viscosity is represented as follows.

$$\mu_m(P, T, X_b) = \mu_w(P, T) f(X_b) \quad (8)$$

where

$$f(X_b) = 1 + v_1 X_b + v_2 X_b^2 + v_3 X_b^3 \quad (9)$$

with default values of  $v_1 = 0.4819$ ,  $v_2 = -0.2774$ , and  $v_3 = 0.7814$ . Different values for the coefficients may be specified by the user.

Gas (air) dissolution in the aqueous phase is modeled by Henry's law (Eq. 6). In saline solutions, gases are generally less soluble than in water ("salting out" effect). For a 5 N (molar) NaCl solution, nitrogen solubility is virtually independent of temperature in the range 0 °C ≤  $T$  ≤ 100 °C, and corresponds to a Henry's constant of  $4.0 \times 10^{10}$   $P_a$  (Cygan, 1991). We retain the value of  $K_h = 10^{10}$   $P_a$  for pure water, and represent air solubility (inverse of Henry's constant) as a linear function of mixture molarity  $N_m$ , as follows.

$$\frac{1}{K_h} = 1.0 \times 10^{-10} + \frac{N_m}{5} \left( \frac{1}{4.0 \times 10^{10}} - 10^{-10} \right) \quad (10)$$

A summary of EOS7 specifications appears in Table 12.

Table 12. Summary of EOS7

<u>Components</u>	# 1: water # 2: brine # 3: air (optional) <sup>†</sup>
<u>Parameter choices</u>	( $NK, NEQ, NPH, NB$ ) = (3, 3, 2, 6) water, brine, air, isothermal (default) (3, 4, 2, 6) water, brine, air, nonisothermal (2, 2, 2, 6) water, brine, isothermal <sup>†</sup> (2, 3, 2, 6) water, brine, nonisothermal <sup>†</sup> molecular diffusion can be modeled by setting $NB = 8$
<u>Primary Variables</u>	single-phase conditions ( $P, X_b, X, T$ ) - (pressure, brine mass fraction, air mass fraction, temperature) two-phase conditions ( $P, X_b, S+10, T$ ) - (gas phase pressure, brine mass fraction, gas saturation plus ten, temperature)

<sup>†</sup> the NK = 2 (no air) option may only be used for problems with single-phase liquid conditions throughout

Users may specify parameters for reference brine in the TOUGH2 input file by means of an optional data block SELEC, as follows.

**SELECTION** keyword to introduce a data block with optional reference brine data.

Record SELEC.1

- |               |  |
|---------------|--|
| Format (I5)   |  |
| IE(I), I=1,16 |  |
| IE(1)         | set equal to 2, to read two additional data records (a larger value with more additional data records is acceptable, but only the first two will be used by EOS7). |

## Record SELEC.2

Format (3E10.4)

$P_0, T_0, \rho_b$

$P_0$  reference pressure, Pa

$T_0$  reference temperature, °C

$\rho_b$  brine density at  $(P_0, T_0)$ , kg/m<sup>3</sup>

If any of these parameters is entered as zero, default values of  $P_0 = 1$  bar,  $T_0 = 25$  °C,  $\rho_b = 1185.1$  kg/m<sup>3</sup> will be used. For  $P_0 < 0$ , brine properties will be assumed identical to water.

## Record SELEC.3

Format (3E10.4)

$v_1, v_2, v_3$

coefficients for salinity correction of aqueous phase viscosity, see Eq. (9).

## 6.7 EOS7R (water, brine, radionuclide 1, radionuclide 2, air)

This is an enhanced version of the EOS7 module in which two additional mass components have been added. These can undergo decay with user-specified half life, with radionuclide 1 (Rn1 for short) being the “parent” and Rn2 the “daughter.” The radionuclides are considered water-soluble as well as volatile, but are not allowed to form a separate non-aqueous fluid phase. Sorption onto the solid grains is also included. Stable trace components, such as volatile and water soluble organic chemicals (VOCs), can be modeled simply by setting half life to very large values. A detailed description of the mathematical model used in EOS7R is available in a laboratory report, which also presents a number of illustrative problems, including verification against analytical solutions (Oldenburg and Pruess, 1995). Here we highlight the main aspects of the thermophysical properties model. A summary of EOS7R input formats is given in Table 13.

Radionuclide decay is described by

$$\frac{dM^\kappa}{dt} = -\lambda_\kappa M^\kappa \quad (11)$$

where  $M^\kappa$  is the mass of radionuclide  $\kappa$  ( $= Rn1, Rn2$ ) per unit volume, and the decay constant  $\lambda_\kappa$  is related to the half life by

$$T_{1/2} = \frac{\ln 2}{\lambda_\kappa} \quad (12)$$

Adsorption of radionuclides on the solid grains is modeled as reversible instantaneous linear sorption, so that mass of radionuclide component  $\kappa$  per unit reservoir volume is given by (compare Eq. A.2 for non-sorbing components)

$$M^\kappa = \phi \sum_\beta S_\beta \rho_\beta X_\beta^\kappa + (1 - \phi) \rho_R \rho_{aq} X_{aq}^\kappa K_d \quad (13),$$

with  $K_d$  the aqueous phase distribution coefficient (de Marsily, 1986, p. 256). Radionuclides partition between aqueous and gaseous phases according to Henry’s law, Eq. (6). The thermophysical properties of the aqueous phase are assumed independent of radionuclide concentrations. Implicit in this approximation is the assumption that aqueous radionuclide concentrations are small. Users need to keep this limitation in mind, because EOS7R does not provide any intrinsic constraints on radionuclide concentrations.

Table 13. Summary of EOS7R

<u>Components</u>	# 1: water # 2: brine # 3: Rn1 (radionuclide 1; “parent”) # 4: Rn2 (radionuclide 2; “daughter”) # 5: air (optional) <sup>†</sup>
<u>Parameter choices</u>	( $NK, NEQ, NPH, NB$ ) <sup>§</sup> = (5, 5, 2, 8) water, brine, Rn1, Rn2, air, isothermal (default) (5, 6, 2, 8) water, brine, Rn1, Rn2, air, nonisothermal (4, 4, 2, 8) water, brine, Rn1, Rn2, no air, isothermal <sup>†</sup> (4, 5, 2, 8) water, brine, Rn1, Rn2, no air, nonisothermal <sup>†</sup>
	molecular diffusion can be suppressed by setting $NB = 6$
<u>Primary Variables</u> <sup>§</sup>	<p>single-phase conditions</p> $(P, X_b, X_{Rn1}, X_{Rn2}, X_{air}, T)$ - (pressure, brine mass fraction, mass fraction of Rn1, mass fraction of Rn2, air mass fraction, temperature) <p>two-phase conditions</p> $(P, X_b, X_{Rn1}, X_{Rn2}, S+10, T)$ - (gas phase pressure, brine mass fraction, mass fraction of Rn1, mass fraction of Rn2, gas saturation plus ten, temperature)*

<sup>†</sup> the no air option ( $NK = 4$ ) may only be used for problems with single-phase liquid conditions throughout

<sup>§</sup> parameter  $NKIN$  following  $NB$  may optionally be set to  $NKIN = NK-2$ , in which case radionuclide mass fractions will be omitted, and initialization will be made from only four EOS7-style variables; radionuclide mass fractions will be initialized as zero;

\* in two-phase conditions,  $X_{Rn1}$  and  $X_{Rn2}$  are mass fractions in the aqueous phase

For the gas phase we assume ideal gas law for air and the radionuclides, and additivity of partial pressures.

$$P_{\text{gas}} = P_{\text{air}} + P_{\text{vapor}} + P_{\text{Rn1}} + P_{\text{Rn2}} \quad (14)$$

Gas phase density is calculated as the sum of the partial densities of gaseous components, while gas phase viscosity and enthalpy are calculated from the same air-vapor mixing models used in EOS3. Apart from these approximations for gas phase viscosity and enthalpy, there is no restriction to “small” radionuclide concentrations in the gas phase. In fact, full allowance for gas

phase radionuclide partial pressures is made for phase change diagnostics, as follows. For single-phase liquid conditions, Henry's law is used to calculate the partial pressures that the non-condensable gases would have if a gas phase were present. The total pressure that a gas phase would have if present is then calculated from Eq. (14), using saturated vapor pressure at prevailing temperature. This is compared with the aqueous phase pressure, and a transition to two-phase conditions is made when  $P_{gas} > P_{aq}$ . In two-phase conditions, the saturation variable is monitored. A phase transition to single-phase liquid occurs when  $S_g < 0$ , while for  $S_g > 1$  a transition to single-phase gas conditions is made. For transitions from two-phase to single-phase liquid conditions, liquid pressure is initialized as  $P_{aq} = (1 + 10^{-6}) * P_{gas}$ , with  $P_{gas}$  given by Eq. (14), while for transitions to single-phase gas conditions, pressure is initialized as  $(1 - 10^{-6}) * P_{gas}$ . For single-phase gas conditions we monitor vapor pressure  $P_{vap} = P_{gas} - P_{air} - P_{Rn1} - P_{Rn2}$ ; a transition to two-phase conditions occurs when  $P_{vap} > P_{gas}$ . As had been pointed out in the EOS7 section, users need to be aware that there are inherent limitations in the ability of a water-brine mixture model to describe processes that involve significant vaporization.

Brine and radionuclide properties are specified in the TOUGH2 input file by means of a data block SELEC, as follows.

**SELECTION** keyword to introduce a data block with reference brine, geometry, dispersion, and radioactive decay data.

#### Record SELEC.1

Format (16I5)

IE(1), NGBINP(1), NGBINP(2), NGBINP(3), NFBL, NFBR, NFBT,  
NFBB

IE(1) set equal to 6 to read six additional records with data for brine and radionuclides, and for hydrodynamic dispersion.

The 7 input variables following IE(1) are for the dispersion module T2DM only and can be left blank if T2DM is not used.

NGBINP(1) number of grid blocks in X (must always be equal to 1).

NGBINP(2) number of grid blocks in Y.

NGBINP(3) number of grid blocks in Z.

NFBL number of the first ("left") column of grid blocks within the flow domain (defaults to 1 if zero or blank).

NFBR	number of the last ("right") column of grid blocks within the flow domain (defaults to NGBINP(2) if zero or blank).
NFBT	number of the first ("top") row of grid blocks within the flow domain (defaults to 1 if zero or blank).
NFBB	number of the last ("bottom") row of grid blocks within the flow domain (defaults to NGBINP(3) if zero or blank).

#### Record SELEC.2

	Format (3E10.4)
	$P_0, T_0, \rho_b$
$P_0$	reference pressure, Pa.
$T_0$	reference temperature, °C.
$\rho_b$	brine density at $(P_0, T_0)$ , $kg/m^3$ .
	If any of these parameters is entered as zero, default values of $P_0 = 1$ bar, $T_0 = 25$ °C, $\rho_b = 1185.1$ $kg/m^3$ will be used. For $P_0 < 0$ , brine properties will be assumed identical to water.

#### Record SELEC.3

	Format (3E10.4)
	$v_1, v_2, v_3$
	coefficients for salinity correction of aqueous phase viscosity, see Eq. (9).

#### Record SELEC.4

	Format (2E10.4)
	ALPHAT, ALPHAL
	Used in T2DM only; otherwise can be left blank.
ALPHAT	transverse dispersivity, m.
ALPHAL	longitudinal dispersivity, m.

#### Record SELEC.5

	Format (6E10.4)
	FDDIAG(NP,NK), $NK=1,2,5$ ; $NP=1,2$
FDDIAG(NP,NK)	molecular diffusivities in units of $m^2/s$ ; first the three gas phase diffusivities for water, brine, and air; then the three aqueous phase diffusivities for water, brine, and air. See section D.4 in Appendix

D for user options. If a data block DIFFU is present, it will override the diffusivity specifications made in SELEC.

#### Record SELEC.6

Format (7E10.4)

XHALF(3), XMW(3), (FDDIAG(NP,NK), NK=3; NP=1,2), blank,  
blank, HCRN1

XHALF(3) half life of parent radionuclide (Rn1, component 3), seconds.

XMW(3) molecular weight of Rn1, g/mol.

FDDIAG(NP,3) molecular diffusivity of Rn1 in the gas phase in m<sup>2</sup>/s;  
followed by molecular diffusivity of Rn1 in the aqueous phase. See  
section D.4 in Appendix D for user options. If a data block DIFFU  
is present, it will override the diffusivity specifications made in  
SELEC.

HCRN1 inverse Henry's constant ( $K_h$ )<sup>-1</sup> (see Eq. 6) for parent radionuclide  
Rn1, Pa<sup>-1</sup>. (The inverse Henry's constant can be thought of as an  
aqueous phase solubility.)

#### Record SELEC.7

Format (7E10.4)

XHALF(4), XMW(4), (FDDIAG(NP,NK), NK=4; NP=1,2), blank,  
blank, HCRN2

XHALF(4) half life of daughter radionuclide (Rn2, component 4), seconds.

XMW(4) molecular weight of Rn2, g/mol.

FDDIAG(NP,4) molecular diffusivity of Rn2 in the gas phase in m<sup>2</sup>/s;  
followed by molecular diffusivity of Rn2 in the aqueous phase. See  
section D.4 in Appendix D for user options. If a data block DIFFU  
is present, it will override the diffusivity specifications made in  
SELEC.

HCRN2 inverse Henry's constant ( $K_h$ )<sup>-1</sup> (see Eq. 6) for daughter  
radionuclide Rn2, Pa<sup>-1</sup>. (The inverse Henry's constant can be  
thought of as an aqueous phase solubility.)

## 6.8 EOS8 (water, air, oil)

This module provides a very basic and simple capability for modeling three fluid phases, including gaseous, aqueous, and oleic phases. EOS8 can represent what in petroleum engineering is often referred to as a "dead oil," meaning a non-aqueous phase liquid that has no volatile or soluble components, so that it is present only in the non-aqueous phase. The thermophysical property description related to the third (oil) phase was intentionally kept very simple and, although EOS8 may be applicable to some flow problems of practical interest as is, it should be considered a development platform rather than a realistic description of three-phase fluid systems.

EOS8 is an enhanced version of EOS3, and was developed from EOS3 by adding a third non-volatile, insoluble component, called "oil," which can only exist in a separate, immiscible phase. To accommodate the third component, the three primary variables used in EOS3 were placed in slots # 1, # 2, and # 4, and a new variable  $S_o$  was added in slot # 3 to represent the saturation of the oil phase (see Table 14). With EOS8 the user can optionally run just two phases (aqueous-gas, without the oil phase), in which case the aqueous-gas process descriptions reduce to those of EOS3.

Table 14. Summary of EOS8

<u>Components</u>	# 1: water # 2: air # 3: oil
<u>Parameter choices</u>	$(NK, NEQ, NPH, NB) =$ (3, 3, 3, 6) water, air, oil, isothermal (default) (3, 4, 3, 6) water, air, oil, nonisothermal (2, 2, 2, 6) water, air, no oil, isothermal (2, 3, 2, 6) water, air, no oil, nonisothermal
<u>Primary Variables</u>	two-phase conditions (gas-oil or aqueous-oil) $(P, X, S_o, T)$ - (pressure, air mass fraction, oil phase saturation, temperature) three-phase conditions (gas-aqueous-oil) $(P_g, S_g + 10, S_o, T)$ - (gas phase pressure, gas saturation plus 10, oil phase saturation, temperature)

The relative permeabilities of the gas and aqueous phases are considered functions of their respective phase saturations only,  $k_{rg} = k_{rg}(S_g)$ ,  $k_{rl} = k_{rl}(S_{aq})$ , and are specified through input data in the usual manner. The oil phase is considered of intermediate wettability, and its relative permeability is described in a schematic fashion that is intended to serve as a template for users.

$$k_{ro} = \frac{S_o - S_{or}}{1 - S_{or}} \quad (15)$$

Here,  $S_{or}$  is the residual oil saturation. Oil phase capillary pressure is neglected. Viscosity, density, and specific enthalpy of the oil phase are described as functions of pressure and temperature through low-order polynomials, with user-specified parameters entered through data block SELEC. More specifically, viscosity is written as

$$\begin{aligned} \mu_{oil} = & a + b(P - P_1) + c(P - P_2)^2 \\ & + d(T - T_1) + e(T - T_2)^2 \end{aligned} \quad (16)$$

Oil density is

$$\rho_{oil} = \rho_0 + C(P - P_0) - E(T - T_0) \quad (17)$$

where  $\rho_0$  is oil density at reference pressure and temperature conditions of  $(P_0, T_0)$ . Specific enthalpy of oil is assumed proportional to temperature (normalized to  $h_{oil} = 0$  at  $T = 0$  °C).

$$h_{oil} = \zeta T \quad (18)$$

All parameters appearing in the oil phase property description are to be provided by the user through data block SELEC. The oil phase property model and the formats for user-definable parameters are described through internal documentation (comments) in the EOS routine, as well as in the sample input file \*rcl8\* (section 9.9), which considers a three-phase flow problem in which water is used to flush a mobile oil down a 1-D column. The property correlations are implemented through arithmetic statement functions at the top of EOS8 in a manner that should be transparent to users. Instructions for preparing EOS8 input data are given through detailed comment statements in the source code.

## 6.9 EOS9 (saturated-unsaturated flow)

This module considers variably saturated flow of a single aqueous phase, which consists entirely of a single water component. The gas phase is treated as a passive bystander at constant pressure, and conditions are assumed to be isothermal. Thus, no mass balance equation for gas and no heat balance is needed, and only a single water mass balance equation is solved for each grid block. This is very efficient numerically, making EOS9 the module of choice for problems for which the underlying approximations are applicable. Liquid flow is described with Eq. (A.16), which represents a slight generalization of the well known Richards' equation (A.17) for unsaturated flow (Richards, 1931). EOS9 can describe flow under partially saturated ( $0 < S_l < 1$ ) as well as fully saturated conditions, and phase changes between the two.

With only a single mass balance equation per grid block, there is only a single primary thermodynamic variable. This is taken to be pressure for single-phase (saturated) conditions, and is water saturation for unsaturated conditions. A distinction between the two is made simply on the basis of the numerical value of the first (and only) primary variable,  $Xl$ . If  $Xl < 1$ , this indicates that  $Xl$  represents water saturation and conditions are unsaturated; if  $Xl$  is larger than a user-specified gas phase reference pressure (default  $P_{gas} = 1.013 \times 10^5 \text{ Pa}$ ), it is taken to be water pressure, and saturated conditions prevail. When phase changes between saturated and unsaturated conditions occur, the primary variable is switched, as follows. The numerical value of  $Xl$  and its change during the Newton-Raphson iteration process is monitored. If  $Xl$  changes from being smaller than 1 to larger than 1, this indicates attainment of fully saturated conditions. In that case  $Xl$  is switched to pressure, and is initialized at a pressure slightly in excess of gas phase reference pressure as  $Xl = P_{gas}(1+\varepsilon)$ , with  $\varepsilon = 10^{-6}$ . If  $Xl$  changes from being larger than  $P_{gas}$  to smaller than  $P_{gas}$ , this indicates a transition from fully to partially saturated conditions.  $Xl$  is then switched to saturation, and is initialized as  $Xl = 1-\varepsilon$ . Actually, a transition from fully to partially saturated conditions is made only when  $Xl$  drops below  $P_{gas}(1-\varepsilon)$ ; test calculations have shown that such a (small) finite-size window for phase change improves numerical stability and efficiency.

In EOS9, the thermophysical properties of water are taken at default reference conditions of  $P = 1.013 \times 10^5 \text{ Pa}$ ,  $T = 15^\circ\text{C}$ . These defaults can be overwritten in a flexible manner by specifying appropriate data in a fictitious ROCKS domain 'REFCO', as follows.

reference pressure:	DROK of REFCO
reference temperature:	POR of REFCO
liquid density:	PER(1) of REFCO
liquid viscosity:	PER(2) of REFCO
liquid compressibility:	PER(3) of REFCO

Note that assignment of thermophysical data through a specially-named domain was set up just as a convenient way of providing floating-point parameters to the code. No volume elements (grid blocks) should be attached to domain ‘REFCO’, as the data in general will not correspond to reasonable hydrogeologic parameters. The above mentioned defaults will be overwritten for any parameters for which a non-zero entry is provided in ‘REFCO’. This allows the generation of these parameters internally for user-defined ( $P$ ,  $T$ ); it also allows for directly assigning user-desired values as, e.g.,  $\rho_{liq} = 1000 \text{ kg/m}^3$ ,  $\mu_{liq} = 10^{-3} \text{ Pa}\cdot\text{s}$  ( $\equiv 1$  centipoise), etc. A summary of EOS9 specifications appears in Table 15.

Table 15. Summary of EOS9

<u>Components</u>	# 1: water
<u>Parameter choices</u>	
$(NK, NEQ, NPH, NB) =$	$(1, 1, 1, 6)$ water, isothermal (default; no other choices available)
<u>Primary Variables</u> *†	<p>saturated conditions  <math>(P_{liq})</math> - (water pressure: <math>P_{liq} \geq P_{gas}</math>)</p> <p>unsaturated conditions  <math>(S_{liq})</math> - (water saturation: <math>0 &lt; S_{liq} &lt; 1</math>)</p>

\* The first primary variable may be initialized as  $X1 < 0$ , in which case it will be taken to denote capillary pressure, and will be converted internally to  $S_{liq}$  in the initialization phase.

† Reference gas phase pressure, flow system temperature, and (optionally) thermophysical parameters of water density, viscosity, and compressibility may be specified through a fictitious ROCKS domain ‘REFCO’.

In addition to specifying the primary thermodynamic variable on a default, domain, or grid block basis, EOS9 offers alternative ways of initializing flow problems. The primary variable may be entered as a negative number upon initialization, in which case it will be taken to denote capillary pressure, and will be internally converted to  $S_{liq}$  in the initialization phase. EOS9 can also initialize a flow problem with gravity-capillary equilibrium, relative to a user-specified reference elevation  $z_{ref}$  of the water table. This type of initialization will be engaged if the user enters a non-zero number in slot CWET in ROCKS domain ‘REFCO’, in which case CWET will be taken to denote the water table elevation  $z_{ref}$ , in units of meters. Water pressure at  $z_{ref}$  is taken equal to reference gas pressure,  $P_{liq}(z_{ref}) = P_{gas}$ , and is initialized as a function of grid block

elevation according to  $P(z) = P_{gas} + (z_{ref} - z) \rho_{liq} g$ . By convention, the z-axis is assumed to point upward. In order to use this facility, the z-coordinates (grid block elevations) must be specified in the ELEME-data, which will be done automatically if internal MESH generation is used.

In the assignment of gravity-capillary equilibrium as just discussed, water saturations at “sufficiently” high elevations above the water table may end up being smaller than the irreducible water saturation  $S_{lr}$  specified in the relative permeability function, which may or may not be consistent with the physical behavior of the flow system. Users may optionally enforce that  $S_l = S_{lr}$  in regions where the capillary pressure function would dictate that  $S_l < S_{lr}$ . This is accomplished by entering an appropriate parameter in slot SPHT of ROCKS domain ‘REFCO’, and works as follows. The irreducible saturation  $S_{lr}$  will be taken to be parameter RP(int(SPHT)) of the relative permeability function. As an example, for the  $IRP = 7$  relative permeability function, irreducible water saturation is the parameter RP(2); therefore, for  $IRP = 7$  the user should specify  $SPHT = 2.0$  in ‘REFCO’ to use this facility.

EOS9 differs from all of the other EOS modules in that, having only a single primary thermodynamic variable, the first (and here only) primary variable does not necessarily denote pressure. This necessitates certain other coding adjustments, as follows. EOS9 comes with its own specially modified version of subroutine MULTI for assembling the flow terms, which does not use the first primary variable  $X1$  as pressure. The slot # 6 of the PAR-array, which normally holds just the capillary pressure, represents total water pressure  $P_{liq} = P_{gas} + P_{cap}$  in EOS9. In order that the special MULTI-subroutine is used, the module eos9.f must be linked with the other TOUGH2 modules ahead of t2f.f, so that the subroutine MULTI of eos9.f rather than the one of t2f.f is used. For some linkers this will create a fatal error of “duplicate names,” which can be avoided by renaming the subroutine MULTI of t2f.f as MULTIX prior to compilation and linking.

The special MULTI subroutine of EOS9 offers one other facility that has not yet been mentioned. Users may optionally assign rock grain density DROK to a value less than zero in selected domains. This will serve as a flag to enforce unit head gradient flow conditions for any flux terms involving grid blocks in the domain with  $DROK < 0$ , which may be used, e.g., to implement unit head gradient boundary conditions. The way this works is that for flux terms involving a domain with  $DROK < 0$  the pressure terms will be ignored, and only the gravity term  $\rho_{liq} g$  will be used. Note that, because no energy equation is solved with EOS9, DROK is not used for anything other than this flux control.

The printed output for EOS9 provides, among other things, information on pressure diffusivities for all grid blocks (output parameter “DIFFUS”, units of  $m^2/s$ ). For saturated conditions, this is calculated as

$$D = \frac{k}{\phi c \mu} \quad (19)$$

where  $k$  is permeability,  $\phi$  is porosity,  $c = c_{liq} + c_\phi$  is the sum of fluid and pore compressibilities, and  $\mu$  is viscosity. For unsaturated conditions,  $k$  in Eq. (19) is replaced by effective liquid phase permeability  $k_{rl}$ , and fluid compressibility is replaced by  $dS_{liq}/dP_{cap}$  (Pruess et al., 1990).

## 6.10 EWASG (water, NaCl, non-condensable gas)

### *Thermophysical properties*

The EWASG (WAter-Salt-Gas) fluid property module was developed by Battistelli et al. (1997) for modeling geothermal reservoirs with saline fluids and non-condensable gas (NCG). In contrast to EOS7, EWASG describes aqueous fluid of variable salinity not as a mixture of water and brine, but as a mixture of water and NaCl. This makes it possible to represent temperature-dependent solubility constraints, and to properly describe precipitation and dissolution of salt. EWASG represents the active system components (water, NaCl, NCG) as three-phase mixtures. Solid salt is the only active mineral phase, and is treated in complete analogy to fluid phases (aqueous, gas), except that, being immobile, its relative permeability is identically zero. From mass balances on salt in fluid and solid phases we calculate the volume fraction of precipitated salt in the original pore space  $\phi_0$ , which is termed “solid saturation,” and denoted by  $S_s$ . A fraction  $\phi_0 S_s$  of reservoir volume is occupied by precipitate, while the remaining void space  $\phi_f = \phi_0 (1 - S_s)$  is available for fluid phases. We refer to  $\phi_f$  as the “active flow porosity.” The reduction in pore space reduces the permeability of the medium (see below).

Several choices are available for the non-condensable gas (CO<sub>2</sub>, air, CH<sub>4</sub>, H<sub>2</sub>, N<sub>2</sub>). Gas dissolution in the aqueous phase is described by Henry’s law, with coefficients that depend not only on temperature but also on salinity to describe the reduction in NCG solubility with increasing salinity (“salting out”). The dependence of brine density, enthalpy, viscosity, and vapor pressure on salinity is taken into account, as are vapor pressure-lowering effects from suction pressures (capillary and vapor adsorption effects). The thermophysical property correlations used in EWASG are accurate for most conditions of interest in geothermal reservoir studies: temperatures in the range from 100 to 350 °C, fluid pressures up to 80 MPa, CO<sub>2</sub> partial pressures up to 10 MPa, and salt mass fraction up to halite saturation. With the exception of brine enthalpy, thermophysical property correlations are accurate to below 10 °C. A full discussion of the thermophysical property correlations used and their empirical basis is given in the original paper (Battistelli et al., 1997).

Primary variables for fluid phases, and phase change diagnostics and variable switching, are similar to EOS7 (see Table 16). Primary variable # 2 (X2) is used for NaCl, and denotes mass fraction X<sub>s</sub> in the aqueous phase when no solid salt is present, while it is solid saturation plus ten ( $S_s + 10$ ) in the presence of precipitated salt. The number 10 is added here to be able to determine whether or not a precipitated phase is present from the numerical range of the second primary variable. Solubility of NaCl in the gas phase is very small at the pressure and temperature conditions considered for EWASG and has been neglected. During the Newton-Raphson iteration

process, possible appearance or disappearance of a solid phase is checked, as follows. If no solid phase was present at the previous iteration, primary variable  $X2$  is known to denote salt mass fraction  $X_s$  in the aqueous phase, and the latest updated value is compared with the equilibrium solubility  $XEQ$ . If  $S_s > XEQ$ , precipitation starts, a small solid phase saturation is initialized as  $S_s = 10^{-6}$ , and the second primary variable is switched to  $X2 = S_s + 10$ . If solid salt had been present at the previous iteration, EWASG checks whether  $S_s = X2 - 10$  is still larger than 0. If not, this indicates that the solid phase disappears; the second primary variable is then switched to dissolved salt mass fraction, and is initialized just below equilibrium solubility as  $S_s = XEQ - 10^{-6}$ .

Table 16. Summary of EWASG

<u>Components</u>	# 1: water # 2: NaCl # 3: NCG (CO <sub>2</sub> , air, CH <sub>4</sub> , H <sub>2</sub> , N <sub>2</sub> ; optional)
<u>Parameter choices</u>	( $NK, NEQ, NPH, NB$ ) = (3, 4, 3, 6) water, NaCl, NCG, nonisothermal (default) (3, 3, 3, 6) water, NaCl, NCG, isothermal (2, 3, 2, 6) water, NaCl, nonisothermal <sup>†</sup> (2, 2, 2, 6) water, NaCl, isothermal <sup>†</sup>
	molecular diffusion can be modeled by setting $NB = 8$
<u>Primary Variables</u>	single fluid phase (only liquid, or only gas) ( $P, X_{sm}, X_3, T$ ) - (pressure, salt mass fraction $X_s$ or solid saturation $S_s+10$ , NCG mass fraction, temperature) two fluid phases (liquid and gas)& ( $P, X_{sm}, S_g+10, T$ ) - (pressure, salt mass fraction $X_s$ or solid saturation $S_s+10$ , gas phase saturation $S_g+10$ , temperature)

<sup>†</sup> the  $NK = 2$  (no NCG) option may only be used for problems with single-phase liquid conditions throughout

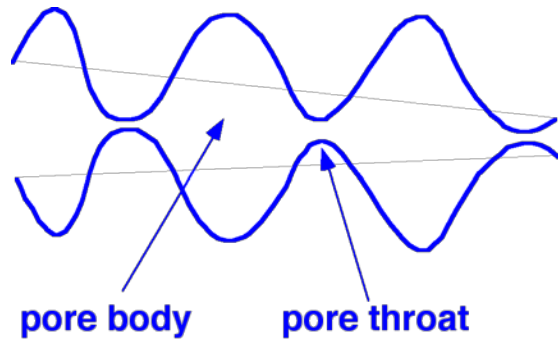
& two-phase conditions may be initialized with variables ( $T, X_{sm}, S_g+10, P_{NCG}$ ), or ( $T, X_{sm}, S_g+10, X_3$ ), where  $P_{NCG}$  is the partial pressure of NCG,  $X_3$  is mass fraction of NCG in the liquid phase; by convention, EWASG will assume the first primary variable to be pressure if it is larger than 370, otherwise it will be taken to be temperature; if the first primary variable is temperature, the last primary variable will be taken to mean mass fraction of NCG if it is less than 1, otherwise it will be taken to mean NCG partial pressure

### Permeability change

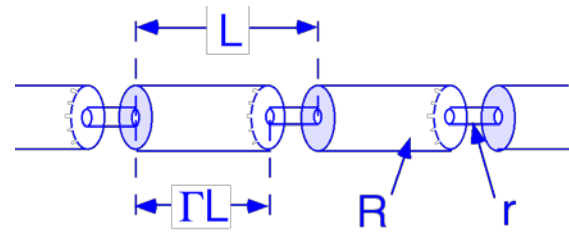
As noted above, the relationship between the amount of solid precipitation and the pore space available to the fluid phases is very simple. The impact of porosity change on formation permeability on the other hand is highly complex. Laboratory experiments have shown that modest reductions in porosity from chemical precipitation can cause large reductions in permeability (Vaughan, 1987). This is explained by the convergent-divergent nature of natural pore channels, where pore throats can become clogged by precipitation while disconnected void spaces remain in the pore bodies (Verma and Pruess, 1988). The permeability reduction effects depend not only on the overall reduction of porosity but on details of the pore space geometry and the distribution of precipitate within the pore space. These may be quite different for different porous media, which makes it difficult to achieve generally applicable, reliable predictions. EWASG offers several choices for the functional dependence of relative change in permeability,  $k/k_0$ , on relative change in active flow porosity.

$$\frac{k}{k_0} = f\left(\frac{\phi_f}{\phi_0}\right) \equiv f(1-S_s) \quad (20)$$

The simplest model that can capture the converging-diverging nature of natural pore channels consists of alternating segments of capillary tubes with larger and smaller radii, respectively; see Fig. 8. While in straight capillary tube models permeability remains finite as long



(a) conceptual model



(b) tubes-in-series

Figure 8. Model for converging-diverging pore channels.

as porosity is non-zero, in models of tubes with different radii in series, permeability is reduced to zero at a finite porosity. From the tubes-in-series model shown in Fig. 8, the following relationship can be derived (Verma and Pruess, 1988)

$$\frac{k}{k_0} = \theta^2 \frac{1 - \Gamma + \Gamma/\omega^2}{1 - \Gamma + \Gamma[\theta/(\theta + \omega - 1)]^2} \quad (21)$$

Here

$$\theta = \frac{1 - S_s - \phi_r}{1 - \phi_r} \quad (22)$$

depends on the fraction  $1 - S_s$  of original pore space that remains available to fluids, and on a parameter  $\phi_r$ , which denotes the fraction of original porosity at which permeability is reduced to zero.  $\Gamma$  is the fractional length of the pore bodies, and the parameter  $\omega$  is given by

$$\omega = 1 + \frac{1/\Gamma}{1/\phi_r - 1} \quad (23)$$

Therefore, Eq. (21) has only two independent geometric parameters that need to be specified,  $\phi_r$  and  $\Gamma$ . As an example, Fig. 9 shows the permeability reduction factor from Eq. (21), plotted against  $\phi/\phi_0 \equiv (1 - S_s)$ , for parameters of  $\phi_r = \Gamma = 0.8$ .

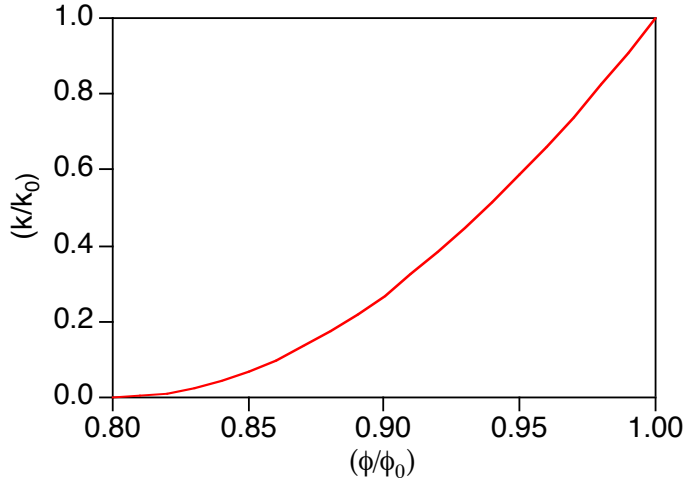


Figure 9. Porosity-permeability relationship for tubes-in-series model, after Verma and Pruess (1988).

For parallel-plate fracture segments of different aperture in series, a relationship similar to Eq. (21) is obtained, the only difference being that the exponent 2 is replaced everywhere by 3 (Verma

and Pruess, 1988). If only straight capillary tubes of uniform radius are considered, we have  $\phi_r = 0$ ,  $\Gamma = 0$ , and Eq. (21) simplifies to

$$k/k_0 = (1 - S_s)^2 \quad (24)$$

### ***Preparation of input data***

Various options for EWASG can be selected through parameter specifications in data block SELEC, as follows.

**SELECTION** keyword to introduce a data block with parameters for EWASG.

#### Record SELEC.1

Format (16I5)  
IE(I), I=1,16

- IE(1) set equal to 1, to read one additional data record (a larger value with more data records is acceptable, but only one additional record will be used by EWASG).
- IE(10) allows to turn vapor pressure lowering on/off.  
0: VPL is off.  
1: VPL is on.
- IE(11) selects dependence of permeability on the fraction  $\phi_f/\phi_0 = (1 - S_s)^\gamma$  of original pore space that remains available to fluids.  
0: permeability does not vary with  $\phi_f$ .  
1:  $k/k_0 = (1 - S_s)^\gamma$ , with  $\gamma = \text{FE}(1)$  (record SELEC.2).  
2: fractures in series, i.e., Eq. (21) with exponent 2 everywhere replaced by 3.  
3: tubes-in-series, i.e., Eq. (21).
- IE(14) allows choice of treatment of thermophysical properties as a function of salinity  
0: full dependence (default).  
1: vapor pressure independent of salinity.  
2: vapor pressure and brine enthalpy independent of salinity.

3: no salinity dependence of thermophysical properties (salt solubility constraints are maintained).

- IE(15) allows choice of correlation for brine enthalpy at saturated vapor pressure  
0: after Michaelides (1981).  
1: after Miller (1978).
- IE(16) allows choice of the type of NCG (default for IE(16)=0 is CO<sub>2</sub>)  
1: air  
2: CO<sub>2</sub>  
3: CH<sub>4</sub>  
4: H<sub>2</sub>  
5: N<sub>2</sub>

Record SELEC.2 introduces parameters for functional dependence of permeability on solid saturation

- Format (8E10.4)  
FE(1), FE(2)  
FE(1) parameter  $\gamma$  (for IE(11)=1); parameter  $\phi_r$  (for IE(11) = 2, 3)  
FE(2) parameter  $\Gamma$  (for IE(11) = 2, 3)

## 7. User Features

### 7.1 Initial Conditions and Restarting

Flow systems are initialized by assigning a complete set of primary thermodynamic variables to all grid blocks into which the flow domain is discretized. Various options are available in a hierarchical system, as follows. During the initialization of a TOUGH2 run, all grid blocks are first assigned to default thermodynamic conditions specified in data block PARAM. The defaults can be overwritten for selected reservoir domains by assigning domain-specific conditions in data block INDOM. These in turn may be superseded by thermodynamic conditions assigned to individual grid blocks in data block INCON. A disk file INCON written to the same specifications as data block INCON may also be used.

Different EOS-modules use different sets of primary variables, and some EOS-modules allow a choice of primary variables for initialization. For a given EOS-module, the primary variables used depend on the fluid phase composition. During phase change primary variables will be automatically switched from one set to another. In multiphase flow systems, therefore, different grid blocks will in general have different sets of primary variables, and must be initialized accordingly.

For many applications, special initial conditions are needed, such as gravity-capillary equilibrium, or steady state corresponding to certain mass and heat flows. This can be realized by performing a series of TOUGH2 runs, in which thermodynamic conditions obtained in one run, and written to disk file SAVE, are used as initial conditions in a subsequent continuation run. For example, in a geothermal reservoir simulation a first run may be made to obtain hydrostatic pressure conditions. These may subsequently be used as boundary conditions in a second run segment to simulate undisturbed natural state conditions with throughflow of mass and heat. This could be followed by a third run segment with fluid production and injection. Restarting of a TOUGH2 run is accomplished by providing file SAVE generated in a previous run as file INCON for initialization. Usually additional (often minor) adjustments will be made for a restart. For example, different specifications for the number of time steps and desired printout times may be made. Some editing of the MESH file may be needed to make certain grid blocks inactive, so that previously calculated pressures can serve as boundary conditions (see below). In a continuation run, simulation time and time step counters may be continuously incremented, or they may be reset to zero. For example, the latter option will be used when simulating production and injection operations following preparation of a “natural” initial state, which may correspond to a large simulation time.

As far as the internal workings of the code is concerned, there is no difference between a fresh start of a simulation and a restart. The only feature that makes a simulation a continuation run is that the INCON-data were generated by a previous TOUGH2 run, rather than having them explicitly provided by the user. File SAVE always ends with a data record with ‘+++’ in the first three columns, followed by one record with restart information (time step and iteration counters, simulation time). To reset all counters to zero, users should simply replace the ‘+++’ with a blank record when using SAVE as file INCON for another TOUGH2 run.

## 7.2 Boundary Conditions and “Inactive” Elements

Boundary conditions can be of two basic types. Dirichlet conditions prescribe thermodynamic conditions, such as pressure, temperature, etc. on the boundary, while Neumann conditions prescribe fluxes of mass or heat crossing boundary surfaces. A special case of Neumann boundary conditions is “no flux,” which in the integral finite difference framework is handled with simplicity itself, namely, by not specifying any flow connections across the boundary. More general flux conditions are prescribed by introducing sinks or sources of appropriate strength into the elements adjacent to the boundary.

Dirichlet conditions can be implemented by assigning very large volumes (e.g.,  $V = 10^{50}$  m<sup>3</sup>) to grid blocks adjacent to the boundary, so that their thermodynamic conditions do not change at all from fluid or heat exchange with finite-size blocks in the flow domain. In addition, a small value (such as  $D = 10^{-9}$  m) should be specified for the nodal distance of such blocks, so that boundary conditions are in fact maintained in close proximity to the surface where they are desired, and not at some distance from it. It is possible to specify a nodal distance that is outright zero; however, this throws certain switches in subroutine MULTI for assignment of interface mobilities that are intended for modeling of fracture-matrix interaction. Therefore, assigning  $D = 0$  should be used with caution.

Time-dependent Neumann conditions can be specified by making sink and source rates time dependent. Time-dependent Dirichlet conditions can also be implemented; these are realized by placing appropriate sinks or sources in the boundary blocks (Moridis and Pruess, 1992). As an example, consider a laboratory experiment reported by Kruger and Ramey (1974) that involved flashing (vaporizing) flow from a sandstone core, with a time-dependent gas pressure boundary condition

$$P_b = P_0 + P_1 t + P_2 t^2 \quad (25)$$

maintained at the outflow end. According to the ideal gas law, the pressure behavior of Eq. (25) can be associated with a time-dependent gas inventory of mass  $M_b$  in a volume  $V$  as follows.

$$M_b = P_b(mV / RT) \quad (26)$$

where  $m$  is the molar weight of the gas,  $R$  the universal gas constant, and  $T$  absolute temperature. The required time dependence of  $M_b$  can be realized by means of a sink/source rate

$$Q_b = dM_b / dt = (mV / RT) dP_b / dt = (mV / RT)(P_1 + 2P_2 t) \quad (27)$$

Therefore, the desired boundary condition can be implemented by means of a grid block with volume  $V$  that is initialized in single-phase gas (e.g., air) conditions, with pressure  $P_0$ , and with a time-dependent sink/source term given by Eq. (27) that would be specified through tabular generation data. In order for the pressure conditions in this block to be negligibly affected by heat and mass exchange with the flow domain, the volume  $V$  should be made very large, e.g.,  $V = 10^{50}$  m<sup>3</sup>, just as for time-independent Dirichlet boundary conditions. The time dependent generation rates from Eq. (27) will then also be very large. The same approach as just outlined for a time-dependent gas pressure boundary can be used to realize other time-dependent Dirichlet conditions, such as prescribed temporal variation of temperature, capillary pressure, and others.

For time-independent Dirichlet boundary conditions, TOUGH2 offers an alternative and more elegant implementation, which provides savings in computational work along with added user conveniences in running simulation problems. This is accomplished with the simple device of “active” and “inactive” elements. By convention, elements encountered in data block ELEME” (or in geometry files MESH or MINC) are taken to be active until the first element entry with a zero or negative volume is encountered. The first element with volume less than or equal to zero, and all subsequent elements, are by convention taken to be inactive. For the inactive elements no mass or energy balance equations are set up, their primary thermodynamic variables are not included in the list of unknowns, and their thermodynamic conditions will remain unchanged. Inactive elements can appear in flow connections and initial condition specifications like all other elements. The computational overhead of inactive elements is small because they do not increase the number of equations to be solved in a flow problem. The easiest way to declare selected grid blocks inactive is to use a text editor to move them to the end of the ELEME data block, and then insert a dummy grid block of zero volume in front of them.

### 7.3 Sinks and Sources

Sinks and sources are introduced through data block GENER in the input file. Several options are available for specifying the production ( $q < 0$ ) or injection ( $q > 0$ ) of fluids and heat. Any of the mass components may be injected in an element at a constant rate, or at time-dependent rates that may be prescribed through user-defined tables. The specific enthalpy of the injected fluid may be specified by the user as either a constant or time dependent value. Heat sources/sinks (with no mass injection) may be either constant or time-dependent.

Fluid production from an element may be handled by prescribing a constant or time-dependent mass rate. In this case, the phase composition of the produced fluid may be determined by the relative phase mobilities in the source element. Alternatively, the produced phase composition may be specified to be the same as the phase composition in the producing element. In either case, the mass fractions of the components in the produced phases are determined by the corresponding component mass fractions in the producing element. Different options are available for interpolating time-dependent rates from user-supplied tabular data; these may be selected through parameter MOP(12).

#### *Deliverability Model*

Production wells may operate on deliverability against a prescribed flowing bottomhole pressure,  $P_{wb}$ , with a productivity index PI (Coats, 1977). With this option, the mass production rate of phase  $\beta$  from a grid block with phase pressure  $P_\beta > P_{wb}$  is (see Appendix A for notation)

$$q_\beta = \frac{k_{r\beta}}{\mu_\beta} \rho_\beta \cdot PI \cdot (P_\beta - P_{wb}) \quad (28).$$

For steady radial flow the productivity index is given by (Coats, 1977; Thomas, 1982)

$$(PI)_l = \frac{2\pi(k\Delta z_l)}{\ln(r_e/r_w) + s - 1/2} \quad (29)$$

Here,  $\Delta z_l$  denotes the layer thickness,  $(k\Delta z)_l$  is the permeability-thickness product in layer  $l$ ,  $r_e$  is the grid block radius,  $r_w$  is the well radius, and  $s$  is the skin factor. If the well is producing from a grid block which does not have cylindrical shape, an approximate PI can be computed by using an effective radius

$$r_e = \sqrt{A/\pi} \quad (30)$$

where  $A$  is the grid block area; e.g.,  $A = \Delta x \cdot \Delta y$  for an areal Cartesian grid. More accurate expressions for specific well patterns and grid block shapes have been given in the literature (e.g., Peaceman, 1977, 1982; Coats and Ramesh, 1982).

The rate of production for mass component  $\kappa$  is

$$\hat{q}^\kappa = \sum_\beta X_\beta^\kappa q_\beta \quad (31)$$

For wells which are screened in more than one layer (element), the flowing wellbore pressure  $P_{wb}$  can be corrected to approximately account for gravity effects according to the depth-dependent flowing density in the wellbore. Assume that the open interval extends from layer  $l = 1$  at the bottom to  $l = L$  at the top. The flowing wellbore pressure in layer  $l$ ,  $P_{wb,l}$ , is obtained from the wellbore pressure in layer  $l + 1$  immediately above it by means of the following recursion formula

$$P_{wb,l} = P_{wb,l+1} + \frac{g}{2} (\rho_l^f \Delta z_l + \rho_{l+1}^f \Delta z_{l+1}) \quad (32)$$

Here,  $g$  is acceleration of gravity, and  $\rho_l^f$  is the flowing density in the tubing opposite layer  $l$ . Flowing densities are computed using a procedure given by Coats (private communication, 1982). If wellbore pressure were zero, we would obtain the following volumetric production rate of phase  $\beta$  from layer  $l$ .

$$r_{l,\beta} = \left( \frac{k_{\beta}}{\mu_\beta} \right)_l (PI)_l P_{l,\beta} \quad (33)$$

The total volumetric flow rate of phase  $\beta$  opposite layer  $l$  is, for zero wellbore pressure

$$r_{l,\beta}^T = \sum_{m=1}^l r_{m,\beta} \quad (34)$$

From this we obtain an approximate expression for flowing density opposite layer  $l$  which can be used in Eq. (32).

$$\rho_l^f = \sum_\beta \rho_{l,\beta} r_{l,\beta}^T / \sum_\beta r_{l,\beta}^T \quad (35)$$

During fluid production or injection, the rate of heat removal or injection is determined by

$$\hat{q}^h = \sum_{\beta} q_{\beta} h_{\beta} \quad (36)$$

where  $h_{\beta}$  is the specific enthalpy of phase  $\beta$ .

### **Coupled Wellbore Flow**

Geothermal production wells typically operate at (nearly) constant wellhead pressures. As flow rate and flowing enthalpy change with time, wellbore pressure gradients and flowing bottomhole pressures will also change. From a conceptual point of view, the most straightforward way to describe production from geothermal wells is to set up and solve equations for flow in the reservoir and flow in the wellbore in a fully coupled manner. This approach was taken by Hadgu et al. (1995) who coupled the reservoir simulator TOUGH (Pruess, 1987) with the wellbore simulator WFS (Hadgu and Freeston, 1990).

As discussed by Murray and Gunn (1993), an alternative approach may be preferable in which the wellbore and reservoir simulations are performed separately. This can be accomplished by running a wellbore flow simulator prior to the reservoir simulation for a range of flow rates  $q$  and flowing enthalpies  $h$ , in order to generate a table of flowing bottomhole pressures  $P_{wb}$ .

$$P_{wb} = P_{wb}(q, h; P_{wh}, z, r_w) \quad (37)$$

In addition to the functional dependence on  $q$  and  $h$ , flowing bottomhole pressure is dependent on a number of well parameters. These include wellhead pressure  $P_{wh}$ , feed zone depth  $z$ , wellbore radius  $r_w$ , friction factors, and possibly others. By interpolating on these tabular data, Eq. (37) can be directly inserted into the well source term, Eq. (28). Reservoir flow equations that include a quasi-steady approximation to wellbore flow can then be solved with little added computational expense compared to the case where no wellbore flow effects are considered. Advantages of representing wellbore flow effects through tabular data include increased robustness and calculational efficiency. It also makes it possible to use different wellbore simulators and two-phase flow correlations without any programming changes in the reservoir simulation code.

We have incorporated a tabular interpolation scheme for dynamic changes of flowing bottomhole pressure into TOUGH2. Flowing enthalpy at the well feed is known from phase

mobilities and enthalpies calculated by the reservoir simulator. The unknown well flow rate and flowing bottomhole pressure are obtained by Newton-Raphson iteration on

$$R(q) = q - \left( \sum \frac{k_{r\beta}}{\mu_\beta} \rho_\beta \right) \cdot PI \cdot (P - P_{wb}(q, h)) = 0 \quad (38)$$

The iterative solution of Eq. (38) was embedded in the outer (Newtonian) iteration performed by TOUGH2 on the coupled mass and heat balance equations. Additional computational work in comparison to conventional simulations with constant downhole pressure is insignificant.

Coupled wellbore flow is invoked in a TOUGH2 simulation by specifying a GENER-type starting with the letters 'F' or 'f'. For example, 'f725d' is a valid GENER-type that will associate the host element with a production well. If this is specified, then the user must supply a disk file named f725d with appropriately formatted data that relate wellhead to flowing bottomhole pressures. Several wells may use the same wellbore pressure table, and multiple data sets for flowing wellbore pressures may be used, e.g., for wells with different diameter, feed zone depth, and wellhead pressure. The well table(s) must be generated by wellbore simulation prior to a TOUGH2 run as ASCII data of 80 characters per record, as follows (see the example given in Table 17). The first record is an arbitrary title. The second record holds the number of flow rate and flowing enthalpy data (table points), NG and NH, respectively, in Format 2I5; in Table 17 we have NG=11, NH=9. This is followed by NG flow rate data in format 8E10.4, and NH enthalpy data also in format 8E10.4. After this come NG sets of NH flowing bottomhole pressure data in format 8E10.4. The data in Table 17 were generated with the HOLA wellbore simulator (Aunzo et al., 1991) for a 0.2 m ( $\approx$  8 inch) inside diameter well of 1,000 m feed zone depth with 7 bars wellhead pressure. Formation temperature for the conductive heat loss calculation in HOLA was assumed to increase linearly from 25 °C at the land surface to 275.5 °C at 750 m depth. Flow rates cover the range from 0.5 to 90.5 kg/s, and flowing enthalpies cover the range from 1,000 to 1,400 kJ/kg. A data record with very large bottomhole pressures of 55.55 MPa was added by hand for a very large hypothetical rate of 1,000 kg/s. This was done to avoid rates going out of table range during Newton-Raphson iteration in a TOUGH2 flow simulation, which results in more robust time stepping behavior, see section 9.5. A contour plot of Table 17 appears in Fig. 10.

The coupled wellbore flow capability as coded in TOUGH2 is limited to wells with a single feed zone and can only handle wellbore pressure effects from changing flow rates and enthalpies. Effects from changing fluid composition, as e.g. variable non-condensable gas content, are not modeled at present.

```

*f725d* - (q,h) from ( .5000E+00, .1000E+07) to ( .9050E+02, .1400E+07)
   11      9
.5000E+00 .1050E+02 .2050E+02 .3050E+02 .4050E+02 .5050E+02 .6050E+02 .7050E+02
.8050E+02 .9050E+02          1.e3
.1000E+07 .1050E+07 .1100E+07 .1150E+07 .1200E+07 .1250E+07 .1300E+07 .1350E+07
.1400E+07
.1351E+07 .1238E+07 .1162E+07 .1106E+07 .1063E+07 .1028E+07 .9987E+06 .9740E+06
.9527E+06
.1482E+07 .1377E+07 .1327E+07 .1299E+07 .1284E+07 .1279E+07 .1279E+07 .1286E+07
.1292E+07
.2454E+07 .1826E+07 .1798E+07 .1807E+07 .1835E+07 .1871E+07 .1911E+07 .1954E+07
.1998E+07
.4330E+07 .3199E+07 .2677E+07 .2280E+07 .2322E+07 .2376E+07 .2434E+07 .2497E+07
.2559E+07
.5680E+07 .4772E+07 .3936E+07 .3452E+07 .2995E+07 .2808E+07 .2884E+07 .2967E+07
.3049E+07
.6658E+07 .5909E+07 .5206E+07 .4557E+07 .4158E+07 .3746E+07 .3391E+07 .3402E+07
.3511E+07
.7331E+07 .6850E+07 .6171E+07 .5627E+07 .5199E+07 .4814E+07 .4465E+07 .4208E+07
.3957E+07
.7986E+07 .7548E+07 .7140E+07 .6616E+07 .6256E+07 .5908E+07 .5634E+07 .5399E+07
.5128E+07
.8621E+07 .8177E+07 .7820E+07 .7560E+07 .7234E+07 .6814E+07 .6624E+07 .6385E+07
.6254E+07
.8998E+07 .8732E+07 .8453E+07 .8124E+07 .7925E+07 .7671E+07 .7529E+07 .7397E+07
.7269E+07
.5555e+08 .5555e+08 .5555e+08 .5555e+08 .5555e+08 .5555e+08 .5555e+08 .5555e+08
.5555e+08

```

Table 17. Flowing bottomhole pressures (in Pa) at 1000 m feed zone depth for a well of 20 cm ( $\approx$  8 inch) inside diameter producing at 7 bar wellhead pressure (calculated from HOLA; Aunzo et al., 1991).

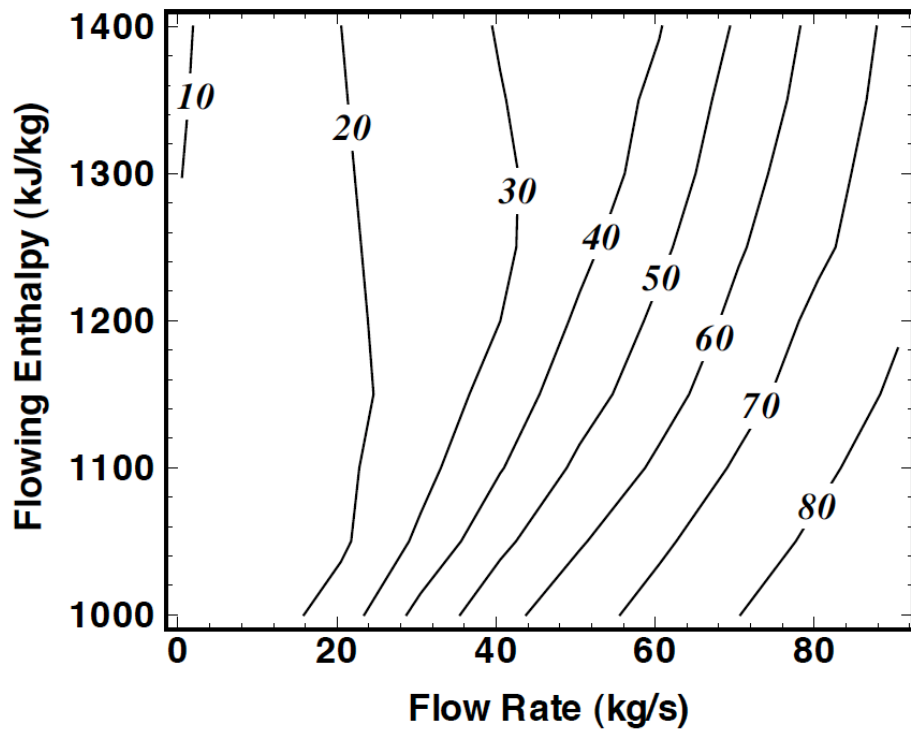


Figure 10. Contour plot of flowing bottomhole pressures, in bars (from Table 17).

## 7.4 Heat Exchange with Confining Beds

One possible approach for modeling heat exchange with confining beds is to simply extend the computational grid into the cap- and base-rock, which would be given small or vanishing permeability. This way heat exchange would be treated no different than flow in the reservoir. A drawback of this approach is that even for modest accuracy requirements, the number of grid blocks in the heat flow domain could easily become comparable to, or even larger than, the number of grid blocks in the reservoir, leading to a very inefficient calculation. A much more efficient alternative is application of a semi-analytical method, which requires no grid blocks outside of the fluid flow domain, and permits better accuracy for short- and long-term heat exchange. TOUGH2 provides an option to use the method of Vinsome and Westerveld (1980), which gives excellent accuracy for heat exchange between reservoir fluids and confining beds such as may arise in geothermal injection and production operations.

Observing that the process of heat conduction tends to dampen out temperature variations, Vinsome and Westerveld suggested that cap- and base-rock temperatures would vary smoothly even for strong and rapid temperature changes at the boundary of the conduction zone. Arguing that heat conduction perpendicular to the conductive boundary is more important than parallel to it, they proposed to represent the temperature profile in a semi-infinite conductive layer by means of a simple trial function, as follows:

$$T(x,t) - T_i = (T_f - T_i + px + qx^2) \exp(-x/d) \quad (39)$$

Here  $x$  is the distance from the boundary,  $T_i$  is initial temperature in cap-or base-rock (assumed uniform),  $T_f$  is the time-varying temperature at the cap- or base-rock boundary,  $p$  and  $q$  are time-varying fit parameters, and  $d$  is the penetration depth for heat conduction, given by

$$d = \sqrt{\Theta t} / 2 \quad (40)$$

where  $\Theta = \lambda/\rho C$  is the thermal diffusivity,  $\lambda$  the thermal conductivity,  $\rho$  the density of the medium, and  $C$  the specific heat. In the context of a finite-difference simulation of nonisothermal flow, each grid block in the top and bottom layers of the computational grid will have an associated temperature profile in the adjacent impermeable rock as given by Eq. (39). The coefficients  $p$  and  $q$  will be different for each grid block; they are determined concurrently with the flow simulation from the physical constraints of (1) continuity of heat flux across the boundary, and (2) energy conservation for the reservoir/confining layer system.

There is no separate input data block for specifying a semi-analytical heat exchange calculation. Instead, a number of parameters have to be specified in different blocks to engage this option, as follows. A semi-analytical heat loss calculation will be performed only when the parameter MOP(15) in record PARAM.1 is set equal to 1. Initial temperature as well as heat capacity and conductivity of the confining beds are specified by means of data provided for the very last volume element in data block ELEME. The initial temperature is taken as the temperature with which the last element is initialized. Heat capacity and conductivity are taken from data provided in block ROCKS for the particular domain to which the last element belongs. Thus, if a semi-analytical heat exchange calculation is desired, the user would append an additional inactive element in block ELEME, and provide the desired parameters as initial conditions and domain data, respectively, for this element. Finally, it is necessary to specify which elements have an interface area with the confining beds, and to give the magnitude of this interface area. This information is input as parameter AHTX in columns 31-40 of volume element data in block ELEME. Volume elements for which a zero-interface area is specified will not be subject to heat exchange.

At the termination of a run the data necessary for continuing the heat exchange calculation in a TOUGH2 continuation run are written onto a disk file TABLE. When restarting a problem, this file has to be provided under the name TABLE. If file TABLE is absent, TOUGH2 assumes that no prior heat exchange with confining beds has taken place, and takes their temperatures to be uniform and equal to the temperature of the very last volume element in block ELEME. An example of the application of a semi-analytical treatment for heat exchange is given in sample problem 3.

## 7.5 Block-by-block Permeability Modification

In previous versions of TOUGH2, heterogeneous flow systems could be specified by providing domains with different hydrogeologic properties, and associating different grid blocks with different domains. Version 2 provides a new feature that applies permeability modification (PM) coefficients for individual grid blocks according to

$$k_n \rightarrow k'_n = k_n \cdot \zeta_n \quad (41)$$

Here,  $k_n$  is the absolute (“reference”) permeability of grid block n, as specified in data block ROCKS for the domain to which that grid block belongs, while  $\zeta_n$  is the permeability modification coefficient. The strength of capillary pressure will be automatically scaled according to (Leverett, 1941)

$$P_{cap,n} \rightarrow P'_{cap,n} = P_{cap,n} / \sqrt{\zeta_n} \quad (42)$$

A new subroutine PMIN was written which is called in RFILE after all MESH data have been processed. PMIN initializes permeability modifiers and generates informative printout. To engage block-by-block permeability modification, users need to specify a (dummy) domain named ‘SEED’ in block ROCKS. No grid blocks should be assigned to this domain; the presence of domain ‘SEED’ simply serves as a flag to put permeability modification into effect, while data provided in domain ‘SEED’ serve to select different options. Random (spatially uncorrelated) PM data can be internally generated in TOUGH2. Alternatively, externally defined permeability modifiers may be provided as part of the geometry data in block ELEME. This feature can be used to apply spatially correlated fields: users can run their own geostatistical package to generate whatever fields they desire, and then use a preprocessing program to place the PM-coefficients into the ELEME data block.

Note that as presently implemented the block-by-block permeability modification affects only grid block permeabilities but not porosities. Full details on the various user options for PM-coefficients are given in informative printout that is automatically generated with each TOUGH2 run. Sample problem 11 (section 9.11) illustrates the use of different permeability modification options.

## 7.6 Linear Equation Solvers

The computational work to be performed in the course of a TOUGH2 simulation includes evaluation of thermophysical properties for all grid blocks, assembly of the vector of residuals and the Jacobian matrix, and solution of the linear equation system for each Newton-Raphson iteration step. Except for small problems with just a few grid blocks, the most computationally intensive of these different tasks is the solution of the linear equation system. TOUGH2 offers a choice of direct or iterative methods for linear equation solution; technical details of the methods and their performance can be found in (Moridis and Pruess, 1998).

The most reliable linear equation solvers are based on direct methods, while the performance of iterative techniques tends to be problem-specific and lacks the predictability of direct solvers. The robustness of direct solvers comes at the expense of large storage requirements and execution times that typically increase with problem size  $N$  (= number of equations solved) proportional to  $N^3$ . In contrast, iterative solvers have much lower memory requirements, and their computational work will increase much less rapidly with problem size, approximately proportional to  $N^\omega$ , with  $\omega \approx 1.4 - 1.6$  (Moridis and Pruess, 1995). For large problems and especially 3-D problems with several thousand grid blocks or more, iterative conjugate gradient (CG) type solvers are therefore the method of choice.

The default linear equation solution technique in TOUGH2 uses DSLUCS, a Lanczos-type bi-conjugate gradient solver, with incomplete LU-factorization as preconditioner. Users need to beware that iterative methods can be quite “fickle” and may fail for matrices with special features, such as many zeros on the main diagonal, large numerical range of matrix elements, and nearly linearly dependent rows or columns. Depending on features of the problem at hand, appropriate matrix preconditioning may be essential to achieve convergence. Poor accuracy of the linear equation solution will lead to deteriorated convergence rates for the Newtonian iteration, and an increase in the number of iterations for a given time step. In severe cases, time steps may fail with residuals either stagnating or wildly fluctuating. Information on the convergence of the linear equation solution is written to disk file LINEQ, which may be examined with any text editor. Users experiencing difficulties with the default settings are encouraged to experiment with the various solvers and preconditioners included in the TOUGH2 package.

The different linear equation solvers included in the TOUGH2 package can be selected by means of parameter MOP(21) in data record PARAM.1, as follows.

MOP(21) = 1: (void)

MOP(21) = 2: DSLUBC, a bi-conjugate gradient solver

MOP(21) = 3: DSLUCS, a Lanczos-type bi-conjugate gradient solver

MOP(21) = 4: DSLUGM, a generalized minimum residual solver

MOP(21) = 5: DLUSTB, a stabilized bi-conjugate gradient solver

MOP(21) = 6: direct solver LUBAND

All iterative solvers selected by means of MOP(21) use incomplete LU-factorization as a preconditioner. Alternative preconditioners and iteration parameters can be selected by means of an optional data block SOLVR in the TOUGH2 input file. If SOLVR is present, its specifications will override the choices made by MOP(21). The default preconditioning with SOLVR is also incomplete LU-factorization. The SOLVR block includes a single data record, as follows.

**SOLVR** keyword to introduce a data block with parameters for linear equation solvers.

Record SOLVR.1

Format (I1,2X,A2,3X,A2,2E10.4)

MATSLV, ZPROCS, OPROCS, RITMAX, CLOSUR

MATSLV      selects the linear equation solver

1: (void)

2: DSLUBC

3: DSLUCS

4: DSLUGM

5: DLUSTB

6: LUBAND

ZPROCS      selects the Z-preconditioning (Moridis and Pruess, 1998). Regardless of user specifications, Z-preprocessing will only be performed when iterative solvers are used ( $2 \leq \text{MATSLV} \leq 5$ ), and if there are zeros on the main diagonal of the Jacobian matrix.

Z0: no Z-preprocessing (default for NEQ=1)

Z1: replace zeros on the main diagonal by a small constant (1.e-25; default for NEQ ≠ 1))

Z2: make linear combinations of equations for each grid block to achieve

	non-zeros on the main diagonal
Z3:	normalize equations, followed by Z2
Z4:	affine transformation to unit main-diagonal submatrices, without center pivoting
OPROCS	selects the O-preconditioning (Moridis and Pruess, 1998).
O0:	no O-preprocessing (default, also invoked for NEQ=1)
O1:	eliminate lower half of the main-diagonal submatrix with center pivoting
O2:	O1, plus eliminate upper half of the main-diagonal submatrix with center pivoting
O3:	O2, plus normalize, resulting in unit main-diagonal submatrices
O4:	affine transformation to unit main-diagonal submatrices, without center pivoting
RITMAX	selects the maximum number of CG iterations as a fraction of the total number of equations ( $0.0 < \text{RITMAX} \leq 1.0$ ; default is RITMAX = 0.1)
CLOSUR	convergence criterion for the CG iterations ( $1.\text{e-}12 \leq \text{CLOSUR} \leq 1.\text{e-}6$ ; default is CLOSUR = 1.e-6)

The newly added solver DLUSTB implements the BiCGSTAB(m) algorithm (Sleijpen and Fokkema, 1993), an extension of the BiCGSTAB algorithm of van der Vorst (1992). DLUSTB provides improved convergence behavior when iterations are started close to the solution, i.e., near steady state. The new preconditioning algorithms can cope with difficult problems in which many of the Jacobian matrix elements on the main diagonal are zero. An example is “two-waters” problems with EOS1 in which typically 2/3 of the elements in the main diagonal are zero. Our tests show that this type of problem can be solved by means of Z2 or Z3 preconditioning (Moridis and Pruess, 1998).

## 8. Output from TOUGH2

TOUGH2 produces a variety of printed output, most of which can be controlled by the user. Information written in the initialization phase to the standard output file includes PARAMETER settings in the main program for dimensioning of problem-size dependent arrays, and disk files in use. This is followed by documentation on block-by-block permeability modification, on settings of the MOP-parameters for choosing program options, and on the EOS-module. During execution TOUGH2 can optionally generate a brief printout for Newtonian iterations and time steps. Standard output at user-specified simulation times or time steps is generated by a subroutine OUT (each EOS module comes with its own routine OUT). This output provides some time-stepping information, and a complete element-by-element report of thermodynamic state variables and other important parameters. Additional optional output is available on mass and heat flow rates and velocities, and on diffusive fluxes of components in phases. Changes in thermodynamic state variables during a time step may also be printed. Examples of TOUGH2-output are reproduced in section 9, most of which should be self-explanatory. There are some minor differences in naming conventions used by different EOS-modules. Here we summarize the main output parameters in alphabetical order.

DELTEX	time step size, seconds
DG	gas phase density, kg/m <sup>3</sup>
DL	liquid (aqueous phase) density, kg/m <sup>3</sup>
DT	time step size, seconds
DW	water (aqueous phase) density, kg/m <sup>3</sup>
DX1, DX2, etc.	changes in first, second, etc. thermodynamic variable
DX1M, DX2M, DX3M	maximum change in first, second, and third primary variable in current time step
ELEM	code name of element
ELEM1, ELEM2	code name of first and second element, respectively, in a flow connection
ENTHALPY	flowing specific enthalpy for mass sinks/sources, J/kg
FF(GAS), FF(LIQ)	mass fraction of flow in gas and liquid phases, respectively (mass production wells only)
FLO(BRINE)	total rate of brine flow, kg/s (positive if from ELEM2 into ELEM1)
FLOF	total rate of fluid flow, kg/s (positive if from ELEM2 into ELEM1)
FLO(GAS)	total rate of gas flow, kg/s (positive if from ELEM2 into ELEM1)

FLOH	total rate of heat flow, W (positive if from ELEM2 into ELEM1)
FLO(LIQ)	total rate of liquid (aqueous phase) flow, kg/s (positive if from ELEM2 into ELEM1)
GENERATION RATE	sink ( $> 0$ ) or source ( $< 0$ ) rate, kg/s (mass), W (heat)
INDEX	internal indexing number of elements, connections, sinks/sources
ITER	number of Newtonian iterations in current time step
ITERC	total cumulative number of Newtonian iterations in simulation run
KCYC	time step counter
KER	index number of equation with largest residual
K(GAS)	gas phase relative permeability
K(LIQ)	liquid (aqueous) phase relative permeability
KON	convergence flag; KON = 2: converged; KON = 1: not converged
MAX. RES.	maximum (relative) residual in any of the mass and energy balance equations (see Eq. B.8)
NER	index number of element (grid block) with largest residual
P	pressure, Pa
PER.MOD.	permeability modification coefficient
PCAP	capillary pressure, Pa
PSAT	saturated vapor pressure, Pa
P(WB)	flowing bottomhole pressure (production wells on deliverability only), Pa
SG	gas saturation
SL	liquid saturation
SOURCE	code name of sink/source
ST	simulation time, in seconds
SW	water (aqueous phase) saturation
T	temperature, °C
TOTAL TIME	simulation time, in seconds
VAPDIF	diffusive vapor flow rate, kg/s (positive if from ELEM2 into ELEM1)
VEL(GAS)	gas phase pore velocity, m/s (positive if from ELEM2 into ELEM1)
VEL(LIQ)	liquid (aqueous) phase pore velocity, m/s (positive if from ELEM2 into ELEM1)

VIS(LIQ)	liquid (aqueous) phase viscosity, $P_a \cdot s$
X1, X2, etc.	first, second, etc. thermodynamic variable (also: water 1, water 2)
XAIRG	mass fraction of air in gas phase
XAIRL	mass fraction of air in liquid phase
XBRINE	brine mass fraction
XRN1	mass fraction of radionuclide 1
XRN2	mass fraction of radionuclide 2

Time series of some parameters for plotting can optionally be written to files FOFT (for elements), COFT (for connections), and GOFT (for sinks and sources). These files are written in subroutine FGTAB, called from and following CYCIT. At present there are no input options to select the parameters to be written out in FGTAB; users desiring different parameters than what is coded in FGTAB should modify that subroutine.

## **9. Sample Problems**

In this section we present and discuss a number of sample problems for TOUGH2. Our emphasis is on demonstrating preparation of input data and illustrating code capabilities to provide benchmarks for proper code installation. Accordingly, most of the problems consist of small and often coarse grid systems. Users are reminded that, for accurate solution to flow problems, careful attention needs to be given to issues of space discretization and time step control. Numerous verification and validation exercises performed with the various TOUGH2 modules are available in separate reports (e.g., Moridis and Pruess, 1992, 1995; Pruess et al., 1996). These demonstrate that the code can obtain accurate solutions to physically and mathematically well-posed problems, and can successfully describe laboratory experiments and field observations on fluid flow and heat transfer processes.

In addition to their primary purpose of documenting and benchmarking code applications, the input data files can also be used as templates to facilitate preparation of input data for new flow problems. We envisage that a user rarely if ever will assemble a new input file from scratch; instead (s)he will modify an existing input file to suit a new application.

In the data records for keywords (such as ROCKS, PARAM, etc.) in TOUGH2 input files, only the first 5 characters are read. As seen in the input files for the sample problems, below, we have adopted a convention of writing column counters following the keywords. This is done as a convenience to facilitate alignment of the fixed-format data with data fields.

## 9.1 Problem No. 1 (\*sam1\*) - Code Demonstration and Comparison with TOUGH (EOS3)

This problem is similar to sample problem 1 from the TOUGH User's Guide (Pruess, 1987) and can serve as a check on proper installation of TOUGH2 as well as for cross-referencing to TOUGH. It uses EOS3 and demonstrates various initialization options and generation specifications. A number of one- and two-element subproblems are simulated which are entirely independent of each other (no flow connections between subproblems), except that being run together they all must go through the same sequence of time steps. The sub-problems perform flow

```

*sam1* CODE DEMONSTRATION: PHASE TRANSITIONS, COMPONENT (DIS-)APPEARANCES
ROCKS---1----*---2---*---3---*---4---*---5---*---6---*---7---*---8
TRANS      2650.      .50      1.E-14                      2.10      1000.
SHOME     2       2650.      .50      1.E-14                      2.10      1000.
                  1.8      .1
            3       .40      .10
            1       1.E5      .2       1.

START---1----*---2---*---3---*---4---*---5---*---6---*---7---*---8
-----*---1 MOP: 123456789*123456789*1234 -----*---5---*---6---*---7---*---8
PARAM---1----*---2---*---3---*---4---*---5---*---6---*---7---*---8
      2       4       1100 30 000000200711
                  -1.          F   1
            1.E2      5.E3

                  45.E5      .5      250.
FOFT ---1----*---2---*---3---*---4---*---5---*---6---*---7---*---8
F   1
abc 2
F   7

GOFT ---1----*---2---*---3---*---4---*---5---*---6---*---7---*---8
F   2
f   1
SHO 9
SHO 2
F   8

RPCAP---1----*---2---*---3---*---4---*---5---*---6---*---7---*---8
      3       .30      .05
      1           1.

TIMES---1----*---2---*---3---*---4---*---5---*---6---*---7---*---8
      1       3       2.E3
      1.E3

ELEME---1----*---2---*---3---*---4---*---5---*---6---*---7---*---8
F   1       9       1TRANS      10.
SHO 1       9       1SHOME      10.
SHO11      1       1SHOME      1.E4

CONNE---1----*---2---*---3---*---4---*---5---*---6---*---7---*---8
F   1F   2           1       5.      5.      1.
F   3F   4           1       5.      5.      1.
F   5F   6           1       5.      5.      1.

```

Figure 11. TOUGH2 input file (first part) for sample problem 1 - code demonstration.

```

INCON---1----*----2----*----3----*----4----*----5----*----6----*----7----*----8
F   1           1.E5          20.          1.
F   2           1.E6          170.          0.
F   3           1.E5          .001         99.5
F   4           99.E5         .999         310.
F   5           1.E6          100.          0.
F   6           10.E6         100.          1.
F   7           1.E5          20.          0.
F   8           1.E7          300.          0.
F   9           1.E5          .99          90.
F  10          40.E5          280.          0.
SH011          50.E5          240.
SH012          40.E5          100.

GENER---1----*----2----*----3----*----4----*----5----*----6----*----7----*----8
f   1AIR          AIR          5.E-3        9.882E4
F   7AIR          AIR          5.E-3        9.882E4
F   8WEL          MASS         -1.5E-2
F   9HOT          HEAT         2.E6
F   10COL         HEAT         -5.E5
SHO 1P  1          MASS1        -1.          1.E6
SHO 2P  2          laff         -1.
SHO 3P  3  2  1  1  4  MASS
      0.           1.E2          2.E2          4.E3
      -0.1         -0.2          -0.3         -1.1
SHO 6P  6  2  1  0  4  MASS1
      0.           1.E2          2.E2          4.E3
      -0.1         -0.2          -0.3         -1.1
      1.E6         2.E6          3.E6          1.1E7
SHO 9P  9          1            DELV         1.E-12        1.E6
SHO10P 10          4            WATE1
      0.           1.E2          2.E2          3.E3
      1.1           1.0           0.9           0.1
      1.E6         1.2E6         1.4E6         3.0E6
SH011WEL00          2            DELV         1.E-12        1.E2
SH012WEL00          DELV         2.E-12        1.E6        1.E2

ENDCY---1----*----2----*----3----*----4----*----5----*----6----*----7----*----8

```

Figure 11. TOUGH2 input file (first part) for sample problem 1 - code demonstration (continued).

and/or injection and withdrawal of water, air, and heat, with highly nonlinear phase and component (dis-)appearances that engage some subtle numerical procedures. A more detailed description is available in the TOUGH User's Guide. The input file for running with the EOS3 fluid properties module is given in Fig. 11 and is similar to that of TOUGH sample problem 1.

Parameter MOP(19) in the first record of data block PARAM was set equal to 1, to permit initialization of the EOS3 module with TOUGH-style primary variables of (P,T,X) for single phase, (P,S,T) for two-phase. Data blocks FOFT and GOFT are used to generate time series for selected grid blocks and generation items that can be used for plotting. We deliberately made some invalid specifications to demonstrate how the code copes with these by generating informative printout (not shown here; “abc 2” in data block FOFT and “f 1” in GOFT are invalid elements, “F 2” in GOFT does not have a valid GENER-item, and “SHO 2” in block GENER has an invalid generation type “laff”).

Figs. 12 - 15 show the disk files MESH, INCON, GENER, and SAVE generated by the TOUGH2 run, and Fig. 16 gives some of the printed output. The results are virtually identical to those obtained with TOUGH and the previous version of TOUGH2, as they should be. Minor differences occur in the maximum residuals (MAX. RES.) during the iteration process. These residuals, being computed as {left hand side} - {right hand side} of the governing balance equations (B.5), involve increasingly severe numerical cancellations as convergence is approached, and therefore constitute a very sensitive check on the numerics.

ELEME								
F 1	1	.1000E+02	.0000E+00	.0000E+00	.0000E+00	.0000E+00	.0000E+00	
F 2	1	.1000E+02	.0000E+00	.0000E+00	.0000E+00	.0000E+00	.0000E+00	
F 3	1	.1000E+02	.0000E+00	.0000E+00	.0000E+00	.0000E+00	.0000E+00	
F 4	1	.1000E+02	.0000E+00	.0000E+00	.0000E+00	.0000E+00	.0000E+00	
F 5	1	.1000E+02	.0000E+00	.0000E+00	.0000E+00	.0000E+00	.0000E+00	
F 6	1	.1000E+02	.0000E+00	.0000E+00	.0000E+00	.0000E+00	.0000E+00	
F 7	1	.1000E+02	.0000E+00	.0000E+00	.0000E+00	.0000E+00	.0000E+00	
F 8	1	.1000E+02	.0000E+00	.0000E+00	.0000E+00	.0000E+00	.0000E+00	
F 9	1	.1000E+02	.0000E+00	.0000E+00	.0000E+00	.0000E+00	.0000E+00	
F 10	1	.1000E+02	.0000E+00	.0000E+00	.0000E+00	.0000E+00	.0000E+00	
SHO 1	2	.1000E+02	.0000E+00	.0000E+00	.0000E+00	.0000E+00	.0000E+00	
SHO 2	2	.1000E+02	.0000E+00	.0000E+00	.0000E+00	.0000E+00	.0000E+00	
SHO 3	2	.1000E+02	.0000E+00	.0000E+00	.0000E+00	.0000E+00	.0000E+00	
SHO 4	2	.1000E+02	.0000E+00	.0000E+00	.0000E+00	.0000E+00	.0000E+00	
SHO 5	2	.1000E+02	.0000E+00	.0000E+00	.0000E+00	.0000E+00	.0000E+00	
SHO 6	2	.1000E+02	.0000E+00	.0000E+00	.0000E+00	.0000E+00	.0000E+00	
SHO 7	2	.1000E+02	.0000E+00	.0000E+00	.0000E+00	.0000E+00	.0000E+00	
SHO 8	2	.1000E+02	.0000E+00	.0000E+00	.0000E+00	.0000E+00	.0000E+00	
SHO 9	2	.1000E+02	.0000E+00	.0000E+00	.0000E+00	.0000E+00	.0000E+00	
SHO10	2	.1000E+02	.0000E+00	.0000E+00	.0000E+00	.0000E+00	.0000E+00	
SHO11	2	.1000E+05	.0000E+00	.0000E+00	.0000E+00	.0000E+00	.0000E+00	
SHO12	2	.1000E+05	.0000E+00	.0000E+00	.0000E+00	.0000E+00	.0000E+00	
CONNE								
F 1F 2	1	.5000E+01	.5000E+01	.1000E+01	.0000E+00	.0000E+00		
F 3F 4	1	.5000E+01	.5000E+01	.1000E+01	.0000E+00	.0000E+00		
F 5F 6	1	.5000E+01	.5000E+01	.1000E+01	.0000E+00	.0000E+00		
+++	1    2    3    4    5    6							

Figure 12. File MESH for sample problem 1.

```

INCON
F 1 .0000000E+00
  .1000000000000E+06 .2000000000000E+02 .1000000000000E+01
F 2 .0000000E+00
  .1000000000000E+07 .1700000000000E+03 .0000000000000E+00
F 3 .0000000E+00
  .1000000000000E+06 .1000000000000E-02 .9950000000000E+02
F 4 .0000000E+00
  .9900000000000E+07 .9990000000000E+00 .3100000000000E+03
F 5 .0000000E+00
  .1000000000000E+07 .1000000000000E+03 .0000000000000E+00
F 6 .0000000E+00
  .1000000000000E+08 .1000000000000E+03 .1000000000000E+01
F 7 .0000000E+00
  .1000000000000E+06 .2000000000000E+02 .0000000000000E+00
F 8 .0000000E+00
  .1000000000000E+08 .3000000000000E+03 .0000000000000E+00
F 9 .0000000E+00
  .1000000000000E+06 .9900000000000E+00 .9000000000000E+02
F 10 .0000000E+00
  .4000000000000E+07 .2800000000000E+03 .0000000000000E+00
SH011 .0000000E+00
  .5000000000000E+07 .2400000000000E+03 .0000000000000E+00
SH012 .0000000E+00
  .4000000000000E+07 .1000000000000E+03 .0000000000000E+00

```

Figure 13. File INCON for sample problem 1.

```

GENER
f 1AIR 0           1     AIR   .5000E-02 .9882E+05 .0000E+00
F 7AIR 0           1     AIR   .5000E-02 .9882E+05 .0000E+00
F 8WEL 0           1     MASS  -.1500E-01 .0000E+00 .0000E+00
F 9HOT 0           1     HEAT  .2000E+07 .0000E+00 .0000E+00
F 10COL 0          1     HEAT  -.5000E+06 .0000E+00 .0000E+00
SHO 1P  1           1     MASS1-1.000 .1000E+07 .0000E+00
SHO 2P  2           1     laff -1.000 .0000E+00 .0000E+00
SHO 3P  3           4     MASS  .0000E+00 .0000E+00 .0000E+00
               .0000000E+00 .1000000E+03 .2000000E+03 .4000000E+04
               -.1000000E+00 -.2000000E+00 -.3000000E+00 -.1100000E+01
SHO 4P  4           4     MASS  .0000E+00 .0000E+00 .0000E+00
               .0000000E+00 .1000000E+03 .2000000E+03 .4000000E+04
               -.1000000E+00 -.2000000E+00 -.3000000E+00 -.1100000E+01
SHO 5P  5           4     MASS  .0000E+00 .0000E+00 .0000E+00
               .0000000E+00 .1000000E+03 .2000000E+03 .4000000E+04
               -.1000000E+00 -.2000000E+00 -.3000000E+00 -.1100000E+01
SHO 6P  6           4     MASS1 .0000E+00 .0000E+00 .0000E+00
               .0000000E+00 .1000000E+03 .2000000E+03 .4000000E+04
               -.1000000E+00 -.2000000E+00 -.3000000E+00 -.1100000E+01
               .1000000E+07 .2000000E+07 .3000000E+07 .1100000E+08
SHO 7P  6           4     MASS1 .0000E+00 .0000E+00 .0000E+00
               .0000000E+00 .1000000E+03 .2000000E+03 .4000000E+04
               -.1000000E+00 -.2000000E+00 -.3000000E+00 -.1100000E+01
               .1000000E+07 .2000000E+07 .3000000E+07 .1100000E+08
SHO 8P  6           4     MASS1 .0000E+00 .0000E+00 .0000E+00
               .0000000E+00 .1000000E+03 .2000000E+03 .4000000E+04
               -.1000000E+00 -.2000000E+00 -.3000000E+00 -.1100000E+01
               .1000000E+07 .2000000E+07 .3000000E+07 .1100000E+08
SHO 9P  9           1     DELV  .1000E-11 .1000E+07 .0000E+00
SHO10P 10          4     WATE1 .0000E+00 .0000E+00 .0000E+00
               .0000000E+00 .1000000E+03 .2000000E+03 .3000000E+04
               .1100000E+01 .1000000E+01 .9000000E+00 .1000000E+00
               .1000000E+07 .1200000E+07 .1400000E+07 .3000000E+07
SHO11WEL 0          2     DELV  .1000E-11 .0000E+00 100.0
SHO12WEL 0          1     DELV  .2000E-11 .1000E+07 100.0
+++
      0    7    8    9    10   11   13   14   15   16   17   18   19   20   21   22

```

Figure 14. File GENER for sample problem 1.

```

INCON -- INITIAL CONDITIONS FOR 22 ELEMENTS AT TIME .195625E+04
F 1 .50000000E+00
.1026783190016E+06 .1099839703607E+02 .2037588882447E+02
F 2 .50000000E+00
.7916370186497E+06 .1000168301021E+02 .1699798522950E+03
F 3 .50000000E+00
.7677482016712E+07 .1179335517890E-04 .1010226763824E+03
F 4 .50000000E+00
.9572079406600E+07 .3232199089739E-02 .3091964900221E+03
F 5 .50000000E+00
.9576155357447E+07 .1000248809440E+02 .1003047579095E+03
F 6 .50000000E+00
.9818168919018E+07 .1000000000000E+01 .9993376313984E+02
F 7 .50000000E+00
.1006737364472E+08 .1000283923305E+02 .2009607456794E+02
F 8 .50000000E+00
.8537862272979E+07 .1000545748692E+02 .2995458360463E+03
F 9 .50000000E+00
.2933407407340E+07 .2741571459748E-01 .3760295466211E+03
F 10 .50000000E+00
.1983600803901E+07 .1099039634618E+02 .2119589075438E+03
SH0 1 .50000000E+00
.4108087712286E+07 .8698644192479E-01 .2567204300811E+03
SH0 2 .50000000E+00
.4500000000000E+07 .1050000000000E+02 .2500000000000E+03
SH0 3 .50000000E+00
.8870946584688E+06 .1073526767326E+02 .1747302885933E+03
SH0 4 .50000000E+00
.8870946584688E+06 .1073526767326E+02 .1747302885933E+03
SH0 5 .50000000E+00
.8870946584688E+06 .1073526767326E+02 .1747302885933E+03
SH0 6 .50000000E+00
.2858980450767E+06 .1075533722368E+02 .8069444982431E+02
SH0 7 .50000000E+00
.2858980450767E+06 .1075533722368E+02 .8069444982431E+02
SH0 8 .50000000E+00
.2858980450767E+06 .1075533722368E+02 .8069444982431E+02
SH0 9 .50000000E+00
.1312984124846E+07 .1069178440957E+02 .1920452237581E+03
SH010 .50000000E+00
.9045343262748E+07 .1009545497753E+02 .2812831401394E+03
SH011 .50000000E+00
.3333056727132E+07 .1000370143276E+02 .2397486286092E+03
SH012 .50000000E+00
.1139849845083E+07 .0000000000000E+00 .9988050365503E+02
+++  

4 25 2 .00000000E+00 .19562500E+04

```

Figure 15. File SAVE for sample problem 1.

```

***** VOLUME- AND MASS-BALANCES ****
***** [KCYC,ITER] = [ 0, 0] ***** THE TIME IS .0000E+00 SECONDS, OR .0000E+00 DA

PHASE VOLUMES IN PLACE
GAS .49950E+02 M**3; LIQUID .10050E+05 M**3

MASS IN PLACE
GAS .14263E+04 KG; LIQUID .89195E+07 KG; AIR .56359E+03 KG; VAPOR .86436E+03 KG; LIQUID WATER .89195E+07

***** ITERATING... AT [ 1, 1] -- DELTEX = .10000E+03 MAX. RES. = .393471E+01 AT ELEMENT SHO 9 EQUATION 2
$$$$$ LIQUID PHASE EVOLVES AT ELEMENT *F 1* $$$$ PS = .12055E+05 PSAT = .23398E+04
$$$$$ GAS PHASE EVOLVES AT ELEMENT *F 5* $$$$ XAIR = .679538E-03 PX = .240543E+07 PG = .432994E+07
$$$$$ GAS PHASE EVOLVES AT ELEMENT *F 7* $$$$ XAIR = .100168E-03 PX = .321052E+06 PG = .625505E+06
... ITERATING... AT [ 1, 2] -- DELTEX = .10000E+03 MAX. RES. = .863043E+00 AT ELEMENT SHO 9 EQUATION 2
... ITERATING... AT [ 1, 3] -- DELTEX = .10000E+03 MAX. RES. = .803189E-02 AT ELEMENT SHO 9 EQUATION 2
F 1( 1, 4) ST = .10000E+03 DT = .10000E+03 DX1= .234670E+04 DX2= .999993E+01 T = 20.006 P = 102347. S = .999928E

*sam1* CODE DEMONSTRATION: PHASE TRANSITIONS, COMPONENT (DIS-)APPEARANCES

OUTPUT DATA AFTER ( 1, 4)-2-TIME STEPS THE TIME IS .11574E-02

TOTAL TIME KCYC ITER ITERC KON DX1M DX2M DX3M MAX. RES. NR KER DELTEX
.10000E+03 1 4 4 2 .16455E+07 .10000E+02 .14654E+02 .11503E-05 19 2 .10000E

ELEM. INDEX P SG SL XAIRC XAIRL PER. MOD. PCAP DG DL
(PA) (DEG-C) (PA) (KG/M**3) (KG/M**3)

F 1 1 .10235E+06 .20006E+02 .99993E+00 .71501E-04 .98565E+00 .16076E-04 .10000E+01 .00000E+00 .12055E+01 .99832
F 2 2 .84410E+06 .16999E+03 .00000E+00 .10000E+01 .00000E+00 .10000E+01 .00000E+00 .00000E+00 .00000E+00 .89734
F 3 3 .10570E+06 .99591E+02 .65930E-03 .99934E+00 .84784E-01 .93960E-06 .10000E+01 .00000E+00 .64424E+00 .95842
F 4 4 .98861E+07 .30990E+03 .99927E+00 .73379E-03 .32622E-02 .47952E-05 .10000E+01 .00000E+00 .54629E+02 .69093
F 5 5 .26455E+07 .10005E+03 .37436E-03 .99963E+00 .97540E+00 .40837E-03 .10000E+01 .00000E+00 .24341E-02 .95931
F 6 6 .99566E+07 .99984E+02 .10000E+01 .00000E+00 .10000E+01 .15959E-02 .10000E+01 .00000E+00 .92941E+02 .00000
F 7 7 .61923E+06 .20005E+02 .13611E-03 .99986E+00 .99765E+00 .99159E-04 .10000E+01 .00000E+00 .73467E+01 .99856
F 8 8 .98110E+07 .29995E+03 .00000E+00 .10000E+01 .00000E+00 .10000E+01 .00000E+00 .00000E+00 .00000E+00 .71508
F 9 9 .15045E+07 .10465E+03 .99017E+00 .98254E-02 .29149E+00 .49979E-05 .10000E+01 .00000E+00 .98336E+00 .95473
F 10 10 .39597E+07 .27628E+03 .10000E+01 .00000E+00 .00000E+00 .00000E+00 .10000E+01 .00000E+00 .18037E+02 .00000
SHO 1 11 .44873E+07 .25017E+03 .52552E+00 .47448E+00 .14192E+00 .80067E-04 .10000E+01 -.65690E+05 .23336E+02 .79951
SHO 2 12 .45000E+07 .25000E+03 .50000E+00 .50000E+00 .14823E+00 .83971E-04 .10000E+01 -.62500E+05 .23463E+02 .79979
SHO 3 13 .43239E+07 .24902E+03 .50401E+00 .49599E+00 .12258E+00 .66147E-04 .10000E+01 -.63001E+05 .22339E+02 .80110
SHO 4 14 .43239E+07 .24902E+03 .50401E+00 .49599E+00 .12258E+00 .66147E-04 .10000E+01 -.63001E+05 .22339E+02 .80110
SHO 5 15 .43239E+07 .24902E+03 .50401E+00 .49599E+00 .12258E+00 .66147E-04 .10000E+01 -.63001E+05 .22339E+02 .80110
SHO 6 16 .44764E+07 .24971E+03 .50405E+00 .49595E+00 .14789E+00 .83275E-04 .10000E+01 -.63006E+05 .23336E+02 .80021
SHO 7 17 .44764E+07 .24971E+03 .50405E+00 .49595E+00 .14789E+00 .83275E-04 .10000E+01 -.63006E+05 .23336E+02 .80021
SHO 8 18 .44764E+07 .24971E+03 .50405E+00 .49595E+00 .14789E+00 .83275E-04 .10000E+01 -.63006E+05 .23336E+02 .80021
SHO 9 19 .32791E+07 .23713E+03 .55068E+00 .44932E+00 .39998E-01 .15625E-04 .10000E+01 -.68834E+05 .165588E+02 .81772
SHO10 20 .45462E+07 .25026E+03 .47289E+00 .52711E+00 .15455E+00 .88636E-04 .10000E+01 -.59111E+05 .23743E+02 .79945
SHO11 21 .45429E+07 .23994E+03 .00000E+00 .10000E+01 .00000E+00 .10000E+01 .00000E+00 .00000E+00 .00000E+00 .81498
SHO12 22 .32957E+07 .99971E+02 .00000E+00 .10000E+01 .00000E+00 .10000E+01 .00000E+00 .00000E+00 .00000E+00 .95968

```

Figure 16. Part of printed output for sample problem 1.

Fig. 17 reproduces the summary of program units used in sample problem 1, as printed at the end of the output file. Besides documenting the versions and dates of subroutines, this listing is instructive as a record of the calling sequence of program units during execution.

UNIT	VERSION	DATE	COMMENTS
IO SECOND	1.0 1.0	15 APRIL 6 September 1994	OPEN FILES *VERS*, *MESH*, *INCON*, *GENER*, *SAVE*, *LINEQ*, AND *TABLE* CPU timing function for IBM RS/6000
TOUGH2	1.20 CG	11 March 1998	MAIN PROGRAM special version for conjugate gradient package includes definition of coordinate arrays and radiative heat transfer capability
INPUT	1.01	28 May 1998	READ ALL DATA PROVIDED THROUGH FILE *INPUT* optional data blocks *FOFT* and *GOFT* for time slices
FLOP	1.0	11 APRIL 1991	CALCULATE NUMBER OF SIGNIFICANT DIGITS FOR FLOATING POINT ARITHMETIC
RFILE	1.1	28 May 1998	INITIALIZE DATA FROM FILES *MESH* OR *MINC*, *GENER*, AND *INCON* also initializes permeability modifiers and coordinate arrays
PMIN	1.0	26 September 1997	and optionally reads tables with flowing wellbore pressures initialize block-by-block permeability modifiers
CYCIT	1.01	28 May 1998	EXECUTIVE ROUTINE FOR MARCHING IN TIME
EOS	1.01	11 January 1999	*EOS3* ... THERMOPHYSICAL PROPERTIES MODULE FOR WATER/AIR
SAT	1.0 S	17 SEPTEMBER 1990	STEAM TABLE EQUATION: SATURATION PRESSURE AS FUNCTION OF TEMPERATURE (M. OS.)
PCAP	1.0	4 MARCH 1991	CAPILLARY PRESSURE AS FUNCTION OF SATURATION
PP	1.0	1 FEBRUARY 1990	CALCULATE VAPOR PRESSURE, DENSITY, INT. ENERGY AS F(P,T,X)
VESCO	1.0	1 FEBRUARY 1990	CALCULATE VISCOSITY OF VAPOR-AIR MIXTURES
COVIS	1.0	1 FEBRUARY 1990	COEFFICIENT FOR GAS PHASE VISCOSITY CALCULATION
VISS	1.0	22 JANUARY 1990	VISCOSITY OF VAPOR AS FUNCTION OF TEMPERATURE AND PRESSURE
VLSW	1.0	22 JANUARY 1990	VISCOSITY OF LIQUID WATER AS FUNCTION OF TEMPERATURE AND PRESSURE
COWAT	1.0 S	17 SEPTEMBER 1990	LIQUID WATER DENSITY AND INT. ENERGY VERSUS TEMPERATURE AND PRESSURE (M. OS.)
SUPST	1.0 S	1 February 1991	VAPOR DENSITY AND INTERNAL ENERGY AS FUNCTION OF TEMPERATURE AND PRESSURE (M. OS.)
RELP	1.0	26 July 1995	LIQUID AND GAS PHASE RELATIVE PERMEABILITIES AS FUNCTIONS OF SATURATION for IRP=7, use Corey-krg when RP(4).ne.0, with Sgr = RP(4)
BALLA	1.0	5 MARCH 1991	PERFORM SUMMARY BALANCES FOR VOLUME, MASS, AND ENERGY
TSTEP	1.0	4 MARCH 1991	ADJUST TIME STEPS TO COINCIDE WITH USER-DEFINED TARGET TIMES
MULTI	1.1	1 March 1999	ASSEMBLE ALL ACCUMULATION AND FLOW TERMS includes capabilities for radiative heat transfer and diffusion in all phases with local equilibrium phase partitioning between gas and liquid allows block-by-block permeability modification
QI	1.1	23 January 1998	ASSEMBLE ALL SOURCE AND SINK TERMS "rigorous" step rate capability for MOP(12) = 2, and capability for flowing wellbore pressure corrections
PHAS	1.0	3 November 1997	calculate composition and enthalpy of source fluid
TTAB	1.0	5 November 1997	Interpolate sink/source rates and enthalpies from tables.
FINDL	1.0	22 JANUARY 1990	INTERPOLATE FROM A TABLE OF TIME-DEPENDENT DATA
QINTER	1.0	22 JANUARY 1990	PERFORM LINEAR INTERPOLATION
HINTER	1.0	22 JANUARY 1990	PERFORM LINEAR INTERPOLATION
PHASD	1.0	27 March 1998	calculate composition, rate and enthalpy for wells on deliverability
GCOR	1.0	27 March 1998	perform simple gravity correction for flowing bottomhole pressure
LINEQ	0.91 CG	31 January 1994	Interface for linear equation solvers can call MA28 or a package of conjugate gradient solvers
CONVER	1.0	4 MARCH 1991	UPDATE PRIMARY VARIABLES AFTER CONVERGENCE IS ACHIEVED
FGTAB	1.00	28 May 1998	Tabulate element, connection, and generation data vs. time for plotting
OUT	1.1	11 January 1999	PRINT RESULTS FOR ELEMENTS, CONNECTIONS, AND SINKS/SOURCES
WRIFI	1.0	22 JANUARY 1990	AT THE COMPLETION OF A TOUGH2 RUN, WRITE PRIMARY VARIABLES ON FILE *SAVE*

Figure 17. Calling sequence of program units in problem 1.

## **9.2 Problem No. 2 (\*rhp\*) - Heat Pipe in Cylindrical Geometry (EOS3, EOS4)**

Heat pipes are systems in which an efficient heat transfer takes place by means of a liquid-vapor counterflow process, with vaporization and condensation occurring at the hot and cold ends, respectively. Heat pipe processes occur naturally on a large scale (kilometers) in two-phase geothermal reservoirs, and they may be induced artificially if heat-generating nuclear waste packages are emplaced above the water table in partially saturated geologic formations.

The present problem models such high-level nuclear waste emplacement in an approximate way. The TOUGH2 input file shown in Fig. 18 specifies a cylindrical heater of 0.3 m radius and 4.5 m height, that provides a constant output of 3 kW into a porous medium with uniform initial conditions of 18 °C temperature, 1 bar pressure, and 20 % gas saturation. The MESHMAKER module is used to generate a one-dimensional radial grid of 120 active elements extending to a radius of 10,000 m (practically infinite for the time scales of interest here), with an additional inactive element of zero volume representing constant boundary conditions. Properly speaking, the problem represents one unit of an infinite linear string of identical heaters; if a single heater were to be modeled, important end effects would occur at the top and bottom, and a two-dimensional R-Z grid would have to be used.

Most of the formation parameters are identical to data used in previous modeling studies of high-level nuclear waste emplacement at Yucca Mountain (Pruess et al., 1990). As we do not include fracture effects in the present simulation, heat pipe effects would be very weak at the low rock matrix permeabilities (of order 1 microdarcy) encountered at Yucca Mountain. To get a more interesting behavior, we have arbitrarily increased absolute permeability by something like a factor 10,000, to 20 millidarcy, and for consistency have reduced capillary pressures by a factor  $(10,000)^{1/2} = 100$  in comparison to typical Yucca Mountain data.

It is well known that for the stated conditions (1-D radial geometry, homogeneous medium, uniform initial conditions, and a constant-rate line source) the problem has a similarity solution: The partial differential equations for this complex two-phase flow problem can be rigorously transformed into a set of ordinary differential equations in the variable  $Z = R/\sqrt{t}$ , which can be easily solved to any degree of accuracy desired by means of one-dimensional numerical integration (O'Sullivan, 1981). Comparison of TOUGH2 simulations with the semi-analytical similarity solution has shown excellent agreement (Doughty and Pruess, 1992). Fig. 19 gives simulation results after  $t = 10$  yr obtained with EOS4, including vapor pressure lowering, plotted as a function of the natural logarithm of the similarity variable  $Z$ .

```

*rhp* 1-D RADIAL HEAT PIPE
MESHMAKER1----*---2----*---3----*---4----*---5----*---6----*---7----*---8
RZ2D
RADII
 1
 0.
EQUID
 1      .3
LOGAR
 99      1.E2
LOGAR
 20      1.E4
EQUID
 1      0.0
LAYER---1----*---2----*---3----*---4----*---5----*---6----*---7----*---8
 1
 4.5

ROCKS---1----*---2----*---3----*---4----*---5----*---6----*---7----*---8
POMED   1      2550.      .10      20.E-15    20.E-15    20.E-15      2.0      800.0
          .25

MULTI---1----*---2----*---3----*---4----*---5----*---6----*---7----*---8
 2      3      2      6
START---1----*---2----*---3----*---4----*---5----*---6----*---7----*---8
-----*---1 MOP: 123456789*123456789*1234 -----*---5----*---6----*---7----*---8
PARAM---1----*---2----*---3----*---4----*---5----*---6----*---7----*---8
 2 250      25000003000000002 47 1 1      1.80
 3.15576E8      -1.
 1.E3      9.E3      9.E4      4.E5
 1.E-5      1.E00
 1.E5      0.20      1.E-7
          18.

diffusivity data are input as follows:
first row water, second row air; first column gas, second column aqueous
DIFFU---1----*---2----*---3----*---4----*---5----*---6----*---7----*---8
 2.13e-5      0.e-8
 2.13e-5      0.e-8
RPCAP---1----*---2----*---3----*---4----*---5----*---6----*---7----*---8
 7      0.45000      9.6E-4      1.
 7      0.45000      1.0E-3      8.0E-05      5.E8      1.
TIMES---1----*---2----*---3----*---4----*---5----*---6----*---7----*---8
 3
 3.15576E7      1.2559E8      3.15576E8
INCON---1----*---2----*---3----*---4----*---5----*---6----*---7----*---8

GENER---1----*---2----*---3----*---4----*---5----*---6----*---7----*---8
A1 1HTR 1      HEAT      3.E3

ENDCY---1----*---2----*---3----*---4----*---5----*---6----*---7----*---8

```

Figure 18. Input file for problem 2 - heat pipe in cylindrical geometry.

To provide a benchmark for proper code installation, we also present portions of the printed output. Fig. 20 shows part of the iteration sequence and thermodynamic data after  $t = 1$  yr for running the input file as given in Fig. 18 with EOS4. Although maximum temperatures exceed saturated vapor temperatures at prevailing pressures, none of the grid blocks dry out because of

vapor pressure lowering effects. The input file in Fig. 18 includes data for vapor-air diffusion, which can be engaged by changing parameter NB in data block MULTI from 6 to 8. Some of the output when diffusion is included is shown in Fig. 21. Comparison with Fig. 20 shows that some air remains in the boiling region near the heater when diffusion is active. Vapor is removed from the hot region at somewhat larger rates, causing liquid saturations to be somewhat smaller. This makes the heat pipe less efficient, and leads to slightly higher temperatures. The input file shown in Fig. 18 can also be run with EOS3. Because this does not include vapor pressure lowering, vaporization is slightly stronger than in the EOS4 run shown in Fig. 20, and temperatures near the heater are approximately 3°C lower (see Fig. 22). EOS3 requires 44 time steps to reach one year as compared to 28 time steps for EOS4. This is explained by the highly nonlinear transition to single-phase vapor conditions in the EOS3 run, which limits time step sizes.

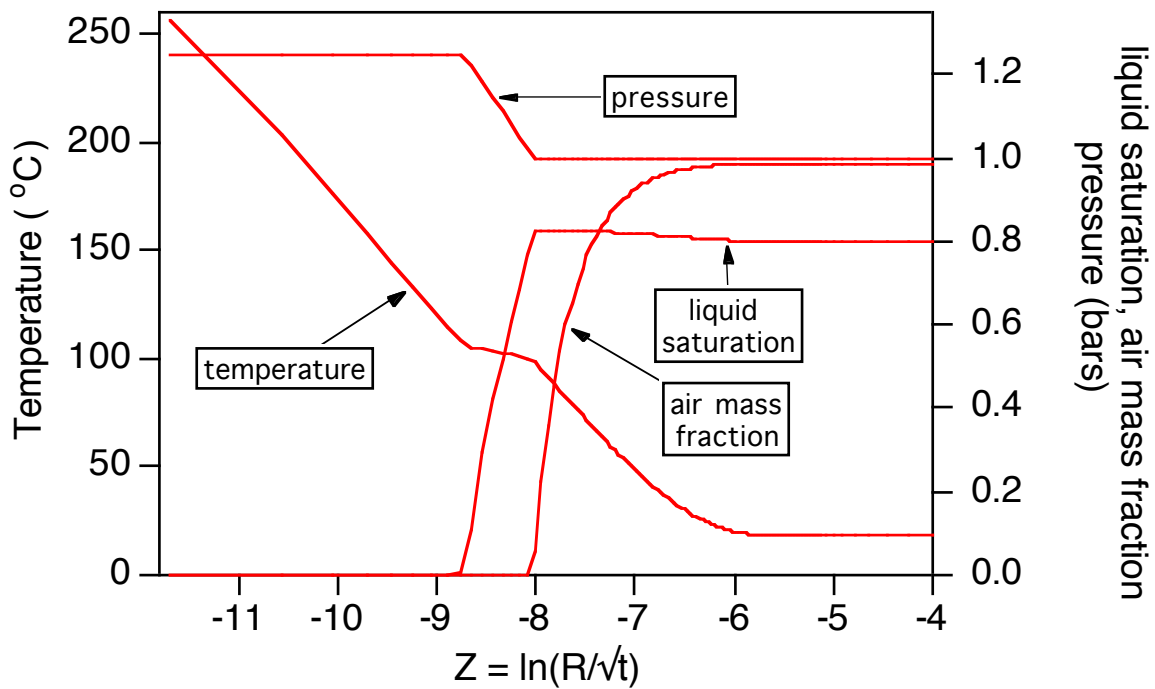


Figure 19. Profiles of temperature, pressure, liquid saturation and air mass fraction.

\*\*\*\*\* VOLUME- AND MASS-BALANCES \*\*\*\*\*

PHASE VOLUMES IN PLACE

THE TIME IS .00000E+00 SECONDS, OR .00000E+00 DAYS

PHASE VOLUMES IN PLACE  
GAS .28274E+08; LIQUID .11310E+09

MASS IN PLACE  
GAS .33561E+08; LIQUID .11295E+12; AIR .34905E+08; VAPOR .43437E+06; LIQUID WATER .11295E+12

```

A1 1( 1, 3) ST = .100000E+04 DT = .100000E+04 DX1= .146786E+02 DX2= -.156853E-03 T = 19.065 P = 100015. S = .199843E-4
A1 1( 2, 4) ST = .100000E+05 DT = .900000E+04 DX1= .744626E+01 DX2= -.128979E-02 T = 27.246 P = 100022. S = .198553E-4
A1 1( 3, 6) ST = .100000E+06 DT = .900000E+05 DX1= .980597E+01 DX2= -.352032E-02 T = 63.142 P = 100032. S = .195033E-4
MATRIX NUMERICALLY SINGULAR ----- PERFORM NEW DECOMPOSITION
A1 1( 4, 8) ST = .500000E+06 DT = .400000E+06 DX1= .457595E+04 DX2= -.11792E+00 T = 100.885 P = 104590. S = .312955E-4
A1 1( 5, 6) ST = .900000E+06 DT = .400000E+06 DX1= .130323E+05 DX2= .228709E+00 T = 104.237 P = 117622. S = .541664E-4
A1 1( 6, 5) ST = .130000E+07 DT = .400000E+06 DX1= .612647E+04 DX2= .670902E-01 T = 105.704 P = 123748. S = .608755E-4
A1 1( 7, 4) ST = .170000E+07 DT = .400000E+06 DX1= .427324E+04 DX2= .345346E-01 T = 106.692 P = 128022. S = .643289E-4
A1 2( 8, 7) ST = .250000E+07 DT = .800000E+06 DX1= .210099E+04 DX2= .573465E-01 T = 100.223 P = 102141. S = .242792E-4
A1 1( 9, 5) ST = .330000E+07 DT = .800000E+06 DX1= .504933E+04 DX2= .720171E-01 T = 109.160 P = 139207. S = .766330E-4
A1 1( 10, 5) ST = .410000E+07 DT = .800000E+06 DX1= .335713E+04 DX2= .523432E-01 T = 109.872 P = 142564. S = .818673E-4
A1 2( 11, 4) ST = .490000E+07 DT = .800000E+06 DX1= .297170E+04 DX2= .479475E-01 T = 103.475 P = 114541. S = .494844E-4
A1 3( 12, 7) ST = .650000E+07 DT = .160000E+07 DX1= .271344E+04 DX2= .482814E-01 T = 100.123 P = 101772. S = .229192E-4
A1 1( 13, 6) ST = .810000E+07 DT = .160000E+07 DX1= .357518E+04 DX2= .430044E-01 T = 112.063 P = 153039. S = .949414E-4
A1 1( 14, 6) ST = .970000E+07 DT = .160000E+07 DX1= .259115E+04 DX2= .234000E-01 T = 112.672 P = 155630. S = .972654E-4
A1 1( 15, 6) ST = .113000E+08 DT = .160000E+07 DX1= .208588E+04 DX2= .120225E-01 T = 113.286 P = 157716. S = .984679E-4
A1 1( 16, 6) ST = .129000E+08 DT = .160000E+07 DX1= .195398E+04 DX2= .805740E-02 T = 114.363 P = 159670. S = .992737E-4
A1 1( 17, 8) ST = .145000E+08 DT = .160000E+07 DX1= .920016E+03 DX2= .375095E-02 T = 116.820 P = 160590. S = .996487E-4
A1 1( 18, 8) ST = .161000E+08 DT = .160000E+07 DX1= .107512E+04 DX2= .143879E-02 T = 122.868 P = 159155. S = .99726E-4
A1 1( 19, 8) ST = .177000E+08 DT = .160000E+07 DX1= .443019E+04 DX2= .522534E-03 T = 134.409 P = 155085. S = .998449E-4
A1 1( 20, 7) ST = .193000E+08 DT = .160000E+07 DX1= .711043E+04 DX2= .188214E-03 T = 148.170 P = 147974. S = .998637E-4
A1 1( 21, 6) ST = .209000E+08 DT = .160000E+07 DX1= .659646E+04 DX2= .737170E-04 T = 159.229 P = 141378. S = .998711E-4
A1 1( 22, 5) ST = .225000E+08 DT = .160000E+07 DX1= .998818E+03 DX2= .150070E-04 T = 162.564 P = 140379. S = .998726E-4
A1 2( 23, 5) ST = .241000E+08 DT = .160000E+07 DX1= .112066E+04 DX2= .133116E-01 T = 109.770 P = 141363. S = .975460E-4
A1 2( 24, 5) ST = .257000E+08 DT = .160000E+07 DX1= .924703E+03 DX2= .865090E-02 T = 110.127 P = 142061. S = .984111E-4
A1 2( 25, 6) ST = .273000E+08 DT = .160000E+07 DX1= .765189E+03 DX2= .555511E-02 T = 110.578 P = 142826. S = .989666E-4
A1 2( 26, 6) ST = .289000E+08 DT = .160000E+07 DX1= .578302E+03 DX2= .350222E-02 T = 111.219 P = 143404. S = .993169E-4
A1 2( 27, 6) ST = .305000E+08 DT = .160000E+07 DX1= .318358E+03 DX2= .255778E-02 T = 112.510 P = 143722. S = .995726E-4
A1 2( 28, 5) ST = .315576E+08 DT = .105760E+07 DX1= .-231627E+03 DX2= .105436E-02 T = 113.937 P = 143491. S = .996781E-4

```

\*rhp\* 1-D RADIAL HEAT PIPE

OUTPUT DATA AFTER ( 28, 5)-2-TIME STEPS

THE TIME IS .36525E+03 DA

```

TOTAL TIME   KCYC   ITER  ITERC   KON    DX1M   DX2M   DX3M   RERM      NER   KER   DEL TEX
.31558E+08    28      5    163     2   .68916E+03   .19043E-01   .263553E+04   .911075E-05

```

ELEM.	INDEX	P	T	SG	SL	XAIRG	XAIRL	PAIR	PCAP	DG	DL	
A1	1	1	.14349E+06	.16750E+03	.99874E+00	.12594E-02	.34883E-25	.50570E-30	.31459E-20	.30149E+09	.71286E+00	.89983E-01
A1	2	2	.14349E+06	.11394E+03	.99678E+00	.32193E-02	.00000E+00	.00000E+00	.00000E+00	.21872E+08	.81859E+00	.94765E-01
A1	3	3	.12974E+06	.10710E+03	.86159E+00	.13841E+00	.63375E-20	.83742E-25	.52096E-15	.14928E+06	.75318E+00	.95289E-01
A1	4	4	.11847E+06	.10445E+03	.60944E+00	.39056E+00	.28844E-15	.34776E-20	.21634E-10	.36757E+05	.69187E+00	.95487E-01
A1	5	5	.10947E+06	.10218E+03	.41314E+00	.58686E+00	.26427E-10	.29414E-15	.18299E-05	.19639E+05	.64255E+00	.95654E-01
A1	6	6	.10179E+06	.10013E+03	.22292E+00	.77708E+00	.26538E-05	.27444E-10	.17073E+00	.10691E+01	.60028E+00	.95803E-01
A1	7	7	.10004E+06	.92618E+02	.17379E+00	.82621E+00	.31731E+00	.36439E-05	.22669E+05	.88079E+04	.68029E+00	.96334E-01
A1	8	8	.10004E+06	.84644E+02	.17497E+00	.82503E+00	.54566E+00	.69191E-05	.43044E+05	.88252E+04	.76792E+00	.96869E-01
A1	9	9	.10004E+06	.77696E+02	.17612E+00	.82388E+00	.67787E+00	.91519E-05	.56934E+05	.88957E+04	.83381E+00	.97399E-01
A1	10	10	.10004E+06	.71563E+02	.17724E+00	.82276E+00	.76175E+00	.10724E-04	.66715E+05	.89379E+04	.88515E+00	.97678E-01
A1	11	11	.10004E+06	.66097E+02	.17833E+00	.82167E+00	.81779E+00	.11860E-04	.73782E+05	.89793E+04	.92630E+00	.97990E-01
A1	12	12	.10004E+06	.61193E+02	.17941E+00	.82059E+00	.85718E+00	.12698E-04	.78997E+05	.90200E+04	.96008E+00	.98256E-01
A1	13	13	.10004E+06	.56766E+02	.18048E+00	.81952E+00	.88570E+00	.13329E-04	.82921E+05	.90604E+04	.98840E+00	.98483E-01
A1	14	14	.10004E+06	.52577E+02	.18154E+00	.81846E+00	.90688E+00	.13811E-04	.85917E+05	.91040E+04	.10125E+01	.98678E-01
A1	15	15	.10004E+06	.49116E+02	.18259E+00	.81741E+00	.92292E+00	.14184E-04	.88238E+05	.91402E+04	.10333E+01	.98847E-01
A1	16	16	.10004E+06	.45806E+02	.18363E+00	.81637E+00	.93528E+00	.14476E-04	.90055E+05	.91798E+04	.10515E+01	.98992E-01
A1	17	17	.10004E+06	.42794E+02	.18467E+00	.81533E+00	.94493E+00	.14707E-04	.91494E+05	.92192E+04	.10764E+01	.99118E-01
A1	18	18	.10004E+06	.40052E+02	.18571E+00	.81429E+00	.95258E+00	.14892E-04	.92645E+05	.92584E+04	.10816E+01	.99227E-01
A1	19	19	.10004E+06	.37558E+02	.18673E+00	.81327E+00	.95869E+00	.15041E-04	.93573E+05	.92974E+04	.10942E+01	.99321E-01
A1	20	20	.10004E+06	.35291E+02	.18775E+00	.81225E+00	.96362E+00	.15163E-04	.94327E+05	.93359E+04	.11054E+01	.99402E-01
A1	21	21	.10004E+06	.33235E+02	.18875E+00	.81125E+00	.96763E+00	.15262E-04	.94944E+05	.93739E+04	.11155E+01	.99472E-01
A1	22	22	.10004E+06	.31374E+02	.18973E+00	.81027E+00	.97029E+00	.15343E-04	.95452E+05	.94112E+04	.11244E+01	.99533E-01
A1	23	23	.10004E+06	.29693E+02	.19069E+00	.80931E+00	.97363E+00	.15411E-04	.95872E+05	.94476E+04	.11325E+01	.99585E-01
A1	24	24	.10004E+06	.28181E+02	.19161E+00	.80839E+00	.97587E+00	.15467E-04	.96221E+05	.94828E+04	.11397E+01	.99629E-01
A1	25	25	.10004E+06	.26824E+02	.19250E+00	.80750E+00	.97774E+00	.15514E-04	.96511E+05	.95166E+04	.11461E+01	.99667E-01
A1	26	26	.10004E+06	.25613E+02	.19334E+00	.80666E+00	.97930E+00	.15553E-04	.96755E+05	.95488E+04	.11518E+01	.99700E-01
A1	27	27	.10004E+06	.24534E+02	.19414E+00	.80586E+00	.98006E+00	.15586E-04	.96959E+05	.95792E+04	.11569E+01	.99728E-01
A1	28	28	.10004E+06	.23579E+02	.19488E+00	.80512E+00	.98170E+00	.15613E-04	.97130E+05	.96076E+04	.11614E+01	.99752E-01
A1	29	29	.10004E+06	.22736E+02	.19557E+00	.80443E+00	.98262E+00	.15636E-04	.97274E+05	.96337E+04	.11653E+01	.99772E-01
A1	30	30	.10004E+06	.21998E+02	.19620E+00	.80380E+00	.98339E+00	.15656E-04	.97395E+05	.96577E+04	.11688E+01	.99789E-01
A1	31	31	.10004E+06	.21354E+02	.19676E+00	.80324E+00	.98404E+00	.15672E-04	.97497E+05	.96794E+04	.11718E+01	.99803E-01
A1	32	32	.10004E+06	.20796E+02	.19727E+00	.80273E+00	.98458E+00	.15686E-04	.97582E+05	.96987E+04	.11744E+01	.99816E-01
A1	33	33	.10004E+06	.20315E+02	.19772E+00	.80228E+00	.98503E+00	.15697E-04	.97653E+05	.97159E+04	.11766E+01	.99826E-01
A1	34	34	.10004E+06	.19903E+02	.19811E+00	.80189E+00	.98541E+00	.15707E-04	.97713E+05	.97305E+04	.11785E+01	.99834E-01
A1	35	35	.10003E+06	.19554E+02	.19845E+00	.80155E+00	.98573E+00	.15715E-04	.97762E+05	.97438E+04	.11802F+01	.99841E-01

Figure 20. Selected output for problem 2 run with EOS4.

Figure 21. Selected output for problem 2, run with EOS4 and including gas diffusion.

\*rhp\* 1-D RADIAL HEAT PIPE

OUTPUT DATA AFTER ( 44, 5)-TIME STEPS

THE TIME IS .36525E+0

TOTAL TIME	KCYC	ITER	ITERC	KON	DX1M	DX2M	DX3M	MAX. RES.	NER	KER	DELT
.31558E+08	44	5	236	2	.42630E+03	.11943E-01	.58034E+00	.10752E-06	2	1	.6576
ELEM.	INDEX	P (PA)	T (DEG-C)	SG	SL	XAIRG	XAIRL	PER. MOD.	PCAP (PA)	DG (KG/M**3)	D (KG/
A1 1	1	.14573E+06	.16412E+03	.10000E+01	.00000E+00	.00000E+00	.00000E+00	.10000E+01	-.50000E+09	.72998E+00	.000
A1 2	2	.14573E+06	.11051E+03	.99743E+00	.25724E-02	.00000E+00	.00000E+00	.10000E+01	-.33327E+08	.83980E+00	.950
A1 3	3	.13007E+06	.10715E+03	.86852E+00	.13148E+00	.70606E-15	.93566E-20	.10000E+01	-.14955E+06	.75504E+00	.952
A1 4	4	.11877E+06	.10451E+03	.61567E+00	.38433E+00	.23223E-14	.28070E-19	.10000E+01	-.37591E+05	.69349E+00	.954
A1 5	5	.10974E+06	.10225E+03	.41885E+00	.58115E+00	.26344E-10	.29395E-15	.10000E+01	-.19979E+05	.64404E+00	.956
A1 6	6	.10204E+06	.10020E+03	.22936E+00	.77064E+00	.26455E-05	.27427E-10	.10000E+01	-.10944E+05	.60170E+00	.957
A1 7	7	.10004E+06	.92930E+02	.17304E+00	.82696E+00	.30601E+00	.34979E-05	.10000E+01	-.87795E+04	.67657E+00	.963
A1 8	8	.10004E+06	.84925E+02	.17425E+00	.82575E+00	.53920E+00	.68171E-05	.10000E+01	-.88254E+04	.76506E+00	.968
A1 9	9	.10004E+06	.77951E+02	.17544E+00	.82456E+00	.67380E+00	.90788E-05	.10000E+01	-.88701E+04	.83155E+00	.972
A1 10	10	.10004E+06	.71794E+02	.17660E+00	.82340E+00	.75884E+00	.10671E-04	.10000E+01	-.89141E+04	.88332E+00	.976
A1 11	11	.10004E+06	.66307E+02	.17775E+00	.82225E+00	.81587E+00	.11820E-04	.10000E+01	-.89575E+04	.92479E+00	.979
A1 12	12	.10004E+06	.61385E+02	.17889E+00	.82111E+00	.85579E+00	.12668E-04	.10000E+01	-.90003E+04	.95881E+00	.982
A1 13	13	.10004E+06	.56941E+02	.18001E+00	.81999E+00	.88468E+00	.13306E-04	.10000E+01	-.90428E+04	.98731E+00	.984
A1 14	14	.10004E+06	.52916E+02	.18112E+00	.81888E+00	.90610E+00	.13793E-04	.10000E+01	-.90849E+04	.10116E+01	.986
A1 15	15	.10004E+06	.49260E+02	.18223E+00	.81777E+00	.92233E+00	.14170E-04	.10000E+01	-.91266E+04	.10325E+01	.988
A1 16	16	.10004E+06	.45937E+02	.18332E+00	.81668E+00	.93482E+00	.14465E-04	.10000E+01	-.91679E+04	.10508E+01	.989
A1 17	17	.10004E+06	.42911E+02	.18440E+00	.81560E+00	.94458E+00	.14699E-04	.10000E+01	-.92088E+04	.10668E+01	.991
A1 18	18	.10004E+06	.40155E+02	.18547E+00	.81453E+00	.95230E+00	.14886E-04	.10000E+01	-.92493E+04	.10811E+01	.992
A1 19	19	.10004E+06	.37648E+02	.18652E+00	.81348E+00	.95848E+00	.15036E-04	.10000E+01	-.92894E+04	.10937E+01	.993
A1 20	20	.10004E+06	.35369E+02	.18756E+00	.81244E+00	.96346E+00	.15159E-04	.10000E+01	-.93288E+04	.11050E+01	.993

Figure 22. Selected output for problem 2 run with EOS3.

### 9.3 Problem No. 3 (\*rvf\*) - Heat Sweep in a Vertical Fracture (EOS1)

In many geothermal fields there is evidence of rapid migration of injected fluids along preferential flow paths, presumably along fractures. The present problem is designed to study thermal interference along such paths, by modeling nonisothermal injection into and production from a single vertical fracture, as illustrated in Fig. 23 (from Pruess and Bodvarsson, 1984). The fracture is bounded by semi-infinite half-spaces of impermeable rock, which provide a conductive heat supply. Initial temperature is 300 °C throughout. Water at 100 °C temperature is injected at one side of the fracture at a constant rate of 4 kg/s, while production occurs at the other side against a specified wellbore pressure. Problem parameters are given in Table 18, and the TOUGH2 input file for injecting at point I and producing at point P is shown in Fig. 24.

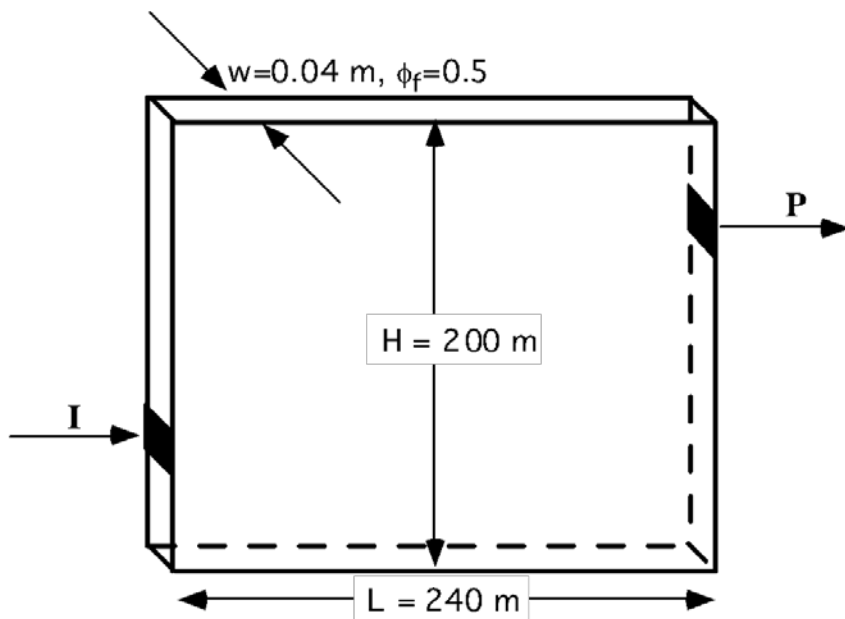


Figure 23. Schematic diagram of injection-production system in vertical fracture.

Injection occurs at  $I$ , production at  $P$ .

A special feature of the problem is that the semi-analytical method is used to describe heat conduction in the confining layers (see section 7.4), reducing the dimensionality of the problem from 3-D to 2-D. Water remains in single-phase liquid conditions throughout, so that no data block RPCAP for relative permeabilities and capillary pressures is needed.

The input file as given in Fig. 24 includes a SOLVR data block for use with the T2CG2 linear equation solution module, selecting the stabilized bi-conjugate gradient solver DLUSTB (MATSLV = 5) with Z1 preconditioning. Other solvers and in particular the T2CG1 module could

Table 18. Parameters for fracture flow problem

Rock	
Thermal conductivity	2.1 W/m°C
Specific heat	1000 J/kg°C
Density	2650 kg/m <sup>3</sup>
Permeability	0
Fracture	
Height	200 m
Length	240 m
Aperture	0.04 m
Permeability	$200 \times 10^{-12} \text{ m}^2$ (200 darcy)
Porosity	50 %
Initial Conditions	
Temperature	300 °C
Pressure	hydrostatic profile
Average pressure	100 bar
Injection	
Enthalpy	$4.2 \times 10^5 \text{ J/kg}$ (appr.100 °C)
Rate	4 kg/s
Production	
Productivity index	$4 \times 10^{-12} \text{ m}^3$
Flowing pressure	96.5 bar

be used for this problem, but the particular solver and preconditioner combination was chosen because it is robust enough to be able to handle a “two waters” variation of the problem (see below).

The problem uses the EOS1 fluid property module, and is run in three separate segments. A first run performs mesh generation only, using the MESHMaker/XYZ module. For this run, the data records from MESHM through ENDFI in the input file are inserted right behind the first record with the problem title. The mesh consists of 12 horizontal by 10 vertical blocks of 20 m × 20 m. Ordinarily, we would specify  $NX = 12$  and  $NZ = 10$  to make such a mesh; however, special considerations arise here because we desire appropriate surface areas for heat conduction to be placed in the MESH file. By default, in the MESHMaker/XYZ module the interface areas with

```

*rvf* - vertical fracture problem for EOS1
ROCKS----1----*---2----*---3----*---4----*---5----*---6----*---7----*---8
FRACT      2650.      .50   200.E-12  200.E-12  200.E-12      0.00    1000.
CONBD      2650.      .00    0.E-12   0.E-12   0.E-12      2.1     1000.

START----1----*---2----*---3----*---4----*---5----*---6----*---7----*---8
----*---1 MOP: 123456789*123456789*1234 ----*---5----*---6----*---7----*---8
PARAM----1----*---2----*---3----*---4----*---5----*---6----*---7----*---8
  1  40      9910000000000001
        1.57788E8      -1.          A1312      9.81
        1.E2       9.E2      9.E3      9.E4      9.E5      2.E6      5.E6
        1.E-5
        100.E5      300.

SOLVR----1----*---2----*---3----*---4----*---5----*---6----*---7----*---8
  5 Z1      00      8.0e-1      1.0e-7
GENER----1----*---2----*---3----*---4----*---5----*---6----*---7----*---8
A18 1INJ 1           COM1      4.      4.2E5
A1312PRO 1           DELV      4.E-12     9.65E6

FOFT ----1----*---2----*---3----*---4----*---5----*---6----*---7----*---8
A1312

ENDCY----1----*---2----*---3----*---4----*---5----*---6----*---7----*---8
INCON----1----*---2----*---3----*---4----*---5----*---6----*---7----*---8

MULTI
  1      1      2      6
ENDCY----1----*---2----*---3----*---4----*---5----*---6----*---7----*---8
con00      CONBD
MESHMAKER1----*---2----*---3----*---4----*---5----*---6----*---7----*---8
XYZ
      90.
NX      12      20.
NY      10      20.
NZ      1       .04

ENDFI----1----*---2----*---3----*---4----*---5----*---6----*---7----*---8
MULTI----1----*---2----*---3----*---4----*---5----*---6----*---7----*---8
  2      3      2      6
A18 1INJ 1           COM2      4.      4.2E5

```

Figure 24. Input file for problem 3 - heat sweep in a vertical fracture.

impermeable confining beds are always taken to be in the X-Y plane, so that in a mesh with vertical Z-axis the interface areas for conductive heat transfer would be assigned to the top and bottom boundaries. To properly assign the desired lateral heat transfer areas, the mesh is generated as an X-Y mesh ( $NX = 12$ ,  $NY = 10$ ,  $NZ = 1$ ), and the Y-axis is specified to make an angle of  $90^\circ$  with the horizontal, i.e., to point in the vertical direction. The MESHMAKER input terminates on ENDFI, to bypass the flow simulation and to limit processing to mesh generation only. Fig. 25 shows the mesh pattern printout generated by TOUGH2. The element “A18 1” corresponds to the injection point I, and “A1312” corresponds to the production point P. The MESH file is then edited, and a dummy element of zero volume is appended at the end of the ELEME block, to provide the thermal data for the conductive boundaries. The input file in Fig. 24 includes a data

```

*****
* CARTESIAN MESH WITH NX*NY*NZ = 12 * 10 * 1 GRID BLOCKS *
*****
*
* THE MESH WILL BE PRINTED AS SLICES FOR K = 1 TO K = NZ = 1 *
*
* IN EACH MESH SLICE, ROWS WILL GO FROM J = 1 TO J = NY = 10 *
*
* IN EACH ROW, COLUMNS WILL GO FROM I = 1 TO I = NX = 12 *
*
*****
SLICE WITH K = 1

COLUMN I = 1 2 3 4 5 6 7 8 9 10 11 12 13 14 15 16 17 18 19 20
ROWS
J = 1 A11 1 A11 2 A11 3 A11 4 A11 5 A11 6 A11 7 A11 8 A11 9 A1110 A1111 A1112
J = 2 A12 1 A12 2 A12 3 A12 4 A12 5 A12 6 A12 7 A12 8 A12 9 A1210 A1211 A1212
J = 3 A13 1 A13 2 A13 3 A13 4 A13 5 A13 6 A13 7 A13 8 A13 9 A1310 A1311 A1312
J = 4 A14 1 A14 2 A14 3 A14 4 A14 5 A14 6 A14 7 A14 8 A14 9 A1410 A1411 A1412
J = 5 A15 1 A15 2 A15 3 A15 4 A15 5 A15 6 A15 7 A15 8 A15 9 A1510 A1511 A1512
J = 6 A16 1 A16 2 A16 3 A16 4 A16 5 A16 6 A16 7 A16 8 A16 9 A1610 A1611 A1612
J = 7 A17 1 A17 2 A17 3 A17 4 A17 5 A17 6 A17 7 A17 8 A17 9 A1710 A1711 A1712
J = 8 A18 1 A18 2 A18 3 A18 4 A18 5 A18 6 A18 7 A18 8 A18 9 A1810 A1811 A1812
J = 9 A19 1 A19 2 A19 3 A19 4 A19 5 A19 6 A19 7 A19 8 A19 9 A1910 A1911 A1912
J = 10 A1A 1 A1A 2 A1A 3 A1A 4 A1A 5 A1A 6 A1A 7 A1A 8 A1A 9 A1A10 A1A11 A1A12
*****
MESH GENERATION COMPLETE --- EXIT FROM MODULE *MESHMAKER*

```

Figure 25. TOUGH2 printout of mesh pattern in problem 3.

record for a suitable dummy element named “con00” after the ENDCY record. This element belongs to domain CONBD with appropriate rock density, thermal conductivity, and specific heat, and it will be initialized with the default conditions of 300 °C temperature.

The next processing step calculates a hydrostatic pressure equilibrium in the fracture under isothermal conditions. This calculation uses the modified MESH file obtained above, and requires several small modifications in the input file of Fig. 24. The time step counter MCYC is changed from 40 to 4, as 4 time steps are sufficient to obtain an accurate gravity equilibrium. The generation items are removed, and the convergence tolerance RE1 is changed from  $1\times 10^{-5}$  to  $1\times 10^{-8}$ , to achieve a tighter control on gravity equilibrium. The ENDCY statement preceding the INCON record is removed, to enforce default initial conditions by way of an empty INCON data block, and to engage the MULTI data block with specifications of (NK,NEQ,NPH,NB) = (1,1,2,6) for an isothermal calculation (mass balance only). We also set MOP(15) = 0, to disengage the semi-analytical heat exchange calculation. Gravity equilibration results in a pressure trend ranging from 106.34175 bars in the bottom row of grid blocks (A1A 1, A1A 2,..., A1A12), to 93.70950 bars in the top row (A11 1, ..., A1112).

The subsequent production/injection run uses the input file exactly as given in Fig. 24, with the MESH file as used in the gravity equilibration. The SAVE file produced by the gravity equilibration run is renamed file INCON and used for initialization, after removing the last two records and replacing them with a blank record, to reset time-step and simulation time counters to

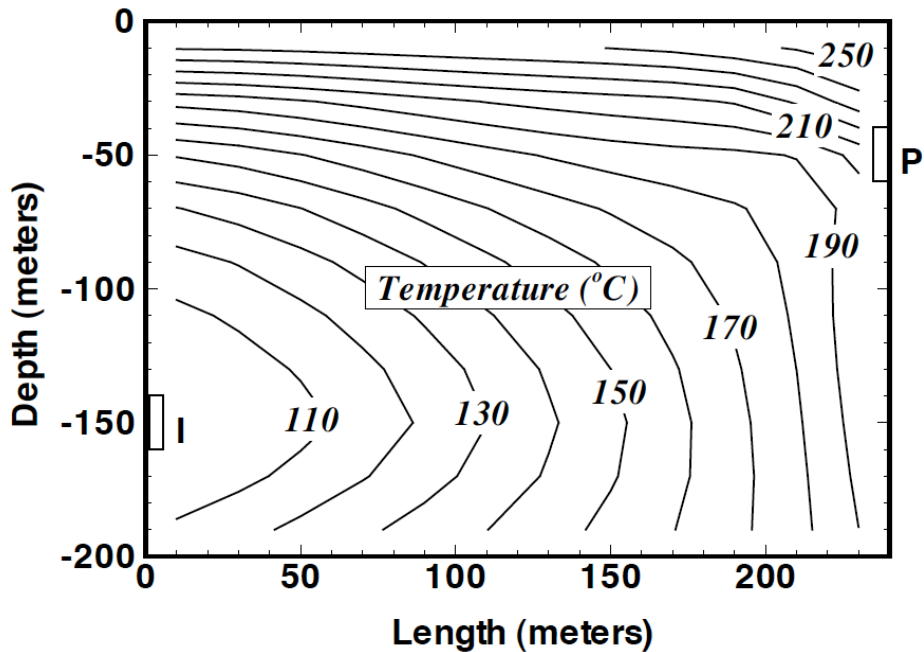


Figure 26. Temperature distribution in fracture plane after 5 years. Injection and production regions are marked I and P, respectively.

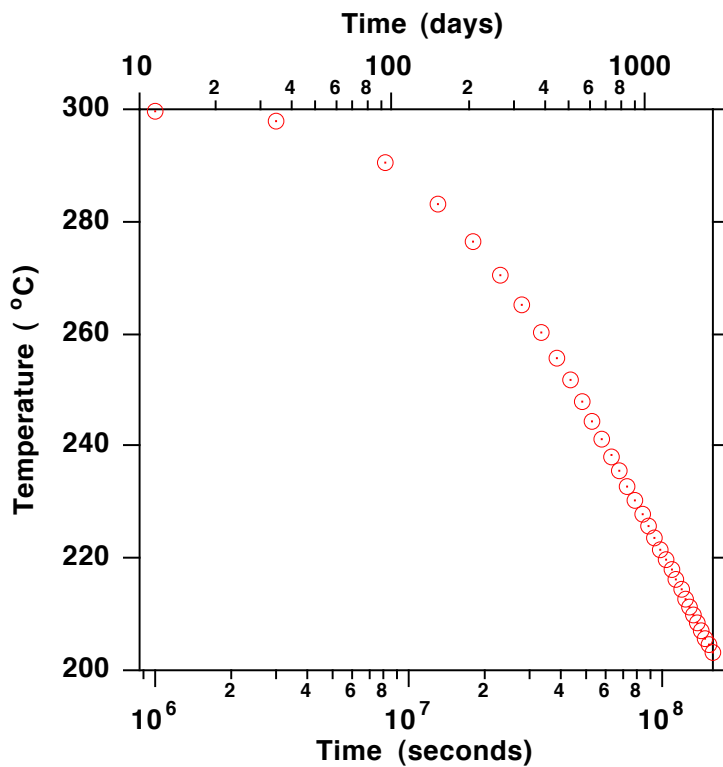


Figure 27. Produced fluid temperature versus time for vertical fracture problem.

zero. The specified maximum time of  $1.57788 \times 10^8$  seconds (5 years) is reached after 37 time steps; at this time production occurs with a rate of 3.9998 kg/s and an enthalpy of 870.31 kJ/kg; temperature in the producing element is 203.25 °C. Fig. 26 shows a contour plot of the temperature distribution in the fracture after 5 years, and a plot of the transient temperature changes at the producing element is given in Fig. 27.

The fracture production/injection problem lends itself to several interesting extensions and variations. These can be implemented by means of small modifications in the input file and are mentioned here without giving calculational results. For example, the problem could be restarted with a zero injection rate to examine the rate of temperature recovery in the production block. Initial conditions could be chosen appropriate for depleted zones in vapor-dominated reservoirs, e.g.,  $T = 240$  °C,  $P = 8$  bars, to examine injection response with strong vaporization effects. Note that for injection into vapor-dominated systems, two-phase conditions will evolve and a data block RPCAP with relative permeability and capillary pressure data will be required. We point out that strong grid orientation effects may arise when modeling water injection into vapor-dominated reservoirs and careful mesh design or inclusion of diffusive effects (capillary pressures) is required to obtain realistic results (Pruess, 1991c).

The problem can be run using “two waters” by specifying a MULTI data block with parameters  $(NK,NEQ,NPH,NB) = (2,3,2,6)$ , along with injection type COM2 instead of COM1, to inject “water 2” and thereby track the advance and arrival of injected water at the production point. The input file as shown in Fig. 24 has appropriate data records at the end for running as a two waters problem. The particular selection of solver and preconditioner in this problem was made to be able to cope with the many zeros that will arise on the main diagonal of the Jacobian matrix for the two waters variation. The problem could also be run with the EOS2 fluid property module, with some CO<sub>2</sub> initially present in the reservoir fluid, to study the changes in non-condensable gas content of produced fluids in response to injection.

#### 9.4 Problem No. 4 (\*rfp\*) - Five-spot Geothermal Production/Injection (EOS1, EOS2)

In geothermal reservoir development, production and injection wells are often sited in more or less regular geometric patterns. The present problem considers a large well field with wells arranged in a “five-spot” configuration (Fig. 28). Because of symmetry only 1/8 of the basic pattern needs to be modeled. The computational grid was generated by means of a separate preprocessor program which has not yet been integrated into the TOUGH2 package. The grid has six rows, each containing between one and eleven elements, for a total of thirty-six volume elements; for simplicity, only a single layer of 305 m thickness is modeled. The problem specifications as given in Table 19 correspond to conditions that may typically be encountered in deeper zones of hot and fairly tight fractured two-phase reservoirs (Pruess and Narasimhan, 1985).

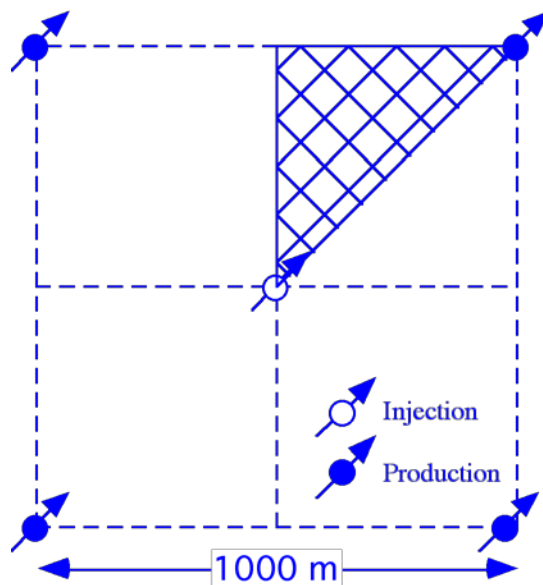


Figure 28. Five-spot well pattern with grid for modeling a 1/8 symmetry domain

The INPUT file for use with the EOS1 fluid property module (Fig. 29) models the system as a fractured medium with embedded impermeable matrix blocks in the shape of cubes. The matrix blocks were assigned a non-vanishing porosity of  $10^{-10}$ , so that they will contain a small amount of water. This has no noticeable impact on fluid and heat flows, and is done to prevent the water mass balance equation from degenerating into the singular form  $0 = 0$ . Running the problem with  $\phi = 0$  in the matrix blocks (domain MATRX) is also possible, but this results in more sluggish convergence and considerably smaller time steps. The MESHMaker module is used to perform MINC-partitioning of the primary grid (partition type THRED with three equal fracture spacings). The first MINC continuum, corresponding to the fracture domain, occupies a volume fraction of

Table 19. Parameters for five-spot problem

Formation	
Rock grain density	2650 kg/m <sup>3</sup>
Specific heat	1000 J/kg°C
Heat conductivity	2.1 W/m°C
Permeable volume fraction	2%
Porosity in permeable domain	50%
Impermeable blocks: cubes with side length	50m, 250 m
Permeability	6.0x10 <sup>-15</sup> m <sup>2</sup>
Thickness	305 m
Relative permeability: Corey curves	
irreducible liquid saturation	0.30
irreducible gas saturation	0.05
Initial Conditions	
Temperature	300 °C
Liquid saturation	0.99
Pressure	85.93 bar
Production/Injection	
Pattern area	1 km <sup>2</sup>
Distance between producers and injectors	707.1 m
Production rate*	30 kg/s
Injection rate*	30 kg/s
Injection enthalpy	500 kJ/kg

\* Full well basis

0.02 and has an intrinsic porosity of 50 %, for an effective fracture porosity of 1 %. By inserting an ENDCY record in front of the MESHMaker data block, the MINC process can be disabled and the problem can be run as an effective porous medium. Figs. 30 and 31 show part of the printout of the MINC simulation run, and Fig. 32 gives temperature profiles along the line connecting the injection and production wells after 36.5 years. It is seen that the MINC results for 50 m fracture spacing are virtually identical to the porous medium results, while another MINC run for 250 m fracture spacing shows lower temperatures, indicating a less complete thermal sweep.

```

*rfp* - 36 BLOCKS PARALLEL FIVE-SPOT GRID (CF. SPE-18426)
ROCKS----1----*----2----*----3----*----4----*----5----*----6----*----7---
POMED      2650.      .01      6.E-15      6.E-15      6.E-15      2.1
FRACT      2650.      .50      6.E-15      6.E-15      6.E-15      2.1
MATRX      2650.      1.E-10     0.E-15     0.E-15     0.E-15      2.1

START----1----*----2----*----3----*----4----*----5----*----6----*----7---
----*----1 MOP: 123456789*123456789*1234 ----*----5----*----6----*----7---
PARAM----1----*----2----*----3----*----4----*----5----*----6----*----7---
   1 99      9900000000000000 4 0
   1.151852E9      -1. 3.15576E7 KA 1
   1.E5
   1.E-5
   300.          0.01          1.E-8
   5.E5
RPCAP----1----*----2----*----3----*----4----*----5----*----6----*----7---
   3      .30      .05
   1      1.
TIMES----1----*----2----*----3----*----4----*----5----*----6----*----7---
   2      2
   1.57788E8 7.88940E8
GENER----1----*----2----*----3----*----4----*----5----*----6----*----7---
AA 1INJ 1           MASS      3.75      5.0E5
KA 1PRO 1           MASS     -3.75

ELEME----1----*----2----*----3----*----4----*----5----*----6----*----7---
AA 1      POMED0.1906E+060.1250E+04      0.      0.      0.1
BA 1      POMED0.7625E+060.5000E+04      0.7071E+020.      0.1
CA 1      POMED0.7625E+060.5000E+04      0.1414E+030.      0.1
DA 1      POMED0.7625E+060.5000E+04      0.2121E+030.      0.1
EA 1      POMED0.7625E+060.5000E+04      0.2828E+030.      0.1
FA 1      POMED0.7625E+060.5000E+04      0.3536E+030.      0.1
GA 1      POMED0.7625E+060.5000E+04      0.4243E+030.      0.1
HA 1      POMED0.7625E+060.5000E+04      0.4950E+030.      0.1
IA 1      POMED0.7625E+060.5000E+04      0.5657E+030.      0.1
JA 1      POMED0.7625E+060.5000E+04      0.6364E+030.      0.1
KA 1      POMED0.1906E+060.1250E+04      0.7071E+030.      0.1
BB 1      POMED0.7625E+060.5000E+04      0.7071E+020.7071E+020.1
CB 1      POMED0.1525E+070.1000E+05      0.1414E+030.7071E+020.1
...
...
GE 1      POMED0.7625E+060.5000E+04      0.4243E+030.2828E+030.1
FF 1      POMED0.3812E+060.2500E+04      0.3536E+030.3536E+030.1
HTX 00    POMED      0.

CONNE----1----*----2----*----3----*----4----*----5----*----6----*----7---
AA 1 BA 1      10.3536E+020.3536E+020.1078E+05
BA 1 CA 1      10.3536E+020.3536E+020.1078E+05
BA 1 BB 1      20.3536E+020.3536E+020.2157E+05
CA 1 DA 1      10.3536E+020.3536E+020.1078E+05
...
...
FE 1 GE 1      10.3536E+020.3536E+020.2157E+05
FE 1 FF 1      20.3536E+020.3536E+020.2157E+05

INCON----1----*----2----*----3----*----4----*----5----*----6----*----7---
MES HMAKER1----*----2----*----3----*----4----*----5----*----6----*----7---
M INC
PART THRED      DFLT
   5 4OUT      50.
   .02      .08      .20      .35

ENDCY----1----*----2----*----3----*----4----*----5----*----6----*----7---

```

Figure 29. TOUGH2/EOS1 input file for problem 4 - five-spot production/injection. (Only part of ELEME and CONNE data blocks is shown.)

```

*****
*          MESHMAKER - MINC: GENERATE MULTIPLE INTERACTING CONTINUA MESH FOR FRACTURED MEDIUM *
*****
FILE *MINC* EXISTS --- OPEN AS AN OLD FILE

CHOICE OF MATRIX-MATRIX FLOW HANDLING: "DFLT"

THE OPTIONS ARE: "      " (DEFAULT), NO GLOBAL MATRIX-MATRIX FLOW; GLOBAL FLOW ONLY THROUGH FRACTURES
                  "MMVER", GLOBAL MATRIX-MATRIX FLOW IN VERTICAL DIRECTION ONLY
                  "MMALL", GLOBAL MATRIX-MATRIX FLOW IN ALL DIRECTIONS

=====
GEOMETRY DATA, NORMALIZED TO A DOMAIN OF UNIT VOLUME =====

CONTINUUM    IDENTIFIER    VOLUME    NODAL DISTANCE    INTERFACE AREA    INTERFACE DISTANCE
                                         FROM FRACTURES

1-FRACTURES   * *     .20000E-01    .00000E+00    .11760E+00    .00000E+00
2-MATRIX       *2*     .80000E-01    .34984E+00    .11111E+00    .69967E+00
3-MATRIX       *3*     .20000E+00    .97637E+00    .93970E-01    .26524E+01
4-MATRIX       *4*     .35000E+00    .23051E+01    .59197E-01    .72627E+01
5-MATRIX       *5*     .35000E+00    .35475E+01

=====
READ PRIMARY MESH FROM FILE *MESH*
THE PRIMARY MESH HAS 37 ELEMENTS ( 36 ACTIVE) AND 55 CONNECTIONS (INTERFACES) BETWEEN THEM

WRITE SECONDARY MESH ON FILE *MINC*
THE SECONDARY MESH HAS 181 ELEMENTS ( 180 ACTIVE) AND 199 CONNECTIONS (INTERFACES) BETWEEN THEM

*****
MESH GENERATION COMPLETE --- EXIT FROM MODULE *MESHMAKER*

```

Figure 30. Output from MINC processing for problem 4.

We mention again a number of problem variations that can be implemented with small modifications in the input file. For example, heat exchange with confining beds can be studied by setting MOP(15) = 1 (an appropriate inactive element to represent thermal parameters has already been included in the input file). This would be expected to be of minor significance for the porous medium and the  $D = 50$  m fracture spacing cases, but could have major effects when fracture spacing is as large as 250 m. The problem could be run with permeable matrix blocks; typical matrix permeabilities in fractured geothermal reservoirs are of the order of 1 to 10 microdarcies ( $10^{-18}$  to  $10^{-17}$  m $^2$ ). It would also be of interest to compare a “production only” case with various different injection scenarios. The input file as is can also be run with the EOS2 module; the third primary variable would then specify a CO<sub>2</sub> partial pressure of 5 bars.

```

KA 1( 1, 6) ST = .100000E+06 DT = .100000E+06 DX1= -.187193E+06 DX2= .199814E+00 T = 298.440 P = 8405499. S = .209814E+00
KA 1( 2, 5) ST = .200000E+06 DT = .100000E+06 DX1= -.299737E+06 DX2= .772235E-01 T = 295.886 P = 8105763. S = .287037E+00
KA 1( 3, 5) ST = .300000E+06 DT = .100000E+06 DX1= -.330969E+06 DX2= .266975E-01 T = 292.981 P = 7774793. S = .313735E+00
KA 1( 4, 4) ST = .400000E+06 DT = .100000E+06 DX1= -.338081E+06 DX2= .171490E-01 T = 289.914 P = 7436712. S = .330884E+00
KA 1( 5, 4) ST = .600000E+06 DT = .200000E+06 DX1= -.749332E+06 DX2= .325955E-01 T = 282.716 P = 6687380. S = .363479E+00
KA 1( 6, 6) ST = .100000E+07 DT = .400000E+06 DX1= -.972591E+06 DX2= .260142E-01 T = 272.391 P = 5714789. S = .389494E+00
KA 1( 7, 4) ST = .140000E+07 DT = .400000E+06 DX1= -.187123E+06 DX2= -.145613E-01 T = 270.253 P = 5527666. S = .374932E+00
KA 1( 8, 4) ST = .220000E+07 DT = .800000E+06 DX1= .151570E+06 DX2= -.262760E-01 T = 271.989 P = 5679236. S = .348656E+00
KA 1( 9, 4) ST = .380000E+07 DT = .160000E+07 DX1= .103832E+06 DX2= -.138883E-01 T = 273.158 P = 5783068. S = .334768E+00
KA 1( 10, 4) ST = .700000E+07 DT = .320000E+07 DX1= .384188E+05 DX2= -.573952E-02 T = 272.728 P = 5744649. S = .329028E+00
KA 1( 11, 5) ST = .134000E+08 DT = .640000E+07 DX1= .265090E+05 DX2= .714484E-02 T = 272.429 P = 5718140. S = .321884E+00
KA 1( 12, 4) ST = .198000E+08 DT = .640000E+07 DX1= .268056E+06 DX2= -.181049E-01 T = 275.399 P = 5986196. S = .303779E+00
KA 1( 13, 5) ST = .326000E+08 DT = .128000E+08 DX1= .452419E+03 DX2= -.184674E-02 T = 275.394 P = 5985744. S = .301932E+00
KA 1( 14, 4) ST = .454000E+08 DT = .128000E+08 DX1= .720842E+05 DX2= .817172E-03 T = 274.606 P = 5913660. S = .302749E+00
KA 1( 15, 4) ST = .710000E+08 DT = .256000E+08 DX1= .277187E+06 DX2= .741455E-02 T = 271.503 P = 5636472. S = .310164E+00
KA 1( 16, 8) ST = .102558E+09 DT = .315576E+08 DX1= .567330E+05 DX2= -.246617E-02 T = 270.854 P = 5579739. S = .307697E+00
KA 1( 17, 5) ST = .134115E+09 DT = .315576E+08 DX1= .586688E+05 DX2= -.702594E-03 T = 270.177 P = 5521071. S = .306995E+00
KA 1( 18, 5) ST = .157788E+09 DT = .236728E+08 DX1= .659227E+05 DX2= .861111E-03 T = 269.410 P = 5455148. S = .307856E+00

```

\*rfp\* - 36 BLOCKS PARALLEL FIVE-SPOT GRID (CF. SPE-18426)

OUTPUT DATA AFTER ( 18, 5)-2-TIME STEPS										THE TIME IS .18262E+04 DAYS			
TOTAL TIME	KCYC	ITER	ITERC	KON	DX1M	DX2M	DX3M	RERM	NER	KER	DELTEX		
.15779E+09	18	5	86	2	.637088E+06	.299967E+03	.000000E+00	.517035E-08	51	2	.236728E+08		
=====													
ELEM.	INDEX	P (PA)	T (DEG-C)	SG	SW	X1	X2	PCAP (PA)	DG (KG/M**3)	DW (KG/M**3)			
AA 1	1	.10328E+08	.13023E+03	.00000E+00	.10000E+01	.10000E+01	.00000E+00	.00000E+00	.15064E+01	.93966E+03			
2AA 1	2	.28232E+06	.13159E+03	.24435E+00	.75565E+00	.10000E+01	.00000E+00	.00000E+00	.15648E+01	.93320E+03			
3AA 1	3	.33065E+06	.13689E+03	.24068E+00	.75932E+00	.10000E+01	.00000E+00	.00000E+00	.18092E+01	.92862E+03			
4AA 1	4	.48442E+06	.15066E+03	.23053E+00	.76947E+00	.10000E+01	.00000E+00	.00000E+00	.25906E+01	.91616E+03			
5AA 1	5	.89267E+06	.17501E+03	.21023E+00	.78977E+00	.10000E+01	.00000E+00	.00000E+00	.46191E+01	.89215E+03			
BA 1	6	.93995E+07	.18697E+03	.00000E+00	.10000E+01	.10000E+01	.00000E+00	.00000E+00	.59990E+01	.88513E+03			
2BA 1	7	.12159E+07	.18856E+03	.19746E+00	.80254E+00	.10000E+01	.00000E+00	.00000E+00	.62051E+01	.87764E+03			
3BA 1	8	.13842E+07	.19451E+03	.19147E+00	.80853E+00	.10000E+01	.00000E+00	.00000E+00	.70289E+01	.87097E+03			
4BA 1	9	.18559E+07	.20863E+03	.17620E+00	.82380E+00	.10000E+01	.00000E+00	.00000E+00	.93339E+01	.85447E+03			
5BA 1	10	.27881E+07	.22981E+03	.14996E+00	.85004E+00	.10000E+01	.00000E+00	.00000E+00	.13944E+02	.82757E+03			
CA 1	11	.91035E+07	.25422E+03	.00000E+00	.10000E+01	.10000E+01	.00000E+00	.00000E+00	.21500E+02	.79864E+03			
2CA 1	12	.43340E+07	.25513E+03	.11161E+00	.88839E+00	.10000E+01	.00000E+00	.00000E+00	.21837E+02	.79146E+03			
3CA 1	13	.45774E+07	.25845E+03	.10584E+00	.89416E+00	.10000E+01	.00000E+00	.00000E+00	.23116E+02	.78634E+03			
4CA 1	14	.51584E+07	.26587E+03	.92199E-01	.90780E+00	.10000E+01	.00000E+00	.00000E+00	.26214E+02	.77455E+03			
5CA 1	15	.60265E+07	.27584E+03	.71923E-01	.92808E+00	.10000E+01	.00000E+00	.00000E+00	.30976E+02	.75784E+03			
DA 1	16	.89587E+07	.28748E+03	.00000E+00	.10000E+01	.10000E+01	.00000E+00	.00000E+00	.37564E+02	.74015E+03			

Figure 31. Selected output from problem 4 flow simulation.

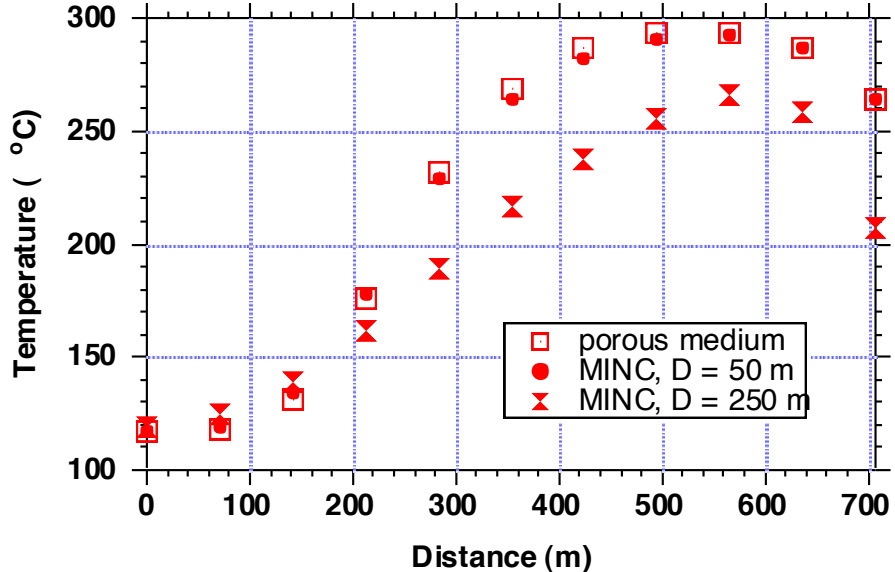


Figure 32. Temperature profiles for problem 4 along a line from injection to production well after 36.5 yrs.

## 9.5 Problem No. 5 (\*r1q\*) - Coupled Wellbore Flow (EOS1)

Application of TOUGH2 to coupled reservoir-wellbore flow is demonstrated with a geothermal production problem similar to Problem 1 of Hadgu et al. (1995). An exact replication of their test problem is not possible because they did not give complete specifications in their paper. A well of 0.2 m inside diameter produces from a 500 m thick two-phase reservoir containing water at initial conditions of  $P = 60$  bars,  $T = T_{sat}(P) = 275.5$  °C,  $S_g = 0.1$ . Wellhead pressure is 7 bars, and feed zone depth is 1000 m.

The input file for TOUGH2/EOS1 as given in Fig. 33 has MESHMaker data for a 1-D radial grid with a wellblock radius of 100 m, as used by Hadgu et al. (1995) to represent a large negative skin factor. The grid extends to a radius of 10,000 m and will be infinite-acting for the time period simulated. Prior to the flow simulation the grid is edited and the first (wellblock) nodal distance is set to a small value; for convenience the original connection record is provided at the end of the input file. In the flow simulation we specify a generation type f725d to engage coupled reservoir-wellbore flow using the flowing bottomhole well pressure data file f725d shown in Table 17 and Fig. 10. Well productivity index is 4.64e-11 m<sup>3</sup>, as used by Hadgu et al. (1995). We also include FOFT and GOFT data blocks to generate data files of time-dependent simulation results suitable for plotting.

The simulation starts with a time step of 1.e5 seconds. Time steps grow rapidly, and the desired simulation time of 10<sup>9</sup> seconds is reached after 30 time steps. Part of the printed output is given in Fig. 34, while Fig. 35 shows the temporal evolution of well flow rate, flowing enthalpy, flowing bottomhole pressure, and wellblock pressure. By replacing the GENER-item in the input file with the DELV item included after the ENDCY-record (see Fig. 33), a problem variation can be run in which production occurs on deliverability against a fixed bottomhole pressure of  $P_{wb} = 57.37$  bars, which is the flowing bottomhole pressure in the coupled reservoir-wellbore system at the end of the first time step (1.e5 seconds). Results obtained for this case are also shown in Fig. 35 and are marked with a subscript “c”.

Our results for flow rates and flowing enthalpies in the coupled model are a few percent higher than those obtained by Hadgu et al., while flowing bottomhole pressures are slightly lower. The simulation with constant bottomhole pressure gives a rapidly declining production rate that agrees well with Hadgu et al. (1995). It is seen that the coupled reservoir-wellbore system sustains long-term production at substantially higher rates, because it predicts a stronger rise in flowing

enthalpy, for which wellbore flow can be sustained at smaller bottomhole driving pressures. The large differences when compared with the simulation with constant bottomhole pressure emphasize the importance of coupled wellbore flow effects for two-phase geothermal production wells.

```

*r1q* --- 1-D radial test problem for flowing wellbore pressure
MESHMAKER1----*---2----*---3----*---4----*---5----*---6----*---7----*---8
RZ2D
RADII
 2
    0.      100.
EQUID
 20
    10.
LOGAR
 30
    1.E3
LOGAR
 30
    1.E4
EQUID
 1
    0.0
LAYER----1----*---2----*---3----*---4----*---5----*---6----*---7----*---8
 1
    500.

ENDFI----1----*---2----*---3----*---4----*---5----*---6----*---7----*---8
ROCKS----1----*---2----*---3----*---4----*---5----*---6----*---7----*---8
POMED      2600.      .10      1.e-13      1.e-13      1.e-13      2.0      1000.0

START----1----*---2----*---3----*---4----*---5----*---6----*---7----*---8
----*---1 MOP: 123456789*123456789*1234 ----*---5----*---6----*---7----*---8
PARAM----1----*---2----*---3----*---4----*---5----*---6----*---7----*---8
 1 100      100100      000000002 30 0 3
      1.e9      -1.

      1.E5      1.E00
      60.E5      0.10
      1.E-7
RPCAP----1----*---2----*---3----*---4----*---5----*---6----*---7----*---8
 3      .30      .05
 1      1.

FOFT ----1----*---2----*---3----*---4----*---5----*---6----*---7----*---8
A1 1

GOFT ----1----*---2----*---3----*---4----*---5----*---6----*---7----*---8

INCON----1----*---2----*---3----*---4----*---5----*---6----*---7----*---8

GENER----1----*---2----*---3----*---4----*---5----*---6----*---7----*---8
A1 1wel 1
      f725d  4.64e-11

ENDCY----1----*---2----*---3----*---4----*---5----*---6----*---7----*---8
GENER----1----*---2----*---3----*---4----*---5----*---6----*---7----*---8
A1 1wel 1
      DELV  4.64e-11  .5737E+07

CONN
A1 1A1 2
      1  .5000E+00  .5000E+01  .3142E+06

```

Figure 33. Input for coupled reservoir-wellbore flow problem for TOUGH2/EOS1.

```

...ITERATING... AT [ 1, 1] --- DELTEX = .100000E+06 MAX. RES. = .618714E-02 AT ELEMENT A1 1 EQUATION 1
...ITERATING... AT [ 1, 2] --- DELTEX = .100000E+06 MAX. RES. = .745132E-04 AT ELEMENT A1 2 EQUATION 1
A1 2( 1, 3) ST = .100000E+06 DT = .100000E+06 DX1= -.444930E+03 DX2= .266564E-02 T = 275.545 P = 599955. S = .102666E+00
...ITERATING... AT [ 2, 1] --- DELTEX = .200000E+06 MAX. RES. = .102796E-01 AT ELEMENT A1 1 EQUATION 1
...ITERATING... AT [ 2, 2] --- DELTEX = .200000E+06 MAX. RES. = .162763E-03 AT ELEMENT A1 2 EQUATION 1
A1 2( 2, 3) ST = .300000E+06 DT = .200000E+06 DX1= -.105296E+04 DX2= .627229E-02 T = 275.533 P = 5998502. S = .108938E+00
...ITERATING... AT [ 3, 1] --- DELTEX = .400000E+06 MAX. RES. = .173616E-01 AT ELEMENT A1 1 EQUATION 1
...ITERATING... AT [ 3, 2] --- DELTEX = .400000E+06 MAX. RES. = .286919E-03 AT ELEMENT A1 2 EQUATION 1
A1 3( 3, 3) ST = .700000E+06 DT = .400000E+06 DX1= -.143401E+04 DX2= .848442E-02 T = 275.525 P = 5997747. S = .113385E+00
...ITERATING... AT [ 4, 1] --- DELTEX = .800000E+06 MAX. RES. = .291114E-01 AT ELEMENT A1 1 EQUATION 1
...ITERATING... AT [ 4, 2] --- DELTEX = .800000E+06 MAX. RES. = .912080E-03 AT ELEMENT A1 2 EQUATION 1
A1 2( 4, 3) ST = .150000E+07 DT = .800000E+06 DX1= -.340359E+04 DX2= .184378E-01 T = 275.475 P = 5993149. S = .138757E+00
...ITERATING... AT [ 5, 1] --- DELTEX = .160000E+07 MAX. RES. = .477432E-01 AT ELEMENT A1 1 EQUATION 1
...ITERATING... AT [ 5, 2] --- DELTEX = .160000E+07 MAX. RES. = .321657E-02 AT ELEMENT A1 2 EQUATION 1
...
...
*r1q* --- 1-D radial test problem for flowing wellbore pressure

        OUTPUT DATA AFTER ( 30, 3)-2-TIME STEPS                                     THE TIME IS .11574E+05 DAYS

@oooooooooooooooooooooooooooooooooooooooooooooooooooooooooooooooooooooooooooooooooooo

TOTAL TIME   KCYC   ITER   ITERC   KON   DX1M      DX2M      DX3M      RERM      NER      KER      DELTEX
.10000E+10    30       3     108      2   .574895E+04   .748790E-02   .000000E+00   .115297E-05     1       1   .945000E+08

@oooooooooooooooooooooooooooooooooooooooooooooooooooooooooooooooooooooooooooooooooooo

ELEM. INDEX      P          T          SG          SW          X1          X2          PCAP         DG          DW
          (PA)        (DEG-C)      (PA)        (PA)          (DEG-C)      (KG/M**3)      (KG/M**3)

A1 1     1   .56974E+07   .27220E+03   .26227E+00   .73773E+00   .10000E+01   .00000E+00   .00000E+00   .29151E+02   .76407E+03
A1 2     2   .57040E+07   .27227E+03   .26172E+00   .73828E+00   .10000E+01   .00000E+00   .00000E+00   .29187E+02   .76394E+03
A1 3     3   .57147E+07   .27239E+03   .26128E+00   .73872E+00   .10000E+01   .00000E+00   .00000E+00   .29246E+02   .76374E+03
A1 4     4   .57246E+07   .27250E+03   .26086E+00   .73914E+00   .10000E+01   .00000E+00   .00000E+00   .29300E+02   .76355E+03
A1 5     5   .57336E+07   .27260E+03   .26047E+00   .73953E+00   .10000E+01   .00000E+00   .00000E+00   .29350E+02   .76338E+03

```

Figure 34. Part of printed output for coupled reservoir-wellbore problem.

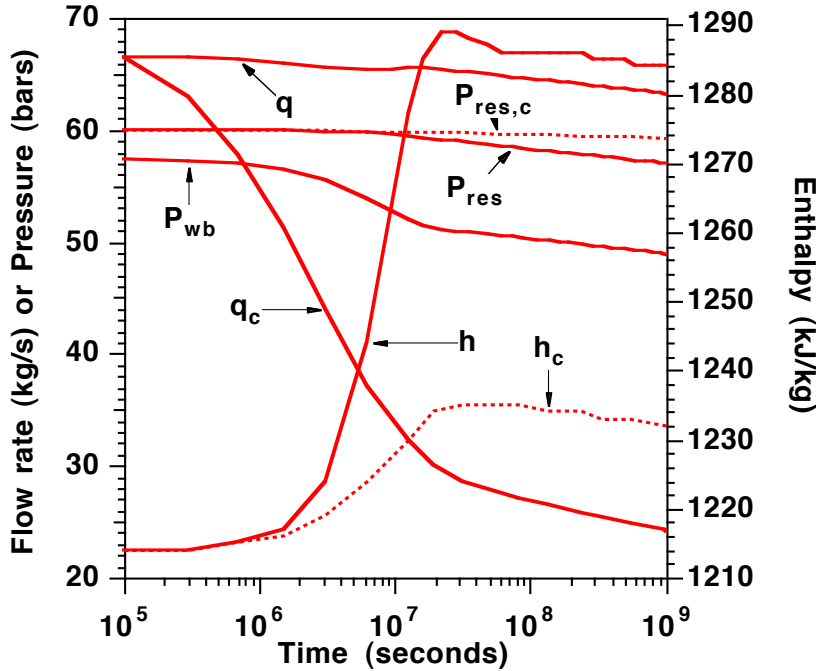


Figure 35. Simulated flow rate ( $q$ ), flowing enthalpy ( $h$ ), flowing bottomhole pressure ( $P_{wb}$ ) and reservoir pressure in well grid block ( $P_{res}$ ) for a problem adapted from Hadgu et al. (1995). Results obtained for constant bottomhole pressure of  $P_{wb} = 57.37$  bars, labeled  $q_c$ ,  $h_c$ , and  $P_{res,c}$ , are also shown.

## **9.6 Problem No. 6 (\*rf1\*) - Multiphase and Nonisothermal Processes in a System with Variable Salinity (EOS7)**

Figures 36 through 38 show specifications and some results for a simulation problem that involves nonisothermal flow of variably saline brine and air. The problem was not designed with an actual “real life” flow problem in mind; rather, the purpose is to demonstrate the use of a variety of thermodynamic conditions and generation options with EOS7, and to provide a benchmark for proper code implementation.

The input file (see Fig. 36) has MESHMAKER specifications for a three-dimensional 5x5x2 X-Y-Z mesh. Data block MULTI specifies that the 3-component option (water, brine, air) is to be used in nonisothermal mode ( $NK = 3$ ,  $NEQ = 4$ ), and “SELEC” chooses default parameters for the reference brine.

Default initial conditions specified in the last record of data block PARAM are: pressure  $P = 10^5 \text{ Pa}$ , brine mass fraction  $X_b = 0.5$ , air mass fraction  $X = 0.$ , and temperature  $T = 25 \text{ }^\circ\text{C}$ . Various different initial conditions are chosen for portions of the flow domain in data block INCON. In the top layer, the first row of grid blocks (A11 1 through A11 5) has  $X_b = 0.0$ , corresponding to single-phase water without salinity; the middle row (A13 1 through A13 5) has  $X_b = 0.0, X = 0.99$ , corresponding to single-phase gas conditions; the last row (A15 1 through A15 5) is initialized with  $X_b = 1.0$ , corresponding to pure brine. In the bottom layer, two-phase conditions with 50 % gas saturation and different salinities are prescribed for the middle row (grid blocks A23 1 through A23 5). In blocks A23 1 and A23 2 the aqueous phase is pure water, in A23 3 it has 50 % brine mass fraction, and in A23 4 and A23 5 it is 100 % brine.

Generation options include a well on deliverability in the upper left corner of the grid (block A11 1), brine injection (COM2) in the upper right hand corner (block A11 5), water injection (COM1) in the lower right hand corner (block A25 5), heat generation in the center block of the lower layer (A23 3), and air injection (COM3) in the lower left corner (block A25 1). Brine enthalpy is  $10^6 \text{ J/kg}$ , corresponding to a temperature of approximately  $233 \text{ }^\circ\text{C}$ , while enthalpy of injected water,  $3 \times 10^5 \text{ J/kg}$ , corresponds to a temperature of approximately  $72 \text{ }^\circ\text{C}$ . Air is injected at a lower rate ( $10^{-4} \text{ kg/s}$ ) and enthalpy ( $2 \times 10^5 \text{ J/kg}$ ). Air specific heat at constant pressure is approximately  $1010 \text{ J/kg }^\circ\text{C}$  (Vargaftik, 1975), so that this enthalpy corresponds to a temperature of approximately  $198 \text{ }^\circ\text{C}$ .

```

*rf1* ... EOS7-test: inject air, heat, brine and fresh water
MESHMAKER1----*---2---*---3---*---4---*---5---*---6---*---7---*---8
XYZ

NX      5      1.
NY      5      1.
NZ      2      1.

ROCKS---1----*---2---*---3---*---4---*---5---*---6---*---7---*---8
POMED    2650.      .25  200.e-15  200.e-15  200.e-15      2.2      1000.

.....specify three components (water, brine, air); solve energy equation
.....no diffusion
MULTI---1----*---2---*---3---*---4---*---5---*---6---*---7---*---8
      3     4     2     6
START---1----*---2---*---3---*---4---*---5---*---6---*---7---*---8
---*---1 MOP: 123456789*123456789*1234 ---*---5---*---6---*---7---*---8
PARAM---1----*---2---*---3---*---4---*---5---*---6---*---7---*---8
      3     99    9910000000000000 4
0.          8.64e4      -1.          9.81
      1.e-9      2.
      1.E-5      1.
      1.e5          0.5          0.0          25.
.....use default parameters for reference brine
SELEC---1----*---2---*---3---*---4---*---5---*---6---*---7---*---8
      2

RPCAP---1----*---2---*---3---*---4---*---5---*---6---*---7---*---8
      1       .30       .05      1.       1.
      1       5.e5       .20      1.
TIMES---1----*---2---*---3---*---4---*---5---*---6---*---7---*---8
      3     3
      1.e-9      2.      8.64e4
GENER---1----*---2---*---3---*---4---*---5---*---6---*---7---*---8
A11 1pro 1           DELV      2.e-13      1.e5
A11 5bri 1           COM2      5.e-2       1.e6
A25 5wtr 1           COM1      5.e-2       3.e5
A23 3hot 1           HEAT      1.e5
A25 1air 1           COM3      1.e-4       2.e5

INCON---1----*---2---*---3---*---4---*---5---*---6---*---7---*---8
A11 1   4   1
      1.e5          0.00          0.0          25.
A13 1   4   1
      1.e5          0.00          0.99          25.
A15 1   4   1
      1.e5          1.0           0.0          25.
A23 1   1   1
      1.e5          0.00         10.50          25.
A23 3
      1.e5          0.50         10.50          25.
A23 4   1   1
      1.e5          1.0          10.50          25.

ENDCY---1----*---2---*---3---*---4---*---5---*---6---*---7---*---8

```

Figure 36. TOUGH2 input file for EOS7 test problem.

The first element-by-element printout occurs at  $10^{-9}$  seconds, giving a record of initial conditions and interblock flow rates. Fig. 37 shows the iteration sequence and part of the printout for time step # 2 with  $\Delta t = 2$  seconds. The strong suction pressures in the single-phase gas blocks A13 1 through A13 5 have drawn in enough aqueous phase to effect a transition to two-phase conditions. The liquid inflow results in a pressure increase which is very small due to the very large compressibility of gas (approximately  $1/P = 10^{-5} \text{ Pa}^{-1}$ ), while pressure decline in the grid blocks that initially were in single-phase liquid conditions is large, due to the small compressibility of liquid water (of order  $10^{-10} \text{ Pa}^{-1}$ ). Gas phase, mostly air with a small fraction of water vapor, flows from the blocks that were initially in single-phase gas or two-phase conditions into the neighboring single-phase liquid blocks, causing phase transitions to two-phase conditions there. The air injection block A25 1 remains in single-phase liquid conditions, because the amount of air injected in 2 seconds is below the solubility limit at prevailing pressures. Note that brine mass fraction in A13 1 is smaller than in A13 5, due to different aqueous phase compositions in the neighboring blocks that provide the liquid inflows.

Figure 37. Iteration sequence and portion of the output after time step # 2.

With automatic time step control, total desired simulation time of 86,400 seconds (1 day) is reached after 52 time steps. Results are shown in Fig. 38. Most of the flow system, except for the vicinity of the block receiving water injection, is now in two-phase conditions. Air is the dominant gas phase component in the cooler regions, while vapor dominates in the hotter regions. Aqueous phase compositions vary over a broad range.  $X_b$  exceeds 1 in a few grid blocks, representing a salinity in excess of that of the reference brine. This effect is due to partial vaporization, and indicates limitations in the water-brine mixing approach used in EOS7.

OUTPUT DATA AFTER ( 52, 5)-2-TIME STEPS											THE TIME IS .10000E+01 DAY			
TOTAL TIME	KCYC	ITER	ITERC	KON	DX1M	DX2M	DX3M	MAX. RES.	NER	KER	DELTEX			
.86400E+05	52	5	274	2	.31302E+05	.47029E-01	.64245E-01	.19448E-07	21	1	.26880E+04			
ELEM.	INDEX	P (PA)	T (DEG-C)	SG	SL	XBRINE(LIQ)	XAIRL	XAIRL	PCAP (PA)	DG (KG/M**3)	DL (KG/M**3)			
A11 1	1	.39334E+06	.10330E+03	.65235E-01	.93476E+00	.52361E+00	.79505E+00	.28542E-04	.40772E+05	.32525E+01	.10424E+04			
A21 1	2	.46677E+06	.10676E+03	.57646E-01	.94235E+00	.41642E+00	.80625E+00	.38910E-04	.36029E+05	.38484E+01	.10207E+04			
A12 1	3	.48283E+06	.10277E+03	.79610E-01	.92039E+00	.42418E+00	.83995E+00	.42324E-04	.49757E+05	.40933E+01	.10253E+04			
A22 1	4	.50510E+06	.14350E+03	.79769E-01	.92023E+00	.29570E+00	.29207E+00	.13719E-04	.49856E+05	.30464E+01	.96820E+04			
A13 1	5	.52397E+06	.86828E+02	.94582E-01	.90542E+00	.45732E+00	.92204E+00	.50867E-04	.59114E+05	.48471E+01	.10431E+04			
A23 1	6	.54844E+06	.15150E+03	.11606E+00	.88394E+00	.25307E+00	.14119E+00	.70894E-05	.72573E+05	.30808E+01	.95368E+04			
A14 1	7	.54799E+06	.28650E+02	.92845E+01	.90716E+00	.69116E+00	.99553E+00	.44101E-04	.58208E+05	.63073E+01	.11190E+04			
A24 1	8	.55699E+06	.55054E+02	.91878E-01	.90812E+00	.35949E+00	.98211E+00	.65815E-04	.57423E+05	.58482E+01	.10455E+04			
A15 1	9	.55951E+06	.25119E+02	.92486E-01	.90751E+00	.95607E+00	.99644E+00	.25066E-04	.57804E+05	.65197E+01	.11756E+04			
A25 1	10	.57128E+06	.26811E+02	.93387E-01	.90616E+00	.43833E+00	.99615E+00	.63807E-04	.58367E+05	.66181E+01	.10714E+04			
A11 2	11	.47108E+06	.12742E+03	.54232E-01	.94577E+00	.69536E+00	.58015E+00	.17805E-04	.33895E+05	.33145E+01	.10530E+04			
A21 2	12	.49637E+06	.12764E+03	.55512E-01	.94449E+00	.54728E+00	.60307E+00	.24289E+00	.34695E+05	.35275E+01	.10257E+04			
A12 2	13	.55925E+06	.15608E+03	.15789E+00	.84211E+00	.47719E+00	.13197E-02	.52004E-07	.98682E+05	.29677E+01	.98563E+04			
A22 2	14	.63604E+06	.16113E+03	.26078E+00	.73922E+00	.36817E+00	.97222E-05	.48970E-09	.16299E+06	.33495E+01	.96233E+04			
A13 2	15	.62725E+06	.16050E+03	.24009E+00	.75991E+00	.40369E+00	.20796E-03	.99713E-08	.15006E+06	.33006E+01	.96871E+04			
A23 2	16	.73174E+06	.16674E+03	.39024E+00	.60976E+00	.17388E+00	.36461E-07	.25068E-11	.24390E+06	.38233E+01	.92613E+04			
A14 2	17	.55409E+06	.61082E+02	.89555E-01	.91045E+00	.56224E+00	.97602E+00	.51916E-04	.55972E+05	.56925E+01	.10790E+04			
A24 2	18	.63197E+06	.16087E+03	.20418E+00	.79582E+00	.14062E+00	.34351E-03	.20805E-07	.12761E+06	.33296E+01	.92708E+04			
A15 2	19	.55901E+06	.26136E+02	.74843E-01	.92152E+00	.84785E+00	.99622E+00	.33441E-04	.49052E+05	.64908E+01	.11520E+04			
A25 2	20	.56668E+06	.43265E+02	.73611E+00	.92639E+00	.21474E+00	.99030E+00	.76948E-04	.46007E+05	.62016E+01	.10261E+04			
A11 3	21	.55593E+06	.15578E+03	.11884E+00	.88116E+00	.91888E+00	.38489E-02	.70461E-07	.74273E+05	.29539E+01	.10668E+04			
A21 3	22	.53052E+06	.13661E+03	.58228E-01	.94177E+00	.67770E+00	.48942E+00	.16766E-04	.36392E+05	.35170E+01	.10408E+04			
A12 3	23	.63557E+06	.16110E+03	.23473E+00	.76527E+00	.63633E+00	.17309E-03	.63634E-08	.14671E+06	.33474E+01	.10979E+04			
A22 3	24	.72330E+06	.16628E+03	.35804E+00	.64196E+00	.46788E+00	.23394E-04	.12155E-08	.22377E+06	.37288E+01	.97327E+04			
A13 3	25	.71853E+06	.16601E+03	.35669E+00	.64391E+00	.35582E+00	.86864E-04	.50245E-08	.22256E+06	.37593E+01	.95522E+04			
A23 3	26	.93376E+06	.17693E+03	.70504E+00	.29496E+00	.44942E+01	.82029E-08	.82150E-13	.44065E+06	.48214E+01	.30985E+04			
A14 3	27	.55833E+06	.13318E+03	.81875E-01	.91813E+00	.36201E+00	.57814E+00	.31718E-04	.51712E+05	.38763E+01	.98874E+04			
A24 3	28	.71046E+06	.16555E+03	.30813E+00	.69187E+00	.33497E-01	.14767E-03	.10881E-07	.19258E+06	.37194E+01	.90660E+04			
A15 3	29	.55756E+06	.30539E+02	.56274E-01	.94373E+00	.52837E+00	.99510E+00	.56172E-04	.35171E+05	.63758E+01	.10869E+04			
A25 3	30	.56472E+06	.87503E+02	.54505E-02	.94595E+00	.41516E-01	.92590E+00	.78383E-04	.33782E+05	.52257E+01	.97343E+04			
A11 4	31	.66388E+06	.16283E+03	.23305E+00	.76695E+00	.11735E+01	.13332E-14	.93566E-20	.14566E+06	.34879E+01	.11113E+04			
A21 4	32	.55613E+06	.13675E+03	.54696E-01	.94303E+00	.87281E+00	.51676E+00	.12872E-04	.34185E+05	.37296E+01	.10781E+04			
A12 4	33	.56471E+06	.13630E+03	.81580E-03	.91842E+00	.85158E+00	.53379E+00	.14301E-04	.50988E+05	.38191E+01	.10744E+04			
A22 4	34	.56590E+06	.14821E+03	.70431E-01	.92957E+00	.49109E+00	.27600E+00	.11912E-04	.44200E+05	.33634E+01	.99607E+04			
A13 4	35	.56135E+06	.13240E+03	.74553E-01	.92545E+00	.34881E+00	.59282E+00	.33321E-04	.46596E+05	.39299E+01	.98727E+04			
A23 4	36	.70573E+06	.16528E+03	.29035E+00	.70965E+00	.75173E-01	.12219E-03	.86939E-08	.18147E+06	.36395E+01	.91293E+04			
A14 4	37	.55773E+06	.33759E+02	.47202E-01	.95280E+00	.33942E+00	.99411E+00	.68461E-04	.29502E+05	.63071E+01	.10513E+04			
A24 4	38	.53501E+06	.12450E+03	.00000E+00	.10000E+01	.18539E-01	.63213E+00	.39871E-04	.00000E+00	.00000E+00	.94104E+04			
A15 4	39	.54756E+06	.38411E+02	.10292E-01	.98971E+00	.17768E+00	.99225E+00	.76777E-04	.64325E+04	.60928E+01	.10219E+04			
A25 4	40	.55350E+06	.63893E+02	.00000E+00	.10000E+01	.16474E-02	.94324E+00	.39635E-04	.00000E+00	.00000E+00	.98160E+04			
A11 5	41	.80134E+06	.17048E+03	.35431E+00	.64569E+00	.11624E+01	.30037E-13	.25367E-18	.22145E+05	.41688E+01	.10995E+04			
A21 5	42	.68772E+06	.16424E+03	.22711E+00	.77289E+00	.10788E+01	.72150E-10	.88688E-15	.14195E+06	.36063E+01	.10895E+04			
A12 5	43	.66813E+06	.21327E+03	.78673E+00	.10844E+01	.11058E-10	.12813E-15	.13329E+00	.35091E+01	.10920E+04				
A22 5	44	.55804E+06	.97576E+02	.29516E-01	.97048E+00	.70391E+00	.88806E+00	.36936E-04	.18448E+05	.49213E+01	.10807E+04			
A13 5	45	.55643E+06	.53735E+02	.38852E-01	.96151E+00	.45408E+00	.98320E+00	.59855E-04	.24283E+05	.58697E+01	.10631E+04			
A23 5	46	.54043E+06	.89515E+02	.00000E+00	.10000E+01	.10495E+00	.90798E+00	.64056E-04	.00000E+00	.00000E+00	.98200E+04			
A14 5	47	.54344E+06	.37933E+02	.00000E+00	.10000E+01	.15532E+00	.97981E+00	.28842E-04	.00000E+00	.00000E+00	.10183E+04			
A24 5	48	.55652E+06	.62803E+02	.00000E+00	.10000E+01	.24840E-02	.23770E+00	.70922E-06	.00000E+00	.00000E+00	.9829E+04			
A15 5	49	.55812E+06	.55943E+02	.00000E+00	.10000E+01	.25454E-01	.30317E+00	.70790E-06	.00000E+00	.00000E+00	.98943E+04			
A25 5	50	.59298E+06	.70933E+02	.00000E+00	.10000E+01	.34700E-06	.00000E+00	.00000E+00	.00000E+00	.00000E+00	.97737E+04			

Figure 38 TOUGH2 output after 1 day of simulation time

## 9.7 Problem No. 7 (\*rdif7\*) - Thermal and Tracer Diffusion (EOS7R)

Fig. 39 shows an input file for a tracer diffusion problem, which serves as an illustration for preparing EOS7R input data, and as a benchmark for code performance. There are in fact two independent flow problems in two separate 1-D grid systems, each with  $1 \text{ m}^2$  cross sectional area and 2 m long, divided into 20 grid blocks of 0.1 m length. The “A-grid” (blocks A 1 through A 20) is initialized in single phase liquid conditions with default parameters of  $P = 10^5 \text{ Pa}$ ,  $T = 8 \text{ }^\circ\text{C}$ , and zero mass fractions for brine, Rn1, Rn2, and air. Boundary conditions provided by inactive block “ina 1” are  $(P, X_b, X_{Rn1}, X_{Rn2}, X, T) = (10^5, 10^{-3}, 10^{-7}, 10^{-8}, 10^{-6}, 9 \text{ }^\circ\text{C})$ . The radionuclide tracers are stable (half life of  $10^{50}$  seconds). Rn1 with an inverse Henry’s constant of  $10^5 \text{ Pa}^{-1}$  has low volatility, while Rn2 is a volatile species with the same inverse Henry’s constant as air,  $10^{-10} \text{ Pa}^{-1}$ . Diffusivities specified in data block DIFFU override parameters in block SELEC; all diffusivities are specified as -1.e-6 so that, for all components, mass diffusion occurs with saturation and tortuosity-independent effective diffusivities of  $10^{-6} \text{ m}^2/\text{s}$ . In addition to mass diffusion, there is also thermal diffusion due to the different temperature at the boundary. Thermal diffusivity is  $d_{th} = \lambda/\rho C \approx 2.5/(2500 \times 1000) = 10^{-6} \text{ m}^2/\text{s}$ , equal to component diffusivities. (Porosity was chosen to be small,  $\phi = 10^{-4}$ , so that fluid contributions to formation specific heat are small.) This parametrization allows a direct comparison between changes for mass fractions and temperatures. The “B-grid” (B 1 through B 20) is initialized in single-phase gas conditions at the same pressure of  $10^5 \text{ Pa}$ , but at a temperature of  $125 \text{ }^\circ\text{C}$ , and also with zero mass fractions of all components other than water. Different non-zero mass fractions for the various components are specified in block ina 2 at the boundary of the B-grid.

Advective effects are suppressed because the medium was assigned zero permeability. Accordingly, the only active processes are mass diffusion of the various components, and thermal diffusion in the A-grid. Portions of the iteration sequence and results obtained after 20 time steps ( $1.427 \times 10^6$  seconds) are shown in Fig. 40. Note that mass fractions for all components are always calculated in both aqueous and gas phases, regardless of phase composition of the fluid (see Appendix D for further discussion). Under the specified conditions, the diffusive profiles are expected to be the same for all components, the only difference being different normalization, because of the different absolute magnitude of the concentration step at the boundary. The liquid phase mass fraction profiles for brine, Rn1, and Rn2 in the A-grid are seen to be in excellent agreement with each other, as well as with the temperature profile from heat conduction. The gas phase radionuclide mass fractions listed for the A-grid are obtained from phase partitioning according to Henry’s law locally; there is no mass inventory associated with these because gas phase saturations are zero. In the single-phase gas conditions in the B-grid, it is the gas phase mass fractions which are to be compared; for all components they agree very well among each other, as

```

*rdif7* ... simple diffusion problem for EOS7R
ROCKS---1----*---2----*---3----*---4----*---5----*---6----*---7----*---8
SANDY   2      2500.    1.e-4     0.e-12    0.e-12    0.e-12    2.5      1000.
          1.e-8           0.25           0.00e-04  0.00E-00
          1.                 0.                1.
          1.                 0.e6               1.

MULTI---1----*---2----*---3----*---4----*---5----*---6----*---7----*---8
      5       6       2       8
START---1----*---2----*---3----*---4----*---5----*---6----*---7----*---8
----*---1 MOP: 123456789*123456789*1234 ---*---5----*---6----*---7----*---8
PARAM---1----*---2----*---3----*---4----*---5----*---6----*---7----*---8
      3      20      201 0 00 00 2 40 0 1
          -1.           1.e5           0.00000
          1.e3
          1.E-08      1.e-3
          1.E5           0.0           0.0           0.0
          0.0           8.0
SELEC---1----*---2----*---3----*---4----*---5----*---6----*---7----*---8
      6

      0.e-0      0.e-1
      0.e-6      0.e-6      0.e-6     -1.e-6     -1.e-6     0.e-6
      1.e50     234.0      0.e-6     -1.e-6
      1.e50     230.0     -1.e-6      0.e-6           1.e+05
                                         1.e-10

diffusivity data are input as follows:
first row: water (gas, liq.)
second row: brine (gas, liq.)
third row: rn1 (gas, liq.)
fourth row: rn2 (gas, liq.)
fifth row: air (gas, liq.)
DIFFU---1----*---2----*---3----*---4----*---5----*---6----*---7----*---8
      -1.e-6     -1.e-6
      -1.e-6     -1.e-6
      -1.e-6     -1.e-6
      -1.e-6     -1.e-6
      -1.e-6     -1.e-6
ELEMEN---1----*---2----*---3----*---4----*---5----*---6----*---7----*---8
A     1      19      1      1      .1
B     1      19      1      1      .1
ina 1
ina 2

CONNE---1----*---2----*---3----*---4----*---5----*---6----*---7----*---8
ina 1A     1           1     1.e-9     .05      1.
A     1A     2      18      1      1     .05     .05      1.
ina 2B     1           1     1.e-9     .05      1.
B     1B     2      18      1      1     .05     .05      1.

INCON---1----*---2----*---3----*---4----*---5----*---6----*---7----*---8
ina 1
          1.E5           1.e-3           1.e-7           1.e-8
          1.e-6           9.0
ina 2
          1.E5           1.e-3           1.e-13          1.e-4
          1.e-5           125.0
B     1     19      1
          1.E5           0.0           0.0           0.0
          0.0           125.0

GENER---1----*---2----*---3----*---4----*---5----*---6----*---7----*---8
ENDCY---1----*---2----*---3----*---4----*---5----*---6----*---7----*---8

```

Figure 39. Diffusion problem for EOS7R.

well as with the diffusion profile calculated for the same diffusivities in the single-phase liquid conditions in the A-grid. (Note that for single phase gas conditions, Xbrine is mass fraction in the gas phase.)

```

...
...ITERATING... AT [ 1, 1] --- DELTEX = .100000E+04 MAX. RES. = .249983E-01 AT ELEMENT A 1 EQUATION 6
...ITERATING... AT [ 1, 2] --- DELTEX = .100000E+04 MAX. RES. = .180243E-06 AT ELEMENT A 1 EQUATION 1
A 1( 1, 3) ST = .100000E+04 DT = .100000E+04 DX1= -.154286E+04 DX2= .154848E-03 T = 8.155 P = 98457. S = .000000
...ITERATING... AT [ 2, 1] --- DELTEX = .200000E+04 MAX. RES. = .379744E-01 AT ELEMENT A 1 EQUATION 6
...ITERATING... AT [ 2, 2] --- DELTEX = .200000E+04 MAX. RES. = .298624E-06 AT ELEMENT A 1 EQUATION 1
A 1( 2, 3) ST = .300000E+04 DT = .200000E+04 DX1= -.193828E+04 DX2= .195959E-03 T = 8.354 P = 96519. S = .000000
...ITERATING... AT [ 3, 1] --- DELTEX = .400000E+04 MAX. RES. = .477807E-01 AT ELEMENT A 1 EQUATION 6
...ITERATING... AT [ 3, 2] --- DELTEX = .400000E+04 MAX. RES. = .355901E-06 AT ELEMENT A 1 EQUATION 2
A 1( 3, 3) ST = .700000E+04 DT = .400000E+04 DX1= -.189247E+04 DX2= .200756E-03 T = 8.555 P = 94626. S = .000000
...ITERATING... AT [ 4, 1] --- DELTEX = .800000E+04 MAX. RES. = .469317E-01 AT ELEMENT A 1 EQUATION 6
...ITERATING... AT [ 4, 2] --- DELTEX = .800000E+04 MAX. RES. = .344587E-06 AT ELEMENT A 1 EQUATION 2
A 2( 4, 3) ST = .150000E+05 DT = .800000E+04 DX1= -.151927E+04 DX2= .156245E-03 T = 8.324 P = 96813. S = .000000
...ITERATING... AT [ 5, 1] --- DELTEX = .160000E+05 MAX. RES. = .375411E-01 AT ELEMENT A 2 EQUATION 6
...ITERATING... AT [ 5, 2] --- DELTEX = .160000E+05 MAX. RES. = .204750E-06 AT ELEMENT A 2 EQUATION 1
A 4( 5, 3) ST = .310000E+05 DT = .160000E+05 DX1= -.922651E+03 DX2= .928678E-04 T = 8.144 P = 98555. S = .000000
...ITERATING... AT [ 6, 1] --- DELTEX = .320000E+05 MAX. RES. = .389930E-01 AT ELEMENT A 2 EQUATION 6
...ITERATING... AT [ 6, 2] --- DELTEX = .320000E+05 MAX. RES. = .191721E-06 AT ELEMENT A 3 EQUATION 1
A 2( 6, 3) ST = .630000E+05 DT = .320000E+05 DX1= -.130064E+04 DX2= .140170E-03 T = 8.629 P = 93941. S = .000000
...ITERATING... AT [ 7, 1] --- DELTEX = .640000E+05 MAX. RES. = .378766E-01 AT ELEMENT A 3 EQUATION 6
...ITERATING... AT [ 7, 2] --- DELTEX = .640000E+05 MAX. RES. = .185728E-06 AT ELEMENT A 4 EQUATION 1
A 3( 7, 3) ST = .127000E+06 DT = .640000E+05 DX1= -.135723E+04 DX2= .145071E-03 T = 8.578 P = 94419. S = .000000
...ITERATING... AT [ 8, 1] --- DELTEX = .100000E+06 MAX. RES. = .290463E-01 AT ELEMENT A 4 EQUATION 6
...ITERATING... AT [ 8, 2] --- DELTEX = .100000E+06 MAX. RES. = .132083E-06 AT ELEMENT A 5 EQUATION 1
A 8( 8, 3) ST = .227000E+06 DT = .100000E+06 DX1= -.110052E+04 DX2= .112158E-03 T = 8.240 P = 97628. S = .000000
...ITERATING... AT [ 9, 1] --- DELTEX = .100000E+06 MAX. RES. = .157680E-01 AT ELEMENT A 6 EQUATION 6
...ITERATING... AT [ 9, 2] --- DELTEX = .100000E+06 MAX. RES. = .509683E-07 AT ELEMENT A 7 EQUATION 1
A 9( 9, 3) ST = .327000E+06 DT = .100000E+06 DX1= -.794751E+03 DX2= .815385E-04 T = 8.270 P = 97332. S = .000000
...
...
OUTPUT DATA AFTER ( 20, 2)-2-TIME STEPS THE TIME IS .165162E+02

```

TOTAL TIME	KCYC	ITER	ITERC	KON	DX1M	DX2M	DX3M	MAX. RES.	NER	KER	DELTI
.142700E+07	20	2	57	2	.31201E+03	.32959E-04	.32959E-08	.80284E-08	20	1	.1000

ELEM.	INDEX	P (PA)	T (DEG-C)	SL	XBRINE(LIQ)	XRN1(LIQ)	XRN2(LIQ)	XAIRG	XRN1(GAS)	XRN2(GAS)	[ KG]
A 1	1	.90821E+05	.89786E+01	.10000E+01	.97865E-03	.97865E-07	.97865E-08	.88727E+00	.88672E-16	.88672E-02	.1000
A 2	2	.91192E+05	.89361E+01	.10000E+01	.93608E-03	.93608E-07	.93608E-08	.88337E+00	.88285E-16	.88285E-02	.1000
A 3	3	.91562E+05	.88939E+01	.10000E+01	.89393E-03	.89393E-07	.89393E-08	.87918E+00	.87868E-16	.87868E-02	.1000
A 4	4	.91928E+05	.88524E+01	.10000E+01	.85244E-03	.85244E-07	.85244E-08	.87470E+00	.87422E-16	.87422E-02	.1000
A 5	5	.92289E+05	.88119E+01	.10000E+01	.81189E-03	.81189E-07	.81189E-08	.86993E+00	.86947E-16	.86947E-02	.1000
A 6	6	.92641E+05	.87725E+01	.10000E+01	.77254E-03	.77254E-07	.77254E-08	.86487E+00	.86444E-16	.86444E-02	.1000
A 7	7	.92982E+05	.87346E+01	.10000E+01	.73462E-03	.73462E-07	.73462E-08	.85955E+00	.85914E-16	.85914E-02	.1000
A 8	8	.93311E+05	.86984E+01	.10000E+01	.69837E-03	.69837E-07	.69837E-08	.85399E+00	.85361E-16	.85361E-02	.1000
A 9	9	.93623E+05	.86640E+01	.10000E+01	.66402E-03	.66402E-07	.66402E-08	.84824E+00	.84788E-16	.84788E-02	.9999
A 10	10	.93918E+05	.86318E+01	.10000E+01	.63178E-03	.63178E-07	.63178E-08	.84235E+00	.84201E-16	.84201E-02	.9999
B 1	21	.99991E+05	.12500E+03	.00000E+00	.97865E-03	.98893E-03	.98893E-09	.97865E-05	.97865E-13	.97865E-04	.9386
B 2	22	.99991E+05	.12500E+03	.00000E+00	.93608E-03	.94596E-03	.94596E-09	.93608E-05	.93608E-13	.93608E-04	.9386
B 3	23	.99992E+05	.12500E+03	.00000E+00	.89393E-03	.90339E-03	.90339E-09	.89393E-05	.89393E-13	.89393E-04	.9386
B 4	24	.99992E+05	.12500E+03	.00000E+00	.85244E-03	.86150E-03	.86150E-09	.85244E-05	.85244E-13	.85244E-04	.9386
B 5	25	.99992E+05	.12500E+03	.00000E+00	.81189E-03	.82055E-03	.82055E-09	.81189E-05	.81189E-13	.81189E-04	.9386
B 6	26	.99993E+05	.12500E+03	.00000E+00	.77254E-03	.78080E-03	.78080E-09	.77254E-05	.77254E-13	.77254E-04	.9386
B 7	27	.99993E+05	.12500E+03	.00000E+00	.73462E-03	.74250E-03	.74250E-09	.73462E-05	.73462E-13	.73462E-04	.9386
B 8	28	.99993E+05	.12500E+03	.00000E+00	.69837E-03	.70589E-03	.70589E-09	.69837E-05	.69837E-13	.69837E-04	.9386
B 9	29	.99994E+05	.12500E+03	.00000E+00	.66402E-03	.67119E-03	.67119E-09	.66402E-05	.66402E-13	.66402E-04	.9386
B 10	30	.99994E+05	.12500E+03	.00000E+00	.63178E-03	.63862E-03	.63862E-09	.63178E-05	.63178E-13	.63178E-04	.9386
ina 1	41	.10000E+06	.90000E+01	.10000E+01	.10000E-02	.10000E-06	.10000E-07	.88912E+00	.88855E-16	.88855E-02	.1000
ina 2	42	.10000E+06	.12500E+03	.00000E+00	.10000E-02	.10106E-02	.10106E-08	.10000E-04	.10000E-12	.10000E-03	.9386

Figure 40. Selected output for problem 7.

## 9.8 Problem No. 8 (\*rdica\*) - Contamination of an Aquifer from VOC Vapors in the Vadose Zone (EOS7R)

This problem uses EOS7R to simulate the diffusive and advective spreading of volatile organic contaminants (VOCs) in the vadose zone, and their migration across the capillary fringe region into an underlying aquifer. Our emphasis is on approach and data preparation for this kind of analysis, and a very simple model system is used (Fig. 41).

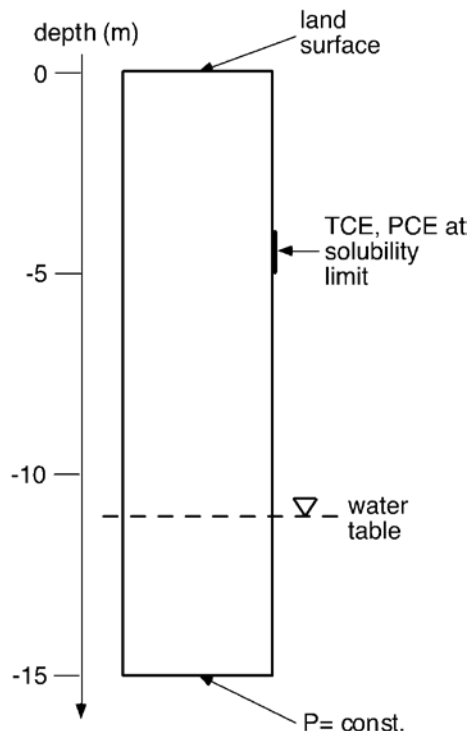


Figure 41. Model system for examining migration of VOC from the vadose zone into an aquifer.

A one-dimensional vertical column of 15 m height and 1 m<sup>2</sup> cross-sectional area is divided into 15 grid blocks of 1 m thickness each; see the MESHMaker data in the input file, Fig. 42. The problem is run in several segments. We first perform a mesh generation run, and then edit the MESH file to place grid block AB1 1 at a depth of -10.5 m in inactive position, and add grid blocks “top” and “bot” that will later serve to maintain boundary conditions at the land surface, and at the bottom of the water table. A first flow simulation is performed with EOS7 for a clean system (no VOC), to obtain a gravity-capillary equilibrium relative to the gas and capillary pressure conditions specified in the inactive block AB1 1. (EOS7R with mass fractions specified as  $X_{Rn1} = X_{Rn2} = 0$  could also be used.) Data block MULTI and initial condition specifications for EOS7, using pure water (zero brine mass fraction), are shown in Fig. 42.

```

MESHMAKER1----*----2----*----3----*----4----*----5----*----6----*----7----*
XYZ
 00.
NX      1      1.0
NY      1      1.0
NZ     15      1.0

ENDFI---1----*----2----*----3----*----4----*----5----*----6----*----7----*
MULTI---1----*----2----*----3----*----4----*----5----*----6----*----7----*
 3      3      2      6
INDOM---1----*----2----*----3----*----4----*----5----*----6----*----7----*
vados
  aquif      1.013e5      0.      10.50
  atmos      1.5e5      0.      1.e-12
  1.013e5      0.      .99

INCON---1----*----2----*----3----*----4----*----5----*----6----*----7----*
AB1 1
  1.013e5      0.      10.20

```

Figure 42. Part of TOUGH2 input data for mesh generation and for initializing an EOS7 run to obtain gravity-capillary equilibrium.

The thermodynamic conditions obtained in this run are then used to initialize an EOS7R run, using parameters of (NK, NEQ, NPH, NB, NKIN) = (5, 5, 2, 8, 3) in data block MULTI. A single small time step of  $\Delta t = 1.e-9$  s is performed, in order to translate the gravity-capillary equilibrium conditions into EOS7R-format. These conditions are used in a subsequent EOS7R run to study migration of TCE and PCE. The VOC data needed for this (aqueous solubilities, inverse Henry's constants) are conveniently obtained with brief T2VOC runs, and are listed in Table 20. The abbreviated TOUGH2 input file for the problem is shown in Fig. 43.

Table 20. TCE and PCE data for VOC contamination problem.

VOC	TCE	PCE
molecular weight	131.389	165.834
aqueous phase mass fraction, ppm	1099.84	200.628
vapor pressure at $T = 20$ °C, Pa	7196	1845
inverse Henry's constant, Pa <sup>-1</sup>	2.0996e-8	1.1816e-8

```

*rdica* ... diffusion in a 1-D column across a capillary fringe
ROCKS---1----*---2----*---3----*---4----*---5----*---6----*---7----*---
vados    2   2600.e00      .35     1.e-11   1.0e-11   1.e-11     2.51      92
                           0.25
    7       .457      .15      1.       .10
    7       .457      .00  5.105e-4      1.e7      1.
...
MULTI---1----*---2----*---3----*---4----*---5----*---6----*---7----*---
      5      5      2      8
START---1----*---2----*---3----*---4----*---5----*---6----*---7----*---
----*---1 MOP: 123456789*123456789*1234 ---*---5----*---6----*---7----*---
PARAM---1----*---2----*---3----*---4----*---5----*---6----*---7----*---
      3 200      999 0 0 0000020000400 00
      3.15576e9      -1.      A51 1      9.81
      1.       9.      9.e1      9.e2      9.e3      9.e4      9.e5      9.e
      1.e-5      1.013e5      0.
      10.50      20.
TIMES---1----*---2----*---3----*---4----*---5----*---6----*---7----*---
      6
      1. 31.5576e6 157.788e6 315.576e6 946.728e6 3.15576e9
SELEC---1----*---2----*---3----*---4----*---5----*---6----*---7----*---
      6
      -1.e5
      0.e-0      0.e-1
      0.e-6      0.e-6      0.e-6      -1.e-6      -1.e-6      0.e-6
      1.e50      131.389      0.e-6      -1.e-6
      1.e50      165.834      -1.e-6      0.e-6
DIFFU---1----*---2----*---3----*---4----*---5----*---6----*---7----*---
      1.e-6      1.e-10
      0.e-6      0.e-6
      1.e-6      1.e-10
      1.e-6      1.e-10
      1.e-6      1.e-10
ELEME---1----*---2----*---3----*---4----*---5----*---6----*---7----*---
A11 1      vados .1000E+01 .1000E+01      .5000E+00 .5000E+00-.5000E+
...
AF1 1      aquif .1000E+01 .1000E+01      .5000E+00 .5000E+00-.1450E+
ina 0
con 0      trapp
top 0      atmos      1.
bot 0      aquif      1.
CONNE---1----*---2----*---3----*---4----*---5----*---6----*---7----*---
con 0A51 1      1      1.e-9      .5      1.e-1
top 0A11 1      3      1.e-9      .5      1.      1.
A11 1A21 1      3 .5000E+00 .5000E+00 .1000E+01 .1000E+01
...
AE1 1AF1 1      3 .5000E+00 .5000E+00 .1000E+01 .1000E+01
AF1 1bot 0      3      .5      1.e-9      1.      1.
INCON -- INITIAL CONDITIONS FOR 19 ELEMENTS AT TIME .100000E-08
A11 1      .35000000E+00
      .1011830232536E+06 .000000000000E+00 .000000000000E+00 .000000000000E+
      .1084703339434E+02 .200000000000E+02
...
con 0      .35000000E+00
      .1012297975914E+06 .000000000000E+00      1.0998e-3      2.0063e
      .1084567823274E+02 .200000000000E+02
bot 0      .35000000E+00
      .1438478256741E+06 .000000000000E+00 .000000000000E+00 .000000000000E+
      .999999999008E-12 .200000000000E+02
GENERAL---1----*---2----*---3----*---4----*---5----*---6----*---7----*---
ENDCY---1----*---2----*---3----*---4----*---5----*---6----*---7----*---

```

Figure 43. Abbreviated TOUGH2/EOS7R input data file for VOC migration problem.

Prior to simulating VOC migration, the mesh is again edited, AB1 1 is returned to active position, and the top and bottom boundary blocks are made inactive, to maintain time-independent land surface and aquifer bottom boundary conditions. An additional inactive grid block containing TCE and PCE is added to the mesh to serve as a VOC source. This block, called “con”, is connected to grid block A51 1 at -4.5 m depth, and is initialized with conditions identical to A51 1, except that components Rn1 and Rn2 were assigned small non-zero mass fractions of 1.0998e-3 and 2.0063e-4, respectively. These correspond to aqueous phase solubilities of TCE and PCE at  $T = 20^\circ\text{C}$ , and model a situation where VOC is present as a free but immobile NAPL (non-aqueous phase liquid). Diffusivities for all components are specified as  $10^{-6} \text{ m}^2/\text{s}$  in the gas phase,  $10^{-10} \text{ m}^2/\text{s}$  in the aqueous phase. The tortuosity factor is 0.25, and relative permeabilities are used as saturation-dependent tortuosity coefficients; no adsorption is included. Part of the printout generated after  $t = 1$  year is shown in Fig. 44; results for the time dependence of VOC concentrations in grid block AC1 1 just below the water table are plotted in Fig. 45 for two variations of the problem with different handling of multiphase diffusion.

Figure 44. Part of printout for VOC contamination problem after  $t = 1$  year.

The general behavior observed in the simulation can be summarized as follows. Transfer of TCE and PCE from the source block into the 1-D column occurs virtually exclusively by gas diffusion, because the liquid phase tortuosity factor near irreducible water saturation is very small, while gas phase tortuosity is near 1. After entering the column, the diffusive spreading of VOCs

upward and downward from grid block A51 1 is nearly symmetric initially, as can be seen from the data printed in Fig 44 (radionuclide mass fractions in A61 1 are close to but slightly larger than those in A41 1, etc.). The asymmetry with larger mass fractions below than above the VOC entry point is caused by buoyancy-driven downflow of soil gas, due to the entry of denser VOC vapors into the vadose zone. These advective flow effects become stronger over time as VOC concentrations and soil gas densities increase. The downflow of soil gas is compensated by upward diffusion of air. Due to the relatively small aqueous phase solubilities, and the much smaller liquid as compared to gas phase diffusivities, there is a large resistance for diffusion across the capillary fringe. This delays entry of VOCs into the aquifer until concentrations above the water table have built up to large values. To illustrate the strong coupling between multiphase diffusion and aqueous-gas phase partitioning, we ran two variations for this problem. By setting  $MOP(24) = 0$  we obtain an accurate, fully coupled treatment of diffusion and phase partitioning. For  $MOP(24) = 1$  diffusive fluxes are calculated separately for the gas and aqueous phases, which can lead to severe underestimate of diffusive fluxes in regions with strong saturation gradients. As is seen in Fig. 45, the aqueous phase concentrations beneath the water table are underestimated by as much as an order of magnitude after 100 years for the  $MOP(24) = 1$  calculation.

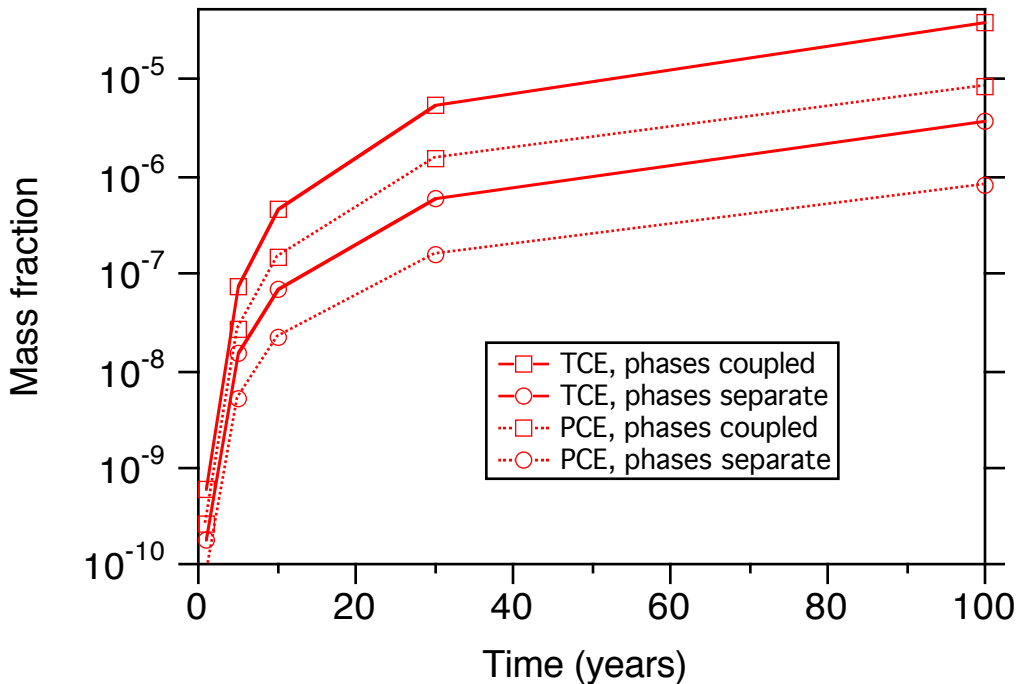


Figure 45. Time dependence of simulated aqueous VOC concentrations below the water table for fully coupled multiphase diffusion, and for separate treatment of gas and aqueous phase diffusive fluxes.

## 9.9 Problem No. 9 (\*rco8\*) - Flushing Oil from a 1-D Column by Water Injection (EOS8)

We consider a 1-D horizontal porous column of 19 m length and 1 m<sup>2</sup> cross-sectional area, divided into 19 grid blocks of 1 m<sup>3</sup> volume each. Initial conditions are uniform, with  $P = 10^5$  Pa,  $T = 15$  °C,  $S_{gas} = 20$  %,  $S_{oil} = 50$  %. These conditions are maintained constant at one end of the column, while water is injected at a rate of 0.03 kg/s and an enthalpy of  $2 \times 10^5$  J/kg, corresponding to a temperature of approximately 48 °C, at the other end. The input file for this problem is shown in Fig. 46. Oil phase specifications include an irreducible saturation  $S_{or} = 0.01$ , constant viscosity of  $0.5 \times 10^{-3}$  P<sub>a</sub>·s, constant density of 800 kg/m<sup>3</sup>, and specific heat of 1000 J/kg°C.

In response to water injection, pressures increase near the injection point, and three-phase flow of gas, aqueous, and oil phases is induced. Air also partially dissolves in the aqueous phase. Fig. 47 shows a portion of the printout, including the iteration sequence during the first few time steps, and results obtained after 10 time steps. At this point, corresponding to a simulated time of 15,900 seconds (4.4 hours), the air that was originally present in the first grid block has been completely removed, mostly through dissolution in the flowing water, with a minor contribution from gas flow at early time. Oil saturations near the inlet have declined, and an oil bank has formed with a broad saturation distribution that peaks at  $S_{oil} = 67.9$  % in grid block F 5. In reality, oil relative permeability will depend on saturation through  $(S_o - S_{or})$  raised to some power larger than 1, and a rather sharp displacement front will develop.

Figure 46. Three-phase flow problem for EOS8: flushing oil from a 1-D column.

```

...ITERATING... AT [ 1, 1] --- DELTEX = .100000E+03 MAX. RES. = .333598E-01 AT ELEMENT F 1 EQUATION 1
...ITERATING... AT [ 1, 2] --- DELTEX = .100000E+03 MAX. RES. = .170349E-03 AT ELEMENT F 1 EQUATION 2
F 1( 1, 3) ST = .100000E+03 DT = .100000E+03 DX1= .498004E+04 DX2= -.985449E-02 T = 15.174 P = 104980. S = .190146E+00
...ITERATING... AT [ 2, 1] --- DELTEX = .200000E+03 MAX. RES. = .645652E-01 AT ELEMENT F 1 EQUATION 1
...ITERATING... AT [ 2, 2] --- DELTEX = .200000E+03 MAX. RES. = .705033E-03 AT ELEMENT F 1 EQUATION 2
F 1( 2, 3) ST = .300000E+03 DT = .200000E+03 DX1= .111254E+05 DX2= -.190128E-01 T = 15.517 P = 116105. S = .171133E+00
...ITERATING... AT [ 3, 1] --- DELTEX = .400000E+03 MAX. RES. = .121293E+00 AT ELEMENT F 1 EQUATION 1
...ITERATING... AT [ 3, 2] --- DELTEX = .400000E+03 MAX. RES. = .292621E-02 AT ELEMENT F 1 EQUATION 2
...ITERATING... AT [ 3, 3] --- DELTEX = .400000E+03 MAX. RES. = .119816E-04 AT ELEMENT F 1 EQUATION 2
F 1( 3, 4) ST = .700000E+03 DT = .400000E+03 DX1= .279660E+05 DX2= -.347199E-01 T = 16.182 P = 144071. S = .136413E+00
...
...
*rcol8* ..... input file for EOS8; flushing oil from 1-D column.

OUTPUT DATA AFTER ( 10, 9)-2-TIME STEPS THE TIME IS .18403E+00 DAYS

oooooooooooooooooooooooooooooooooooooooooooooooooooooooooooooooooooo
TOTAL TIME KCYC ITER ITERC KON DX1M DX2M DX3M MAX. RES. NER KER DELTEX
.15900E+05 10 9 49 2 .41813E+06 .69685E-01 .15242E+00 .45792E-05 15 3 .32000E+04
oooooooooooooooooooooooooooooooooooooooooooooooooooooooooooo
ELEM. INDEX P T SG SL S(oil) VIS(oil) XAIRG XAIRL PSAT PCAP
(Pa) (deg-C) (Pa*s) (Pa) (Pa)
F 1 1 .19071E+07 .30971E+02 .00000E+00 .92951E+00 .70491E-01 .50000E-03 .00000E+00 .11155E-03 .44836E+04 .00000E+00
F 2 2 .16931E+07 .19870E+02 .26364E-02 .83950E+00 .15786E+00 .50000E-03 .99915E+00 .27176E-03 .23179E+04 -.10478E+04
F 3 3 .13968E+07 .15968E+02 .10699E-01 .65522E+00 .33409E+00 .50000E-03 .99919E+00 .22422E-03 .18130E+04 -.23020E+04
F 4 4 .10434E+07 .15155E+02 .15505E-01 .36907E+00 .61543E+00 .50000E-03 .99897E+00 .16743E-03 .17210E+04 -.28432E+04
F 5 5 .81521E+06 .15069E+02 .20653E-01 .30067E+00 .67867E+00 .50000E-03 .99869E+00 .13076E-03 .17115E+04 -.33521E+04
F 6 6 .61886E+06 .15049E+02 .28592E-01 .30001E+00 .67140E+00 .50000E-03 .99828E+00 .99201E-04 .17093E+04 -.40494E+04
F 7 7 .43960E+06 .15032E+02 .41641E-01 .30002E+00 .65834E+00 .50000E-03 .99758E+00 .70387E-04 .17074E+04 -.50587E+04
F 8 8 .29095E+06 .15018E+02 .65334E-01 .30002E+00 .63464E+00 .50000E-03 .99634E+00 .46494E-04 .17059E+04 -.66638E+04
F 9 9 .18843E+06 .15009E+02 .10330E+00 .30002E+00 .59668E+00 .50000E-03 .99435E+00 .30015E-04 .17049E+04 -.89658E+04
F 10 10 .13365E+06 .15003E+02 .14783E+00 .30001E+00 .55215E+00 .50000E-03 .99420E+00 .21209E-04 .17043E+04 -.11532E+05
F 11 11 .11125E+06 .15001E+02 .17936E+00 .30001E+00 .52063E+00 .50000E-03 .99041E+00 .17609E-04 .17040E+04 -.13355E+05
F 12 12 .10372E+06 .15000E+02 .19347E+00 .30000E+00 .50653E+00 .50000E-03 .98971E+00 .16398E-04 .17040E+04 -.14186E+05
F 13 13 .10125E+06 .15000E+02 .19794E+00 .30000E+00 .50205E+00 .50000E-03 .98945E+00 .16001E-04 .17039E+04 -.14452E+05
F 14 14 .10042E+06 .15000E+02 .19932E+00 .30000E+00 .50068E+00 .50000E-03 .98937E+00 .15868E-04 .17039E+04 -.14534E+05
F 15 15 .10014E+06 .15000E+02 .19977E+00 .30000E+00 .50023E+00 .50000E-03 .98934E+00 .15823E-04 .17039E+04 -.14561E+05
F 16 16 .10005E+06 .15000E+02 .19992E+00 .30000E+00 .50008E+00 .50000E-03 .98933E+00 .15808E-04 .17039E+04 -.14570E+05
F 17 17 .10002E+06 .15000E+02 .19997E+00 .30000E+00 .50003E+00 .50000E-03 .98932E+00 .15803E-04 .17039E+04 -.14573E+05
F 18 18 .10001E+06 .15000E+02 .19999E+00 .30000E+00 .50001E+00 .50000E-03 .98932E+00 .15801E-04 .17039E+04 -.14574E+05
F 19 19 .10000E+06 .15000E+02 .20000E+00 .30000E+00 .50000E+00 .50000E-03 .98932E+00 .15801E-04 .17039E+04 -.14574E+05
F 20 20 .10000E+06 .15000E+02 .20000E+00 .30000E+00 .50000E+00 .50000E-03 .98932E+00 .15801E-04 .17039E+04 -.14574E+05
oooooooooooooooooooooooooooooooooooooooooooooooooooo

```

Figure 47. Portion of printed output for 3-phase flow problem.

## **9.10 Problem No. 10 (\*reos9a\*) - Demonstration of Equilibrium (EOS9)**

This problem uses EOS9 to demonstrate initialization of a flow problem with gravity-capillary equilibrium. MESHMaker is used to generate a vertical 1-D column consisting of 10 grid blocks with 10 m height and 1 m<sup>2</sup> cross-sectional area. Nodal point elevations range from -5 m at the top (block A11 1) to -95 m at the bottom (block AA1 1). In domain REFCO a water table elevation of -75 m is specified, corresponding to the center of grid block A81 1. Other problem specifications can be read from the input file, Fig. 48.

Some of the printed output is shown in Fig. 49. The printout after the first infinitesimal time step of  $\Delta t = 1.e-9$  s shows the initialization made by EOS9, with unsaturated conditions above block A81 1 and saturated conditions below. Mass fluxes obviously vanish in the region above grid block A61 1, because water saturations are below the irreducible value of  $S_{liq} = 0.15$  there. Very small water flow velocities of order  $10^{-20}$  m/s are present in the mobile portion of the unsaturated zone, while considerably larger albeit still small flow velocities of order  $10^{-10}$  m/s (approximately 3 mm/yr) are seen between the saturated zone blocks. The reason for gravity-capillary equilibrium being slightly less accurate in the saturated zone is that water density will slightly increase with increasing pressure, which is neglected in the assignment of pressure conditions in EOS9. A time step of  $10^9$  seconds is then performed for which convergence is obtained after a single Newton-Raphson iteration. The maximum pressure change in any grid block is 8.7 Pa, and a more accurate gravity-capillary equilibrium is obtained, with saturated zone flow velocities reduced by another six orders of magnitude.

The input file includes alternative REFCO specifications after the ENDCY record. If these are used, all unsaturated zone grid blocks will be initialized at irreducible water saturation of 15%.

Figure 48. EOS9 input file for demonstration of gravity-capillary equilibrium.

Figure 49. Portion of the printed output for the gravity-capillary equilibrium problem.

## 9.11 Problem No. 11 (\*rpm\*) - Demonstration of Permeability Modification Options (EOS9)

Here we present a small, coarsely gridded problem to illustrate the various block-by-block permeability modification options. The TOUGH2 input file as shown in Fig. 50 is for use with EOS9 and applies internally generated “logarithmic” random permeability modifiers (Option 3). Fig. 51 shows the MESHMaker data that were used to generate the grid, and provides alternative data for domain SEED that can be used instead of the SEED data in Fig. 50 to select linear random permeability modifiers (Option 2), or user-supplied permeability modifiers in data block ELEME (Option 1). The problem can alternatively be run with EOS3; appropriate initialization data to replace the EOS9 initialization data are also shown in Fig. 51.

In assembling the input file of Fig. 50, we first performed a MESH generation run, and then added arbitrary PM-coefficients to the ELEME-data using a text editor. Reference hydrogeologic conditions feature typical parameters for a coarse sand, with permeability of  $10^{-11}$  m $^2$  (10 darcy). Default initial water saturation is 14.99 %, just below the irreducible level of 15 %, and the top three grid blocks are initialized at a large water saturation of 99 % (A11 1, A11 2, A11 3; note that the y-axis of the grid has been rotated by 90 ° about the x-axis, so that it is pointing downward).

In the input file as shown in Fig. 50, the explicitly provided PM-coefficients will not be used; instead the domain SEED data will cause a set  $\{s_n; n = 1, \dots, NEL\}$  of random numbers in the interval [0, 1] to be internally generated, with a random number seed of 0.5 (POR-parameter in domain SEED). The permeability modifiers will be calculated as (logarithmic permeability modification)

$$\xi_n = \max\{\exp(-\sigma \cdot s_n) - \Delta, 0\} \quad (43).$$

where  $\sigma = \text{PER}(1) = 6.909$  is a scale factor, which will cause permeability modifiers to cover the range from  $\exp(-6.909) \approx 10^{-3}$  to  $\exp(0) = 1$ , and  $\Delta = \text{PER}(2) = 0.01$  is a shift parameter. The input data in Fig. 50 require a first small time step of  $\Delta t = 10^{-9}$  s, after which the initial conditions are printed prior to any changes. Fig. 52 shows part of the iteration sequence starting from time step # 2, and the output data after 10 time steps, corresponding to a simulated time of  $2.56 \times 10^5$  seconds. Basically what is happening in the problem is that water is flowing downward under gravity, in a manner that is affected by capillary pressure variations. Grid block A12 1 is impermeable, so that outflow from block A11 1 above it can only occur sideways, by capillary force, into block A11 2.

Figure 50. EOS9 input file for demonstrating “logarithmic” permeability modifiers.

Figure 51. MESHMaker input, alternative SEED data, and EOS3-type initial conditions for permeability modification problem.

Replacing the default (block PARAM) and INCON initial conditions with data appropriate for EOS3 from Fig. 51, the problem can be run with an active gas phase using EOS3. The results are quite similar to what was obtained with EOS9; see Fig. 53. As a benchmark we also provide portions of the printout from EOS9 runs that use internally generated random linear permeability modifiers with a shift of  $\Delta = 1.2$  (Fig. 54), and the explicitly provided permeability modifiers in the ELEME-block with a shift of  $\Delta = 1.5$  (Fig. 55). These permeability fields are very different from the previous case and, accordingly, rather different saturation distributions are obtained.

Figure 52. Part of printed output for running the input file of Fig. 50 with TOUGH2/EOS9, demonstrating “logarithmic” permeability modification.

```

...
ITERATING... AT [ 2, 1] --- DELTEX = .100000E+04 MAX. RES. = .466840E+00 AT ELEMENT A12 2 EQUATION 1
ITERATING... AT [ 2, 2] --- DELTEX = .100000E+04 MAX. RES. = .112216E+00 AT ELEMENT A12 2 EQUATION 1
ITERATING... AT [ 2, 3] --- DELTEX = .100000E+04 MAX. RES. = .602940E-02 AT ELEMENT A12 2 EQUATION 1
ITERATING... AT [ 2, 4] --- DELTEX = .100000E+04 MAX. RES. = .170452E-04 AT ELEMENT A12 2 EQUATION 1
A12 2( 2, 5) ST = .100000E+04 DT = .100000E+04 DX1= .272347E+01 DX2= -.342742E-01 T = 20.000 P = 100003. S = .815826E+00
ITERATING... AT [ 3, 1] --- DELTEX = .100000E+04 MAX. RES. = .186079E+00 AT ELEMENT A12 2 EQUATION 1
ITERATING... AT [ 3, 2] --- DELTEX = .100000E+04 MAX. RES. = .131069E-01 AT ELEMENT A12 2 EQUATION 1
ITERATING... AT [ 3, 3] --- DELTEX = .100000E+04 MAX. RES. = .686726E-04 AT ELEMENT A12 2 EQUATION 1
A12 2( 3, 4) ST = .200000E+04 DT = .100000E+04 DX1= -.669621E+00 DX2= -.238092E-01 T = 20.000 P = 100002. S = .792017E+00
...
*rpmp3* ... 4-5-99: adapted from rpm for EOS3

      OUTPUT DATA AFTER ( 10, 4)-2-TIME STEPS                               THE TIME IS .29630E+01 DAYS

=====
TOTAL TIME   KCYC   ITER   ITERC   KON      DX1M      DX2M      DX3M      MAX. RES.      NER      KER      DELTEX
.25600E+06    10       4     38       2     .90932E+01    .72489E-01    .86561E-06    .47967E-07     8       1     .12800E+06

=====
ELEM. INDEX      P      T      SG      SL      XAIRG      XAIRL      PER.MOD.      PCAP      DG      DL
          (PA)    (DEG-C)                    (PA)      (KG/M**3)    (KG/M**3)

A11 1   1   .99977E+05   .20000E+02   .30437E+00   .69563E+00   .98532E+00   .15695E-04   .94364E+00   -.22391E+04   .11774E+01   .99832E+03
A12 1   2   .10000E+06   .20000E+02   .85010E+00   .14990E+00   .98532E+00   .15699E-04   .00000E+00   -.18517E+05   .11777E+01   .99832E+03
A13 1   3   .10000E+06   .20000E+02   .85010E+00   .14990E+00   .98532E+00   .15699E-04   .00000E+00   -.18517E+05   .11777E+01   .99832E+03
A11 2   4   .99980E+05   .20000E+02   .27798E+00   .72202E+00   .98532E+00   .15696E-04   .53022E-01   -.86878E+04   .11774E+01   .99832E+03
A12 2   5   .99998E+05   .20000E+02   .49187E+00   .50813E+00   .98532E+00   .15699E-04   .33181E+00   -.66084E+04   .11777E+01   .99832E+03
A13 2   6   .10001E+06   .20000E+02   .72348E+00   .27652E+00   .98532E+00   .15701E-04   .20459E+00   -.19288E+05   .11778E+01   .99832E+03
A11 3   7   .99979E+05   .20000E+02   .17091E+00   .82909E+00   .98532E+00   .15696E-04   .55940E-02   -.18112E+05   .11774E+01   .99832E+03
A12 3   8   .10000E+06   .20000E+02   .62016E+00   .37984E+00   .98532E+00   .15699E-04   .12133E+00   -.16569E+05   .11777E+01   .99832E+03
A13 3   9   .10001E+06   .20000E+02   .84163E+00   .15837E+00   .98532E+00   .15701E-04   .11803E+00   -.50436E+05   .11778E+01   .99832E+03

```

Figure 53. Part of printed output for running modified input file of Fig. 50 with TOUGH2/EOS3 for “logarithmic” permeability modification.

Figure 54. Part of printed output for running modified input file of Fig. 50 with TOUGH2/EOS9 for “linear” permeability modification.

Figure 55. Part of printed output for running modified input file of Fig. 50 with TOUGH2/EOS9, using permeability modifiers provided in ELEME data block.

## 9.12 Problem No. 12 (\*rhbc\*) - Production from a Geothermal Reservoir with Hypersaline Brine and CO<sub>2</sub> (EWASG)

This problem examines production from a hypothetical geothermal reservoir with high salinity and CO<sub>2</sub>. A single well produces at a constant rate of 65 kg/s from an infinite-acting reservoir in 1-D radial flow geometry. The reservoir is in two-phase conditions initially, with uniform initial conditions of  $P = 60$  bar,  $T = 275.55$  °C; other problem parameters are given in Table 21, and Fig. 56 shows the TOUGH2 input file. The choices made with SELEC-data are: no vapor pressure lowering (IE(10) = 0), a tubes-in-series model for permeability reduction from precipitation (IE(11) = 3), full dependence of thermophysical properties on salinity (IE(14) = 0), Michaelides correlation for brine enthalpy (IE(15) = 0), and CO<sub>2</sub> as non-condensable gas (IE(16) = 2). The permeability-porosity relationship for the parameters used here (IE(11) = 3, FE(1) = FE(2) = 0.8) is shown in Fig. 9.

Table 21. Parameters for production from a saline reservoir with CO<sub>2</sub>.

Reservoir thickness	500 m
Permeability	$50 \times 10^{-15}$ m <sup>2</sup>
Porosity	0.05
Relative permeability Corey curves with $S_{lr} =$	0.30
$S_{gr} =$	0.05
Rock grain density	2600 kg/m <sup>3</sup>
Specific heat	1000 J/kg °C
Thermal conductivity	2.1 W/m °C
Initial conditions	
Temperature	275.55 °C
Gas saturation	0.45
Pressure	60.0 bar
NaCl mass fraction in liquid phase	0.30
CO <sub>2</sub> partial pressure	14.79 bar
Wellblock radius	5 m
Production rate	65 kg/s

Fluid withdrawal causes pressures to drop near the production well. Boiling of reservoir fluid gives rise to dilution of CO<sub>2</sub> in the gas phase and to increased concentrations of dissolved NaCl, which begins to precipitate when the aqueous solubility limit is reached. As the boiling front

```

*rhbc* - 1-D radial flow problem for EWASG, with NaCl and CO2
MESHMAKER1-----*----2----*----3----*----4----*----5----*----6----*----7----*----8
RZ2D
RADII
 1
 5.
EQUID
 1           2.
LOGAR
 50          1.E2
LOGAR
 20          1.E3
EQUID
 1           0.0
LAYER-----1----*----2----*----3----*----4----*----5----*----6----*----7----*----8
 1
 500.

ROCKS-----1----*----2----*----3----*----4----*----5----*----6----*----7----*----8
POMED    2      2600.     .05   50.e-15   50.e-15   50.e-15     2.0    1000.0

 3      .30       .05
 1           1.

SELEC-----2----3----4----5----6----7----8----9----10----11----12----13----14----15----16
 1
  .8     .8
..... IE(16) = 2 chooses CO2 .....
MULTI-----1----*----2----*----3----*----4----*----5----*----6----*----7----*----8
 3      4      3      6
START-----1----*----2----*----3----*----4----*----5----*----6----*----7----*----8
-----*----1----MOP:123456789012345678901234-----*----5----*----6----*----7----*----8
PARAM-----1----*----2----*----3----*----4----*----5----*----6----*----7----*----8
 1 100      100100 3000000002 40 0 3
 2.e6      -1.

 1.E4
 1.E-5     1.E00
 60.e5      .30
 1.E-7
 10.45
 275.55
TIMES-----1----*----2----*----3----*----4----*----5----*----6----*----7----*----8
 1      1
 5.e5

RPCAP-----1----*----2----*----3----*----4----*----5----*----6----*----7----*----8
 3      .30       .05
 1           1.

INCON-----1----*----2----*----3----*----4----*----5----*----6----*----7----*----8

GENER-----1----*----2----*----3----*----4----*----5----*----6----*----7----*----8
A1 1wel 1
  MASS      -65.

ENDCY-----1----*----2----*----3----*----4----*----5----*----6----*----7----*----8

```

Figure 56. TOUGH2/EWASG input data for constant-rate production from a 1-D cylindrical reservoir.

recedes from the well, solid precipitate fills approximately 10 % of the original void space (see Fig. 57), causing permeability to decline to approximately 28 % of its original value.

Specifications of this problem (1-D radial geometry, uniform initial conditions, constant well rate) were chosen so that a similarity solution would be applicable, which should depend on radius  $R$  and time  $t$  only through the similarity variable  $x = R^2/t$  (O'Sullivan, 1981). This similarity property should hold even when all complexities of two-phase flow with nonlinear relative permeabilities,  $\text{CO}_2$  exsolution effects, salt precipitation, and associated porosity and permeability effects are taken into account. The agreement between results for two different times ( $5 \times 10^5$  and  $2 \times 10^6$  seconds) when plotted as a function of the similarity variable shows that the similarity property holds very accurately for all thermodynamic variables (Fig. 57). As a benchmark for proper code installation, we also provide printout for the first few time steps of the TOUGH2 run, Fig. 58.

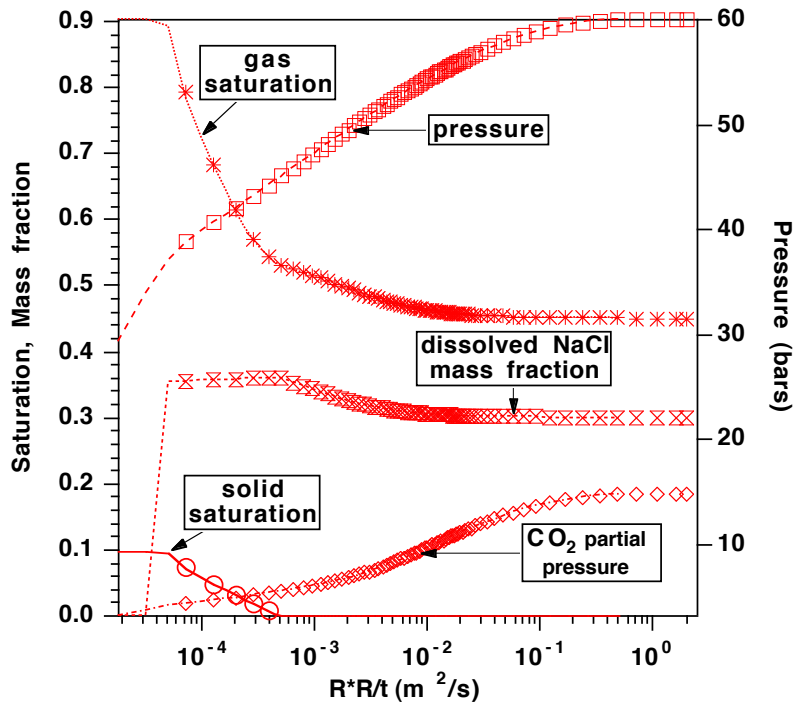


Figure 57. Simulated thermodynamic conditions for 1-D radial flow problem with salinity and non-condensable gas, plotted as a function of the similarity variable  $x = R^2/t$ . Results at  $2 \times 10^6$  seconds are shown as lines, while the data at  $t = 5 \times 10^5$  seconds are given as symbols.

```

...ITERATING... AT [ 1, 1] --- DELTEX = .100000E+05 MAX. RES. = .588696E+01 AT ELEMENT A1 1 EQUATION 3
...ITERATING... AT [ 1, 2] --- DELTEX = .100000E+05 MAX. RES. = .174318E+01 AT ELEMENT A1 1 EQUATION 3
...ITERATING... AT [ 1, 3] --- DELTEX = .100000E+05 MAX. RES. = .150080E+00 AT ELEMENT A1 1 EQUATION 3
...ITERATING... AT [ 1, 4] --- DELTEX = .100000E+05 MAX. RES. = .141958E-02 AT ELEMENT A1 1 EQUATION 3
A1 1( 1, 5) ST = .100000E+05 DT = .100000E+05 DX1= -.887887E+06 DX2= .178902E-01 T = 274.471 P = 5112113. S = .483674E+00
...ITERATING... AT [ 2, 1] --- DELTEX = .100000E+05 MAX. RES. = .154696E+00 AT ELEMENT A1 1 EQUATION 3
...ITERATING... AT [ 2, 2] --- DELTEX = .100000E+05 MAX. RES. = .120755E-01 AT ELEMENT A1 1 EQUATION 3
A1 1( 2, 3) ST = .200000E+05 DT = .100000E+05 DX1= -.242572E+06 DX2= .129321E-01 T = 273.754 P = 4869541. S = .502173E+00
...ITERATING... AT [ 3, 1] --- DELTEX = .200000E+05 MAX. RES. = .918414E-01 AT ELEMENT A1 1 EQUATION 1
...ITERATING... AT [ 3, 2] --- DELTEX = .200000E+05 MAX. RES. = .407143E-01 AT ELEMENT A1 1 EQUATION 3
...ITERATING... AT [ 3, 3] --- DELTEX = .200000E+05 MAX. RES. = .803879E-04 AT ELEMENT A1 1 EQUATION 3
A1 1( 3, 4) ST = .400000E+05 DT = .200000E+05 DX1= -.218945E+06 DX2= .161757E-01 T = 272.909 P = 4650596. S = .520622E+00
...ITERATING... AT [ 4, 1] --- DELTEX = .400000E+05 MAX. RES. = .102523E+00 AT ELEMENT A1 1 EQUATION 1
=====PRECIPITATION STARTS AT ELEMENT *A1 1* XSM=.365355E+00 XS=.365355E+00 XEQ = .360175E+00
...ITERATING... AT [ 4, 2] --- DELTEX = .400000E+05 MAX. RES. = .819347E+00 AT ELEMENT A1 1 EQUATION 3
...ITERATING... AT [ 4, 3] --- DELTEX = .400000E+05 MAX. RES. = .661370E-02 AT ELEMENT A1 1 EQUATION 3
A1 1( 4, 4) ST = .800000E+05 DT = .400000E+05 DX1= -.214641E+06 DX2= .965782E+01 T = 271.647 P = 4435955. S = .543653E+00
...ITERATING... AT [ 5, 1] --- DELTEX = .800000E+05 MAX. RES. = .143447E+00 AT ELEMENT A1 1 EQUATION 1
=====PRECIPITATION STARTS AT ELEMENT *A1 2* XSM=.367276E+00 XS=.367276E+00 XEQ = .360084E+00
...ITERATING... AT [ 5, 2] --- DELTEX = .800000E+05 MAX. RES. = .190705E+01 AT ELEMENT A1 2 EQUATION 3
...ITERATING... AT [ 5, 3] --- DELTEX = .800000E+05 MAX. RES. = .628951E-01 AT ELEMENT A1 2 EQUATION 3
...ITERATING... AT [ 5, 4] --- DELTEX = .800000E+05 MAX. RES. = .202622E-04 AT ELEMENT A1 2 EQUATION 3
A1 1( 5, 5) ST = .160000E+06 DT = .800000E+05 DX1= -.207023E+06 DX2= .234897E-01 T = 268.781 P = 4228932. S = .608426E+00

```

Figure 58. Iteration sequence for first five time steps of the hypersaline reservoir problem.

## **10. Concluding Remarks**

TOUGH2, Version 2.0, provides flexible capabilities for modeling multicomponent multiphase fluid and heat flows in permeable media. TOUGH2 implements the general MULKOM architecture that separates and interfaces the flow and transport aspects of the problem (which do not depend on the nature and number of fluid components and phases) from the fluid property and phase composition aspects (which are specific to the particular fluid mixture under study). Another important aspect of TOUGH2 is the integral finite difference method used for space discretization of the flow system. This method provides a high degree of flexibility in the description of flow geometry. One-, two-, and three-dimensional flow problems with regular or irregular gridding can be treated on the same footing, and special discretization schemes for fractured media, or for higher-order differencing approximations, can be implemented through appropriate preprocessing of geometric data. For regular grid systems, the integral finite difference method is equivalent to conventional finite differences.

The emphasis in the development of the MULKOM concept, and its implementation in the TOUGH2 code, has been on flexibility and robustness. TOUGH2 is an adaptable research tool, that in the present form can handle a wide variety of flow problems in the fields of geothermal reservoir engineering, nuclear waste isolation, environmental assessment and remediation, and unsaturated and saturated zone hydrology.

TOUGH2 is intended to be a “general purpose” simulator. Applications to many different kinds of flow problems are possible, but should be made with caution. The diversity of multiphase fluid and heat flow problems is enormous, and careful consideration must be given to the peculiar features of any given problem if a reasonably accurate and efficient solution is to be obtained. A case in point is multiphase flow in composite (layered) media, in which discontinuous permeability changes occur at the boundaries between different geologic units. It is well known that for single-phase flow, the appropriate interface weighting scheme for absolute permeability is harmonic weighting. For two-phase flow, the added problem of relative permeability weighting arises. It has been established that for transient flow problems in homogeneous media, relative permeability must be upstream weighted, or else phase fronts may be propagated with erroneous speed (Aziz and Settari, 1979). Studies at the Lawrence Berkeley National Laboratory have shown that for transient two-phase problems in composite media, both absolute and relative permeability must be fully upstream weighted to avoid the possibility of gross errors (Tsang and Pruess, 1990; Wu et al., 1993). The applicable weighting schemes for different flow problems are summarized in Fig. 59. Our somewhat disturbing conclusion is that there is no single weighting scheme for

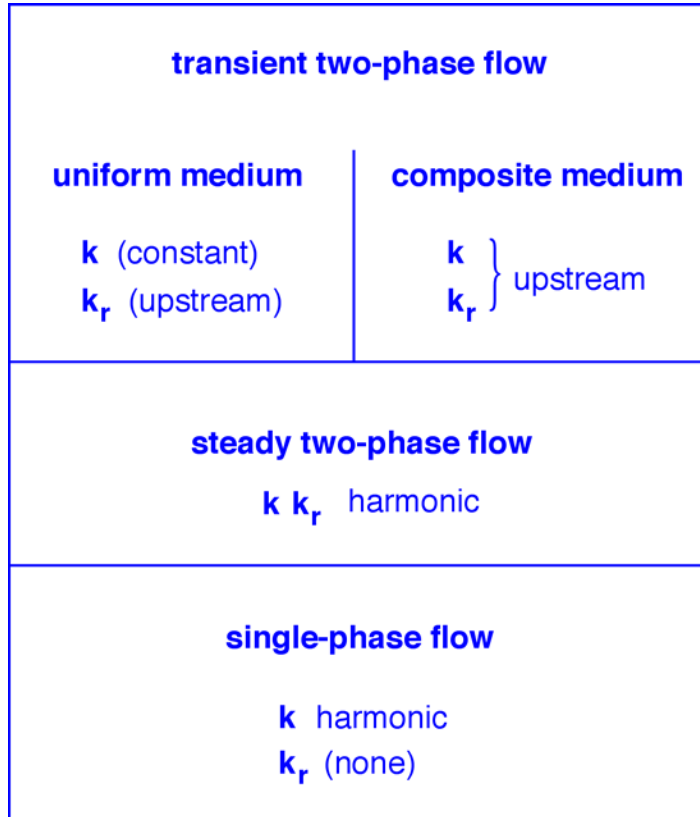


Figure 59. Weighting procedures for absolute ( $k$ ) and relative permeability ( $k_r$ ) at grid block interfaces.

general two-phase flows in composite media that would at the same time preserve optimal accuracy for single-phase or steady two-phase flows. Another interesting problem is the weighting scheme for interface densities. For proper modeling of gravity effects, it is necessary to define interface density as the arithmetic average between the densities of the two adjacent grid blocks, regardless of nodal distances from the interface. An unstable situation may arise when phases (dis-)appear, because interface density may then have to be “switched” to the upstream value when the phase in question is not present in the downstream block. For certain flow problems spatial interpolation of densities may provide more accurate answers.

Issues of interface weighting and associated discretization errors are especially important when non-uniform or irregular grids are used. Additional complications related to interface weighting arise in flow problems that involve hydrodynamic instabilities. Examples include immiscible displacements with unfavorable mobility ratio where a less viscous fluid displaces a fluid of higher viscosity (viscous instability), and flow problems where a denser fluid invades a zone with less dense fluid from above (gravity instability). These instabilities can produce very

large grid orientation errors, i.e., simulated results can depend strongly on the orientation of the computational grid (Yanosik and McCracken, 1979; Pruess and Bodvarsson, 1983; Pruess, 1991c; Brand et al., 1991).

These examples are by no means exhaustive; they are intended to illustrate potential subtle and not so subtle pitfalls in the modeling of multiphase flows. Generally speaking, in the design and implementation of numerical schemes for such flows, there appears to be a trade-off between accuracy and efficiency on the one hand, and flexibility and robustness on the other. For any given problem, small modifications in the source code will often allow substantial gains in accuracy and efficiency. In some cases it may be advisable to use higher-order differencing schemes. Various higher-order differencing methods have been explored with TOUGH2 and its predecessors, although none are included in the present version. Grid orientation effects can be reduced by using 7-point or 9-point differencing instead of the common 5-point “stencil,” to achieve a higher degree of rotational invariance in the finite difference approximations of the fundamental differential operators. In the integral finite difference method, these higher-order schemes can be implemented through preprocessing of geometry data, without any coding changes, by assigning additional flow connections with appropriate weighting factors between elements of the computational grid (Pruess and Bodvarsson, 1983; Pruess, 1991c). However, reduction or elimination of grid orientation effects as such does not necessarily achieve a better numerical approximation. It may just amount to reducing the anisotropy of space discretization errors but not their magnitude, creating an illusion of a better approximation by making space discretization effects less obvious (Pruess, 1991c).

The 7- and 9-point differencing methods are “static,” in the sense that they can be implemented by appropriate assignment of geometric data ahead of a simulation. There are also “dynamic” higher-order schemes that adjust interface weighting parameters in a dynamical way during the course of a simulation, depending on spatial variability of concentration, temperature, and phase saturation gradients. Higher-order TVD (total variation diminishing) methods can strongly reduce front smearing relative to the standard single-point upstream weighting used in the current version of TOUGH2. For upstream weighting to achieve a similar reduction in numerical dispersion would require grid refinement by a factor of order 5 - 10; however, when using TVD-schemes time steps tend to be more restricted (Oldenburg and Pruess, 1998). Program modules for various higher-order methods are expected to be released in the future, and will be made available for downloading from the TOUGH2 web site at <http://esd.lbl.gov/TOUGH2/>.

## **Acknowledgement**

Code development leading up to the current Version 2.0 of TOUGH2, and accompanying documentation, was supported by the Assistant Secretary for Energy Efficiency and Renewable Energy, Office of Geothermal and Wind Technologies, of the U.S. Department of Energy under Contract No. DE-AC03-76SF00098. Development of multiphase fluid and heat flow simulation capabilities at LBNL was initiated in the late 1970s and has continued with primary support from DOE's geothermal program. Various stages in the development of the TOUGH family of simulators received partial funding from other DOE programs, including the offices of Basic Energy Sciences, and Civilian Radioactive Waste Management. Significant support in an earlier phase had also been provided by Sandia National Laboratories, and by the U.S. Nuclear Regulatory Commission. The senior author would like to thank his colleagues at LBNL and elsewhere for many stimulating discussions and helpful suggestions throughout the development of the TOUGH codes. T.N. Narasimhan of LBNL/University of California at Berkeley and M.J. O'Sullivan of the University of Auckland, New Zealand, made important contributions to the development of capabilities for simulating flow in fractured media and to modeling of fluid mixtures. Y. Tsang and C. Doughty of LBNL, S. Webb and M. Fewell of Sandia National Laboratories, M.J. O'Sullivan and D. Bullivant of the University of Auckland, and D. Holford of PNNL assisted in testing earlier versions of TOUGH2, and made suggestions for improvements. Beta-testing of Version 2.0 was performed by Stefan Finsterle and Yu-Shu Wu of LBNL, Alfredo Battistelli of Aquater, Italy, Grimur Bjornsson of Orkustofnun, Iceland, and Steve Webb of Sandia National Laboratories. We are very grateful for their careful scrutiny of computer code, input files, and documentation, and for the many excellent suggestions for improvements.

## References

- Atkinson, P.G., R. Celati, R. Corsi and F. Kucuk. Behavior of the Bagnore Steam/ CO<sub>2</sub> Geothermal Reservoir, Italy, *Soc. Pet. Eng. J.*, 228 - 238, 1980.
- Aunzo, Z.P., G. Bjornsson and G.S. Bodvarsson. Wellbore Models GWELL, GWNACL, and HOLA, Lawrence Berkeley National Laboratory Report LBL-31428, Berkeley, CA, October 1991.
- Aziz, K. and A. Settari. *Petroleum Reservoir Simulation*, Elsevier, London and New York, 1979.
- Battistelli, A., C. Calore and K. Pruess. The Simulator TOUGH2/EWASG for Modeling Geothermal Reservoirs with Brines and Non-Condensable Gas, *Geothermics*, Vol. 26, No. 4, pp. 437 - 464, 1997.
- Bird, R., W.E. Stewart and E.N. Lightfoot. *Transport Phenomena*, John Wiley & Sons, New York, NY, 1960.
- Brand, C.W., J.E. Heinemann and K. Aziz. The Grid Orientation Effect in Reservoir Simulation, Paper SPE-21228, presented at Society of Petroleum Engineers Eleventh Symposium on Reservoir Simulation, Anaheim, CA, February 1991.
- Cass, A., G.S. Campbell and T.L. Jones. Enhancement of Thermal Water Vapor Diffusion in Soil. *Soil Sci. Soc. Am. J.*, Vol. 48, no. 1, pp. 25 - 32, 1984.
- Coats, K.H. Geothermal Reservoir Modeling, paper SPE-6892, presented at the 52nd Annual Fall Technical Conference and Exhibition of the SPE, Denver, Colorado, October 1977.
- Coats, K.H. and A.B. Ramesh. Effects of Grid Type and Difference Scheme on Pattern Steamflood Simulation Results, paper SPE-11079, presented at the 57th Annual Fall Technical Conference and Exhibition of the Society of Petroleum Engineers, New Orleans, LA, September 1982.
- Corey, A.T. The Interrelation Between Gas and Oil Relative Permeabilities, *Producers Monthly*, 38-41, November 1954.
- Cygan, R.T. The Solubility of Gases in NaCl Brine and a Critical Evaluation of Available Data, SAND90-2848, Sandia National Laboratories, Albuquerque, New Mexico, 1991.
- Dean, J.A. (ed.). *Lange's Handbook of Chemistry*, McGraw Hill, Thirteenth Edition, New York, 1985.
- de Marsily, G. *Quantitative Hydrogeology*, Academic Press, Orlando, FL, 1986.
- Doughty, C. and K. Pruess. A Similarity Solution for Two-Phase Water, Air and Heat Flow Near a Linear Heat Source in a Porous Medium, *J. of Geophys. Res.*, 97 (B2), 1821-1838, 1992.
- Edlefsen, N.E. and A.B.C. Anderson. Thermodynamics of Soil Moisture, *Hilgardia*, 15 (2), 31-298, 1943.
- Edwards, A.L. TRUMP: A Computer Program for Transient and Steady State Temperature Distributions in Multidimensional Systems, National Technical Information Service, National Bureau of Standards, Springfield, VA, 1972.

- Falta, R.W., K. Pruess, I. Javandel and P.A. Witherspoon. Density - Driven Flow of Gas in the Unsaturated Zone Due to the Evaporation of Volatile Organic Compounds, *Water. Resour. Res.*, Vol. 25, No. 10, pp. 2159 - 2169, 1989.
- Falta, R.W., K. Pruess, S. Finsterle, and A. Battistelli. T2VOC User's Guide, Lawrence Berkeley Laboratory Report LBL-36400, Berkeley, CA, March 1995.
- Fatt, I. and W.A. Klikoff. Effect of Fractional Wettability on Multiphase Flow Through Porous Media, *AIME Transactions*, 216, 246, 1959.
- Faust, C.R. and J.W. Mercer. Summary of Our Research in Geothermal Reservoir Simulation, Proc. Workshop on Geothermal Reservoir Engineering, Stanford University, Stanford, CA, SGP-TR-12, 1975.
- Finley, N.C. and M. Reeves. Swift Self-Teaching Curriculum, Report SAND81-0410, Sandia National Laboratory, Albuquerque, NM, 1982.
- Grant, M.A. Permeability Reduction Factors at Wairakei, paper 77-HT-52, presented at AIChE-ASME Heat Transfer Conference, Salt Lake City, Utah, August 1977.
- Hadgu, T. and D.H. Freeston. A Multi-Purpose Wellbore Simulator. *Geothermal Resources Council Transactions*, Vol. 14, pp. 1279 - 1286, 1990.
- Hadgu, T., R.W. Zimmerman and G.S. Bodvarsson. Coupled Reservoir-Wellbore Simulation of Geothermal Reservoir Behavior. *Geothermics*, Vol. 24, No. 2, pp. 145-166, 1995.
- Herbert, A.W., C.P. Jackson and D.A. Lever. Coupled Groundwater Flow and Solute Transport with Fluid Density Strongly Dependent on Concentration, *Water Resour. Res.*, Vol. 24, No. 10, pp. 1781 - 1795, 1988.
- Hirschfelder, J.O., C.F. Curtiss and R.B. Bird. *Molecular Theory of Gases and Liquids*, John Wiley & Sons, New York, NY, 1954.
- International Formulation Committee. *A Formulation of the Thermodynamic Properties of Ordinary Water Substance*, IFC Secretariat, Düsseldorf, Germany, 1967.
- Jury, W.A., W.F. Spencer and W.J. Farmer. Behavior Assessment Model for Trace Organics in Soil: I. Model Description, *J. Environ. Qual.*, Vol. 12, No. 4, pp. 558 - 564, 1983.
- Klinkenberg, L.J. The Permeability of Porous Media to Liquids and Gases, in *API Drilling and Production Practice*, pp. 200-213, 1941.
- Kruger, P. and H.J. Ramey, Jr. Stimulation and Reservoir Engineering of Geothermal Resources, Stanford Geothermal Program Report SGR-TR-1, Stanford University, Stanford, CA, 1974.
- Lam, S.T., A. Hunsbedt, P. Kruger and K. Pruess. Analysis of the Stanford Geothermal Reservoir Model Experiments Using the LBL Reservoir Simulator, *Geothermics*, 17 (4), 595 - 605, LBL-25957, 1988.
- Leverett, M.C. Capillary Behavior in Porous Solids, *Trans. Soc. Pet. Eng. AIME*, 142, 152-169, 1941.
- Loomis, A.G. Solubilities of Gases in Water, in: *International Critical Tables*, Vol. III, E. W. Washburn, (ed.), McGraw-Hill, New York, NY, pp. 255-257, 1928.

- Mason, E.A. and A.P. Malinauskas. *Gas Transport in Porous Media: The Dusty Gas Model*, Elsevier, Amsterdam, The Netherlands, 1983.
- Michaelides, E.E. Thermodynamic Properties of Geothermal Fluids, Geothermal Resources Council Transactions, Vol. 5, pp. 361 - 364, 1981.
- Miller, A.B. A Brine-Steam Properties Computer Program for Geothermal Energy Calculations, Lawrence Livermore National Laboratory Report UCRL-52495, Livermore, CA, June 1978.
- Millington, R.J. and J.P. Quirk. Permeability of Porous Solids, *Trans. Faraday Soc.*, 57, 1200-1207, 1961.
- Milly, P.C.D. Moisture and Heat Transport in Hysteretic, Inhomogeneous Porous Media: A Matric-Head Based Formulation and a Numerical Model, *Water Resour. Res.*, Vol. 18, No. 3, pp. 489 - 498, 1982.
- Moridis, G. and K. Pruess. TOUGH Simulations of Updegraff's Set of Fluid and Heat Flow Problems, Lawrence Berkeley Laboratory Report LBL-32611, Berkeley, CA, November 1992.
- Moridis, G. and K. Pruess. Flow and Transport Simulations Using T2CG1, a Package of Conjugate Gradient Solvers for the TOUGH2 Family of Codes, Lawrence Berkeley Laboratory Report LBL-36235, Berkeley, CA, 1995.
- Moridis, G. and K. Pruess. T2SOLV: An Enhanced Package of Solvers for the TOUGH2 Family of Reservoir Simulation Codes, *Geothermics*, Vol. 27, No. 4, pp. 415 - 444, 1998.
- Mualem, Y. A New Model for Predicting the Hydraulic Conductivity of Unsaturated Porous Media, *Water Resour. Res.*, Vol. 12, No. 3, pp. 513 - 522, 1976.
- Murray, L. and C. Gunn. Toward Integrating Geothermal Reservoir and Wellbore Simulation: TETRAD and WELLSIM, Proc. 15th NZ Geothermal Workshop, Auckland, New Zealand, 1993.
- Narasimhan, T.N. and P.A. Witherspoon. An Integrated Finite Difference Method for Analyzing Fluid Flow in Porous Media, *Water Resour. Res.*, Vol. 12, No. 1, pp. 57 – 64, 1976.
- Narasimhan, T.N., P.A. Witherspoon and A.L. Edwards. Numerical Model for Saturated-Unsaturated Flow in Deformable Porous Media, Part 2: The Algorithm, *Water Resour. Res.*, 14 (2), 255-261, 1978.
- Oldenburg, C.M. and K. Pruess. A Two-Dimensional Dispersion Module for the TOUGH2 Simulator, Lawrence Berkeley Laboratory Report LBL-32505, Berkeley, CA, September 1993.
- Oldenburg, C.M. and K. Pruess. EOS7R: Radionuclide Transport for TOUGH2, Lawrence Berkeley Laboratory Report LBL-34868, Berkeley, CA, November 1995.
- Oldenburg, C.M. and K. Pruess. Higher-Order Differencing for Phase Front Propagation in Geothermal Systems, Proc., Twenty-Third Workshop on Geothermal Reservoir Engineering, Stanford University, January 1998.
- O'Sullivan, M.J. A Similarity Method for Geothermal Well Test Analysis, *Water Resour. Res.*, Vol. 17, No. 2, pp. 390 – 398, 1981.

- O'Sullivan, M.J., G.S. Bodvarsson, K. Pruess and M.R. Blakeley. Fluid and Heat Flow in Gas-Rich Geothermal Reservoirs, *Society of Petroleum Engineers Journal*, Vol. 25, No. 2, pp. 215 - 226, April 1985.
- Peaceman, D.W. *Fundamentals of Numerical Reservoir Simulation*, Elsevier, Amsterdam, The Netherlands, 1977.
- Peaceman, D.W. Interpretation of Well-Block Pressures in Numerical Reservoir Simulation with Nonsquare Grid Blocks and Anisotropic Permeability, paper SPE-10528, presented at the Sixth SPE Symposium on Reservoir Simulation of the Society of Petroleum Engineers, New Orleans, LA, January 1982.
- Pickens, J.F., R.W. Gillham and D.R. Cameron. Finite Element Analysis of the Transport of Water and Solutes in Tile-Drained Soils, *J. of Hydrology*, 40, 243-264, 1979.
- Potter, J.M. and D.L. Brown. The Volumetric Properties of Aqueous Sodium Chloride Solutions, U. S. Geological Survey, Bulletin 1421-C, 1977.
- Pritchett, J.W. Numerical Calculation of Multiphase Fluid and Heat Flow in Hydrothermal Reservoirs, Proc. Workshop on Geothermal Reservoir Engineering, Stanford University, Stanford, CA, pp. 201-205, SGP-TR-12, 1975.
- Pritchett, J.W., M.H. Rice and T.D. Riney. Equation-of-State for Water-Carbon Dioxide Mixtures: Implications for Baca Reservoir, Report DOE/ET/27163-8, Systems, Science and Software, La Jolla, CA, February 1981.
- Pruess, K. GMINC - A Mesh Generator for Flow Simulations in Fractured Reservoirs, Lawrence Berkeley Laboratory Report LBL-15227, Berkeley, CA, March 1983.
- Pruess, K. TOUGH User's Guide, Nuclear Regulatory Commission Report NUREG/CR-4645; also Lawrence Berkeley Laboratory Report LBL-20700, 1987.
- Pruess, K. TOUGH2 - A General Purpose Numerical Simulator for Multiphase Fluid and Heat Flow, Lawrence Berkeley Laboratory Report LBL-29400, Berkeley, CA, 1991a.
- Pruess, K. EOS7, An Equation-of-State Module for the TOUGH2 Simulator for Two-Phase Flow of Saline Water and Air, Lawrence Berkeley Laboratory Report LBL-31114, Berkeley, CA, 1991b.
- Pruess, K. Grid Orientation and Capillary Pressure Effects in the Simulation of Water Injection into Depleted Vapor Zones, *Geothermics*, Vol. 20, No. 5/6, pp. 257 - 277, 1991c.
- Pruess, K., ECO2N: A TOUGH2 Fluid Property Module for Mixtures of Water, NaCl, and CO<sub>2</sub>, Lawrence Berkeley National Laboratory Report LBNL-57952, Berkeley, Calif., 2005.
- Pruess, K., ECO2M: A TOUGH2 Fluid Property Module for Mixtures of Water, NaCl, and CO<sub>2</sub>, Including Super- and Sub-Critical Conditions, and Phase Change Between Liquid and Gaseous CO<sub>2</sub>, Lawrence Berkeley National Laboratory Report LBNL-4590E, Berkeley, Calif., 2011.
- Pruess, K., J.M. Zerzan, R.C. Schroeder and P.A. Witherspoon. Description of the Three-Dimensional Two-Phase Simulator SHAFT78 for Use in Geothermal Reservoir Studies, paper SPE-7699, presented at the Fifth SPE Symposium on Reservoir Simulation, Denver, CO, February 1979.

- Pruess, K. and R.C. Schroeder. SHAFT 79 User's Manual, Lawrence Berkeley Laboratory Report LBL-10861, Berkeley, CA, March 1980.
- Pruess, K., and T.N. Narasimhan. On Fluid Reserves and the Production of Superheated Steam from Fractured, Vapor-Dominated Geothermal Reservoirs, *J. Geophys. Res.*, Vol. 87, No. B11, pp. 9329 - 9339, 1982.
- Pruess, K. and G.S. Bodvarsson. A Seven-Point Finite Difference Method for Improved Grid Orientation Performance in Pattern Steam Floods, *Proceedings*, Seventh Society of Petroleum Engineers Symposium on Reservoir Simulation, Paper SPE-12252, pp. 175 - 184, San Francisco, CA, 1983.
- Pruess, K. and G.S. Bodvarsson. Thermal Effects of ReInjection in Geothermal Reservoirs with Major Vertical Fractures, *J. Pet. Tech.*, Vol. 36, No. 10, pp. 1567 – 1578, 1984.
- Pruess, K. and T.N. Narasimhan. A Practical Method for Modeling Fluid and Heat Flow in Fractured Porous Media, *Soc. Pet. Eng. J.*, Vol. 25, No. 1, pp. 14 - 26, February 1985.
- Pruess, K., J.S.Y. Wang and Y.W. Tsang. On Thermohydrological Conditions Near High-Level Nuclear Wastes Emplaced in Partially Saturated Fractured Tuff. Part 2. Effective Continuum Approximation, *Water Resour. Res.*, Vol. 26, No. 6, pp. 1249 - 1261, 1990.
- Pruess, K., A. Simmons, Y.S. Wu and G. Moridis. TOUGH2 Software Qualification, Lawrence Berkeley National Laboratory Report LBL-38383, Berkeley, CA, February 1996.
- Reeves, M., D. S. Ward, N. D. Johns and R. M. Cranwell. Theory and Implementation of Swift II, The Sandia Waste-Isolation Flow and Transport Model for Fractured Media, Report No. SAND83-1159, Sandia National Laboratory, Albuquerque, NM, 1986.
- Richards, L.A. Capillary Conduction of Liquids Through Porous Mediums, *Physics*, Vol. 1, pp. 318 - 333, 1931.
- Sleijpen, G.L.G. and D. Fokkema. BiCGSTAB(m) for Linear Equations Involving Unsymmetric Matrices with Complex Spectrum, *Electronic Transactions on Numerical Analysis*, Vol. 1, pp. 11 - 32, 1993.
- Sutton, F.M. and A. McNabb. Boiling Curves at Broadlands Field, New Zealand, *N. Z. J. Sci.*, Vol. 20, pp. 333 - 337, 1977.
- Thomas, G.W. *Principles of Hydrocarbon Reservoir Simulation*. International Human Resources Development Corporation, Boston, 1982.
- Tsang, Y.W. and K. Pruess. Further Modeling Studies of Gas Movement and Moisture Migration at Yucca Mountain, Nevada, Lawrence Berkeley Laboratory Report LBL-29127, Berkeley, CA, 1990.
- Udell, K.S. and J.S. Fitch. Heat and Mass Transfer in Capillary Porous Media Considering Evaporation, Condensation, and Non-Condensable Gas Effects, paper presented at 23rd ASME/AIChE National Heat Transfer Conference, Denver, CO, 1985.
- van der Vorst, H.A. Bi-CGSTAB: A Fast and Smoothly Converging Variant of BiCG in the Presence of Rounding Errors, *SIAM J. Sci. Statist. Comput.*, Vol. 13, pp. 631 - 644, 1992.
- van Genuchten, M.Th. A Closed-Form Equation for Predicting the Hydraulic Conductivity of Unsaturated Soils, *Soil Sci. Soc. Amer. J.*, Vol. 44, pp. 892 - 898, 1980.

- Vargaftik, N.B. *Tables on the Thermophysical Properties of Liquids and Gases*, 2nd Ed., John Wiley & Sons, New York, NY, 1975.
- Vaughan, P.J. Analysis of Permeability Reduction During Flow of Heated, Aqueous Fluid Through Westerly Granite, in C.F. Tsang (ed.), *Coupled Processes Associated with Nuclear Waste Repositories*, pp. 529 - 539, Academic Press, New York, 1987.
- Verma, A.K., K. Pruess, C.F. Tsang and P.A. Witherspoon. A Study of Two-Phase Concurrent Flow of Steam and Water in an Unconsolidated Porous Medium, Proc. 23rd National Heat Transfer Conference, Am. Society of Mechanical Engineers, Denver, CO, 135–143, 1985.
- Verma, A. and K. Pruess. Thermohydrologic Conditions and Silica Redistribution Near High-Level Nuclear Wastes Emplaced in Saturated Geological Formations, *J. of Geophys. Res.*, Vol. 93, No. B2, pp. 1159-1173, 1988.
- Vinsome, P.K.W. and J. Westerveld. A Simple Method for Predicting Cap and Base Rock Heat Losses in Thermal Reservoir Simulators, *J. Canadian Pet. Tech.*, Vol. 19, No. 3, pp. 87 – 90, July-September 1980.
- Walker, W.R., J.D. Sabey, and D.R. Hampton. Studies of Heat Transfer and Water Migration in Soils, Final Report, Department of Agricultural and Chemical Engineering, Colorado State University, Fort Collins, CO, 80523, April 1981.
- Warren, J.E. and P.J. Root. The Behavior of Naturally Fractured Reservoirs, *Soc. Pet. Eng. J., Transactions, AIME*, 228, 245-255, September 1963.
- Webb, S.W. Gas-Phase Diffusion in Porous Media - Evaluation of an Advection-Dispersive Formulation and the Dusty Gas Model for Binary Mixtures, *J. Por. Media*, Vol. 1, No. 2, pp. 187 - 199, 1998.
- Webb, S.W. and C.K. Ho. Review of Enhanced Vapor Diffusion in Porous Media, in: K. Pruess (ed.), *Proceedings of the TOUGH Workshop '98*, Lawrence Berkeley National Laboratory Report LBNL-41995, pp. 257 - 262, Berkeley, CA, 1998a.
- Webb, S.W. and C.K. Ho. Enhanced Vapor Diffusion in Porous Media - LDRD Final Report, Sandia National Laboratories Report SAND98-2772, Albuquerque, NM, 1998b.
- Wu, Y.S., K. Pruess and Z.X. Chen. Buckley-Leverett Flow in Composite Media, *SPE Advanced Technology Series*, Vol. 1, No. 2, pp. 36 - 42, 1993.
- Yanosik, J.L. and T.A. McCracken. A Nine-Point, Finite Difference Reservoir Simulator for Realistic Prediction of Adverse Mobility Ratio Displacements, *Soc. Pet. Eng. J.*, 253 – 262, 1979.

## Appendix A. Mass and Energy Balances

The basic mass- and energy balance equations solved by TOUGH2 can be written in the general form

$$\frac{d}{dt} \int_{V_n} M^\kappa dV_n = \int_{\Gamma_n} \mathbf{F}^\kappa \cdot \mathbf{n} d\Gamma_n + \int_{V_n} q^\kappa dV_n \quad (\text{A.1})$$

The integration is over an arbitrary subdomain  $V_n$  of the flow system under study, which is bounded by the closed surface  $\Gamma_n$ . The quantity  $M$  appearing in the accumulation term (left hand side) represents mass or energy per volume, with  $\kappa = 1, \dots, NK$  labeling the mass components (water, air,  $H_2$ , solutes, ...), and  $\kappa = NK + 1$  the heat “component.”  $\mathbf{F}$  denotes mass or heat flux (see below), and  $q$  denotes sinks and sources.  $n$  is a normal vector on surface element  $d\Gamma_n$ , pointing inward into  $V_n$ .

The general form of the mass accumulation term is

$$M^\kappa = \phi \sum_\beta S_\beta \rho_\beta X_\beta^\kappa \quad (\text{A.2})$$

The total mass of component  $\kappa$  is obtained by summing over the fluid phases  $\beta$  (= liquid, gas, NAPL).  $\phi$  is porosity,  $S_\beta$  is the saturation of phase  $\beta$  (i.e., the fraction of pore volume occupied by phase  $\beta$ ),  $\rho_\beta$  is the density of phase  $\beta$ , and  $X_\beta^\kappa$  is the mass fraction of component  $\kappa$  present in phase  $\beta$ . A more general form of the mass accumulation term that includes equilibrium sorption on the solid grains is given in Eq. (13). Similarly, the heat accumulation term in a multiphase system is

$$M^{NK+1} = (1 - \phi) \rho_R C_R T + \phi \sum_\beta S_\beta \rho_\beta u_\beta \quad (\text{A.3})$$

where  $\rho_R$  and  $C_R$  are, respectively, grain density and specific heat of the rock,  $T$  is temperature, and  $u_\beta$  is specific internal energy in phase  $\beta$ .

Advective mass flux is a sum over phases,

$$\mathbf{F}^\kappa \Big|_{adv} = \sum_\beta X_\beta^\kappa \mathbf{F}_\beta \quad (\text{A.4})$$

and individual phase fluxes are given by a multiphase version of Darcy's law:

$$\mathbf{F}_\beta = \rho_\beta \mathbf{u}_\beta = -k \frac{k_{r\beta} \rho_\beta}{\mu_\beta} (\nabla P_\beta - \rho_\beta \mathbf{g}) \quad (\text{A.5})$$

Here  $u_\beta$  is the Darcy velocity (volume flux) in phase  $\beta$ ,  $k$  is absolute permeability,  $k_{r\beta}$  is relative permeability to phase  $\beta$ ,  $\mu_\beta$  is viscosity, and

$$P_\beta = P + P_{c\beta} \quad (\text{A.6})$$

is the fluid pressure in phase  $\beta$ , which is the sum of the pressure  $P$  of a reference phase (usually taken to be the gas phase), and the capillary pressure  $P_{c\beta}$  ( $\leq 0$ ).  $\mathbf{g}$  is the vector of gravitational acceleration. Vapor pressure lowering due to capillary and phase adsorption effects is modeled by Kelvin's equation (Edlefsen and Anderson, 1943),

$$P_v(T, S_l) = f_{VPL}(T, S_l) P_{sat}(T) \quad (\text{A.7}),$$

where

$$f_{VPL} = \exp \left[ \frac{M_w P_{cl}(S_l)}{\rho_l R (T + 273.15)} \right] \quad (\text{A.8})$$

is the vapor pressure lowering factor.  $P_{sat}$  is the saturated vapor pressure of bulk aqueous phase,  $P_{cl}$  is the difference between aqueous and gas phase pressures,  $M_w$  is the molecular weight of water, and  $R$  is the universal gas constant.

Heat flux includes conductive and convective components

$$\mathbf{F}^{NK+1} = -\lambda \nabla T + \sum_\beta h_\beta \mathbf{F}_\beta \quad (\text{A.9})$$

where  $\lambda$  is thermal conductivity, and  $h_\beta$  is specific enthalpy in phase  $\beta$ . Radiative heat transfer according to the Stefan-Boltzmann law can also be modeled (see Eq. E.2).

Absolute permeability of the gas phase increases at low pressures according to the relation given by Klinkenberg (1941)

$$k = k_\infty \left( 1 + \frac{b}{P} \right) \quad (\text{A.10})$$

where  $k_\infty$  is the permeability at “infinite” pressure, and  $b$  is the Klinkenberg parameter. In addition to Darcy flow, mass transport can also occur by diffusion and hydrodynamic dispersion, as follows (de Marsily, 1986).

$$\mathbf{F}^\kappa|_{dis} = - \sum_{\beta} \rho_{\beta} \bar{\mathbf{D}}_{\beta}^{\kappa} \nabla X_{\beta}^{\kappa} \quad (\text{A.11})$$

The hydrodynamic dispersion tensor is given by

$$\bar{\mathbf{D}}_{\beta}^{\kappa} = D_{\beta,T}^{\kappa} \mathbf{I} + \frac{\left( D_{\beta,L}^{\kappa} - D_{\beta,T}^{\kappa} \right)}{u_{\beta}^2} \mathbf{u}_{\beta} \mathbf{u}_{\beta} \quad (\text{A.12})$$

where

$$D_{\beta,L}^{\kappa} = \phi \tau_0 \tau_{\beta} d_{\beta}^{\kappa} + \alpha_{\beta,L} u_{\beta} \quad (\text{A.13a})$$

$$D_{\beta,T}^{\kappa} = \phi \tau_0 \tau_{\beta} d_{\beta}^{\kappa} + \alpha_{\beta,T} u_{\beta} \quad (\text{A.13b})$$

are longitudinal and transverse dispersion coefficients, respectively.  $d_{\beta}^{\kappa}$  is the molecular diffusion coefficient for component  $\kappa$  in phase  $\beta$ ,  $\tau_0 \tau_{\beta}$  is the tortuosity which includes a porous medium dependent factor  $\tau_0$  and a coefficient that depends on phase saturation  $S_{\beta}$ ,  $\tau_{\beta} = \tau_{\beta}(S_{\beta})$ , and  $\alpha_L$ ,  $\alpha_T$  are the longitudinal and transverse dispersivities. Full hydrodynamic dispersion is included only in special versions of TOUGH2, while molecular diffusion in all phases is now part of the standard code. The mass flux from molecular diffusion alone is obtained by setting  $\alpha_L = \alpha_T = 0$  in Eq. (A.11 - A.13); diffusive flux of component  $\kappa$  in phase  $\beta$  is given by (see Appendix D)

$$\mathbf{f}_{\beta}^{\kappa} = -\phi \tau_0 \tau_{\beta} \rho_{\beta} d_{\beta}^{\kappa} \nabla X_{\beta}^{\kappa} \quad (\text{A.14})$$

By applying Gauss’ divergence theorem, Eq. (A.1) can be converted into the following PDE

$$\frac{\partial M^{\kappa}}{\partial t} = -\operatorname{div} \mathbf{F}^{\kappa} + q^{\kappa} \quad (\text{A.15})$$

which is the form commonly used as the starting point for deriving finite difference or finite element discretization approaches. Of special interest is a simplified version of Eq. (A.15) for an approximate description of water seepage in the unsaturated zone. Neglecting phase change effects and assuming that the gas phase acts as a “passive bystander” with negligible gas pressure gradients, the following equation for liquid phase flow is obtained

$$\frac{\partial}{\partial t} \phi S_l \rho_l = \operatorname{div} \left[ k \frac{k_{rl}}{\mu_l} \rho_l \nabla (P_l + \rho_l g z) \right] \quad (\text{A.16})$$

where  $z$  is defined positive upward. Neglecting variations in liquid phase density and viscosity, as is appropriate for (nearly) isothermal conditions, Eq. (A.16) simplifies to Richards' equation (1931)

$$\frac{\partial}{\partial t} \theta = \operatorname{div} [K \nabla h] \quad (\text{A.17})$$

where  $\theta = \phi S_l$  is specific volumetric moisture content,  $K = k k_{rl} \rho_l g / \mu_l$  is hydraulic conductivity, and  $h = z + P_l / \rho_l g$  is the hydraulic head.

## Appendix B. Space and Time Discretization

The continuum equations (A.1) are discretized in space using the integral finite difference method (IFD; Edwards, 1972; Narasimhan and Witherspoon, 1976). Introducing appropriate volume averages, we have

$$\int_{V_n} M dV = V_n \bar{M}_n \quad (\text{B.1})$$

where  $M$  is a volume-normalized extensive quantity, and  $\bar{M}_n$  is the average value of  $M$  over  $V_n$ . Surface integrals are approximated as a discrete sum of averages over surface segments  $A_{nm}$ :

$$\int_{\Gamma_n} \mathbf{F}^\kappa \cdot \mathbf{n} d\Gamma = \sum_m A_{nm} F_{nm} \quad (\text{B.2})$$

Here  $F_{nm}$  is the average value of the (inward) normal component of  $\mathbf{F}$  over the surface segment  $A_{nm}$  between volume elements  $V_n$  and  $V_m$ . The discretization approach used in the integral finite difference method and the definition of the geometric parameters are illustrated in Fig. 60.

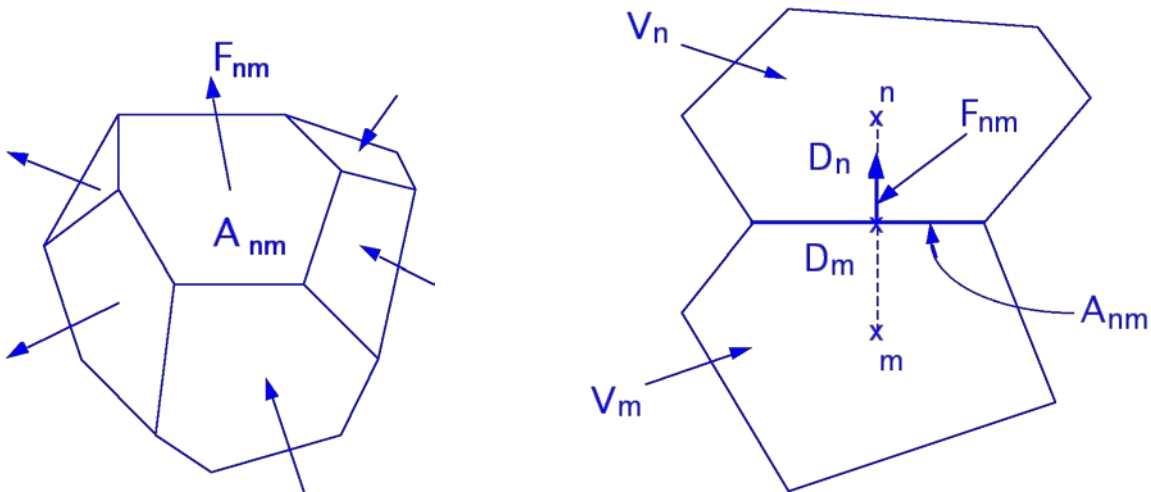


Figure 60. Space discretization and geometry data in the integral finite difference method.

The discretized flux is expressed in terms of averages over parameters for elements  $V_n$  and  $V_m$ . For the basic Darcy flux term, Eq. (A.5), we have

$$F_{\beta,nm} = -k_{nm} \left[ \frac{k_{r\beta} \rho_\beta}{\mu_\beta} \right]_{nm} \left[ \frac{P_{\beta,n} - P_{\beta,m}}{D_{nm}} - \rho_{\beta,nm} g_{nm} \right] \quad (\text{B.3})$$

where the subscripts  $(nm)$  denote a suitable averaging at the interface between grid blocks  $n$  and  $m$  (interpolation, harmonic weighting, upstream weighting).  $D_{nm} = D_n + D_m$  is the distance between the nodal points  $n$  and  $m$ , and  $g_{nm}$  is the component of gravitational acceleration in the direction from  $m$  to  $n$ . Discretization of diffusive fluxes raises some subtle issues and is discussed separately in Appendix D.

Substituting Eqs. (B.1) and (B.2) into the governing Eq. (A.1), a set of first-order ordinary differential equations in time is obtained.

$$\frac{dM_n^\kappa}{dt} = \frac{1}{V_n} \sum_m A_{nm} F_{nm}^\kappa + q_n^\kappa \quad (\text{B.4})$$

Time is discretized as a first-order finite difference, and the flux and sink and source terms on the right-hand side of Eq. (B.4) are evaluated at the new time level,  $t^{k+1} = t^k + \Delta t$ , to obtain the numerical stability needed for an efficient calculation of multiphase flow. This treatment of flux terms is known as “fully implicit,” because the fluxes are expressed in terms of the unknown thermodynamic parameters at time level  $t^{k+1}$ , so that these unknowns are only implicitly defined in the resulting equations (see, e.g., Peaceman, 1977). The time discretization results in the following set of coupled non-linear, algebraic equations

$$R_n^{\kappa,k+1} = M_n^{\kappa,k+1} - M_n^{\kappa,k} - \frac{\Delta t}{V_n} \left\{ \sum_m A_{nm} F_{nm}^{\kappa,k+1} + V_n q_n^{\kappa,k+1} \right\} = 0 \quad (\text{B.5})$$

where we have introduced residuals  $R_n^{\kappa,k+1}$ . For each volume element (grid block)  $V_n$ , there are  $NEQ$  equations ( $\kappa = 1, 2, \dots, NEQ$ ; usually,  $NEQ = NK + 1$ ), so that for a flow system with  $NEL$  grid blocks (B.5) represents a total of  $NEL \times NEQ$  coupled non-linear equations. The unknowns are the  $NEL \times NEQ$  independent primary variables  $\{x_i; i = 1, \dots, NEL \times NEQ\}$  which completely define the state of the flow system at time level  $t^{k+1}$ . These equations are solved by Newton/Raphson iteration, which is implemented as follows. We introduce an iteration index  $p$  and expand the residuals  $R_n^{\kappa,k+1}$  in Eq. (B.5) at iteration step  $p + 1$  in a Taylor series in terms of those at index  $p$ .

$$R_n^{\kappa,k+1}(x_{i,p+1}) = R_n^{\kappa,k+1}(x_{i,p}) + \sum_i \frac{\partial R_n^{\kappa,k+1}}{\partial x_i} \Big|_p (x_{i,p+1} - x_{i,p}) + \dots = 0 \quad (\text{B.6})$$

Retaining only terms up to first order, we obtain a set of  $\text{NEL} \times \text{NEQ}$  linear equations for the increments ( $x_{i,p+1} - x_{i,p}$ ):

$$-\sum_i \frac{\partial R_n^{\kappa,k+1}}{\partial x_i} \Big|_p (x_{i,p+1} - x_{i,p}) = R_n^{\kappa,k+1}(x_{i,p}) \quad (\text{B.7})$$

All terms  $\partial R_n/\partial x_i$  in the Jacobian matrix are evaluated by numerical differentiation. Eq. (B.7) is solved by sparse direct matrix methods or iteratively by means of preconditioned conjugate gradients (Moridis and Pruess, 1995, 1998). Iteration is continued until the residuals  $R_n^{\kappa,k+1}$  are reduced below a preset convergence tolerance.

$$\left| \frac{R_{n,p+1}^{\kappa,k+1}}{M_{n,p+1}^{\kappa,k+1}} \right| \leq \varepsilon_1 \quad (\text{B.8})$$

The default (relative) convergence criterion is  $\varepsilon_1 = 10^{-5}$  (TOUGH2 input parameter *RE1*). When the accumulation terms are smaller than  $\varepsilon_2$  (TOUGH2 input parameter *RE2*, default  $\varepsilon_2 = 1$ ), an absolute convergence criterion is imposed,

$$|R_n^{\kappa,k+1}| \leq \varepsilon_1 \bullet \varepsilon_2 \quad (\text{B.9}).$$

Convergence is usually attained in 3 - 4 iterations. If convergence cannot be achieved within a certain number of iterations (default 8), the time step size  $\Delta t$  is reduced and a new iteration process is started.

It is appropriate to add some comments about our space discretization technique. The entire geometric information of the space discretization in Eq. (B.5) is provided in the form of a list of grid block volumes  $V_n$ , interface areas  $A_{nm}$ , nodal distances  $D_{nm}$  and components  $g_{nm}$  of gravitational acceleration along nodal lines. There is no reference whatsoever to a global system of coordinates, or to the dimensionality of a particular flow problem. The discretized equations are in fact valid for arbitrary irregular discretizations in one, two or three dimensions, and for porous as well as for fractured media. This flexibility should be used with caution, however, because the accuracy of solutions depends upon the accuracy with which the various interface parameters in

equations such as (B.3) can be expressed in terms of average conditions in grid blocks. A general requirement is that there exists approximate thermodynamic equilibrium in (almost) all grid blocks at (almost) all times (Pruess and Narasimhan, 1985). For systems of regular grid blocks referenced to global coordinates (such as  $r - z$ ,  $x - y - z$ ), Eq. (B.5) is identical to a conventional finite difference formulation (e.g., Peaceman, 1977; Moridis and Pruess, 1992).

## Appendix C. Description of Flow in Fractured Media

Figure 61 illustrates the classical double-porosity concept for modeling flow in fractured-porous media as developed by Warren and Root (1963). Matrix blocks of low permeability are embedded in a network of interconnected fractures. Global flow in the reservoir occurs only through the fracture system, which is described as an effective porous continuum. Rock matrix and fractures may exchange fluid (or heat) locally by means of “interporosity flow,” which is driven by the difference in pressures (or temperatures) between matrix and fractures. Warren and Root approximated the interporosity flow as being quasi-steady, with rate of matrix-fracture interflow proportional to the difference in (local) average pressures.

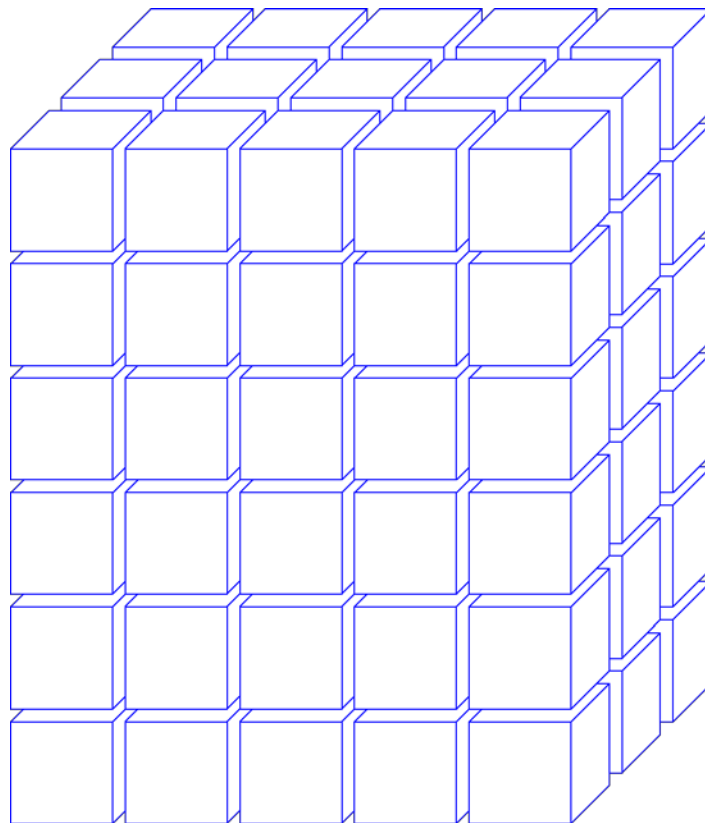


Figure 61. Idealized double porosity model of a fractured porous medium.

The quasi-steady approximation is applicable to isothermal single-phase flow of fluids with small compressibility, where pressure diffusivities are large, so that pressure changes in the fractures penetrate quickly all the way into the matrix blocks. However, for multiphase flows, or coupled fluid and heat flows, the transient periods for interporosity flow can be very long (tens of years). In order to accurately describe such flows it is necessary to resolve the driving pressure, temperature, and mass fraction gradients at the matrix/fracture interface. In the method of

"multiple interacting continua" (MINC; Pruess and Narasimhan, 1982, 1985), resolution of these gradients is achieved by appropriate subgridding of the matrix blocks, as shown in Fig. 62. The MINC concept is based on the notion that changes in fluid pressures, temperatures, phase compositions, etc. due to the presence of sinks and sources (production and injection wells) will propagate rapidly through the fracture system, while invading the tight matrix blocks only slowly. Therefore, changes in matrix conditions will (locally) be controlled by the distance from the fractures. Fluid and heat flow from the fractures into the matrix blocks, or from the matrix blocks into the fractures, can then be modeled by means of one-dimensional strings of nested grid blocks, as shown in Fig. 62.

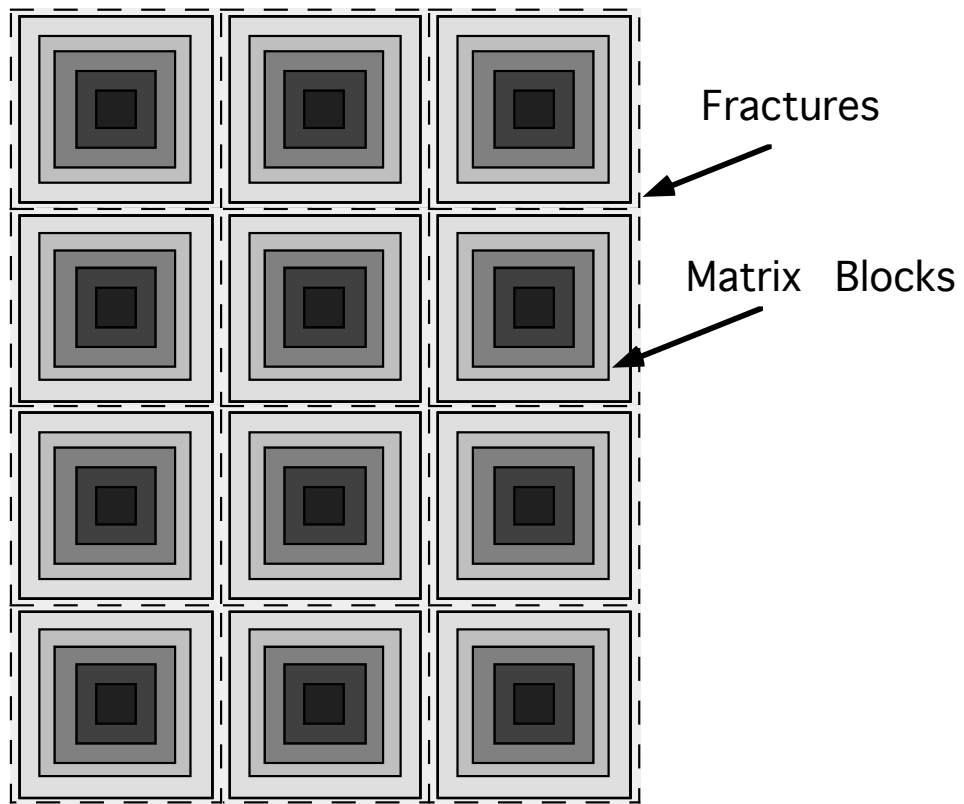


Figure 62. Subgridding in the method of "multiple interacting continua" (MINC).

In general it is not necessary to explicitly consider subgrids in all of the matrix blocks separately. Within a certain reservoir subdomain (corresponding to a finite difference grid block), all fractures will be lumped into continuum # 1, all matrix material within a certain distance from the fractures will be lumped into continuum # 2, matrix material at larger distance becomes continuum # 3, and so on. Quantitatively, the subgridding is specified by means of a set of volume fractions  $VOL(j)$ ,  $j = 1, \dots, J$ , into which the primary porous medium grid blocks are partitioned.

The MINC-process in the MESHMAKER module of TOUGH2 operates on the element and connection data of a porous medium mesh to calculate, for given data on volume fractions, the volumes, interface areas, and nodal distances for a secondary fractured medium mesh. The information on fracturing (spacing, number of sets, shape of matrix blocks) required for this is provided by a “proximity function” PROX( $x$ ) which expresses, for a given reservoir domain  $V_o$ , the total fraction of matrix material within a distance  $x$  from the fractures. If only two continua are specified (one for fractures, one for matrix), the MINC approach reduces to the conventional double-porosity method. Full details are given in a separate report (Pruess, 1983).

The MINC-method as implemented in the MESHMaker module can also describe global matrix-matrix flow. Fig. 63 shows the most general approach, often referred to as “dual permeability,” in which global flow occurs in both fracture and matrix continua. It is also possible to permit matrix-matrix flow only in the vertical direction. For any given fractured reservoir flow problem, selection of the most appropriate gridding scheme must be based on a careful consideration of the physical and geometric conditions of flow. The MINC approach is not applicable to systems in which fracturing is so sparse that the fractures cannot be approximated as a continuum.

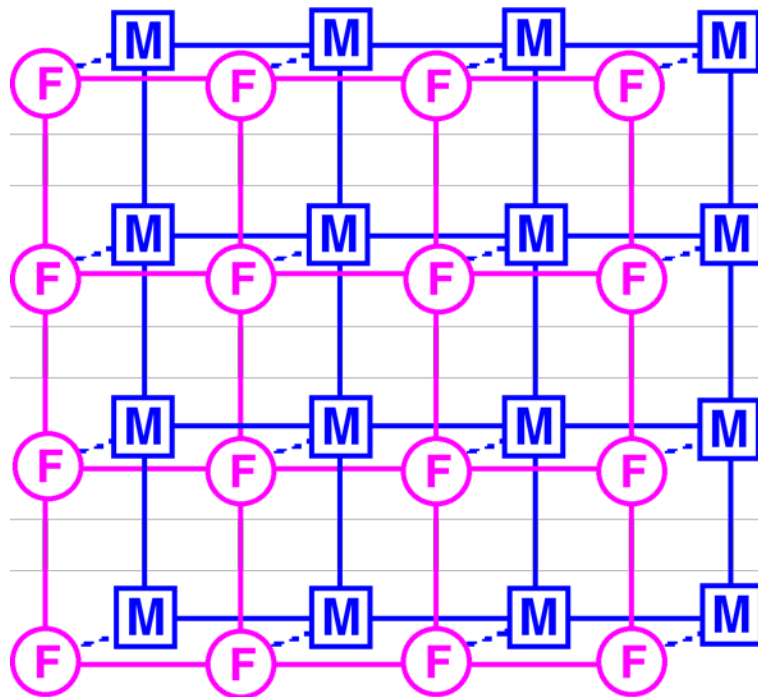


Figure 63. Flow connections in the “dual permeability” model. Global flow occurs between both fracture ( $F$ ) and matrix ( $M$ ) grid blocks. In addition there is  $F$ - $M$  interporosity flow.

## Appendix D. Multiphase Diffusion

### D.1 General Considerations

Molecular diffusion plays a minor role in many subsurface flow processes, but may become a significant and even dominant mechanism for mass transport when advective velocities are small. Diffusive flux is usually written as being proportional to the gradient in the concentration of the diffusing component (Fick's law)

$$\mathbf{f} = -d\nabla C \quad (\text{D.1})$$

where  $d$  is an effective diffusivity, which in general will depend on properties of the diffusing component, the pore fluid, and the porous medium. The concentration variable  $C$  may be chosen in a number of different ways (mass per unit volume, moles per unit volume, mass or mol fraction, etc.; Bird et al., 1960; de Marsily, 1986).

The basic Fick's law Eq. D.1 works well for diffusion of tracer solutes that are present at low concentrations in a single phase aqueous solution at rest with respect to the porous medium. However, many subtleties and complications arise when multiple components diffuse in a multiphase flow system. Effective diffusivities in general may depend on all concentration variables, leading to non-linear behavior especially when some components are present in significant (non-tracer) concentrations. Additional nonlinear effects arise from the dependence of tortuosity on phase saturations, and from coupling between advective and diffusive transport. For gases the Fickian model has serious limitations even at low concentrations, which prompted the development of the “dusty gas” model that entails a strong coupling between advective and diffusive transport (Mason and Malinauskas, 1983; Webb, 1998), and accounts for molecular streaming effects (Knudsen diffusion) that become very important when the mean free path of gas molecules is comparable to pore sizes. Further complications arise for components that are both soluble and volatile, in which case diffusion in aqueous and gaseous phases may be strongly coupled via phase partitioning effects. An extreme case is the well-known enhancement of vapor diffusion in partially saturated media, that is attributed to pore-level phase change effects (Cass et al., 1984; Webb and Ho, 1998a, b).

### D.2 Formulation Used in TOUGH2

Because of the difficulties mentioned above, it is not possible to formulate a model for multiphase diffusion that would be accurate under all circumstances. We have used a pragmatic approach in which diffusive flux of component  $\kappa$  in phase  $\beta$  (= liquid, gas) is written as

$$\mathbf{f}_\beta^\kappa = -\phi \tau_0 \tau_\beta \rho_\beta d_\beta^\kappa \nabla X_\beta^\kappa \quad (\text{D.2})$$

where  $\phi$  is porosity,  $\tau_0 \tau_\beta$  is the tortuosity which includes a porous medium dependent factor  $\tau_0$  and a coefficient that depends on phase saturation  $S_\beta$ ,  $\tau_\beta = \tau_\beta(S_\beta)$ ,  $\rho_\beta$  is density,  $d_\beta^\kappa$  is the diffusion coefficient of component  $\kappa$  in bulk fluid phase  $\beta$ , and  $X_\beta^\kappa$  is the mass fraction of component  $\kappa$  in phase  $\beta$ . For later developments it will be useful to define a single diffusion strength factor which combines all material constants and tortuosity factors into a single effective multiphase diffusion coefficient, as follows.

$$\Sigma_\beta^\kappa = \phi \tau_0 \tau_\beta \rho_\beta d_\beta^\kappa \quad (\text{D.3})$$

For general two-phase conditions, the total diffusive flux is then given by

$$\mathbf{f}^\kappa = -\Sigma_l^\kappa \nabla X_l^\kappa - \Sigma_g^\kappa \nabla X_g^\kappa \quad (\text{D.4}).$$

The saturation dependence of tortuosity is not well known at present. For soils the Millington and Quirk (1961) model has frequently been used (Jury et al., 1983; Falta et al., 1989)

$$\tau_0 \tau_\beta = \phi^{1/3} S_\beta^{10/3} \quad (\text{D.5})$$

which yields non-zero tortuosity coefficients as long as phase saturation is non-zero. It stands to reason that diffusive flux should vanish when a phase becomes discontinuous at low saturations, suggesting that saturation-dependent tortuosity should be related to relative permeability; e.g.  $\tau_\beta(S_\beta) \approx k_{r\beta}(S_\beta)$ . However, for components that partition between liquid and gas phases more complex behavior may be expected. For example, consider the case of a volatile and water-soluble compound diffusing under conditions of low gas saturation where the gas phase is discontinuous. In this case we have  $k_{rg}(S_g) = 0$  (because  $S_g < S_{gr}$ ), and  $k_{rl}(S_l = 1-S_g) < 1$ , so that a model equating saturation-dependent tortuosity to relative permeability would predict weaker diffusion than in single-phase liquid conditions. For compounds with “significant” volatility this would be unrealistic, as diffusion through isolated gas pockets would tend to enhance overall diffusion relative to single-phase liquid conditions.

### D.3 Space Discretization

Space discretization of diffusive flux in multiphase conditions raises some subtle issues. A finite difference formulation for total diffusive flux, Eq. (D.4), may be written as

$$(f^\kappa)_{nm} = -(\Sigma_l^\kappa)_{nm} \frac{(X_l^\kappa)_m - (X_l^\kappa)_n}{D_{nm}} - (\Sigma_g^\kappa)_{nm} \frac{(X_g^\kappa)_m - (X_g^\kappa)_n}{D_{nm}} \quad (D.6),$$

This expression involves the as yet unknown diffusive strength coefficients  $(\Sigma_l^\kappa)_{nm}$  and  $(\Sigma_g^\kappa)_{nm}$  at the interface, which must be expressed in terms of the strength coefficients in the participating grid blocks. Invoking conservation of diffusive flux across the interface between two grid blocks leads in the usual way to the requirement of harmonic weighting of the diffusive strength coefficients. However, such weighting may in general not be applied separately to the diffusive fluxes in gas and liquid phases, because these may be strongly coupled by phase partitioning effects. This can be seen by considering the extreme case of diffusion of a water-soluble and volatile compound from a grid block in single-phase gas conditions to an adjacent grid block which is in single-phase liquid conditions. Harmonic weighting applied separately to liquid and gas diffusive fluxes would result in either of them being zero, because for each phase effective diffusivity is zero on one side of the interface. Thus total diffusive flux would vanish in this case, which is unphysical. In reality, tracer would diffuse through the gas phase to the gas-liquid interface, would establish a certain mass fraction in the aqueous phase by dissolution, and would then proceed to diffuse away from the interface through the aqueous phase. Similar arguments can be made in the less extreme situation where liquid saturation changes from a large to a small value rather than from 1 to 0, as may be the case in the capillary fringe, during infiltration events, or at fracture-matrix interfaces in variably saturated media.

TOUGH2 features a fully coupled approach in which the space-discretized version Eq. (D.6) of the total multiphase diffusive flux Eq. (D.4) is re-written in terms of an effective multiphase diffusive strength coefficient and a single mass fraction gradient. Choosing the liquid mass fraction for this we have

$$(f^\kappa)_{nm} = - \left\{ \Sigma_l^\kappa + \Sigma_g^\kappa \frac{(X_g^\kappa)_m - (X_g^\kappa)_n}{(X_l^\kappa)_m - (X_l^\kappa)_n} \right\}_{nm} \frac{(X_l^\kappa)_m - (X_l^\kappa)_n}{D_{nm}} \quad (D.7),$$

where the gas phase mass fraction gradient has been absorbed into the effective diffusive strength term (in braces). As is well known, flux conservation at the interface then leads to the requirement

of harmonic weighting for the full effective strength coefficient. In order to be able to apply this scheme to the general case where not both phases may be present on both sides of the interface, we always define both liquid and gas phase mass fractions in all grid blocks, regardless of whether both phases are present. Mass fractions are assigned in such a way as to be consistent with what would be present in an evolving second phase. This procedure is applicable to all possible phase combinations, including the extreme case where conditions at the interface change from single phase gas to single phase liquid. Note that, if the diffusing tracer exists in just one of the two phases, harmonic weighting of the strength coefficient in Eq. (D.7) will reduce to harmonic weighting of either  $\Sigma_l^\kappa$  or  $\Sigma_g^\kappa$ .

The simpler scheme of separate harmonic weighting for individual phase diffusive fluxes is retained as an option, see below.

#### D.4 User Options

The treatment of multiphase diffusion requires parameter specifications in several different data blocks. In order to engage diffusion, the user must set the number of secondary parameters  $NB = 8$  in data block MULTI; the alternative value  $NB = 6$  will give a “no diffusion” calculation. Diffusivities are input through a new data block DIFFU; however, for the EOS7R module data block DIFFU may be omitted, and diffusivities may be input via data block SELEC, see p. 47. Specifications in the DIFFU block will override those in SELEC.

Diffusion coefficients for gases depend on pressure and temperature as (Vargaftik, 1975; Walker et al., 1981)

$$d_\beta^\kappa(P, T) = d_\beta^\kappa(P_0, T_0) \frac{P_0}{P} \left[ \frac{T+273.15}{273.15} \right]^\theta \quad (\text{D.8})$$

At standard conditions of  $P_0 = 1$  atm = 1.01325 bar,  $T_0 = 0^\circ\text{C}$ , the diffusion coefficient for vapor-air mixtures has a value of  $2.13 \times 10^{-5}$  m<sup>2</sup>/s; parameter  $\theta$  for the temperature dependence is 1.80. TOUGH2 can model a temperature dependence of gas phase diffusion coefficients according to Eq. (D.8) by specifying parameter  $\theta = \text{TEXP}$  in the first record of data block PARAM (see p. 166). Presently there are no provisions for inputting different values for the parameter  $\theta$  of temperature dependence for different gas phase components. Aqueous phase diffusion coefficients and Henry’s law coefficients (Eq. 6) are taken as constants, with no provisions for temperature dependence of these parameters.

Tortuosity effects have a porous medium-dependent part  $\tau_0$  and a saturation-dependent part  $\tau_\beta$ , see Eq. (D.2). The following three alternative formulations are available.

1. Relative permeability model.

For domains for which a tortuosity parameter  $\tau_0 = \text{TORTX} \neq 0$  is specified in data block ROCKS, tortuosity will be taken as  $\tau_0\tau_\beta(S_\beta) = \tau_0 k_{r\beta}(S_\beta)$ .

2. Millington-Quirk model.

For domains in which  $\text{TORTX} = 0$ , the Millington-Quirk model as given in Eq. (D.5) will be used.

3. Constant diffusivity.

When diffusivities  $d_\beta^\kappa$  are specified as negative numbers,  $\tau_0\tau_\beta = S_\beta$  will be used. Diffusivities will be taken to be the absolute values of the user inputs.

Alternative 3 corresponds to the formulation for gas diffusion in previous versions of TOUGH2. In the absence of phase partitioning and adsorptive effects, it amounts to effective diffusivity being approximately equal to  $d_\beta^\kappa$ , independent of saturation. This can be seen by noting that the accumulation term in the phase  $\beta$  contribution to the mass balance equation for component  $\kappa$  is given by  $\phi S_\beta \rho_\beta X_\beta^\kappa$ , approximately canceling out the  $\phi S_\beta \rho_\beta$  coefficient in the diffusive flux.

A crude (saturation-independent) enhancement of vapor diffusion can be chosen by specifying a suitable value, typically of order 1, for the parameter group  $B = \phi\tau_0\tau_\beta$ . This is to be entered as parameter BE in the first record in data block PARAM (see p. 166).

As had been discussed above, two alternative discretization schemes are implemented in TOUGH2. The default option is selected for  $\text{MOP}(24) = 0$  and applies harmonic weighting to the full multiphase effective diffusion strength (see Eq. D.7). This includes contributions from gas and aqueous phases, accounts for coupling of diffusion with phase partitioning effects, and can cope with the most general case of diffusion across a phase boundary. As an alternative, by setting  $\text{MOP}(24) = 1$ , harmonic weighting can be performed separately for the diffusive fluxes in gas and aqueous phases.

The multiphase diffusion treatment discussed here has not been implemented in T2VOC. T2VOC models only gas phase diffusion, as discussed in the report by Falta et al. (1995).

## Appendix E. TOUGH2 Input Formats

This appendix covers input data for the core modules of TOUGH2 (EOS1 - EOS5). Additional input data for the new EOS modules are discussed elsewhere in this report. Separate reports are available for T2VOC (Falta et al., 1995) and hydrodynamic dispersion (T2DM; Oldenburg and Pruess, 1993, 1995).

**TITLE** is the first record of the input file, containing a header of up to 80 characters, to be printed on output. This can be used to identify a problem. If no title is desired, leave this record blank.

**MESHM** introduces parameters for internal mesh generation and processing. The MESHMaker input has a modular structure which is organized by keywords. Detailed instructions for preparing MESHMaker input are given in Appendix F.

Record MESHM.1      Format (A5)  
                          WORD

**WORD** enter one of several keywords, such as RZ2D, RZ2DL, XYZ, MINC, to generate different kinds of computational meshes.

Record MESHM.2    A blank record closes the MESHM data block.

**ENDFI** is a keyword that can be used to close a TOUGH2 input file when no flow simulation is desired. This will often be used for a mesh generation run when some hand-editing of the mesh will be needed before the actual flow simulation.

**ROCKS** introduces material parameters for up to 27 different reservoir domains.

Record ROCKS.1  
                          Format (A5, I5, 7E10.4)  
                          MAT, NAD, DROK, POR, (PER (I), I = 1,3), CWET, SPHT

**MAT** material name (rock type).

**NAD** if zero or negative, defaults will take effect for a number of parameters (see below);

$\geq 1$ : will read another data record to override defaults.

$\geq 2$ : will read two more records with domain-specific parameters for relative permeability and capillary pressure functions.

**DROK** rock grain density ( $\text{kg}/\text{m}^3$ )

**POR** default porosity (void fraction) for all elements belonging to domain "MAT" for which no other porosity has been specified in block INCON. Option "START" is necessary for using default porosity.

PER(I),	I = 1,3 absolute permeabilities along the three principal axes, as specified by ISOT in block CONNE.
CWET	formation heat conductivity under fully liquid-saturated conditions (W/m °C).
SPHT	rock grain specific heat (J/kg °C). Domains with SPHT > 10 <sup>4</sup> J/kg °C will not be included in global material balances. This provision is useful for boundary nodes, which are given very large volumes so that their thermodynamic state remains constant. Because of the large volume, inclusion of such nodes in global material balances would make the balances useless.

Record ROCKS.1.1 (optional, NAD ≥ 1 only)

Format (7E10.4)

COM, EXPAN, CDRY, TORTX, GK, XKD3, XKD4

COM	pore compressibility ( $\text{Pa}^{-1}$ ), $(1/\phi)(\partial\phi/\partial P)_T$	(default is 0).
EXPAN	pore expansivity (1/ °C), $(1/\phi)(\partial\phi/\partial T)_P$	(default is 0).
CDRY	formation heat conductivity under desaturated conditions (W/m °C), (default is CWET).	
TORTX	tortuosity factor for binary diffusion. If TORTX = 0, a porosity and saturation-dependent tortuosity will be calculated internally from the Millington and Quirk (1961) model, Eq. (D.5).	
GK	Klinkenberg parameter b ( $\text{Pa}^{-1}$ ) for enhancing gas phase permeability according to the relationship $k_{\text{gas}} = k * (1 + b/P)$ .	
XKD3	Distribution coefficient for parent radionuclide, Component 3, in the aqueous phase, $\text{m}^3 \text{ kg}^{-1}$ (EOS7R only).	
XKD4	Distribution coefficient for daughter radionuclide, Component 4, in the aqueous phase, $\text{m}^3 \text{ kg}^{-1}$ (EOS7R only).	

Record ROCKS.1.2 (optional, NAD ≥ 2 only)

Format (I5, 5X,7E10.4)

IRP, (RP(I), I= 1,7)

IRP integer parameter to choose type of relative permeability function (see Appendix G).

RP(I), I = 1, ..., 7 parameters for relative permeability function (Appendix G).

Record ROCKS.1.3 (optional, NAD ≥ 2 only)

Format (I5, 5X,7E10.4)

ICP, (CP(I), I = 1,7)

ICP	integer parameter to choose type of capillary pressure function (see Appendix H).
CP(I)	I = 1, ..., 7 parameters for capillary pressure function (Appendix H).  Repeat records 1, 1.1, 1.2, and 1.3 for up to 27 reservoir domains.
<b>Record ROCKS.2</b>	A blank record closes the ROCKS data block.
<b>MULTI</b>	permits the user to select the number and nature of balance equations that will be solved. The keyword MULTI is followed by a single data record. For most EOS modules this data block is not needed, as default values are provided internally. Available parameter choices are different for different EOS modules (see Section 6).
<b>Record MULTI.1</b>	Format (5I5) NK, NEQ, NPH, NB, NKIN
NK	number of mass components.
NEQ	number of balance equations per grid block. Usually we have NEQ = NK + 1, for solving NK mass and one energy balance equation. Some EOS modules allow the option NEQ = NK, in which case only NK mass balances and no energy equation will be solved.
NPH	number of phases that can be present (2 for most EOS modules).
NB	number of secondary parameters in the PAR-array (see Fig. 3) other than component mass fractions. Available options include NB = 6 (no diffusion) and NB = 8 (include diffusion).
NKIN	number of mass components in INCON data (default is NKIN = NK). This parameter can be used, for example, to initialize an EOS7R simulation (NK = 4 or 5) from data generated by EOS7 (NK = 2 or 3). If a value other than the default is to be used, then data block MULTI must appear before any initial conditions in data blocks PARAM, INDOM, or INCON.
<b>START</b>	(optional) A record with START typed in columns 1-5 allows a more flexible initialization. More specifically, when START is present, INCON data can be in arbitrary order, and need not be present for all grid blocks (in which case defaults will be used). Without START, there must be a one-to-one correspondence between the data in blocks ELEME and INCON.
<b>PARAM</b>	introduces computation parameters, time stepping information, and default initial conditions.

**Record PARAM.1**

Format (2I2, 3I4, 24I1, 10X, 2E10.4).  
NOITE, KDATA, MCYC, MSEC, MCYPR, (MOP(I), I = 1, 24), TEXP, BE

NOITE	specifies the maximum number of Newtonian iterations per time step (default is 8)
KDATA	<p>specifies amount of printout (default is 1).</p> <p>0 or 1: print a selection of the most important variables.</p> <p>2: in addition, print mass and heat fluxes and flow velocities.</p> <p>3: in addition, print primary variables and their changes.</p> <p>If the above values for KDATA are increased by 10, printout will occur after each Newton-Raphson iteration (not just after convergence).</p>
MCYC	maximum number of time steps to be calculated.
MSEC	maximum duration, in CPU seconds, of the simulation (default is infinite).
MCYPR	printout will occur for every multiple of MCYPR steps (default is 1).
MOP(I), I = 1,24	allows choice of various options, which are documented in printed output from a TOUGH2 run.
MOP(1)	<p>if unequal 0, a short printout for non-convergent iterations will be generated.</p> <p>MOP(2) through MOP(6) generate additional printout in various subroutines, if set unequal 0. This feature should not be needed in normal applications, but it will be convenient when a user suspects a bug and wishes to examine the inner workings of the code. The amount of printout increases with MOP(I) (consult source code listings for details).</p>
MOP(2)	CYCIT (main subroutine).
MOP(3)	MULTI (flow- and accumulation-terms).
MOP(4)	QU (sinks/sources).
MOP(5)	EOS (equation of state).
MOP(6)	LINEQ (linear equations).
MOP(7)	<p>if unequal 0, a printout of input data will be provided.</p> <p>Calculational choices are as follows:</p>
MOP(9)	<p>determines the composition of produced fluid with the MASS option (see GENER, below). The relative amounts of phases are determined as follows:</p> <p>0: according to relative mobilities in the source element.</p>

- 1: produced source fluid has the same phase composition as the producing element.
- MOP(10) chooses the interpolation formula for heat conductivity as a function of liquid saturation ( $S_l$ )
- 0:  $C(S_l) = CDRY + SQRT(S_l) * [CWET - CDRY]$
- 1:  $C(S_l) = CDRY + S_l * (CWET - CDRY)$
- MOP(11) determines evaluation of mobility and permeability at interfaces.
- 0: mobilities are upstream weighted with WUP (see PARAM.3), permeability is upstream weighted.
- 1: mobilities are averaged between adjacent elements, permeability is upstream weighted.
- 2: mobilities are upstream weighted, permeability is harmonic weighted.
- 3: mobilities are averaged between adjacent elements, permeability is harmonic weighted.
- 4: mobility and permeability are both harmonic weighted.
- MOP(12) determines interpolation procedure for time dependent sink/source data (flow rates and enthalpies).
- 0: triple linear interpolation; tabular data are used to obtain interpolated rates and enthalpies for the beginning and end of the time step; the average of these values is then used.
- 1: step function option; rates and enthalpies are taken as averages of the table values corresponding to the beginning and end of the time step.
- 2: rigorous step rate capability for time dependent generation data.

A set of times  $t_i$  and generation rates  $q_i$  provided in data block GENER is interpreted to mean that sink/source rates are piecewise constant and change in discontinuous fashion at table points. Specifically, generation is assumed to occur at constant rate  $q_i$  during the time interval  $[t_i, t_{i+1})$ , and changes to  $q_{i+1}$  at  $t_{i+1}$ . Actual rate used during a time step that ends at time  $t$ , with  $t_i \leq t \leq t_{i+1}$ , is automatically adjusted in such a way that total cumulative exchanged mass at time  $t$

$$Q(t) = \int_0^t q dt' = \sum_{j=1}^{i-1} q_j (t_{j+1} - t_j) + q_i (t - t_i) \quad (\text{E.1})$$

is rigorously conserved. If also tabular data for enthalpies are given, an analogous adjustment is made for fluid enthalpy, to preserve  $\int qhdt$ .

- MOP(13) used by dispersion module T2DM.
- MOP(14) (void)
- MOP(15) determines conductive heat exchange with impermeable confining layers (see section 7.4).
  - 0: heat exchange is off.
  - 1: heat exchange is on (for grid blocks that have a non-zero heat transfer area; see data block ELEME).
- MOP(16) provides automatic time step control. Time step size will be doubled if convergence occurs within  $ITER \leq MOP(16)$  Newton-Raphson iterations. It is recommended to set MOP(16) in the range of 2 - 4.
- MOP(17) (void)
- MOP(18) selects handling of interface density.
  - 0: perform upstream weighting for interface density.
  - >0: average interface density between the two grid blocks. However, when one of the two phase saturations is zero, upstream weighting will be performed.
- MOP(19) switch used by different EOS modules for conversion of primary variables; see EOS description, section 6.
- MOP(20) switch for vapor pressure lowering in EOS4; see Table 10.
- MOP(21) selects the linear equation solver (see section 7.6).
  - 0: defaults to  $MOP(21) = 3$ , DSLUCS, Lanczos-type preconditioned bi-conjugate gradient solver.
  - 1: (void)
  - 2: DSLUBC, bi-conjugate gradient solver.
  - 3: DSLUCS (default).
  - 4: DSLUGM, generalized minimum residual preconditioned conjugate gradient solver.
  - 5: DLUSTB, stabilized bi-conjugate gradient solver.
  - 6: LUBAND, banded direct solver.

All conjugate gradient solvers use incomplete LU-factorization as a default preconditioner. Other preconditioners may be chosen by means of a data block SOLVR (see section 7.6).

MOP(22)	used by dispersion module T2DM.
MOP(23)	used by dispersion module T2DM.
MOP(24)	determines handling of multiphase diffusive fluxes at interfaces. 0: harmonic weighting of fully coupled effective multiphase diffusivity. 1: separate harmonic weighting of gas and liquid phase diffusivities.
TEXP	parameter for temperature dependence of gas phase diffusion coefficient (see Eq. D.8).
BE	(optional) parameter for effective strength of enhanced vapor diffusion; if set to a non-zero value, will replace the parameter group $\phi\tau_0\tau_\beta$ for vapor diffusion (see Eq. D.3 and section D.4).

<u>Record PARAM.2</u>	Format (4E10.4, A5, 5X,3E10.4) TSTART, TIMAX, DELTEN, DELTMX, ELST, GF, REDLT, SCALE
TSTART	starting time of simulation in seconds (default is 0).
TIMAX	time in seconds at which simulation should stop (default is infinite).
DELTEN	length of time steps in seconds. If DELTEN is a negative integer, DELTEN = -NDLT, the program will proceed to read NDLT records with time step information. Note that - NDLT must be provided as a floating point number, with decimal point.
DELMX	upper limit for time step size in seconds (default is infinite)
ELST	set equal to the name of one element to obtain a short printout after each time step.
GF	magnitude (m/sec <sup>2</sup> ) of the gravitational acceleration vector. Blank or zero gives "no gravity" calculation.
REDLT	factor by which time step is reduced in case of convergence failure or other problems (default is 4).
SCALE	scale factor to change the size of the mesh (default = 1.0).

<u>Record PARAM.2.1, 2.2, etc.</u>	
	Format (8E10.4)

(DLT(I), I = 1, 100)

DLT(I) Length (in seconds) of time step I.

This set of records is optional for DELTEN = - NDLT, a negative integer. Up to 13 records can be read, each containing 8 time step data. If the number of simulated time steps exceeds the number of DLT(I), the simulation will continue with time steps equal to the last non-zero DLT(I) encountered. When automatic time step control is chosen (MOP(16) > 0), time steps following the last DLT(I) input by the user will increase according to the convergence rate of the Newton-Raphson iteration. Automatic time step reduction will occur if the maximum number of Newton-Raphson iterations is exceeded (parameter NOITE, record PARAM.1)

<u>Record PARAM.3</u>	Format (6E10.4) RE1, RE2, U, WUP, WNR, DFAC
RE1	convergence criterion for relative error, see Appendix B (default= $10^{-5}$ ).
RE2	convergence criterion for absolute error, see Appendix B (default= 1).
U	(void).
WUP	upstream weighting factor for mobilities and enthalpies at interfaces (default = 1.0 is recommended). $0 \leq WUP \leq 1$ .
WNR	weighting factor for increments in Newton/Raphson - iteration (default = 1.0 is recommended). $0 < WNR \leq 1$ .
DFAC	increment factor for numerically computing derivatives (default value is $DFAC = 10^{-k/2}$ , where k, evaluated internally, is the number of significant digits of the floating point processor used; for 64-bit arithmetic, $DFAC \approx 10^{-8}$ ).

Record PARAM.4 introduces a set of primary variables which are used as default initial conditions for all grid blocks that are not assigned by means of data blocks INDOM or INCON. Option START is necessary to use default INCON.

Format (4E20.13)  
DEP(I), I = 1, NKIN+1

The number of primary variables, NKIN+1, is normally assigned internally in the EOS module, and is usually equal to the number NEQ of equations solved per grid block. See data block MULTI for special assignments of NKIN. When more than four primary variables are used more than one line (record) must be provided

Different sets of primary variables are in use for different EOS modules; see the description of EOS modules, section 6.

**INDOM** introduces domain-specific initial conditions. These will supersede default initial conditions specified in PARAM.4, and can be overwritten by element-specific initial conditions in data block INCON. Option START is needed to use INDOM conditions.

Record INDOM.1 Format (A5)  
MAT

MAT name of a reservoir domain, as specified in data block ROCKS.

Record INDOM.2 Format (4E20.13)  
X1, X2, X3, ...

A set of primary variables assigned to all grid blocks in the domain specified in record INDOM.1. Different sets of primary variables are used for different EOS modules; see the description of EOS modules in section 6.

Record INDOM.3

A blank record closes the INDOM data block. Repeat records INDOM.1 and INDOM.2 for as many domains as desired. The ordering is arbitrary and need not be the same as in block ROCKS.

**INCON** introduces element-specific initial conditions.

Record INCON.1 Format (A3, I2, 2I5, E15.9)  
EL, NE, NSEQ, NADD, PORX

EL, NE code name of element.

NSEQ number of additional elements with the same initial conditions.

NADD increment between the code numbers of two successive elements with identical initial conditions.

PORX porosity; if zero or blank, porosity will be taken as specified in block ROCKS if option START is used.

Record INCON.2 specifies primary variables.

Format (4E20.14)  
X1, X2, X3, ...

A set of primary variables for the element specified in record INCON.1. INCON specifications will supersede default conditions specified in PARAM.4, and domain-specific conditions that may have been specified in data block INDOM. Different sets of primary variables are used for different EOS modules; see the description of EOS modules, section 6.

**Record INCON.3** A blank record closes the INCON data block. Alternatively, initial condition information may terminate on a record with ‘+++’ typed in the first three columns, followed by time stepping information. This feature is used for a continuation run from a previous TOUGH2 simulation.

**SOLVR** (optional) introduces a data block with parameters for linear equation solvers.

**Record SOLVR.1** Format (I1,2X,A2,3X,A2,2E10.4)  
MATSLV, ZPROCS, OPROCS, RITMAX, CLOSUR

The SOLVR parameter choices are explained in section 7.6.

**FOFT** (optional) introduces a list of elements (grid blocks) for which time-dependent data are to be written out for plotting to a file called FOFT during the simulation.

**Record FOFT.1** Format (A5)  
EOFT(I)

EOFT is an element name. Repeat for up to 100 elements, one per record.

**Record FOFT.2** A blank record closes the FOFT data block.

**COFT** (optional) introduces a list of connections for which time-dependent data are to be written out for plotting to a file called COFT during the simulation.

**Record COFT.1** Format (A10)  
ECOFT(I)

ECOFT is a connection name, i.e., an ordered pair of two element names. Repeat for up to 100 connections, one per record.

**Record COFT.2** A blank record closes the COFT data block.

**GOFT** (optional) introduces a list of sinks/sources for which time-dependent data are to be written out for plotting to a file called GOFT during the simulation.

**Record GOFT.1** Format (A5)  
EGOFT(I)

EGOFT is the name of an element in which a sink/source is defined. Repeat for up to 100 sinks/sources, one per record. When no sinks or sources are specified here, by default tabulation will be made for all.

**Record GOFT.2** A blank record closes the GOFT data block.

**NOVERSION** (optional) One record with NOVER typed in columns 1-5 will suppress printing of a summary of versions and dates of the program units used in a TOUGH2 run.

**DIFFUSION** (optional; needed only for NB  $\geq$  8) introduces diffusion coefficients.

Record DIFFU.1

Format (8E10.4)

FDDIAG(I,1), I=1,NPH

diffusion coefficients for mass component # 1 in all phases (I=1: gas; I=2: aqueous; etc.)

Record DIFFU.2

Format (8E10.4)

FDDIAG(I,2), I=1,NPH

diffusion coefficients for mass component # 2 in all phases (I=1: gas; I=2: aqueous; etc.)

provide a total of NK records with diffusion coefficients for all NK mass components. See Appendix D for additional parameter specifications for diffusion.

**SELECTION** (optional) introduces a number of integer and floating point parameters that are used for different purposes in different TOUGH2 modules (EOS7, EOS7R, EWASG, T2DM).

Record SELEC.1

Format (16I5)

IE(I), I=1,16

IE(1) number of records with floating point numbers that will be read (default is IE(1) = 1; maximum values is 64).

Record SELEC.2, SELEC.3, ..., SELEC.IE(1)\*8

Format (8E10.4)

FE(I), I=1,IE(1)\*8

provide as many records with floating point numbers as specified in IE(1), up to a maximum of 64 records.

**RPCAP**

introduces information on relative permeability and capillary pressure functions, which will be applied for all flow domains for which no data were specified in records ROCKS.1.2 and ROCKS.1.3. A catalog of relative permeability and capillary pressure functions is presented in Appendix G and Appendix H, respectively.

Record RPCAP.1

Format (I5,5X,7E10.4)

IRP, (RP(I), I = 1, 7)

IRP

integer parameter to choose type of relative permeability function

(see Appendix G).

RP(I), I = 1, ..., 7 parameters for relative permeability function (Appendix G).

**Record RPCAP.2** Format (I5,5X,7E10.4)  
ICP, (CP(I), I = 1, 7)

**ICP** integer parameter to choose type of capillary pressure function  
(see Appendix H).

**CP(I)** I = 1, ..., 7 parameters for capillary pressure function (Appendix H).

**TIMES** permits the user to obtain printout at specified times (optional). This  
printout will occur in addition to printout specified in record PARAM.1.

**Record TIMES.1** Format (2I5,2E10.4)  
ITI, ITE, DELAF, TINTER

**ITI** number of times provided on records TIMES.2, TIMES.3, etc.,  
(see below; restriction: ITI ≤ 100).

**ITE** total number of times desired (ITI ≤ ITE ≤ 100; default is ITE = ITI).

**DELAF** maximum time step size after any of the prescribed times have been reached  
(default is infinite ).

**TINTER** time increment for times with index ITI, ITI+1, ..., ITE.

**Record TIMES.2, TIMES.3, etc.**

Format (8E10.4)  
(TIS(I), I = 1, ITI)

**TIS(I)** list of times (in ascending order) at which printout is desired.

**ELEME** introduces element (grid block) information.

**Record ELEME.1**

Format (A3, I2, 2I5, A3, A2, 6E10.4)  
EL, NE, NSEQ, NADD, MA1, MA2, VOLX, AHTX, PMX, X, Y, Z

**EL, NE** five-character code name of an element. The first three characters are  
arbitrary, the last two characters must be numbers.

**NSEQ** number of additional elements having the same volume and belonging to  
the same reservoir domain.

**NADD** increment between the code numbers of two successive elements. (Note: the  
maximum permissible code number NE + NSEQ \*NADD is ≤ 99.)

MA1, MA2	a five-character material identifier corresponding to one of the reservoir domains as specified in block ROCKS. If the first three characters are blanks and the last two characters are numbers then they indicate the sequence number of the domain as entered in ROCKS. If both MA1 and MA2 are left blank the element is by default assigned to the first domain in block ROCKS.
VOLX	element volume ( $\text{m}^3$ ).
AHTX	interface area ( $\text{m}^2$ ) for heat exchange with semi-infinite confining beds. Internal MESH generation via MESHMaker will automatically assign AHTX.
PMX	permeability modifier (optional, active only when a domain ‘SEED’ has been specified in the ROCKS block; see section 7.5). Will be used as multiplicative factor for the permeability parameters from block ROCKS. Simultaneously, strength of capillary pressure will be scaled as $1/\text{SQRT(PMX)}$ . PMX = 0 will result in an impermeable block.  Random permeability modifiers can be generated internally, see detailed comments in the TOUGH2 output file. The PMX may be used to specify spatially correlated heterogeneous fields, but users need their own preprocessing programs for this, as TOUGH2 provides no internal capabilities for generating such fields.
X, Y, Z	Cartesian coordinates of grid block centers. These may be included in the ELEME data to make subsequent plotting of results more convenient. Generally speaking, the coordinate data are not used in TOUGH2; the single exception is for optional initialization of a gravity-capillary equilibrium with EOS9 (see sections 6.9 and 9.10).  Repeat record ELEME.1 for the number of elements desired.

Record ELEME.2    A blank record closes the ELEME data block.

**CONNE**    introduces information for the connections (interfaces) between elements.

Record CONNE.1

Format (A3, I2, A3, I2, 4I5, 5E10.4)  
EL1, NE1, EL2, NE2, NSEQ, NAD1, NAD2, ISOT, D1, D2, AREAX,  
BETAX, SIGX

EL1, NE1    code name of the first element.

EL2, NE2    code name of the second element.

NSEQ        number of additional connections in the sequence.  
NAD1        increment of the code number of the first element between two successive connections.

NAD2	increment of the code number of the second element between two successive connections.
ISOT	set equal to 1, 2, or 3; specifies absolute permeability to be PER(ISOT) for the materials in elements (EL1, NE1) and (EL2, NE2), where PER is read in block ROCKS. This allows assignment of different permeabilities, e.g., in the horizontal and vertical direction.
D1      }	distance (m) from first and second element, respectively, to their common interface.
D2      }	
AREAX	interface area ( $\text{m}^2$ ).
BETAX	cosine of the angle between the gravitational acceleration vector and the line between the two elements. GF * BETAX > 0 (<0) corresponds to first element being above (below) the second element.
SIGX	“radiant emittance” factor for radiative heat transfer, which for a perfectly “black” body is equal to 1. The rate of radiative heat transfer between the two grid blocks is

$$G_{\text{rad}} = \text{SIGX} * \sigma_0 * \text{AREAX} * (T_2^4 - T_1^4) \quad (\text{E.2})$$

where  $\sigma_0 = 5.6687 \times 10^{-8} \text{ J/m}^2 \text{ K}^4 \text{ s}$  is the Stefan-Boltzmann constant, and  $T_1$  and  $T_2$  are the absolute temperatures of the two grid blocks. SIGX may be entered as a negative number, in which case the absolute value will be used, and heat conduction at the connection will be suppressed. SIGX = 0 will result in no radiative heat transfer.

Repeat record CONNE.1 for the number of connections desired.

**Record CONNE.2** A blank record closes the CONNE data block. Alternatively, connection information may terminate on a record with ‘+++’ typed in the first three columns, followed by element cross-referencing information. This is the termination used when generating a MESH file with TOUGH2.

**GENER** introduces sinks and/or sources.

**Record GENER.1**

Format (A3, I2, A3, I2, 4I5, 5X, A4, A1, 3E10.4)  
 EL, NE, SL, NS, NSEQ, NADD, NADS, LTAB, TYPE, ITAB, GX, EX, HX

EL, NE code name of the element containing the sink/source.

SL, NS code name of the sink/source. The first three characters are arbitrary, the last two characters must be numbers.

NSEQ	number of additional sinks/sources with the same injection/production rate (not applicable for TYPE = DELV).
NADD	increment between the code numbers of two successive elements with identical sink/source.
NADS	increment between the code numbers of two successive sinks/sources.
LTAB	number of points in table of generation rate versus time. Set 0 or 1 for constant generation rate. For wells on deliverability, LTAB denotes the number of open layers, to be specified only for the bottommost layer.
TYPE	specifies different options for fluid or heat production and injection. For example, different fluid components may be injected, the nature of which depends on the EOS module being used. Different options for considering wellbore flow effects may also be specified.
HEAT	introduces a heat sink/source.
COM1	- component 1 (water).
WATE	
COM2	- component 2
COM3	- component 3
...	
COMn	- component n
MASS	- mass production rate specified.
DELV	- well on deliverability, i.e., production occurs against specified bottomhole pressure. If well is completed in more than one layer, bottommost layer must be specified first, with number of layers given in LTAB. Subsequent layers must be given sequentially for a total number of LTAB layers.
F---	- well on deliverability against specified wellhead pressure. By convention, when the first letter of a type specification is F or f, TOUGH2 will perform flowing wellbore pressure corrections using tabular data of flowing bottomhole pressure vs. flow rate and flowing enthalpy. The tabular data used for flowing wellbore correction must be generated by means of a wellbore simulator ahead of a TOUGH2 run according to certain format specifications (see Table 17, section 7.3). The data must be provided by means of a disk file, whose name consists of the four characters of the TYPE specification, and the one character of the following ITAB

parameter. For example, to use wellbore pressure data in a disk file called f120a, specify TYPE as ‘f120’, and specify ITAB as ‘a’. Different wellbore tables, representing e.g. wells with different diameter, feed zone depth, and flowing wellhead pressure, may be used simultaneously in a TOUGH2 simulation. Also, several wells completed in different grid blocks may reference the same wellbore table.

The capability for flowing wellbore pressure correction is presently only available for wells with a single feed zone.

ITAB	unless left blank, table of specific enthalpies will be read (LTAB > 1 only). When time-dependent injection is used, ITAB must be specified non-blank, and specific enthalpy data must be given.
GX	constant generation rate; positive for injection, negative for production; GX is mass rate (kg/sec) for generation types COM1, COM2, COM3, etc., and MASS; it is energy rate (J/s) for a HEAT sink/source. For wells on deliverability, GX is productivity index PI ( $\text{m}^3$ ), Eq. (29).
EX	fixed specific enthalpy (J/kg) of the fluid for mass injection (GX>0). For wells on deliverability against fixed bottomhole pressure, EX is bottomhole pressure $P_{\text{wb}}$ (Pa), at the center of the topmost producing layer in which the well is open.
HG	thickness of layer (m; wells on deliverability with specified bottomhole pressure only).

Record GENER.1.1 (optional, LTAB > 1 only)

Format (4E14.7)  
F1(L), L=1, LTAB

F1 generation times

Record GENER.1.2 (optional, LTAB > 1 only)

Format (4E14.7)  
F2(L), L=1, LTAB

F2 generation rates.

Record GENER.1.3 (optional, LTAB > 1 and ITAB non-blank only; this data must be provided for injection at time-dependent rates)

Format (4E14.7)  
F3(L), L=1, LTAB

F3 specific enthalpy of produced or injected fluid.  
Repeat records GENER.1, 1.1, 1.2, and 1.3 for the number of sinks/sources desired.

Record GENER.2 A blank record closes the GENER data block.

Alternatively, generation information may terminate on a record with ‘+++’ typed in the first three columns, followed by element cross-referencing information.

**ENDCY**      closes the TOUGH2 input file and initiates the simulation.

#### **Note on closure of blocks CONNE, GENER, and INCON**

The ordinary way to indicate the end of any of the above data blocks is by means of a blank record. There is an alternative available if the user makes up an input file from files MESH, GENER, or SAVE, which have been generated by a previous TOUGH2 run. These files are written exactly according to the specifications of data blocks ELEME and CONNE (file MESH), GENER (file GENER), and INCON (file SAVE), except that the CONNE, GENER, and INCON data terminate on a record with "+++" in columns 1-3, followed by some cross-referencing and restart information. TOUGH2 will accept this type of input, and in this case there is no blank record at the end of the indicated data blocks.

## Appendix F. Input Formats for MESHMAKER

The MESHMaker module performs internal mesh generation and processing. The input for MESHMaker has a modular structure and a variable number of records; it begins with keyword MESHM and ends with a blank record (see Fig. 64).

At the present time there are three sub-modules available in MESHMaker: keywords RZ2D or RZ2DL invoke generation of a one or two-dimensional radially symmetric R-Z mesh; XYZ initiates generation of a one, two, or three dimensional Cartesian X-Y-Z mesh; and MINC calls a modified version of the GMINC program (Pruess, 1983) to sub-partition a primary porous medium mesh into a secondary mesh for fractured media, using the method of “multiple interacting continua” (Pruess and Narasimhan, 1982, 1985). The meshes generated under keyword RZ2D or XYZ are internally written to file MESH. The MINC processing operates on the data in file MESH, so that invoking the RZ2D or XYZ options, or assignment of ELEME and CONNE blocks in the INPUT file must precede the MESHMaker/MINC data. We shall now separately describe the preparation of input data for the three MESHMaker sub-modules.

### *Generation of radially symmetric grids*

Keyword RZ2D (or RZ2DL) invokes generation of a radially symmetric mesh. Values for the radii to which the grid blocks extend can be provided by the user or can be generated internally (see below). Nodal points will be placed half-way between neighboring radial interfaces. When RZ2D is specified, the mesh will be generated by columns; i.e., in the ELEME block we will first have the grid blocks at smallest radius for all layers, then the next largest radius for all layers, and so on. With keyword RZ2DL the mesh will be generated by layers; i.e., in the ELEME block we will first have all grid blocks for the first (top) layer from smallest to largest radius, then all grid blocks for the second layer, and so on. Apart from the different ordering of elements, the two meshes for RZ2D and RZ2DL are identical. The reason for providing the two alternatives is as a convenience to users in implementing boundary conditions by way of inactive elements (see Section 6.4). Assignment of inactive elements would be made by using a text editor on the RZ2D-generated MESH file, and moving groups of elements towards the end of the ELEME block, past a dummy element with zero volume. RZ2D makes it easy to declare a vertical column inactive, facilitating assignment of boundary conditions in the vertical, such as a gravitationally equilibrated pressure gradient. RZ2DL on the other hand facilitates implementation of areal (top and bottom layer) boundary conditions.

MESHMAKER - Two-dimensional R-Z Grids							
	1	2	3	4	5	6	7
MESHMAKER							
RZ2D1							
RAD111							
NRAD							
RC(1)	RC(2)	RC(3)				RC(NRAD)	
EQU1D							
HQU		DR					
LLOG1R							
NLOG		RLOG	DR				
LAYER							
NLAY	H(1)	H(2)	H(3)			H(NLAY)	

MESHMAKER-Rectilinear Grids							
	1	2	3	4	5	6	7
MESHMAKER							
XIYZ1	DEG						
N1X1	<input type="checkbox"/> N01	DEL					
DX(1)		DX(2)	DX(3)			DX(N01)	
N2X1		N02	DEL				
DX(N01+1)		DX(N01+2)					DX(N01+N02)
N1Y1	<input type="checkbox"/> N0	DEL					
DY(1)		DY(2)	DY(3)			DY(N0)	
N2Y1		N0	DEL				
DZ(1)		DZ(2)	DZ(3)			DZ(N0)	

MESHMAKER - MINC Processing for Fractured Media							
	1	2	3	4	5	6	7
MESHMAKER							
MINC1	TYPE	<input type="checkbox"/> DUAL					
PAR1	J	NUOLHERE	PAR(1)	PAR(2)	PAR(3)	PAR(4)	PAR(5)
							PAR(6) PAR(7)
		VOL(1)	VOL(2)	VOL(3)			
						VOL(NVOL)	

Figure 64. MESHMaker input formats.

**RADII** is the first keyword following RZ2D; it introduces data for defining a set of interfaces (grid block boundaries) in the radial direction.

Record RADII.1 Format (I5)  
NRAD

NRAD number of radius data that will be read. At least one radius must be provided, indicating the inner boundary of the mesh.

Record RADII.2, RADII.3, etc.

Format (8E10.4)  
RC(I), I = 1, NRAD

RC(I) a set of radii in ascending order.

**EQUIDistant** introduces data on a set of equal radial increments.

Record EQUID.1 Format (I5, 5X, E10.4)  
NEQU, DR

NEQU number of desired radial increments.  
DR magnitude of radial increment.

Note: At least one radius must have been defined via block RADII before EQUID can be invoked.

**LOGARithmic** introduces data on radial increments that increase from one to the next by the same factor ( $\Delta R_{n+1} = f \cdot \Delta R_n$ ).

Record LOGAR.1 Format (I5, 5X, 2E10.4)  
NLOG, RLOG, DR

NLOG number of additional interface radii desired.  
RLOG desired radius of the last (largest) of these radii.  
DR reference radial increment: the first  $\Delta R$  generated will be equal to  $f \cdot DR$ , with  $f$  internally determined such that the last increment will bring total radius to RLOG.  $f < 1$  for decreasing radial increments is permissible. If DR is set equal to zero, or left blank, the last increment DR generated before keyword LOGAR will be used as default.

Additional blocks RADII, EQUID, and LOGAR can be specified in arbitrary order.

Note: At least one radius must have been defined before LOGAR can be invoked. If DR = 0, at least two radii must have been defined.

**LAYER** introduces information on horizontal layers, and signals closure of RZ2D input data.

Record LAYER.1 Format (I5)  
NLAY

NLAY number of horizontal grid layers.

Record LAYER.2 Format (8E10.4)  
H(I), I = 1, NLAY

H(I) a set of layer thicknesses, from top layer downward. By default, zero or blank entries for layer thickness will result in assignment of the last preceding non-zero entry. Assignment of a zero layer thickness, as needed for inactive layers, can be accomplished by specifying a negative value.

The LAYER data close the RZ2D data block. Note that one blank record must follow to indicate termination of the MESHM data block. Alternatively, keyword MINC can appear to invoke MINC-processing for fractured media (see below).

### *Generation of rectilinear grids*

**XYZ** invokes generation of a Cartesian (rectilinear) mesh.

Record XYZ.1 Format (E10.4)  
DEG

DEG angle (in degrees) between the Y-axis and the horizontal. If gravitational acceleration (parameter GF in record PARAM.2) is specified positive,  $-90^\circ < \text{DEG} < 90^\circ$  corresponds to grid layers going from top down. Grids can be specified from bottom layer up by setting GF or BETA negative. Default (DEG = 0) corresponds to horizontal Y- and vertical Z-axis. X-axis is always horizontal.

Record XYZ.2 Format (A2, 3X, I5, E10.4)  
NTYPE, NO, DEL

NTYPE set equal to NX, NY or NZ for specifying grid increments in X, Y, or Z direction.

NO number of grid increments desired.

DEL constant grid increment for NO grid blocks, if set to a non zero value.

Record XYZ.3 (optional, DEL = 0. or blank only)

Format (8E10.4)  
DEL(I), I = 1, NO

DEL(I) a set of grid increments in the direction specified by NTYPE in record XYZ.2. Additional records with formats as XYZ.2 and XYZ.3 can be provided, with X, Y, and Z-data in arbitrary order.

Record XYZ.4 a blank record closes the XYZ data block.

Note that the end of block MESHMaker is also marked by a blank record. Thus, when MESHMaker/XYZ is used, there will be two blank records at the end of the corresponding input data block.

### *MINC processing for fractured media*

**MINC** invokes postprocessing of a primary porous medium mesh from file MESH. The input formats in data block MINC are identical to those of the GMINC program (Pruess, 1983), with two enhancements: there is an additional facility for specifying global matrix-matrix connections (“dual permeability”); further, only active elements will be subjected to MINC-processing, the remainder of the MESH remaining unaltered as porous medium grid blocks. See Appendix C for further discussion.

**PART** is the first keyword following MINC; it will be followed on the same line by parameters TYPE and DUAL with information on the nature of fracture distributions and matrix-matrix connections.

Format (2A5, 5X, A5)  
PART, TYPE, DUAL

PART identifier of data block with partitioning parameters for secondary mesh.

TYPE a five-character word for selecting one of the six different proximity functions provided in MINC (Pruess, 1983).

ONE-D: a set of plane parallel infinite fractures with matrix block thickness between neighboring fractures equal to PAR(1).

TWO-D: two sets of plane parallel infinite fractures, with arbitrary angle between them. Matrix block thickness is PAR(1) for the first set, and PAR(2) for the second set. If PAR(2) is not specified explicitly, it will be set equal to PAR(1).

THRED: three sets of plane parallel infinite fractures at right angles, with matrix block dimensions of PAR(1), PAR(2), and

PAR(3), respectively. If PAR(2) and/or PAR(3) are not explicitly specified, they will be set equal to PAR(1) and/or PAR(2), respectively.

- STANA: average proximity function for rock loading of Stanford large reservoir model (Lam et al., 1988).
- STANB: proximity function for the five bottom layers of Stanford large reservoir model.
- STANT: proximity function for top layer of Stanford large reservoir model.

Note: a user wishing to employ a different proximity function than provided in MINC needs to replace the function subprogram PROX(x) in file meshm.f with a routine of the form:

```
FUNCTION PROX(x)
PROX = (arithmetic expression in x)
RETURN
END
```

It is necessary that PROX(x) is defined even when  $x$  exceeds the maximum possible distance from the fractures, and that PROX = 1 in this case. Also, when the user supplies his/her own proximity function subprogram, the parameter TYPE has to be chosen equal to ONE-D, TWO-D, or THRED, depending on the dimensionality of the proximity function. This will assure proper definition of innermost nodal distance (Pruess, 1983).

DUAL is a five-character word for selecting the treatment of global matrix matrix flow.

blank: (default) global flow occurs only through the fracture continuum, while rock matrix and fractures interact locally by means of interporosity flow (“double-porosity” model).

MMVER: global matrix-matrix flow is permitted only in the vertical; otherwise like the double-porosity model; for internal consistency this choice should only be made for flow systems with one or two predominantly vertical fracture sets.

MMALL: global matrix-matrix flow in all directions; for internal consistency only two continua, representing matrix and fractures, should be specified (“dual-permeability”).

Record PART.1 Format (2I3, A4, 7E10.4)  
J, NVOL, WHERE, (PAR(I), I = 1, 7)

J	total number of multiple interacting continua (J < 36).
NVOL	total number of explicitly provided volume fractions (NVOL < J). If NVOL < J, the volume fractions with indices NVOL+1, ..., J will be internally generated; all being equal and chosen such as to yield proper normalization to 1.
WHERE	specifies whether the sequentially specified volume fractions begin with the fractures (WHERE = 'OUT ') or in the interior of the matrix blocks (WHERE = 'IN ').
PAR(I), I = 1, 7	holds parameters for fracture spacing (see above).
<u>Record PART.2.1, 2.2, etc.</u>	Format (8E10.4) (VOL(I), I = 1, NVOL)
VOL(I)	volume fraction (between 0 and 1) of continuum with index I (for WHERE = 'OUT ') or index $J + l - I$ (for WHERE = 'IN '). NVOL volume fractions will be read. For WHERE = 'OUT ', I = 1 is the fracture continuum, I = 2 is the matrix continuum closest to the fractures, I = 3 is the matrix continuum adjacent to I = 2, etc. The sum of all volume fractions must not exceed 1.

## Appendix G. Relative Permeability Functions

IRP = 1      **linear functions**

$k_{rl}$  increases linearly from 0 to 1 in the range

$$RP(1) \leq S_l \leq RP(3);$$

$k_{rg}$  increases linearly from 0 to 1 in the range

$$RP(2) \leq S_g \leq RP(4)$$

Restrictions:  $RP(3) > RP(1)$ ;  $RP(4) > RP(2)$ .

IRP = 2       $k_{rl} = S_l^{**} RP(1)$

$$k_{rg} = 1.$$

IRP = 3      **Corey's curves** (1954)

$$k_{rl} = \hat{S}^4$$

$$k_{rg} = (1 - \hat{S})^2 (1 - \hat{S}^2)$$

where  $\hat{S} = (S_l - S_{lr}) / (1 - S_{lr} - S_{gr})$

with  $S_{lr} = RP(1)$ ;  $S_{gr} = RP(2)$

Restrictions:  $RP(1) + RP(2) < 1$

IRP = 4      **Grant's curves** (Grant, 1977)

$$k_{rl} = \hat{S}^4$$

$$k_{rg} = 1 - k_{rl}$$

where  $\hat{S} = (S_l - S_{lr}) / (1 - S_{lr} - S_{gr})$

with  $S_{lr} = RP(1)$ ;  $S_{gr} = RP(2)$

Restrictions:  $RP(1) + RP(2) < 1$

IRP = 5      **all phases perfectly mobile**

$k_{rg} = k_{rl} = 1$  for all saturations; no parameters

IRP = 6

### functions of Fatt and Klikoff (1959)

$$k_{rl} = (S^*)^3$$

$$k_{rg} = (1 - S^*)^3$$

where  $S^* = (S_l - S_{lr}) / (1 - S_{lr})$

with  $S_{lr} = RP(1)$ .

Restriction:  $RP(1) < 1$ .

IRP = 7

### van Genuchten-Mualem model (Mualem, 1976; van Genuchten, 1980)

$$k_{rl} = \begin{cases} \sqrt{S^*} \left\{ 1 - (1 - [S^*]^{1/\lambda})^\lambda \right\}^2 & \text{if } S_l < S_{ls} \\ 1 & \text{if } S_l \geq S_{ls} \end{cases}$$

Gas relative permeability can be chosen as one of the following two forms, the second of which is due to Corey (1954)

$$k_{rg} = \begin{cases} 1 - k_{rl} & \text{if } S_{gr} = 0 \\ (1 - \hat{S})^2 (1 - \hat{S}^2) & \text{if } S_{gr} > 0 \end{cases}$$

subject to the restriction  $0 \leq k_{rl}, k_{rg} \leq 1$

Here,  $S^* = (S_l - S_{lr}) / (S_{ls} - S_{lr})$ ,  $\hat{S} = (S_l - S_{lr}) / (1 - S_{lr} - S_{gr})$

Parameters:  $RP(1) = \lambda$

$RP(2) = S_{lr}$

$RP(3) = S_{ls}$

$RP(4) = S_{gr}$

Notation: Parameter  $\lambda$  is  $m$  in van Genuchten's notation, with  $m = 1 - 1/n$ ; parameter  $n$  is often written as  $\beta$ .

IRP = 8      function of Verma et al. (1985)

$$k_{rl} = \hat{S}^3$$

$$k_{rg} = A + B\hat{S} + C\hat{S}^2$$

where  $\hat{S} = (S_l - S_{lr}) / (S_{ls} - S_{lr})$

Parameters as measured by Verma et al. (1985) for steam-water flow in an unconsolidated sand:

$$S_{lr} = RP(1) = 0.2$$

$$S_{ls} = RP(2) = 0.895$$

$$A = RP(3) = 1.259$$

$$B = RP(4) = -1.7615$$

$$C = RP(5) = 0.5089$$

If the user wishes to employ other relative permeability relationships, these need to be programmed into subroutine RELP in module t2f.f. The routine has the following structure:

```
SUBROUTINE RELP( . . . )  
    . . .  
    GOTO(10,11,12, . . . ),IRP  
  
10  CONTINUE  
(IRP = 1)    . . .  
    . . .  
    REPL= . . .  
    REPG= . . .  
    RETURN  
  
11  CONTINUE  
(IRP = 2)    . . .  
    . . .  
    REPL= . . .  
    REPG= . . .  
    RETURN  
    . . .  
    . . .  
    END
```

To code an additional relative permeability function, the user needs to insert a code segment analogous to those shown above, beginning with a statement number which would also appear in the GOTO statement. The RP( ) parameters as read in input can be utilized as parameters in the assignment of liquid and gas relative permeability (REPL and REPG, respectively).

## Appendix H. Capillary Pressure Functions

ICP = 1      **linear function**

$$P_{cap} = \begin{cases} -CP(1) & \text{for } S_l \leq CP(2) \\ 0 & \text{for } S_l \geq CP(3) \\ -CP(1) \frac{CP(3)-S_l}{CP(3)-CP(2)} & \text{for } CP(2) < S_l < CP(3) \end{cases}$$

Restriction:  $CP(3) > CP(2)$ .

ICP = 2      **function of Pickens et al. (1979)**

$$P_{cap} = -P_0 \left\{ \ln \left[ \frac{A}{B} \left( 1 + \sqrt{1 - B^2/A^2} \right) \right] \right\}^{1/x}$$

with

$$A = (1 + S_l/S_{l0})(S_{l0} - S_{lr})/(S_{l0} + S_{lr})$$

$$B = 1 - S_l/S_{l0}$$

where

$$P_0 = CP(1) \quad S_{lr} = CP(2) \quad S_{l0} = CP(3) \quad x = CP(4)$$

Restrictions:  $0 < CP(2) < 1 \leq CP(3); \quad CP(4) \neq 0$

ICP = 3      **TRUST capillary pressure** (Narasimhan et al., 1978)

$$P_{cap} = \begin{cases} -P_e - P_0 \left[ \frac{1-S_l}{S_l - S_{lr}} \right]^{1/\eta} & \text{for } S_l < 1 \\ 0 & \text{for } S_l \geq 1 \end{cases}$$

where

$$P_0 = CP(1) \quad S_{lr} = CP(2) \quad \eta = CP(3) \quad P_e = CP(4)$$

Restrictions:  $CP(2) \geq 0; \quad CP(3) \neq 0$

ICP = 4

**Milly's function** (Milly, 1982)

$$P_{cap} = -97.783 \times 10^A$$

with

$$A = 2.26 \left( \frac{0.371}{S_l - S_{lr}} - 1 \right)^{1/4}$$

where  $S_{lr} = CP(1)$

Restriction:  $CP(1) \geq 0.$

ICP = 6

**Leverett's function** (Leverett, 1941; Udell and Fitch, 1985)

$$P_{cap} = -P_0 \cdot \sigma(T) \cdot f(S_l)$$

with

$\sigma(T)$  - surface tension of water (supplied internally in TOUGH2)

$$f(S_l) = 1.417 (1 - S^*) - 2.120 (1 - S^*)^2 + 1.263 (1 - S^*)^3$$

where

$$S^* = (S_l - S_{lr}) / (1 - S_{lr})$$

Parameters:  $P_0 = CP(1)$      $S_{lr} = CP(2)$

Restriction:  $0 \leq CP(2) < 1$

ICP = 7

**van Genuchten function** (van Genuchten, 1980)

$$P_{cap} = -P_0 \left[ [S^*]^{-1/\lambda} - 1 \right]^{1-\lambda}$$

subject to the restriction

$$-P_{max} \leq P_{cap} \leq 0$$

Here,

$$S^* = (S_l - S_{lr}) / (S_{ls} - S_{lr})$$

Parameters:  $CP(1) = \lambda = 1 - 1/n$

$CP(2) = S_{lr}$  (should be chosen smaller than the corresponding parameter in the relative permeability function; see note below.)

$$CP(3) = 1/P_0 = \alpha/\rho_w g \text{ (proportional to } \sqrt{k} \text{ )}$$

$$CP(4) = P_{max}$$

$$CP(5) = S_{ls}$$

Notation: Parameter  $\lambda$  is  $m$  in van Genuchten's notation, with  $m = 1 - 1/n$ ; parameter  $n$  is often written as  $\beta$ .

Note on parameter choices: In van Genuchten's derivation (1980), the parameter  $S_{lr}$  for irreducible water saturation is the same in the relative permeability and capillary pressure functions. As a consequence, for  $S_l \not\equiv S_{lr}$  we have  $k_{rl} \not\equiv 0$  and  $P_{cap} \not\equiv -\infty$ , which is unphysical because it implies that the radii of capillary menisci go to zero as liquid phase is becoming immobile (discontinuous). In reality, no special capillary pressure effects are expected when liquid phase becomes discontinuous. Accordingly, we recommend to always choose a smaller  $S_{lr}$  for the capillary pressure as compared to the relative permeability function.

## ICP = 8      **no capillary pressure**

$$P_{cap} \equiv 0 \quad \text{for all saturations; no parameters}$$

## Subject Index

### A

Accumulation terms 16, 38, 144  
Accuracy 7, 12, 30, 69, 72, 87, 135, 136, 151  
Active blocks 27, 63  
Adsorption 44, 117  
Advection 111, 114, 118, 144  
Air 35, 37, 39, 40, 44, 107  
Anisotropy (of space discretization errors) 136  
Aqueous 14, 33, 40, 44, 46, 49, 51, 55, 75, 107, 111, 115, 119, 130, 145, 155  
Aquifer 114, 118  
Architecture 2, 6, 8, 134  
Arrays 7, 11, 13, 14, 16, 17, 18  
Automatic time stepping 6, 165

### B

Balance equations 11, 16, 63, 144, 162  
Benchmark 78, 88, 107, 132  
Biconjugate gradients 93  
Black body 173  
Boiling 89, 130  
Boundary conditions 19, 27, 61, 62, 114, 177  
time-dependent 62  
Brine 40, 55, 107, 130  
specifications 42, 46  
Buoyancy 118

### C

Cancellation, numerical 81  
Capillary 122  
effects 30, 145  
fringe 114, 118  
pressure 37, 52, 71, 98, 145, 160, 162, 170, 188

Carbon dioxide 33  
CO<sub>2</sub> 33, 98, 102, 130  
Code installation 4  
COFT (keyword) 169  
COMMON blocks 8, 17, 18  
Compilation 4, 17, 53  
Components 11, 29, 44, 55, 80, 144, 155, 162, 174  
Composite media 134  
Compressibility 41, 51, 54, 109, 152, 161  
Computational work 72  
Computer hardware 4  
Concentration 155  
Condensation 87  
Confining beds 69, 95  
Conjugate gradient solvers 72, 150, 166  
CONNE (keyword) 173  
Connections (interfaces) 19, 25, 172  
Constitutive relations 19, 184, 188  
Contamination 114  
Continuation run (see Restarting)  
Continuum 28, 100, 153  
Convergence  
check 9, 10, 17  
criterion 150, 167  
flag 9  
tolerance 96, 150  
Coordinates 27, 151, 172  
Corey's curves (relative permeability) 184  
Corrosion 39  
Cylindrical geometry 87

### D

Darcy's law 144  
Data  
blocks 19, 20, 176  
geometry 25  
Daughter (radionuclide) 44  
Decay, radionuclide 44  
Defaults 21, 61  
Deliverability (well) 64, 104, 107, 174, 175

Density 13, 30, 38, 39, 40, 45, 50, 65, 135, 144, 160, 165  
 Derivatives, numerical 14, 16, 167  
 DIFFU (keyword) 170  
 Diffusion  
     coefficient 14, 146, 156, 158, 166, 169  
     molecular 30, 89, 111, 114, 117, 146, 155  
     vapor 155, 159  
 Diffusive flux 146, 155, 166  
 Diffusivity  
     molecular 47, 111, 117, 159  
     pressure 54, 152  
     thermal 69, 111  
 Dilution 130  
 Dimensioning (of arrays) 17, 18, 75  
 Direct solvers (linear equations) 72, 150  
 Dirichlet boundary conditions 27, 62  
 Discretization 6, 134, 135, 147, 148, 150, 157  
 Disk files 8, 21, 24, 81, 176  
 Dispersion 1, 46, 146  
 Dissolution 2, 33, 35, 41, 55, 119  
 Distribution coefficient (Kd) 44, 161  
 Domain (reservoir) 19, 21, 27, 160, 170, 172  
 Double porosity 6, 152, 182  
 Double precision 4  
 Dual permeability 154, 182  
 Duplicate names (of subroutines) 4  
 Dusty gas 155

## E

ELEME (keyword) 172  
 Elements (see Volume elements)  
 Elevation 52  
 ENDCY (keyword) 176  
 ENDFI (keyword) 160  
 Energy  
     balances 6, 11, 15, 144  
     internal 30  
     rate 175  
 Enhanced vapor diffusion 155, 159

Enthalpy 30, 45, 50, 55, 59, 66, 98, 106, 107, 130, 165, 174  
 EOS modules 2, 7, 8, 13, 29, 30, 61  
 Equations (see Balance, Energy, Governing, Mass)  
 EQUID (keyword) 179  
 Equilibrium 11, 151  
     gravity-capillary 52, 61, 114, 122, 172  
     solubility 56  
 Error 17, 134  
     absolute 167  
     duplicate names 4, 53  
     grid orientation 135  
     relative 167  
 Executable 29  
 Execution 9  
 Expansivity 41, 161  
 Exsolution 132

## F

Feed zone 66, 67, 104  
 Fick's law 155  
 Finite differences 6, 69, 134, 151, 157  
 Five-spot 99  
 Flow  
     rates 104, 174  
     terms 16, 38  
 Flux 6, 16, 53, 62, 69, 144, 148, 156, 166  
 FOFT (keyword) 169  
 Formats  
     data blocks 21  
     disk files 21  
     input 22  
 FORTRAN 4  
 Fracture 93, 96, 102  
     spacing 182  
 Fractured media 1, 25, 28, 99, 152  
 Front smearing 136

## G

Gas 33, 39, 147  
     constant 145  
     diffusion 155, 157, 166

ideal 39, 45, 63  
 non-condensible 33, 40, 55, 98, 130  
 Gauss' divergence theorem 146  
 GENER (keyword) 174  
 Generation 79, 104, 107, 164, 174, 175  
 Geometry 25, 134, 136, 148, 150  
     Cartesian 25  
     cylindrical 87  
     data 25, 26, 27  
 Geothermal  
     fields, reservoirs 87, 93, 99, 130  
     production 99, 104  
 Gibbs' phase rule 11  
 GOFT (keyword) 170  
 Governing equations 7, 144  
 Gradient 53, 66, 118, 136, 147, 152, 155, 158, 177  
 Grant's curves (relative permeability) 184  
 Gravity 65, 96, 122, 125, 167, 173  
 Gravity-capillary equilibrium 52, 122  
 Grid (see also MESH) 99  
     block 11, 13, 16, 25, 29, 61, 135, 149  
     Cartesian 25, 65, 95, 180  
     generation 19, 26, 28, 95, 177  
     irregular 135  
     nested 153  
     orientation 98, 135, 136  
     primary 28, 100  
     radial 87, 104, 131

## H

Half life 44  
 Hardware 4  
 Harmonic (see Weighting)  
 Heat  
     conduction 69, 93, 94, 145  
     conductivity 161, 164  
     convection 145  
     exchange 69, 102, 165, 172  
     generation 87, 107  
     pipe 87  
     sink/source 174  
     specific 107, 144, 161

sweep 93  
 transfer 87, 95, 145, 174  
 Henry's  
     constant 35, 111, 115, 159  
     law 33, 41, 55  
 Heterogeneity 71  
 Higher-order methods 25, 136  
 Humidity, relative 37, 38  
 Hydraulic  
     conductivity 147  
     head 147  
 Hydrodynamic  
     dispersion 1, 46, 146  
     instability 135  
 Hydrogen 39  
 Hydrostatic 96  
 Hypersaline 130

## I

Ideal gas (see Gas, ideal)  
 Impermeable 99, 165  
 Implicit time differencing 6, 149  
 Inactive blocks 27, 61, 62, 63, 102, 117, 177  
 INCON (keyword) 168  
 Increments 14, 16, 17  
 INDOM (keyword) 168  
 Initial conditions 19, 61, 96, 107, 114  
 Initialization 21, 31, 35, 37, 61, 79, 96, 115  
 Injection 80, 93, 95, 96, 98, 99, 107, 119, 174  
 Input data 19, 20, 42, 46, 59, 78, 160, 177  
 Instability 135  
 Installation (of code) 4  
 Integral finite differences (IFD) 6, 25, 134, 148  
 Integration 144  
 Interface 6, 18, 25, 62, 70, 134, 149, 164, 172, 173  
 International Formulation Committee 30, 35  
 Internet (see Web)  
 Interpolation 64, 135, 149, 164  
 Inward unit normal 148  
 Irreducible (see Saturation)  
 Isothermal 30, 96, 152

Isotropy 173  
Iteration 8, 9, 109  
Iterative solvers (linear equations) 72, 150

## J

Jacobian matrix 10, 14, 15, 16, 17, 72, 98, 150, 165

## K

Kelvin's equation 37, 38, 145  
Keywords 19, 20, 78, 160, 177  
Klinkenberg parameter 146, 161  
Knudsen diffusion 155

## L

LAYER (keyword) 179  
Line source 87  
Linear  
    equations 9, 14, 15, 16, 17, 72, 150  
    solvers 7, 72, 93, 165  
Linking 4  
Liquid 31, 51, 147  
LOGAR (keyword) 179

## M

Mass  
    balances 6, 11, 15, 29, 51, 55, 96, 99, 144  
    component 144, 162  
    exchange 164  
    flux 144  
    fraction 111, 117, 144, 156, 158  
    injection 174  
    production 174  
    rate 175  
    transport 146  
Matrix blocks 99, 102, 152  
Memory requirements 5, 72  
MESH (see also Grid)  
    Cartesian 25, 177, 180  
    file 25  
    generation 19, 27, 28, 95, 160, 177

radial 25, 87, 177  
rectilinear 25, 27  
MESHM (keyword) 160  
Migration (of contaminants) 115  
MINC (keyword) 181  
MINC (multiple interacting continua) 25, 26, 28, 100, 153, 177, 181  
Mixture 40, 110  
Mobility 62, 64, 67, 135, 164, 167  
Modular architecture 7, 8, 25  
Moisture content 147  
Molar weight 48, 63, 145  
Molecular diffusion (see Diffusion)  
MOP options 163  
MULKOM 7  
MULTI (keyword) 162  
Multiphase 6, 12, 61, 107, 117, 152, 155

## N

NaCl 40, 55  
NAPL (non-aqueous phase liquid) 117  
Neumann boundary conditions 62  
Newton-Raphson iteration 6, 14, 16, 55, 72, 122, 149, 163, 167  
Nitrogen 41  
Nodal  
    distance 149, 182  
    line 25  
    points 177  
Non-aqueous phase 44  
Nonisothermal 40, 69, 93, 107  
NOVER (keyword) 170  
Nuclear waste 87  
Numerical dispersion 136

## O

Oil 49, 119  
O-preconditioning 73  
Output 75

## P

PAR array 13  
PARAM (keyword) 163  
PARAMETER statement 17, 75  
Parameters  
    hydrogeologic 19  
    secondary 13, 14, 29, 158, 162  
    thermophysical 7, 13, 14, 16  
Parent (radionuclide) 44  
PART (keyword) 181  
Permeability 164  
    absolute 145, 161  
    change 56  
    effective 54  
    matrix 102  
    modification 71, 125, 128, 172  
    reduction 58, 130  
    relative 13, 50, 55, 56, 145, 156,  
        160, 161, 170, 184  
    -thickness 64  
Phase 144, 162  
    adsorption 145  
    appearance 29, 55, 80  
    aqueous 109, 111, 118, 119  
    change 11, 29, 31, 32, 46, 51, 55  
    conditions 29  
    diagnostic 31  
    disappearance 29, 55, 80  
    distribution 11, 29  
    front 134  
    gas 14, 30, 33, 35, 40, 45, 51, 55,  
        75, 109, 111, 117  
    liquid 32  
    partitioning 44, 111, 118, 155, 157  
    reference 29  
    single 11, 31, 107, 109  
    transition 12, 109  
Pivot 165, 167  
Plotting 77, 81, 104, 168  
    contour 68, 98  
Pore 57, 155  
    model 57  
    velocity 76  
Porosity 54, 56, 99, 111, 130, 144, 160,  
        176

Porous medium 1, 24, 25, 27, 28, 57, 102  
Precipitation 40, 55, 130  
Precision (of arithmetic) 4  
Preconditioning (linear equations) 72, 94,  
        98, 165  
Preferential flow 93  
Pressure 11, 29  
    bottomhole 64, 66, 68, 104, 174  
    capillary 37, 52, 71, 87, 98, 145,  
        162, 170, 188  
    equilibrium 96  
    liquid 38  
    partial 37, 45, 55, 102  
    trend 96  
    vapor 12, 30, 37, 145, 165  
wellbore 65, 93  
    wellhead 66, 104, 174  
Primary variables 6, 8, 11, 13, 30, 31, 51,  
        61, 165, 167, 170, 176  
Printout 75, 163, 171  
Produced fluid 164  
Production 93, 95, 96, 130, 174  
    rate 64, 65, 104  
    well 64, 99, 104  
Productivity index (PI) 64, 104, 175  
Program structure 7, 9  
Proximity function 154, 181

## Q

Quasi-steady 66, 152

## R

RADIAL (keyword) 179  
Radial flow 64, 130  
Radiant emittance 174  
Radiative heat transfer 145, 174  
Radionuclide 44, 111  
    specifications 46  
Random 71, 125, 172  
Records (data) 94, 96  
Relative (see Permeability)  
Reservoir 104  
    domains 19  
    two-phase 104

vapor-dominated 98  
Residual 81, 149  
computation 8, 14, 72  
formulation 6, 149  
Restarting 61, 62  
Richards' equation 51, 147  
ROCKS (keyword) 160  
RPCAP (keyword) 171

## S

Salinity 1, 40, 55, 59, 107, 110, 130  
Salt 40, 55, 132  
Salting out 41  
Sand 125  
Saturated-unsaturated flow 51, 122  
Saturation 11, 40, 55, 117, 125, 144  
gradient 118  
irreducible 53, 119, 122, 190  
line 30  
Scaling 165  
Secondary parameters 7, 8, 13  
Segments (of a simulation run) 94, 114  
SELEC (keyword) 42, 46, 59, 171  
Semi-analytical 69, 87, 93  
SI units 19  
Similarity solution 87, 131  
Single precision 4  
Sinks/sources 8, 16, 19, 62, 63, 64, 173  
Skin factor 64, 104  
Soil 118, 156  
Solid 40, 44, 55, 131  
Solubility 35, 39, 40, 55, 109, 115, 117, 130  
Soluble 44  
Solute 155  
Solver (linear) 72, 98, 165  
SOLVR (keyword) 73, 93, 169  
Source (see Sink)  
Standard conditions 157  
START (keyword) 162  
Steady (flow, state) 10, 61, 135  
Steam  
superheated 30, 31  
tables 30, 35  
Stefan-Boltzmann (law, constant) 145, 174

Step function 164  
Subdomain 144  
Subroutines 8, 9

## T

T2DM (dispersion module) 1, 160, 169  
T2VOC (module for volatile organic chemicals) 1, 115, 159, 160  
Temperature 11  
distribution 97  
profile 103  
recovery 98  
Templates 78  
Text editor 21, 27  
Thermal expansivity 161  
Thermodynamic  
state 11  
variables 7, 11, 13, 14, 61  
Thermophysical properties 7, 13, 14, 19, 29  
Three-phase 1, 119  
Time  
automatic 10, 165  
discretization 149  
series 77, 81  
stepping 6, 9, 17, 19, 75, 96, 104, 163, 165, 166, 167  
TIMES (keyword) 171  
Title 19, 160  
Tortuosity 111, 117, 146, 155, 159, 161  
TOUGH 7, 35, 79  
Tracer 30, 31, 111, 155  
Transient 11, 134, 152  
TVD (total variation diminishing) 136  
Two-phase 11, 30, 105, 109, 130  
Two waters 30, 74, 94, 98

## U

Unit head gradient 53  
Units 19  
Unsaturated 51, 122, 147  
Upstream (see Weighting)

## V

Vadose zone 114  
Validation (of code) 78  
van Genuchten - Mualem model 185  
Vapor 30  
    diffusion 155, 159, 166  
    pressure 30, 145  
    pressure lowering 12, 30, 37, 38,  
        55, 87, 89, 130, 145, 165  
Vaporization 87, 89, 98  
Variable salinity 41, 107  
Variables  
    persistent 12  
    primary 11, 12, 13, 14, 16, 29, 30,  
        31, 167, 170, 176  
    secondary 13, 14  
    switching 12, 29, 32, 56, 61  
Variably saturated flow 51  
Velocity (pore) 76  
Verification (of code) 78  
Version control 3, 86  
Viscosity 13, 31, 34, 35, 39, 40, 41, 50,  
    145  
Void space 55, 131  
Volatile 44, 111, 155  
    organic chemical (VOC) 1, 44, 114,  
        117

Volume elements (see also Grid blocks) 13,  
    19, 25, 29, 148, 172  
    active 27, 63  
    inactive 27, 61, 62, 63, 87, 177

## W

Water 2, 30  
    injection 93, 119  
    subcooled 30  
    table 39, 52, 114, 117, 122  
Web (Internet) 2, 136  
Weighting  
    harmonic 134, 149, 157, 159, 164,  
        166  
    interface 6, 134, 135, 149, 164  
    upstream 6, 134, 136, 149, 164,  
        167

## Well

block 104  
coupled to reservoir 66, 104  
field 99  
injection 99  
pattern 99  
pressure 64, 66  
production 64, 99, 130  
radius 64  
rate 67  
specifications 174

## Wellbore

flow 66, 104, 174  
pressure 8, 93  
simulator 66, 174

## X

XY grid 95  
XYZ (keyword) 180

## Y

Yucca Mountain 87

## Z

Z-preconditioning 73, 93